Triangular-n Postmaster: Technical Dossier and Empirical Context

Volume I — the proofs behind the Reading Volume – v5.1

Jeffery Huckstead   ORCID 0009-0007-0234-2177   Cerebral Graphix

September 2026

RH STATUS: OPEN

Contents

Abstract

This Dossier supplies the proofs, finite certificates, countermodels, and separately marked empirical material behind *Triangular-n Postmaster, Volume I*. The analytic coordinate is $q_\rho = \rho(1-\rho) = -2T_{\rho-1}$, indexed by reflection orbits $[\rho] = \{\rho, 1-\rho\}$ with multiplicity m_ρ. An off-line quartet contributes two conjugate folded nodes. This convention controls the canonical product, resolvent, Widder and heat identities, and the Li sum. Conjugation is not silently included in the quotient.

The chapters develop the triangular arithmetic, the completed source, finite positivity certificates, and exact obstructions to several proposed shortcuts. The inherited analytic source result covers W_1; the v5.0 computer-assisted certificates cover W_2–W_6 on their stated domains. The independent source proof at W_7, the all-node matrix inequality, and the specified uniform energy and arithmetic bounds remain open. This edition clarifies the interface and closes with a local summary; it adds no RH implication and invokes no companion entropy paper.

The v5.0 certificate programs and receipts are retained unchanged as provenance. They have not been re-executed for this editorial revision. The current receipt distinguishes preservation and interface checks from those inherited mathematical certificates.

How to use this Dossier

This is the second of two documents. The **Reading Volume** carries the continuous argument from the triangular primitive to the research boundary, in reader sections **§R1–§R25**. This Dossier carries the proofs, the finite certificates, the countermodels, and the empirical context that supports none of them.

A section number without an R is here. References of the form §34, §104 or §166C name sections of this Dossier; references of the form §R12 or §R23 name sections of the Reading Volume. Equation tags are shared: (33.1), (SW.4b) and (166C.25) name the same equations in both documents, and the identifiers under which the proofs were derived have not been renumbered.

The signed coefficient grid $c_{k,j} = (-1)^j \binom{k}{j}$ referred to throughout is printed in full, for $0 \le k \le 17$, as the coefficient-grid figure of the Reading Volume.

Chapters follow mathematical dependency, not reading order:

chapter	subject	supports
I–II	discrete primitives, factorial families, the fractional grid, worked triangular arithmetic (§§169–172)	§§R1–R5E
III	centered geometry and operator models	§§R6–R8
IV	completion, folded support, the Gamma source	§§R9–R10B
V–VI	flux geometry, rational witnesses, Widder source proofs	§§R11–R14
VII–VIII	one-scale moment criteria, finite Löwner certificates	§§R14–R16
IX–XI	cyclic arithmetic, prime wave packets, finite Weil models	§§R17–R17E
XII–XIV	dilation, completion forms, completed Bernstein rows, prime cutoffs	§§R17F–R17H
XV	remaining proof obligations and countermodels	§§R22–R25
Part E	empirical context and historical transcriptions	nothing

Status tags in this Dossier use the **single master key in the Reading Volume front matter**. The certificate that carries the source rungs of §74A is bundled with this edition and re-executed by the v5.0 build; software versions, precisions and run dates are recorded in the package's QA receipt rather than in the text. The Riemann hypothesis is open, and no result in this Dossier is offered as a proof of it.

Labels and vocabulary. Labels such as PP85 or PP190-T name the author's numbered working papers, where a result or certificate was first produced. They are kept as provenance tags only: each result is stated here with its own status, and the working papers are not part of this publication. An *adversarial replay* reruns a certificate with every material numerical parameter changed at once (precision, partition and expansion orders), so that agreement is not an artifact of one configuration. The other working terms (source, owner, rung, carrier, rail) are defined in the glossary of the Reading Volume.

Classical sources. Classical results are cited where they are used, and the lineage table of the Reading Volume maps each part of the argument to its sources. Reference numbers are shared with the Reading Volume; entries 83–120 were added in the previous edition.

What changed in v5.1. The abstract, the folded-multiplicity explanation in Section 32, and the technical summary make the object and the open boundary explicit. No theorem status changed.

Retained from v5.0. Section 155A now prints the diagonal specializations (155A.4a) of its two product identities, so the square form of every reflected Li rung, odd and even, appears in one place, and cross-references Reading Volume §R10C, the new one-orbit coordinate dictionary. Section 74A is unchanged and still carries the five certified source rungs $W_2, \ldots, W_6$ in one certificate — one partition of $1 \leq s \leq 128$, one exact tail for $s \geq 128$, and two programs that share no arithmetic — re-executed by the v5.0 build on both backends. No status changed, and the Riemann hypothesis remains open.

Technical chapter I. Discrete primitives and factorial families

Primitive identities generate discrete ladders. Factorial and Pell classifications retain their exact integer conditions.

5. Discrete ladders: squaring, perfect numbers, and Pell

Reader §R1A proves the primitive identities (TDP.1)–(TDP.5). This section derives their repeated-square and Pell consequences. All statements here are arithmetic; none assumes a zero-location theorem.

Theorem TDP-A - Square-index triangular conjugacy

Fix a positive integer n and define

$$m_0 = n, \qquad m_{k+1} = m_k^2 = n^{2^{k+1}} \qquad U_k = T_{m_k - 1}, \quad V_k = T_{m_k} \tag{TDP.A1}$$

Then

$$m_{k+1} = U_k + V_k, \qquad V_{k+1} = U_k^2 + V_k^2$$

and therefore

$$\boxed{(U_{k+1}, V_{k+1}) = (U_k^2 + V_k^2 - U_k - V_k,\ U_k^2 + V_k^2)} \tag{TDP.A2}$$

This recurrence is exactly one-dimensional on its invariant curve. Put

$$D_k = V_k - U_k, \qquad S_k = U_k + V_k$$

Consecutiveness gives $D_k = m_k$ and $S_k = m_k^2 = D_k^2$. Under (TDP.A2),

$$\boxed{D_{k+1} = S_k = D_k^2, \qquad S_{k+1} = D_k^4} \tag{TDP.A3}$$

Thus the two-component polynomial recurrence is conjugate to $D \mapsto D^2$ on the parabola $S = D^2$.

For $n = 2$ the first steps are

k	m_k	(U_k, V_k)
0	2	$(1, 3)$
1	4	$(6, 10)$
2	16	$(120, 136)$
3	256	$(32640, 32896)$

Equivalently, every step gives

$$T_{n^{2^{k+1}}} = T^2_{n^{2^k}-1} + T^2_{n^{2^k}} \tag{TDP.A4}$$

Corollary TDP-B - Exact Euclid–Euler intersection

The Euclid–Euler theorem says that an even perfect number is exactly

$$2^{p-1}(2^p - 1) = T_q \qquad q = 2^p - 1 \text{ prime} \tag{TDP.B1}$$

On the lower $n = 2$ ladder, $q_k = m_k - 1 = 2^{2^k} - 1$. At $k = 0$, $q_0 = 1$ is not prime; at $k = 1$, $q_1 = 3$ gives $T_3 = 6$. For every $k \geq 2$, the exponent 2^k is composite, and $2^{2^k} - 1$ is correspondingly composite by the factorization of $X^{ab} - 1$. Hence

$$\boxed{\{T_{q_k} : q_k \text{ is a Mersenne-prime index}\} = \{T_3\} = \{6\}} \tag{TDP.B2}$$

The next even perfect number $T_7 = 28$ lies in the full Euclid–Euler family, not in this repeated-square subfamily. This corollary concerns even perfect numbers only.

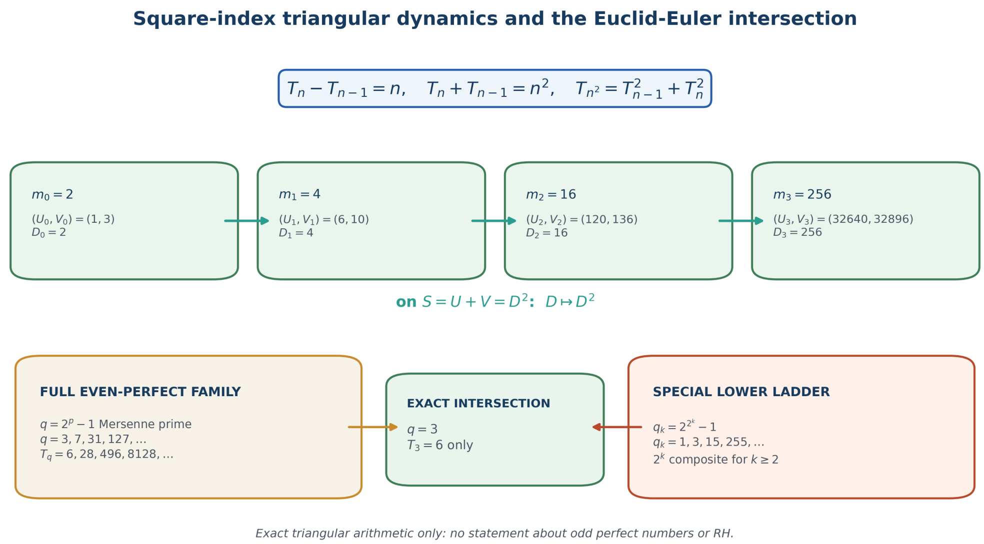

Figure 1: The square-index triangular recurrence is scalar squaring on the invariant parabola, while its lower n=2 branch meets the Euclid–Euler family only at 6.

Theorem TDP-C - Pell companion and the unique fourth-power lock

For nonnegative integers a, b with $a + b > 0$,

$$b^2 - a^2 = T_{a+b} \quad \Longleftrightarrow \quad b = 3a + 1 \tag{TDP.C1}$$

Indeed, cancellation of $a + b$ reduces the equation to $2(b - a) = a + b + 1$. If $a = T_r$ and $b = T_s$, (TDP.C1) becomes

$$T_s = 3T_r + 1 \quad \Longleftrightarrow \quad (2s+1)^2 - 3(2r+1)^2 = 6 \tag{TDP.C2}$$

All nonnegative solutions form one Pell orbit. From $(r_0, s_0) = (0, 1)$,

$$\boxed{r_{k+1} = 2r_k + s_k + 1 \qquad s_{k+1} = 3r_k + 2s_k + 2} \tag{TDP.C3}$$

The first pairs are

$$(0, 1), (2, 4), (9, 16), (35, 61), (132, 229), (494, 856), \ldots$$

and every pair satisfies

$$\boxed{T_s^2 - T_r^2 = T_{T_s + T_r}} \tag{TDP.C4}$$

Completeness follows by writing $x = 2s + 1$, $y = 2r + 1$ and descending every solution with $y > 1$ by

$$(x, y) \longmapsto (2x - 3y,\ 2y - x)$$

The first nontrivial pair carries one extra identity, and it is unique. Put $t = T_r$, so $T_s = 3t + 1$. Equality of the fourth-power and square-difference constructions factors as

$$t^4 + 3t + 1 = 8t^2 + 6t + 1 \quad \Longleftrightarrow \quad \boxed{t(t - 3)(t^2 + 3t + 1) = 0} \tag{TDP.C5}$$

Thus $t = 0$ is trivial and $t = 3$ is the unique nontrivial nonnegative solution. Consequently

$$\boxed{T_2^4 + T_4 = T_4^2 - T_2^2 = T_{13} = 91} \tag{TDP.C6}$$

This Pell ladder is independent of the repeated-square dynamical ladder in Theorem TDP-A. Neither has an RH implication.

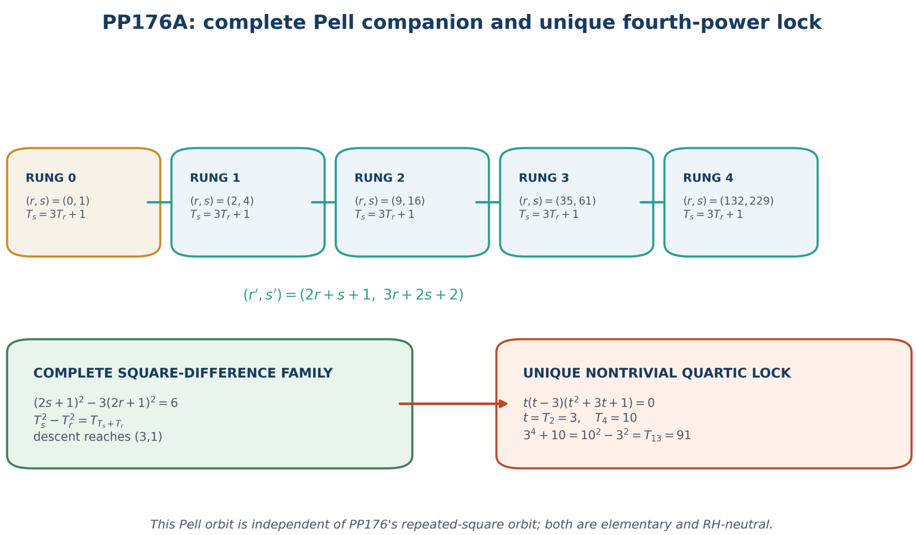

Figure 2: The repeated-square ladder and the Pell companion are distinct exact triangular ladders: repeated squaring on one side, and a complete Pell orbit with a unique fourth-power lock on the other.

6. Simplex hierarchy and factorial absorption

The qth simplex polynomial is

$$S_q(x) = \binom{x + q}{q} = \frac{1}{q!} \prod_{j=1}^{q} (x + j)$$

Every factor is an adjacent triangular difference. Consequently every simplex polynomial is a normalized product of consecutive triangular legs. Its reflection-completed centered roots form a symmetric arithmetic progression, producing central-factorial parity formulas.

For integer $n \geq 1$,

$$\frac{T_n}{n!} = \frac{n+1}{2(n-1)!}$$

With

$$g_n = \gcd(n+1, 2(n-1)!)$$

the reduced numerator and denominator are

$$A_n = \frac{n+1}{g_n}, \qquad B_n = \frac{2(n-1)!}{g_n}$$

For $n \geq 2$, the reduced numerator U_n obeys the exact successor gate

$$\boxed{U_n = \begin{cases} n+1, & n+1 \text{ prime} \\ 1, & n+1 \text{ composite} \end{cases}}$$

The prime 2 is the explicit base exception. Therefore $\epsilon_n = (U_n - 1)/n$ is the successor-prime indicator and

$$\zeta(s) = \frac{1}{1-2^{-s}} \prod_{n \geq 2} \left(1 - (n+1)^{-s}\right)^{-\epsilon_n} \qquad \Re s > 1$$

This is an exact encoding of existing prime support, not an estimate of prime distribution.

Proposition 6.1 - Ideal-lattice and radical form

The divisibility reversal in the ideal lattice of $\mathbb{Z}$ is

$$\boxed{d \mid n \iff (n) \subseteq (d)}$$

Suppose the triangular-factorial equation

$$T_m = n!$$

holds. Then

$$m(m+1) = 2n!$$

Since consecutive integers are coprime,

$$(m) + (m+1) = \mathbb{Z}$$

For comaximal ideals, product and intersection agree, so

$$\boxed{(m)\cap(m+1)=(m)(m+1)=(2n!)}$$

For $n\geq 2$, taking the ideal radical yields

$$\boxed{\sqrt{(2n!)}=\bigcap_{p\leq n}(p)=\left(\prod_{p\leq n}p\right)}$$

The logarithm of the positive generator is therefore Chebyshev's function

$$\log\prod_{p\leq n}p=\sum_{p\leq n}\log p=\vartheta(n)$$

Thus the exact structural lane is

$$\text{triangular successor pair}\longrightarrow\text{comaximal ideal factorization}$$
$$\longrightarrow\text{radical prime support}\longrightarrow\vartheta(n)$$

This reformulation does not estimate $\vartheta(n)$ and hence does not supply prime cancellation. Its durable lesson is categorical: in extensions where element factorization can fail, prime ideals rather than prime elements are the stable transport objects.

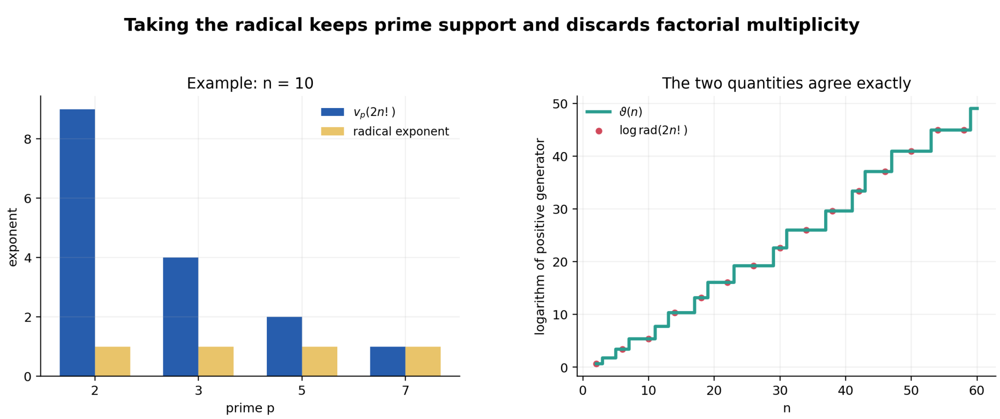

Figure 3: The ideal radical preserves prime support while discarding factorial multiplicity.

156. The factorial triangular switch and its diagonal defect

For integer $x\geq 1$,

$$\boxed{\frac{(x+1)!}{2(x-1)!}=\frac{x(x+1)}{2}=T_x} \tag{156.1}$$

The same cancellation can be displayed in the factored form noticed in the exploratory round:

$$\boxed{\left(\frac{x!}{2}\right)\left(\frac{x+1}{(x-1)!}\right)=\frac{1}{2}\left(\frac{x!}{(x-1)!}\right)(x+1)=\frac{x(x+1)}{2}} \tag{156.2}$$

This is elementary, but structurally useful: inserting the factorial turns a reduced rational successor gate into an exact diagonal polynomial. Gamma continuation shows its natural domain:

$$\frac{\Gamma(x+2)}{2\Gamma(x)}=\frac{x(x+1)}{2} \tag{156.3}$$

where the quotient is regular, and everywhere after filling its removable values.

The mixed expression

$$F_{\triangle}(x,y):=\frac{(y+1)!}{2(x-1)!}=\frac{\Gamma(y+2)}{2\Gamma(x)} \tag{156.4}$$

restricts to the triangular polynomial on its diagonal:

$$\boxed{F_{\triangle}(x,x)=T_x} \tag{156.5}$$

The diagonal is therefore an equality or balance locus. At regular points with $T_x \neq 0$, the exact signed off-diagonal defect and relative defect are

$$\boxed{\Delta_{\triangle}(x,y)=F_{\triangle}(x,y)-T_x=T_x\left(\frac{\Gamma(y+2)}{\Gamma(x+2)}-1\right), \qquad \frac{F_{\triangle}(x,y)}{T_x}=\frac{\Gamma(y+2)}{\Gamma(x+2)}} \tag{156.6}$$

Near $y=x$, with $y=x+\varepsilon$,

$$\frac{\Delta_{\triangle}(x,x+\varepsilon)}{T_x}=\varepsilon\psi(x+2)+O(\varepsilon^2) \tag{156.7}$$

Thus the graph's immediate departure from the diagonal is controlled by the digamma slope. For integer $y>x$ the ratio in (156.6) is the product $\prod_{k=x+2}^{y+1} k$, explaining the rapid visual growth.

The successor-prime information in the reduced rational

$$\frac{x+1}{2(x-1)!} \tag{156.8}$$

does remain visible **inside that factor before the product is reduced**: for $x \geq 2$, its reduced numerator is $x+1$ when $x+1$ is prime and 1 when $x+1$ is composite. It is not preserved as a separate invariant of (156.2), because multiplying by $x!$ introduces the cancellation $x!/(x-1)!=x$ and the whole expression becomes the integer T_x. The switch is real; the prime recognizer and triangular polynomial are two different reductions of the same displayed factorization.

76. Dyadic triangular factorials and the reciprocal simplex operator

The unrestricted equation $T_m = n!$ remains open. Its dyadic branch, however, closes completely.

Theorem 76.1 (complete dyadic classification). The positive integer solutions of

$$2^{k-1}(2^k - 1) = n! \tag{76.1}$$

are exactly

$$\boxed{(k, n) = (1, 1), (2, 3), (4, 5)} \tag{76.2}$$

Proof. Taking 2-adic valuations and using Legendre's identity gives

$$k - 1 = v_2(n!) = n - s_2(n) \qquad k = n - s_2(n) + 1 \le n \tag{76.3}$$

For $n \ge 3$, k must be even because $3 \mid n!$. The lifting-the-exponent formula then gives

$$v_3(2^k - 1) = 1 + v_3(k/2) \le 1 + \log_3 n \tag{76.4}$$

On the other hand $v_3(n!) \ge \lfloor n/3 \rfloor$. Hence a solution must satisfy

$$\left\lfloor \frac{n}{3} \right\rfloor \le 1 + \log_3 n \tag{76.5}$$

The inequality fails for $n = 12, 13, 14$. Replacing n by $n + 3$ raises its left side by one and its right side by $\log_3(1 + 3/n) < 1$, so it fails for every $n \ge 12$. Exact evaluation of (76.3) for $1 \le n \le 11$ leaves precisely (76.2). □

The square form is exactly equivalent:

$$\boxed{(2^{k+1} - 1)^2 = 8n! + 1} \tag{76.6}$$

because the difference between the left side and 1 is eight times the left side of (76.1). All three solutions, including the unit seed, therefore give

$$\boxed{8 \cdot 1! + 1 = 3^2, \qquad 8 \cdot 3! + 1 = 7^2, \qquad 8 \cdot 5! + 1 = 31^2} \tag{76.6a}$$

They are $1! = T_1$, $3! = T_3$, and $5! = T_{15}$. The next odd factorial fails the square test:

$$\boxed{200^2 = 40000 < 8 \cdot 7! + 1 = 40321 < 40401 = 201^2} \tag{76.6b}$$

There is also a local arithmetic obstruction. Since $7! \equiv 2 \pmod{11}$, $8 \cdot 7! + 1 \equiv 6 \pmod{11}$, whereas the square residues modulo 11 are $0, 1, 3, 4, 5, 9$. Thus $7! = 5040$ is not triangular; indeed $T_{99} = 4950 < 5040 < T_{100} = 5050$.

The odd-factorial step itself is exact: $(2r + 1)! = 2T_{2r}(2r - 1)!$. At $r = 3$ it gives $7!/240 = 21 = T_6$. This multiplication identity does not preserve triangularity: the square test remains necessary. Theorem 76.1 closes only the subfamily $m = 2^k - 1$. Neither that theorem nor the rejection of 7! proves that $1!, 3!, 5! = 1, 6, 120$ exhaust all triangular factorials.

The reciprocal arithmetic connects the same triangular coordinates:

$$\boxed{\frac{1}{7!} = \frac{1}{56 \cdot 90} = \frac{1}{4T_7T_9}, \qquad \frac{7!}{T_{44}} = \frac{5040}{990} = \frac{56}{11} = 5 + \frac{1}{11}} \tag{76.6c}$$

Here $56 = 7 \cdot 8$, $90 = 9 \cdot 10$, and $990 = 11 \cdot 90 = T_{44}$. Thus the recurring decimal $5.\overline{09}$ is the exact quotient $56/11$; it is not another solution of $T_m = n!$. The two factors 56 and 90 are also the real source coordinates $x = s(s - 1)$ at $s = 8$ and $s = 10$ used in §147. Their analytic sign certificates have the scope stated there. The same 7! normalizes the fourth Widder row in (32.4): $W_4(0)/7! = \mu_3$. This is the factorial rung normalization, distinct from asserting that 7! itself is triangular.

The independent near-integer $\pi^3 \approx 31.0062766803$ has a convergent triangular owner, rather than a factorial square-test proof. From (4.4f) and Basel, $\pi^2 = 10 - \frac{1}{8}\sum_{n\geq 1} T_n^{-3}$. Since $T_n \geq n^2/2$ and the tail is strictly positive,

$$\sum_{n=1}^{3} T_n^{-3} = \frac{25}{24}, \qquad 0 < \sum_{n>N} T_n^{-3} < \frac{8}{5N^5}, \qquad \frac{1895}{192} - \frac{1}{1215} < \pi^2 < \frac{1895}{192} \tag{76.6d}$$

The tail estimate follows by comparison with $8\int_N^\infty t^{-6}dt$. Exact rational comparison, with all quantities positive, gives

$$31^2 < \left(\frac{1895}{192} - \frac{1}{1215}\right)^3 < \pi^6 < \left(\frac{1895}{192}\right)^3 < \left(\frac{3101}{100}\right)^2 \tag{76.6e}$$

Taking positive square roots proves $31 < \pi^3 < 31.01$. Meanwhile the factor 960/961 in (PR.10d) comes from $T_{15} = 5!$ and $8T_{15} + 1 = 31^2$. These are two exact, distinct connections to the earlier triangular formulas. The denominator 7! reappears in W_4, and the next Widder normalization grows by $2T_{2k}$ in (SW.4d).

The neighbouring value 91 has its own proved identity in (TDP.C6): $T_{13} = T_2^4 + T_4 = T_4^2 - T_2^2 = 91 = 2T_9 + 1$. That unique nonzero intersection uses the triangular value $T_2 = 3$ and $T_4 = 10$; $T_3 = 6$ belongs to a different index. This connects the reciprocal scale 90 to the arithmetic branch already established in Reading Volume §R1A.

The reciprocal digit mechanism is elementary: $1/5040 = 0.0001\overline{984126}$ has period six after a four-digit prefix, whereas $5040/990 = 5.\overline{09}$ has period two. Their denominator orders explain these distinct repetitions.

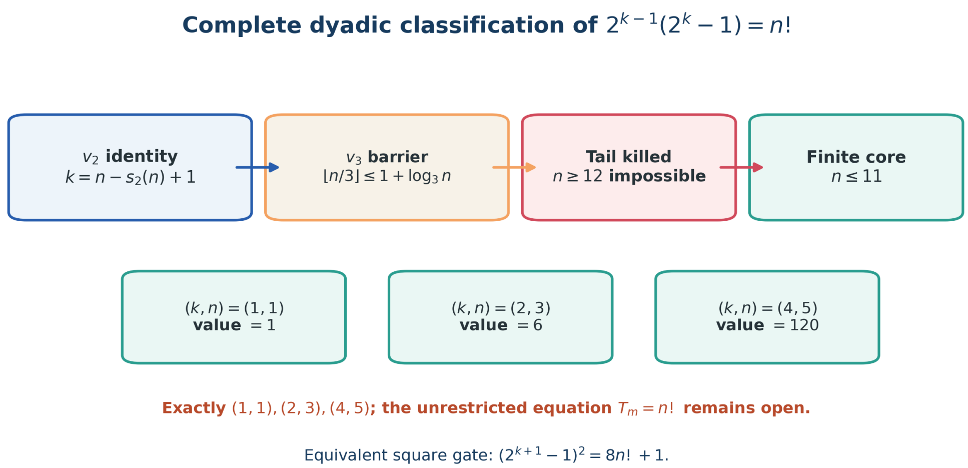

Figure 4: The dyadic subfamily is completely classified by a valuation tail and an eleven-case exact core.

The same packet contains a useful simplex identity. Put

$$\Sigma_d(m)=\binom{m+d-1}{d}$$

Then for $d\ge 2$,

$$\boxed{\frac{1}{\Sigma_d(m)}=\frac{d}{d-1}\left(\frac{1}{\Sigma_{d-1}(m)}-\frac{1}{\Sigma_{d-1}(m+1)}\right)} \tag{76.7}$$

Consequently

$$\boxed{\sum_{m=1}^{N}\frac{1}{\Sigma_d(m)}=\frac{d}{d-1}\left(1-\frac{1}{\Sigma_{d-1}(N+1)}\right)\qquad \sum_{m\ge 1}\frac{1}{\Sigma_d(m)}=\frac{d}{d-1}} \tag{76.8}$$

For $d=2$, this is the familiar handshake identity

$$\frac{1}{T_m}=2\left(\frac{1}{m}-\frac{1}{m+1}\right)$$

The coefficient $d/(d-1)$ in higher dimension is algebraic; it is not an orientation multiplicity. The value 120 has the exact face-count packet

$$120=\Sigma_2(15)=\Sigma_3(8)=\Sigma_7(4)=\Sigma_{14}(3)=5! \tag{76.9}$$

but this is a cardinal resonance, not a prime selector or a zeta-zero theorem.

120. Scope of the repeated-square perfect-number intersection

Theorem TDP-A and Corollary TDP-B are the controlling square-index statements. They use only the primitive identities

$$T_n - T_{n-1} = n \qquad T_n + T_{n-1} = n^2$$

so the cubic difference and the square-index identity are derived, rather than presented as isolated coincidences. Exact integer replay verifies (TDP.1)–(TDP.A4) for $1 \leq n \leq 1000$ and the recurrence through every staged ladder step.

The Euclid–Euler corollary is narrower than the full perfect-number family. It says only that the special lower indices $1, 3, 15, 255, \ldots$ meet the Mersenne-prime index set at 3. In particular, $T_7 = 28$ remains the next even perfect number and is not discarded; it simply does not lie on the repeated-square ladder. No part of PP176 changes an analytic, Löwner, source, zero-density, or RH grade.

128. Scope of the Pell fourth-power intersection

Theorem TDP-C supplies the exact arithmetic companion to the square-index ladder. Its square-difference identity is not merely a list of examples: (TDP.C2) is a complete Pell classification, with forward recurrence (TDP.C3) and a strict descent proof. The extra fourth-power lock is not a scan. Its exact factored equation is

$$t(t-3)(t^2+3t+1) = 0$$

so $(T_2, T_4) = (3, 10)$ is the unique nontrivial nonnegative intersection. PP176A is an elementary side rail and changes no analytic grade.

162. Two Pell orbits and the dyadic restriction

The finite-dyadic terminal of (139.4) gives $(s_6, n_6, x_6) = (32, 31, 992)$. Its arithmetic companion is

$$2T_{31} = 992 = T_{44} + 2 \qquad T_{31} = 496 \qquad T_{44} = 990 \tag{162.1}$$

The value $496 = 2^4 \cdot 31$ belongs to the even-perfect-number family because $31 = 2^5 - 1$ is prime. This is separate from the repeated-square subfamily of Theorem TDP-B.

For $m \geq 0, n \geq 1$, the complete companion problem is

$$2T_n = T_m + 2 \iff X^2 - 2Y^2 = -17 \qquad X = 2m+1, \quad Y = 2n+1 \tag{162.2}$$

Theorem 162.1 — two complete Pell orbits. All solutions of (162.2) form exactly two forward families, with seeds $(m,n) = (0,1)$ and $(4,3)$, under

$$m' = 3m + 4n + 3, \qquad n' = 2m + 3n + 2$$

For strictly positive m, omit only $(0,1)$.

The first members are

family	first four pairs (m,n)
first	$(0,1), (7,5), (44,31), (259,183)$
second	$(4,3), (27,19), (160,113), (935,661)$

Proof. Multiplication of $X + Y\sqrt{2}$ by $3 + 2\sqrt{2}$ gives the displayed recurrence and preserves the norm. Conversely, every positive solution has odd X, Y by reduction modulo 2 and 4. For $Y \geq 9$, the norm equation implies $4/3 < X/Y < \sqrt{2}$ and $X > Y$. The inverse transformation

$$(X,Y) \mapsto (3X - 4Y,\ 3Y - 2X) \tag{162.3}$$

therefore keeps both coordinates positive and decreases Y. Descent terminates at odd $Y \leq 7$. Checking $Y = 1,3,5,7$ leaves exactly $(X,Y) = (1,3)$ and $(9,7)$, proving completeness. □

The dyadic intersection is an additional restriction:

$$Y = 2^N - 1 \qquad X^2 = 2^{2N+1} - 2^{N+2} - 15 \tag{162.4}$$

The exact hits $N = 2,3,6$ give $m = 0,4,44$ respectively. The first uses $T_0 = 0$. A finite scan reported in the PP230 directive found no others through $N = 100$; that scan is not a completeness proof. Modulo 5 excludes $N \equiv 0 \pmod 4$, and modulo 7 excludes $N \equiv 1 \pmod 3$. Thus

$$N \bmod 12 \in \{2,3,5,6,9,11\} \tag{162.5}$$

is necessary, not sufficient. An additional modulus 9 test sharpens it. With $u = 2^N$, the right side of (162.4) is $2u^2 - 4u - 15$. For $N = 0,1,\ldots,5 \pmod 6$, its residues modulo 9 are $1,3,1,0,1,6$ respectively. Since squares modulo 9 are $0,1,4,7$, the classes $N \equiv 1,5 \pmod 6$ are excluded. Thus

$$\boxed{N \bmod 12 \in \{2,3,6,9\}} \tag{162.5a}$$

This remains only a necessary condition. Global completeness of the dyadic intersection is open in the present work.

Two scalar relations have exact family explanations. For any offset c,

$$2T_n = T_m + c \iff (2m+1)^2 - 2(2n+1)^2 = -(8c+1) \tag{162.6}$$

Thus the number 17 is generated by offset 2; this does not independently select the modulus $1009 = 992 + 17$. Also, with $x = 2T_n$,

$$2j_n^2 = 8x + 2 \qquad 2(j_n+1)^2 - 2j_n^2 = 4j_n + 2 \tag{162.7}$$

For the dyadic terminal, $j_n = 2^N - 1$ and $2(j_n+1)^2 = 2^{2N+1}$. At $N = 6$ these endpoints are 7938 and 8192. This is a centered-coordinate boundary identity. It adds no sign theorem to the source obstruction (139.3).

The $\sqrt{2}$ norm -17 family is distinct from the $\sqrt{3}$ norm 6 family in Theorem TDP-C. The complete arithmetic classification is retained as a sidecar; no transport from it to the all-node Gamma/prime inequality has been proved.

The completed derivative array determines signed Bernstein rows, their exact Laguerre energy, and a limiting measure under a variation bound. The proofs below establish the ordinary growth rate and identify the remaining fixed-scale source estimate. That estimate remains open.

Technical chapter II. The fractional grid, reciprocal moments, and decimal coordinates

Native addresses retain their gcd and denominator. Reciprocal sums give exact measures and scale laws; spacing experiments are assessed separately.

7. Native Triangular-Fractional Grid

The native cell and cumulative address are

$$a(n,k) = n - 1 + \frac{k}{n}, \qquad 1 \le k \le n$$

$$\rho(n,k) = T_{n-1} + k$$

Chamber n contains exactly n cells, and the number of cells through chamber N is T_N. Reduction of k/n is not allowed to erase the ambient denominator: if X/n reduces to p/q, then

$$q = \frac{n}{\gcd(X,n)}$$

and the gcd is part of the unreduced record.

The native center is

$$c_n = n - \frac{1}{2}$$

With

$$\eta = k - \frac{n}{2}, \qquad j = 2\eta = 2k - n$$

one has

$$\boxed{j \equiv n \pmod 2}$$

Adjacent chambers therefore populate complementary parity sheets. Even chambers contain the midpoint; odd chambers have the two nearest cells

$$c_n \pm \frac{1}{2n}$$

The parity rule matches the indexing grammar of the two-channel finite-Weil construction. It does not by itself prove an operator intertwiner, equal channel mass, or positivity.

8. The centered rational collar

The centered displacement of a native cell inside its unit chamber is

$$c_{n,k} = \left|\frac{k}{n} - \frac{1}{2}\right| = \frac{|2k-n|}{2n}$$

Define

$$\mathcal{C}_\triangle = \left\{\frac{|2k-n|}{2n} : n \geq 2,\ 1 \leq k \leq n,\ 0 < |2k-n| < n\right\}$$

Proposition 8.1 - Exact rational coverage

$$\boxed{\mathcal{C}_\triangle = \mathbb{Q} \cap (0, 1/2)}$$

Proof. Every displayed cell displacement is rational and lies in the required interval. Conversely, let $c = r/s$ with $0 < r/s < 1/2$. Set

$$n = 2s, \qquad k = s + 2r$$

Then $1 \leq k \leq n$ and

$$\frac{|2k-n|}{2n} = \frac{4r}{4s} = \frac{r}{s} \qquad \square$$

This exact coverage becomes load-bearing in the rational RH witness theorem of Part V.

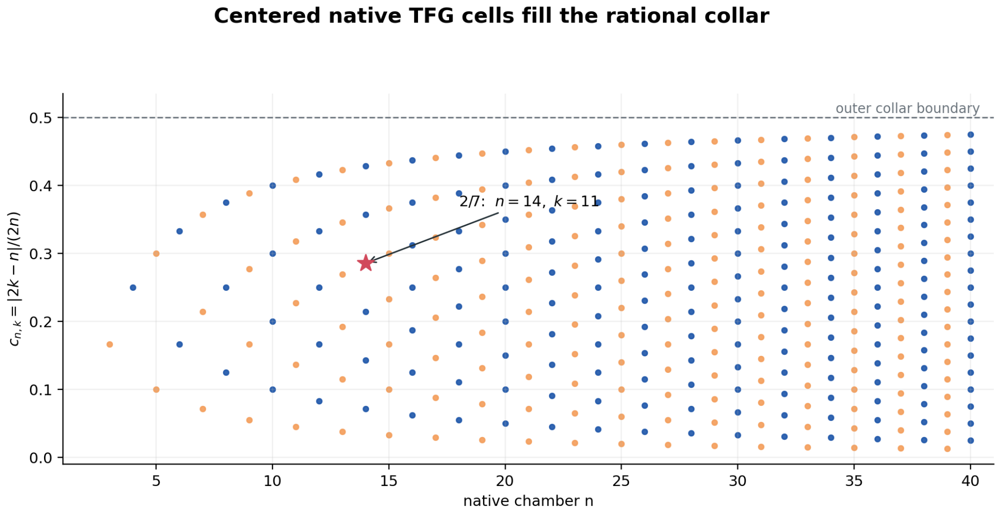

Figure 5: Centered native cells through chamber 40 in the rational collar.

9. Cyclic orders and denominator moments

Let $q_{n,k}$ be the reduced denominator of $a(n,k)$. Then

$$\boxed{q_{n,k} = \frac{n}{\gcd(k,n)} = \mathrm{ord}_{\mathbb{Z}/n\mathbb{Z}}([k])}$$

For $j \geq 0$, define

$$M_j(n) = \sum_{d|n} d^j \varphi(d)$$

The chamber/cyclic-order identity is

$$\boxed{M_j(n) = \sum_{k=1}^{n} q_{n,k}^j = \sum_{g \in \mathbb{Z}/n\mathbb{Z}} \mathrm{ord}(g)^j}$$

The functions M_j are multiplicative and, for prime powers,

$$M_j(p^a) = 1 + (p-1)p^j \frac{p^{(j+1)a} - 1}{p^{j+1} - 1}$$

Their Dirichlet series is

$$\boxed{F_j(s) = \sum_{n \geq 1} \frac{M_j(n)}{n^s} = \zeta(s)\frac{\zeta(s-j-1)}{\zeta(s-j)} \qquad \Re s > j+2}$$

$s = \sigma + it$

For $j \geq 1$, a nontrivial zero ρ of ζ appears as an inherited pole at $s = j + \rho$. This is an exact pole transport, not a restriction on ρ.

Triangularizing a reduced cell A/b gives

$$\mathrm{den}(T_{A/b}) = \begin{cases} b^2, & b \text{ odd} \\ 2b^2, & b \text{ even} \end{cases}$$

The local factor at 2 is essential. Its resulting even-moment rail selects ambient dimensions $d = 4m + 1$.

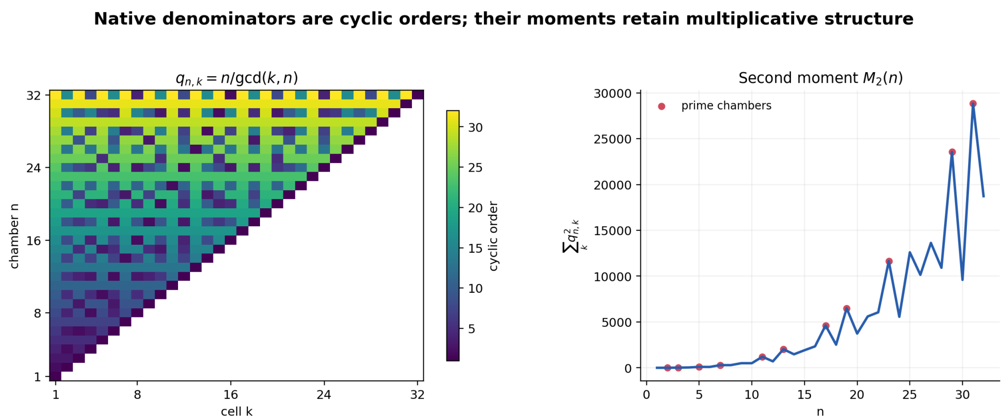

Figure 6: Cyclic orders across native chambers and their second denominator moment.

84. Reduced-denominator rays, the prime sieve, and the trace law

The one-based chamber distinguishes two exact partitions: reduced-denominator rays and prime-divisibility layers. For native cell (n, k),

$$q_{n,k} = \frac{n}{\mathrm{gcd}(n, k)} \tag{84.1}$$

is the reduced denominator of k/n, and $q_{dn,dk} = q_{n,k}$. Every cell factors transversely as

$$(n, k) = m(q, a), \qquad m = \mathrm{gcd}(n, k), \qquad \mathrm{gcd}(q, a) = 1 \tag{84.2}$$

The non-coprime cells form the prime-layer sieve

$$\{(n, k) : \mathrm{gcd}(n, k) > 1\} = \bigcup_{p \text{ prime}} \{(n, k) : p \mid n,\ p \mid k\} \tag{84.3}$$

At $N = 32$ the exact counts are 204 non-coprime cells, 176 in the $p = 2, 3$ sieve, and 28 structured higher-prime residuals. At $N = 64$ the corresponding counts are 820, 704, and 116.

The magenta family in the audit is the distinct constant ray $q_{2m,m} = 2$.

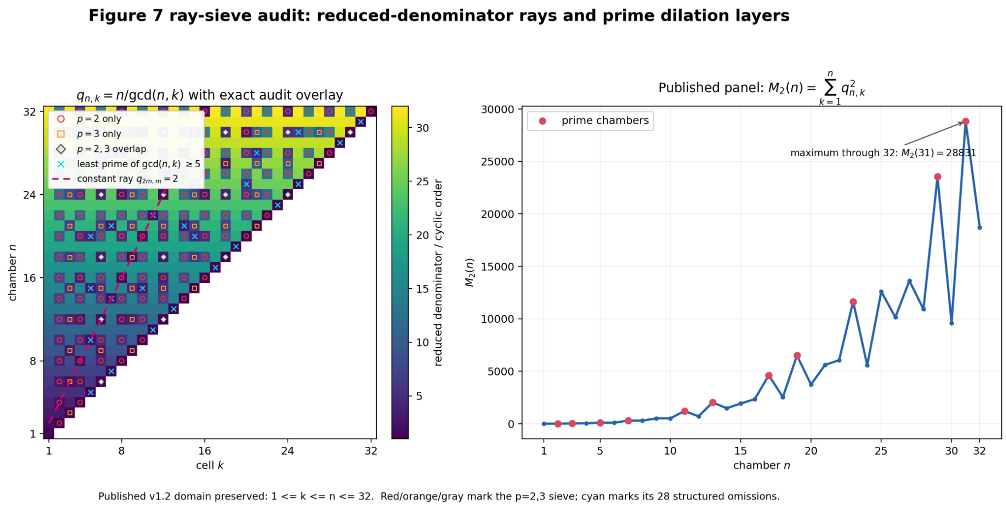

Figure 7: One-based $N = 32$ chamber: red/gray marks the $p = 2, 3$ divisibility sieve within the drawn region; magenta marks the reduced-denominator $q = 2$ ray.

For reduced a/q, the triangular fold has exact denominator

$$\mathrm{den}\left(\frac{a(a+q)}{2q^2}\right) = \eta(q)q^2 \qquad \eta(q) = \begin{cases} 1, & q \text{ odd} \\ 2, & q \text{ even} \end{cases} \tag{84.4}$$

Thus $Q_{m+1} = \eta(Q_m)Q_m^2$. If q is odd, $Q_m = q^{2^m}$; if $q = 2^e u$ with u odd and $e \geq 1$, then

$$Q_m = 2^{2^m(e+1)-1} u^{2^m} \tag{84.5}$$

The separate one-based $N = 64$ sidecar has maximum $2 \cdot 64^2 = 8192$.

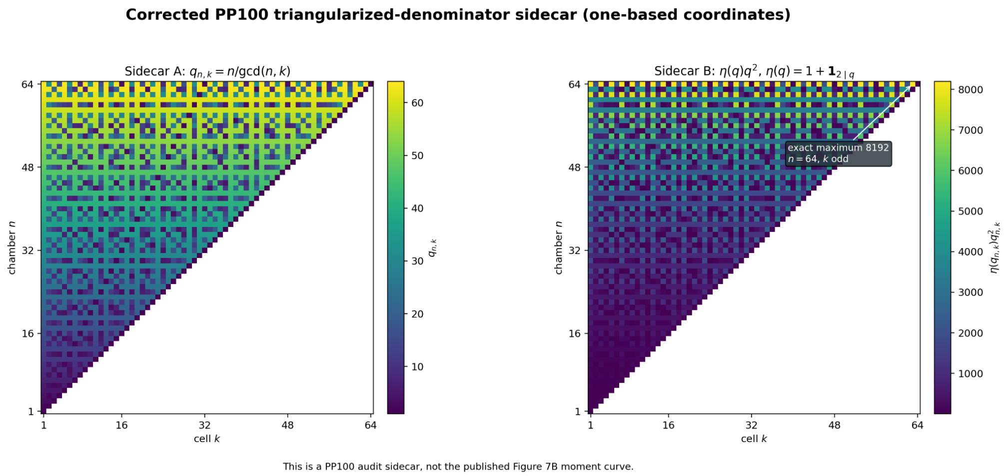

Figure 8: The one-based $N = 64$ triangularized-denominator chamber has maximum $2 \cdot 64^2 = 8192$.

The row identity

$$\sum_{k=1}^{n} F(q_{n,k}) = \sum_{d|n} \varphi(d)F(d) \tag{84.6}$$

has a finite Vandermonde–Hankel owner and a rational Padé generating model. These are exact arithmetic statements. The map from this finite arithmetic owner into the Löwner matrix (53.4), the moment–Casimir operator, or the source kernel remains open.

94. Reciprocal-triangular telescope and the forced dyadic ladder

Write

$$\mathsf{T}_n = \frac{n(n+1)}{2}$$

Then

$$\boxed{\frac{1}{\mathsf{T}_n} = 2\left(\frac{1}{n} - \frac{1}{n+1}\right) \qquad \sum_{n=a}^{\infty} \frac{1}{\mathsf{T}_n} = \frac{2}{a}} \tag{94.1}$$

More strongly, for every $a \geq 1$ and $j \geq 0$,

$$\boxed{\sum_{n=a2^j}^{a2^{j+1}-1} \frac{1}{\mathsf{T}_n} = \frac{1}{a2^j}} \tag{94.2}$$

Thus consecutive dyadic blocks of the reciprocal-triangular series are exactly the terms of the reciprocal powers-of-two series. If block endpoints b_j are required to have mass $1/b_j$, the telescope forces $b_{j+1} = 2b_j$. Doubling is also the unique dilation for which the removed block and surviving tail have equal mass. Its endpoint pair $(2m, m)$ is exactly the singleton $q = 2$ ray.

The ordinary generating function is

$$\sum_{n\geq 1} \frac{z^n}{\mathsf{T}_n} = 2\left[1 + \frac{1-z}{z}\log(1-z)\right] \qquad |z| < 1 \tag{94.3}$$

95. Centered c-geometry, spectral product, and the rational π collar

The centered identity

$$\boxed{8\mathsf{T}_n + 1 = (2n+1)^2} \tag{95.1}$$

gives

$$\mathsf{T}_n - c = \frac{1}{2}\left[\left(n + \frac{1}{2}\right)^2 - \left(\frac{1}{4} + 2c\right)\right] \tag{95.2}$$

At $c = 1/8$ the centered roots are $\pm 1/\sqrt{2}$. At $c = 1/2$ the factors are the golden reciprocal pair

$$n(n+1) - 1 = (n - \phi^{-1})(n + \phi) \tag{95.3}$$

The genus-zero triangular product is

$$\boxed{\mathcal{E}(c) = \prod_{n\geq 1}\left(1 - \frac{c}{\mathsf{T}_n}\right) = -\frac{\cos\left(\frac{\pi}{2}\sqrt{1+8c}\right)}{2\pi c}} \tag{95.4}$$

with the value at zero filled by continuity. Its logarithmic derivative is meromorphic away from $c = \mathsf{T}_n$ and generates every reciprocal-power sum.

Tying c to the sidecar value $a(q) = \eta(q)q^2$ gives $a(2) = 8$, $c_2 = 1/8$, and the first resolvent term $1/(8\mathsf{T}_1 - 1) = 1/7$.

The visible 1/8–1/7 trap is the proved rational collar

$$\boxed{\frac{1}{8} < \pi - 3 < \frac{1}{7}} \quad \Longleftrightarrow \quad \frac{25}{8} < \pi < \frac{22}{7} \tag{95.5}$$

It yields

$$\boxed{8-\frac{1}{7}<11-\pi<8-\frac{1}{8}<8<8+\frac{1}{8}<\pi+5<8+\frac{1}{7}} \tag{95.6}$$

Here $56/7 = 8$ with $56 = 2\mathsf{T}_7$, while $64/8 = 8$ with $64 = 8^2$. The same upper bound is $7\pi/8 < 11/4 = 2.75$. These are scalar rational inequalities, not zeta-zero constraints.

95A. Catalan normalization, Beta products, and the odd sine slice

Let $C_m = \binom{2m}{m}/(m+1)$ for $m \ge 0$. These are integers because $C_m = \binom{2m}{m} - \binom{2m}{m+1}$. Since $T_{2m+1} = (2m+1)(m+1)$, cancellation gives the all-index identity

$$\boxed{(2m+1)! = T_{2m+1}(m!)^2 C_m, \qquad \frac{T_{2m+1}}{(2m+1)!} = \frac{1}{(m!)^2 C_m}.} \tag{95A.1}$$

In particular $180 = (3!)^2 C_3$. The first denominators are $1, 1, 8, 180, 8064, 604800, 68428800$. Every odd index belongs to this slice. The successor-prime numerator transition $p \to 1$ belongs specifically to indices $p-1 \to p$ for an odd prime p; it is not a property of every odd index. At $8 \to 9$ both reduced numerators are 1.

Put $D = z\,d/dz$. Since $D(z^n) = nz^n$, triangular coefficient weighting is $T_D = D(D+1)/2$. Termwise differentiation of the entire sine series gives

$$\boxed{\sum_{m\ge 0} \frac{(-1)^m z^{2m+1}}{(m!)^2 C_m} = T_D \sin z = z\cos z - \frac{z^2}{2}\sin z.} \tag{95A.2}$$

This coefficient operator is different from the interval operator in Section 12A. Neither operation supplies a completed-source sign.

Proposition 95A.1 (a specified product of moment measures). With the Beta filter $b_m = 4^m (m!)^2/(2m+1)!$ of Section 104A,

$$\boxed{b_m \frac{C_m}{4^m} = \frac{1}{T_{2m+1}}.} \tag{95A.3}$$

The product of independent variables with densities $2\pi^{-1}\sqrt{(1-u)/u}$ and $1/(2\sqrt{1-v})$ on $(0,1)$ has density $(t^{-1/2}-1)dt$ on $(0,1)$.

Proof. On $0 < y < 4$ define the probability measures

$$d\eta(y) = \frac{dy}{\pi\sqrt{y(4-y)}}, \qquad d\nu_C(y) = \frac{4-y}{2}\, d\eta(y), \qquad d\omega(y) = \frac{y}{2}\, d\eta(y). \tag{95A.4}$$

The substitution $y = 4\sin^2(\theta/2)$ gives $d\eta = d\theta/\pi$. Even-sine integration yields $\int y^j \, d\eta = \binom{2j}{j}$, and hence

$$\int y^j \, d\nu_C = \frac{1}{2}\left[4\binom{2j}{j} - \binom{2j+2}{j+1}\right] = C_j.$$

The reflected-polynomial orthogonality measure is ω, not ν_C; they are interchanged by $y \mapsto 4 - y$. Scaling $y = 4u$ gives the first claimed density and moments $C_m/4^m$. The second variable has moments b_m. Independence and (95A.1) give (95A.3). Finally

$$\int_0^1 t^m (t^{-1/2} - 1) dt = \frac{2}{2m+1} - \frac{1}{m+1} = \frac{1}{T_{2m+1}}. \tag{95A.5}$$

Equality of all polynomial integrals determines finite measures on a compact interval, proving the product law. Equivalently the last density is the pushforward of $2(1-v)dv$ under $t = v^2$. □

These are identities between specified comparison measures. They do not identify any of them with the folded-zero functional or reverse a failed finite-matrix Beta implication. Section 155C uses ν_C in a positive comparison whose arithmetic defect is kept separately.

96. The reciprocal-triangular Hausdorff benchmark

The telescope normalizes the probability measure

$$d\nu_{\triangle}(t) = \frac{1}{2}\sum_{n\geq 1} \frac{1}{\mathsf{T}_n}\, \delta_{1/\mathsf{T}_n}(dt) \tag{96.1}$$

Its moments $m_k = \frac{1}{2}\sum_n \mathsf{T}_n^{-(k+1)}$ form a Hausdorff moment sequence, and every finite Hankel matrix $H_N^{\triangle} = [m_{i+j}]_{i,j=0}^{N-1}$ is strictly positive definite. Cauchy–Binet gives

$$\boxed{\det H_N^{\triangle} = 2^{-N} \sum_{n_1<\cdots<n_N} \frac{\prod_{r<s}(\mathsf{T}_{n_s} - \mathsf{T}_{n_r})^2}{\prod_r \mathsf{T}_{n_r}^{2N-1}} > 0} \tag{96.2}$$

For comparison define the synthetic moment matrix

$$G_N^{(a)}(0) = \sum_\nu a_\nu^{-1} v_N(a_\nu^{-1}) v_N(a_\nu^{-1})^{\mathsf{T}}, \qquad v_N(t) = (1, t, \ldots, t^{N-1})^{\mathsf{T}}$$

where the sums converge. At $a_\nu = \mathsf{T}_\nu$,

$$H_N^{\triangle} = \frac{1}{2} G_N^{(a_\nu = \mathsf{T}_\nu)}(0) \tag{96.3}$$

The determinant factor is therefore 2^{-N} and the net atom exponent is exactly $2N-1$. Same Gram grammar does not identify the synthetic atoms with the actual folded parameters

$q_\rho = \rho(1-\rho)$. Off RH those parameters may be nonreal, so the actual folded atomic functional is not known to be a positive real measure. The first missing line is an RH-free positive kernel or uniform Gram domination transporting $2\nu_\triangle$ to that functional.

More generally, for distinct positive a_ν with $\sum_\nu a_\nu^{-1} < \infty$, extend the synthetic matrix to $x \geq 0$ by

$$\begin{aligned} G_N^{(a)}(x) &= \left[\sum_\nu \frac{a_\nu}{(x+a_\nu)^{i+j+2}}\right]_{i,j=0}^{N-1}, \\ \det G_N^{(a)}(x) &= \sum_{\nu_1<\cdots<\nu_N} \frac{\prod_r a_{\nu_r} \prod_{r<s}(a_{\nu_s}-a_{\nu_r})^2}{\prod_r (x+a_{\nu_r})^{2N}} \end{aligned} \tag{96.4}$$

Finite Cauchy–Binet gives the identity, and entry convergence together with the increasing nonnegative determinant sums gives the infinite limit. There is strict positivity whenever at least N distinct atoms occur. At $x = 0$ the exponent reduces to $2N-1$, recovering (96.2)–(96.3). The positive-real-atom hypothesis is essential for this comparison.

96A. Euler's constant, the reciprocal-triangular zeta series, and a simplex ladder

Reader §R4A states these results, and this section proves them. Throughout, $T_k = k(k+1)/2$, $H_n = \sum_{k\leq n} 1/k$, $\psi = \Gamma'/\Gamma$, and γ_{E} is Euler's constant. Every statement is **PROVED**. Their substance is classical [95–109, 112]. The replay `qa/audit_gamma_bridge.py` checks every display, and its receipt is `qa/GAMMA_BRIDGE.json`.

96A.1 The mirror lemma and Ramanujan's coefficients

Lemma 96A.1 (mirror parity). Put $u = n + \frac{1}{2}$. As $n \to \infty$,

$$\psi(n+1) - \tfrac{1}{2}\log\bigl(n(n+1)\bigr) \sim \sum_{m\geq 1} \frac{c_m}{u^{2m}}, \qquad c_m = \frac{(1-2^{1-2m})B_{2m} + 2^{-2m}}{2m}. \tag{96A.1}$$

The formal expansion is invariant under $n \mapsto -1-n$, equivalently under $u \mapsto -u$, and it is a power series in $1/T_n$.

Proof. Differentiating the generalized Stirling series [2, §5.11] gives, for fixed h, $\psi(z+h) \sim \log z - \sum_{k\geq 1}(-1)^k B_k(h)/(kz^k)$. Take $z = u$ and $h = \frac{1}{2}$, so that $z + h = n + 1$. Since $B_k(1-x) = (-1)^k B_k(x)$, every odd-order $B_k(\frac{1}{2})$ vanishes, and $B_{2m}(\frac{1}{2}) = -(1-2^{1-2m})B_{2m}$ [2, §24.4]. Hence $\psi(n+1) \sim \log u + \sum_{m\geq 1}(1-2^{1-2m})B_{2m}/(2m\,u^{2m})$. Also $n(n+1) = u^2 - \frac{1}{4}$, so $\frac{1}{2}\log(n(n+1)) = \log u - \sum_{m\geq 1}(2m)^{-1}(4u^2)^{-m}$. Subtracting the two expansions gives (96A.1). Both sides are even in u, and $u^2 = 2T_n + \frac{1}{4}$. $\square$

The uncentered subtraction $\psi(n+1) - \log n$ keeps the odd term $1/(2n)$. The centered subtractions $\log(n+\frac{1}{2})$ [100, 120] and $\frac{1}{2}\log(n(n+1))$ are both even in u, and that is why both converge faster.

Corollary 96A.2 (Ramanujan's expansion). Since $\psi(n+1) = H_n - \gamma_{\mathrm{E}}$, (96A.1) together with $u^{-2} = (2T_n)^{-1}\bigl(1+(8T_n)^{-1}\bigr)^{-1}$ gives

$$H_n \sim \gamma_{\mathrm{E}} + \tfrac{1}{2}\log(2T_n) + \sum_{k\geq 1} \frac{\varrho_k}{T_n^k}, \tag{96A.1a}$$

with the coefficients

k	1	2	3	4	5
ϱ_k	$\frac{1}{12}$	$-\frac{1}{120}$	$\frac{1}{630}$	$-\frac{1}{1680}$	$\frac{1}{2310}$
k	6	7	8	9	10
ϱ_k	$-\frac{191}{360360}$	$\frac{29}{30030}$	$-\frac{2833}{1166880}$	$\frac{140051}{17459442}$	$-\frac{6525613}{193993800}$

These agree with the values in the literature [97, 99, 119]. Matching (96A.1a) against the $1/n$ expansion is an overdetermined linear system, with twenty equations for ten unknowns; it is consistent precisely because of the parity in Lemma 96A.1. At $n = 5$, 10 and 40, truncation after ϱ_6 leaves an error smaller than $|\varrho_7|\, T_n^{-7}$. The coincidences $\varrho_1 = -\zeta(-1)$ and $\varrho_2 = -\zeta(-3)$ do not continue: $\varrho_3 = \frac{1}{630}$, while $-\zeta(-5) = \frac{1}{252}$. $\square$

96A.2 The reciprocal-triangular zeta series

Theorem 96A.3.

$$\sum_{k\geq 2} \frac{\zeta(k)}{T_k} = \log(2\pi) - \gamma_{\mathrm{E}} = 1.26066140150781262295\ldots \tag{96A.2}$$

First proof (Raabe). For $|w| < 1$, $\log\Gamma(1-w) = \gamma_{\mathrm{E}} w + \sum_{k\geq 2}\zeta(k)w^k/k$ [2, §5.7]. For $0 < w < 1$ every term is positive, so monotone convergence allows termwise integration over $[0,1]$. The left side is integrable at $w = 1$, since $\log\Gamma(1-w) \sim -\log(1-w)$. Use $\int_0^1 w^k/k\, dw = 1/(k(k+1)) = 1/(2T_k)$ and Raabe's integral $\int_0^1 \log\Gamma(v)\, dv = \frac{1}{2}\log(2\pi)$ [95]. They give $\frac{1}{2}\log(2\pi) = \frac{1}{2}\gamma_{\mathrm{E}} + \frac{1}{2}\sum_{k\geq 2}\zeta(k)/T_k$. $\square$

Second proof (moment form). By (4.5), $1/T_k = \int_0^1 u^{k-1}\, 2(1-u)\, du$, and $\sum_{k\geq 2}\zeta(k)u^{k-1} = -\gamma_{\mathrm{E}} - \psi(1-u)$ for $0 \leq u < 1$. All terms are nonnegative, and $2(1-u)\psi(1-u)$ stays bounded as $u \to 1$. So the sum equals $-\gamma_{\mathrm{E}} - 2\int_0^1 v\,\psi(v)\, dv$. Integrating by parts against Raabe's integral gives $\int_0^1 v\psi(v)\, dv = -\frac{1}{2}\log(2\pi)$. $\square$

Third proof (triangular telescope and Stirling). Evaluate (94.3) at $z = 1/m$ and remove the $n = 1$ term. For $m \geq 2$ this gives

$$\sum_{k\geq 2} \frac{m^{-k}}{T_k} = 2 - \frac{1}{m} + 2(m-1)\log\Bigl(1 - \frac{1}{m}\Bigr), \tag{96A.2a}$$

and at $m = 1$ the value is 1, by Mengoli's telescope [91]. Sum over $m = 1, \dots, M$ and write $a_m = m \log m$. The logarithmic terms then telescope to $2(\log M! - M \log M)$. For the truncated zeta function $\zeta_M(k) = \sum_{m \le M} m^{-k}$ this gives

$$\boxed{\sum_{k \ge 2} \frac{\zeta_M(k)}{T_k} = 2M - H_M - 2 \log \frac{M^M}{M!}.} \tag{96A.3}$$

By Stirling's formula [94], $2 \log M! - 2M \log M = -2M + \log(2\pi M) + O(1/M)$. The right side of (96A.3) is therefore $\log(2\pi) - (H_M - \log M) + O(1/M)$, which tends to $\log(2\pi) - \gamma_{\mathrm{E}}$; the error is $-\frac{1}{3M} + \frac{1}{12M^2} + O(M^{-3})$. □

Corollary 96A.4 (unit-interval masses and the norm). For $m \ge 1$,

$$\sum_{k \ge 2} \frac{m^{-k}}{T_k} = \int_{m-1}^{m} \Big(\frac{\{x\}}{x} \Big)^2 dx, \tag{96A.4}$$

and

$$\log(2\pi) - \gamma_{\mathrm{E}} = \int_0^\infty \Big(\frac{\{x\}}{x} \Big)^2 dx = \int_0^\infty \{1/y\}^2 \, dy = \frac{1}{2\pi} \int_{-\infty}^{\infty} \frac{|\zeta(\frac12 + it)|^2}{\frac14 + t^2} \, dt. \tag{96A.5}$$

Proof. On $[m-1, m]$ we have $\{x\} = x - (m-1)$, and

$$\int_{m-1}^{m} \Big(1 - \frac{m-1}{x} \Big)^2 dx = 1 - 2(m-1) \log \frac{m}{m-1} + \frac{m-1}{m},$$

which equals (96A.2a). For $m = 1$ both sides equal 1. Summing over m and using Theorem 96A.3 gives the first equality in (96A.5), and the substitution $y = 1/x$ gives the second. For $0 < \sigma < 1$, $\zeta(s)/s = -\int_0^\infty \{1/y\} \, y^{s-1} \, dy$ (from [3, (2.1.5)] after $x = 1/y$), and $\{1/y\} \in L^2(0, \infty)$. The Mellin–Plancherel theorem [117] on $\sigma = \frac12$ then gives the last equality, because $|s|^2 = \frac14 + t^2$ there. □

The same constant is the squared Hardy norm (155G.6). Under $z = 1 - 1/s$, the unit circle maps onto $\sigma = \frac12$ with $|dz| = dt/(\frac14 + t^2)$, and $|\mathcal{B}(z)| = |\zeta(s)|$ on it. So $\sum_n (b_n^{\mathrm{den}})^2$ is exactly the last integral in (96A.5). The fractional-part function in (96A.5) is the one in the Nyman–Beurling closure problem [106–109]. A numerical evaluation of the critical-line integral, up to $|t| = 200$ plus the second-moment tail, agrees with $\log(2\pi) - \gamma_{\mathrm{E}}$ to 10^{-4}. That check is a sanity check, not a certificate; the proof above is the certificate.

96A.3 The simplex ladder

Theorem 96A.5. For $d \ge 2$,

$$\sum_{k \ge 2} \frac{\zeta(k)}{\binom{k+d-1}{d}} = d(d-1) \int_0^1 u^{d-2} \log \Gamma(u) \, du - \gamma_{\mathrm{E}}, \tag{96A.6}$$

and, for $m \geq 1$, with $(m)_{j-1} = m(m-1)\cdots(m-j+2)$,

$$\int_0^1 u^m \log\Gamma(u)\,du = \frac{\log(2\pi)}{2(m+1)} - \sum_{j=1}^{m} \frac{(m)_{j-1}(-1)^j}{j!}\Big[\zeta'(-j) + H_j\,\zeta(-j)\Big]. \qquad (96\text{A}.7)$$

Proof. The Beta integral gives $1/\binom{k+d-1}{d} = d\,B(k,d) = d\int_0^1 u^{k-1}(1-u)^{d-1}\,du$. As in the second proof of Theorem 96A.3, and since $d\int_0^1 (1-u)^{d-1}du = 1$, the sum equals $-\gamma_{\mathrm{E}} - d\int_0^1 v^{d-1}\psi(v)\,dv$. Integration by parts gives $\int_0^1 v^{d-1}\psi(v)\,dv = -(d-1)\int_0^1 v^{d-2}\log\Gamma(v)\,dv$; the boundary terms vanish for $d \geq 2$. This proves (96A.6).

For (96A.7), start from Lerch's formula $\log\Gamma(u) = \zeta'(0,u) + \frac{1}{2}\log(2\pi)$ [2, §25.11]. Apply $\partial_u\zeta(s-1,u) = -(s-1)\zeta(s,u)$ repeatedly, integrating by parts each time, and continue analytically. This gives the Hurwitz moments $\int_0^1 u^m\zeta(s,u)\,du = -\sum_{j=1}^{m}(m)_{j-1}\,\zeta(s-j)/\prod_{i=1}^{j}(s-i)$. Differentiating at $s=0$ gives (96A.7); compare [104]. □

Corollary 96A.6 (first rungs). With $\log A = \frac{1}{12} - \zeta'(-1)$ [105] and $\zeta'(-2) = -\zeta(3)/(4\pi^2)$,

$$\begin{aligned} d = 2:&\quad \log(2\pi) - \gamma_{\mathrm{E}},\\ d = 3:&\quad \tfrac{3}{2}\log(2\pi) - 6\log A - \gamma_{\mathrm{E}},\\ d = 4:&\quad 2\log(2\pi) - 12\log A + \frac{3\zeta(3)}{\pi^2} - \gamma_{\mathrm{E}}. \end{aligned} \qquad (96\text{A}.8)$$

Written in the constants $\log(2\pi)$, γ_{E} and $\zeta'(-j)$, every rung has γ_{E}-coefficient -1, which comes only from the term isolated in the proof of (96A.6), and $\log(2\pi)$-coefficient $d/2$, from (96A.7). Rung d introduces $\zeta'(2-d)$. At even arguments, differentiating the functional equation [2, §25.4] at the trivial zero $-2j$ gives $\zeta'(-2j) = (-1)^j(2j)!\,\zeta(2j+1)/(2(2\pi)^{2j})$, so odd zeta values enter exactly there. The replay evaluates $d = 2, \ldots, 9$ in three independent ways (the series, quadrature of the moment, and (96A.7)), and they agree to 35 digits. With every $\zeta(k)$ replaced by 1, the left side of (96A.6) becomes the reciprocal simplex telescope of §76, which sums to $d/(d-1)$ from $k=1$. □

96A.4 Where Euler's constant meets the zeros

Corollary 96A.7. $\lambda_1 = \sum_{[\rho]} m_\rho/q_\rho = 1 + \frac{1}{2}\gamma_{\mathrm{E}} - \frac{1}{2}\log(4\pi)$, and

$$\sum_{k\geq 2}\frac{\zeta(k)}{T_k} + 2\lambda_1 = 2 - \log 2 = \sum_{k\geq 1}\frac{1}{T_k} - \log 2. \qquad (96\text{A}.9)$$

Proof. Davenport's constant $B = -\frac{1}{2}\gamma_{\mathrm{E}} - 1 + \frac{1}{2}\log(4\pi)$ in the Hadamard product of ξ satisfies $B = -\sum_\rho \Re\rho^{-1}$ [110, 112, Ch. 12]. The orbit pairing of (9.7) gives $\sum_{[\rho]} m_\rho/q_\rho = \sum_\rho \rho^{-1}$; equivalently, $\lambda_1 = -\xi'(0)/\xi(0) = \xi'(1)/\xi(1)$. Add twice this to (96A.2). □

The replay confirms $\xi'(1)/\xi(1) = \lambda_1$ to fifteen digits. It also recovers λ_1 to within 10^{-5} from the first hundred zeros and the smooth Riemann–von Mangoldt tail [111]. (96A.9) is the triangular zero-sum formula for γ_{E}, written in the folded coordinate. It is an identity, not a positivity statement.

96A.5 Recomputed enclosures for §R12

These enclosures are computed in ball arithmetic: the zeta-zero routine returns rigorous enclosures of the first two zeros, and every other input is an exact constant. Every value below is CERTIFIED.

quantity	enclosure
λ_1	$0.0230957089661210338143102479065 \pm 4.8 \times 10^{-33}$
$q_1 = \frac{1}{4} + \gamma_1^2$	$200.0404548323868594633651859 61 \pm 4.1 \times 10^{-28}$
$q_2 = \frac{1}{4} + \gamma_2^2$	$442.1761505740824903204606887 68 \pm 2.1 \times 10^{-28}$
q_1/q_2	$0.45239991929160355477 \pm 2.7 \times 10^{-21}$
$C_0 = q_2(\lambda_1 - 1/q_1)$	$8.0019380461602012294410 97 \pm 9.7 \times 10^{-26}$

The verified height $H = 3{,}000{,}175{,}332{,}800$ of §R13 enters through (12.7a), which gives $C_0 \le C \le C_0 + q_2\lambda_1/(2H^2)$. Hence $C = 8.00193804616020122944\ldots$, and $C(q_1/q_2)^3 = 0.7409053672828\ldots < 1$. These recomputed enclosures replace the carried decimals of §R12.

An independent mpmath evaluation agrees with q_1 and q_2 to twelve decimals. These enclosures were recomputed by the v5.0 build; the receipt is `qa/GAMMA_BRIDGE.json` and is bundled.

97. Dyadic Gram amplification and the triangular exponent law

Use $v_N(t) = (1, t, \ldots, t^{N-1})^{\mathsf{T}}$. For a dyadic block beginning at m, set

$$C_{m,N} = \sum_{n=m}^{2m-1} \frac{1}{2\mathsf{T}_n} v_N(1/\mathsf{T}_n) v_N(1/\mathsf{T}_n)^{\mathsf{T}} \tag{97.1}$$

Its rank is $\min(m, N)$, and it is positive definite exactly when $m \ge N$. After the exact congruence with $D_m = \operatorname{diag}(1, m^2, \ldots, m^{2(N-1)})$,

$$C_{m,N} = \frac{1}{2m} D_m^{-1} G_{m,N} D_m^{-1} \tag{97.2}$$

Therefore

$$\boxed{\det C_{m,N} = 2^{-N} m^{-\mathsf{T}_{2N-1}} \det G_{m,N} \qquad \mathsf{T}_{2N-1} = N(2N-1)} \tag{97.3}$$

The ordered block eigenvalues have the exact scale ladder

$$\boxed{\lambda_{r+1}(C_{m,N}) = \Theta_N(m^{-(4r+1)}) \qquad r = 0, \ldots, N-1, \qquad m \ge 2N} \tag{97.4}$$

The exponents $1, 5, 9, \ldots, 4N-3$ sum to $N(2N-1) = \mathsf{T}_{2N-1}$. In particular, rank four has determinant exponent $\mathsf{T}_7 = 28$; under one asymptotic doubling its block determinant ratio tends to 2^{-28}.

Define the normalized full tail

$$R_{m,N} = mD_m \left[\sum_{n \geq m} \frac{1}{2\mathsf{T}_n} v_N(1/\mathsf{T}_n) v_N(1/\mathsf{T}_n)^{\mathsf{T}} \right] D_m$$

Splitting that tail at $2m$ gives the exact renormalization

$$R_{m,N} = \frac{1}{2} G_{m,N} + \frac{1}{2} E R_{2m,N} E \qquad E = \operatorname{diag}(1, 4^{-1}, \dots, 4^{-(N-1)}) \tag{97.5}$$

The normalized cores converge at an explicit $O_N(m^{-2})$ rate to the compact Gram measure $dy/\sqrt{2y}$ on $[1/2, 2]$. This is the solved synthetic analogue of the moving normalized source core. PP132 package SHA-256: `6861f7a7e4d2d69541d953ead56a078c5f0790787696221a5f59cf720875add6`.

98. Decimal, cyclotomic, and divisor-ray exponents

If

$$\mathsf{T}_n = 2^{\alpha_n} 5^{\beta_n} m_n \qquad (m_n, 10) = 1$$

then the decimal preperiod of $1/\mathsf{T}_n$ is $\max(\alpha_n, \beta_n)$ and its period is $\operatorname{ord}_{m_n}(10)$ when $m_n > 1$; for $m_n = 1$ it terminates and the period is recorded as zero. The recurring remainders in the nonterminating case form a coset $r_n\langle 10 \rangle$ in the primitive m_n-ray labels, covering all labels exactly when $\operatorname{ord}_{m_n}(10) = \varphi(m_n)$.

For $n = 7$,

$$\frac{1}{28} = 0.03\overline{571428} \qquad (\text{prefix length}, \text{period length}) = (2, 6) \tag{98.1}$$

Independently,

$$\boxed{2\mathsf{T}_n + 1 = \Phi_3(n) \qquad \operatorname{ord}_{2\mathsf{T}_n+1}(n) = 3 \quad (n > 1)} \tag{98.2}$$

At $n = 7$, $57 = 111_7$ and $1 \mapsto 7 \mapsto 49 \mapsto 1 \pmod{57}$. This order-three base-seven cycle is distinct from $\operatorname{ord}_{57}(10) = 18$ and $\operatorname{ord}_7(10) = 6$. A universal 57-prefix digit rule is false; $n = 6$ already gives $2\mathsf{T}_6 + 1 = 43$ but $1/\mathsf{T}_6 = 0.\overline{047619}$.

There is nevertheless a complete radix exponent ladder. For every radix $b \geq 2$, integer $h \geq 1$, and prime ℓ, put $Q = \Phi_\ell(b^h)$. Then

$$\boxed{\operatorname{ord}_Q(b) = \ell h \qquad \frac{1}{Q} = 0.\overline{\underbrace{00\cdots0}_{(\ell-1)h}\underbrace{(b-1)\cdots(b-1)}_{h}}_{\,b}} \tag{98.3}$$

For $\ell = 3$, $Q = 2\mathsf{T}_{b^h} + 1$ and the exact exponent sequence is $3h$. The complementary identity

$$\Phi_3(n) = 2\mathsf{T}_n + 1 = \Phi_6(n+1)$$

gives orders 3 and 6 for the bases n and $n+1$ modulo the same number. At $n = 7$, the centered triad is $55, 56, 57$; modulo 57, the subgroups generated by 7, 8, and 10 have orders 3, 6, and 18, with $\langle 8\rangle \cap \langle 10\rangle = \langle 7\rangle$ and together the larger two generate all 36 primitive labels. These exact arithmetic orbits do not select the $q = 57$ determinant margin; the certificate geometry does.

The exact reciprocal-triangular divisor trace is

$$\sum_{k=1}^{n} \frac{1}{\mathsf{T}_{q_{n,k}}} = \sum_{d|n} \frac{2\varphi(d)}{d(d+1)} \tag{98.4}$$

An elementary base-100 seed illustrates this cyclic viewpoint: the coefficients $14, 28, 56, \ldots$ generate $1/7$ before carrying, and $1/T_7 = \frac{1}{4}(1/7)$ transports its periodic tail. The multiplicative order determines the period after the factors of the base are removed.

The arithmetic trace also explains the visible bands in the chamber below. For each reduced denominator q, the rays have slopes $k/n = a/q$ with $\gcd(a, q) = 1$. Each ray contains $\lfloor N/q\rfloor$ native cells, so

$$\boxed{C_N(q) = \varphi(q)\lfloor N/q\rfloor} \tag{98.5}$$

Here $C_N(q)$ counts cells in the whole q-family, including $q = 1$ on the boundary $k = n$. The low-denominator bands at $N = 256$ are:

q	Reduced ray slopes k/n	Colour value $\eta(q)q^2$	Family cells
1	1 (boundary diagonal)	1	256
2	$1/2$	8	128
3	$1/3, 2/3$	9	170
4	$1/4, 3/4$	32	128
5	$1/5, 2/5, 3/5, 4/5$	25	204
6	$1/6, 5/6$	72	84
7	$1/7, 2/7, \ldots, 6/7$	49	216
8	$1/8, 3/8, 5/8, 7/8$	128	128

The colour is constant along each listed ray. It is not monotone in q: the even denominator $q = 4$ has colour value 32, exceeding the value 25 at $q = 5$. Horizontal and vertical crosshatching additionally records the gcd/divisibility layers of (84.3); it is not a second collection of constant-q rays.

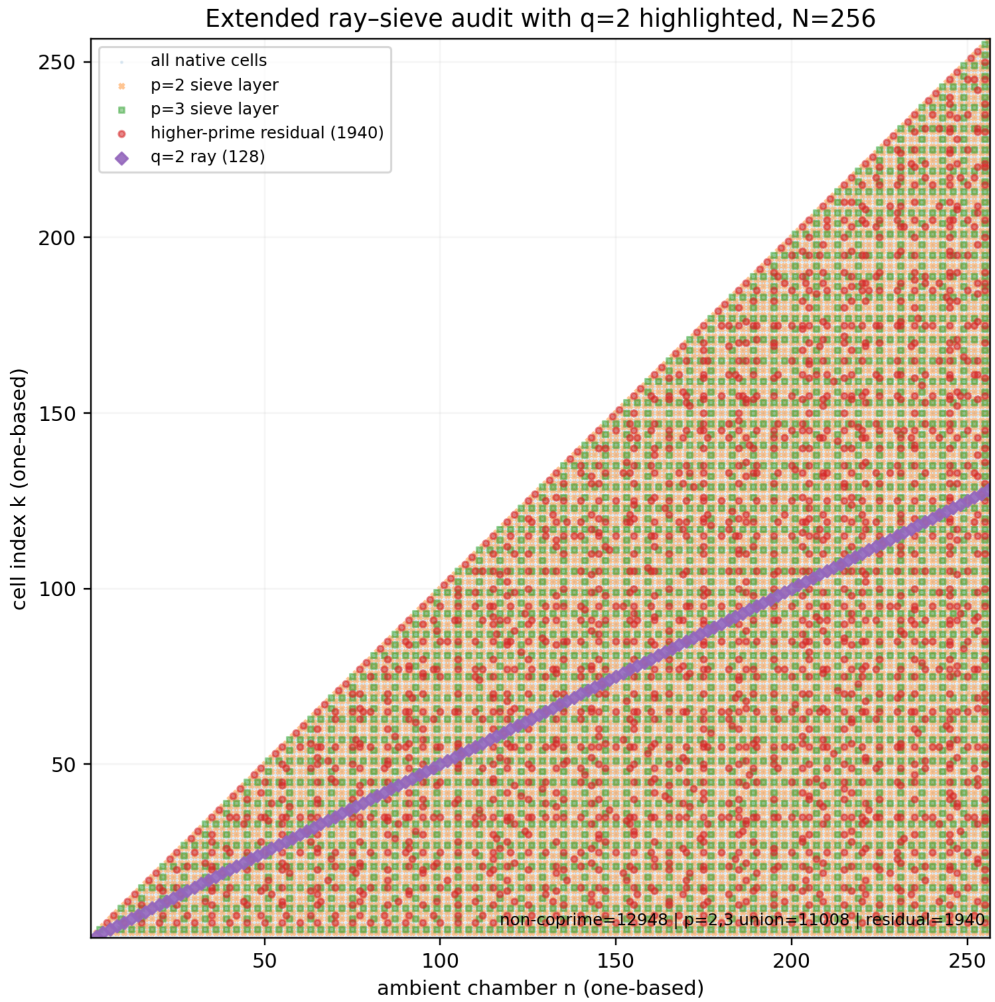

Figure 9: Extended one-based ray–sieve audit with the singleton $q = 2$ family highlighted.

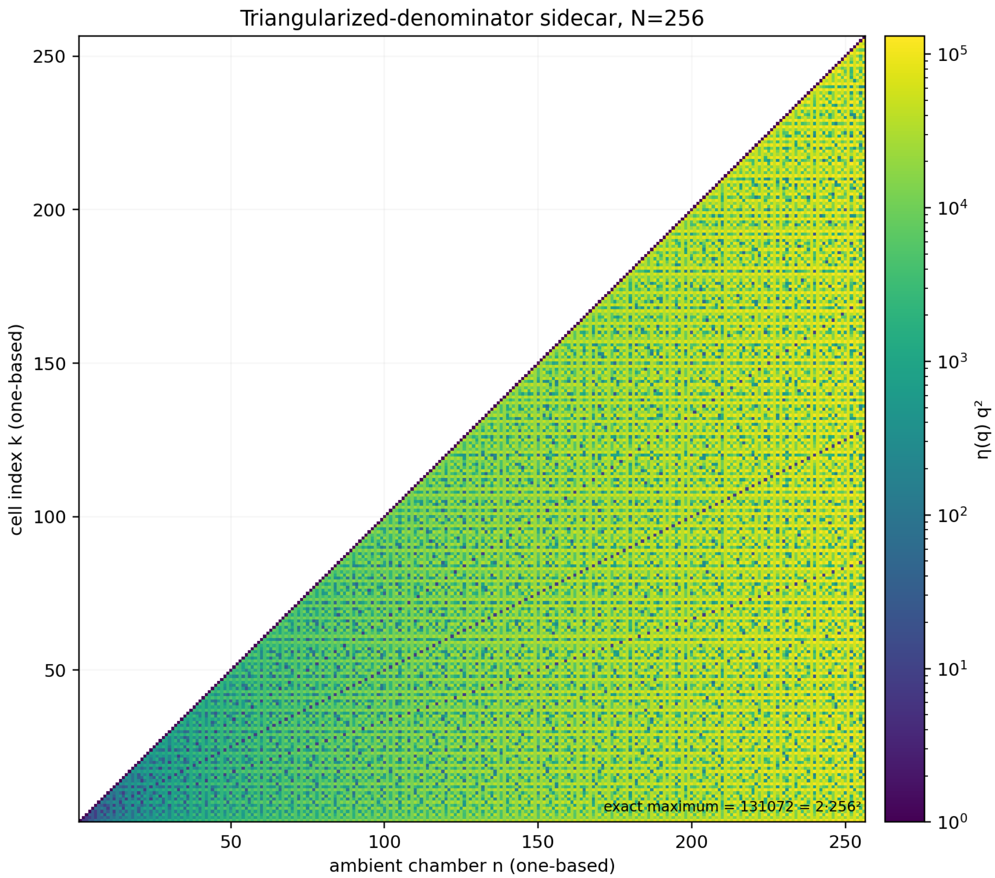

Figure 10: Triangularized-denominator chamber at $N = 256$, coloured by $\eta(q)q^2$. The boundary has $q = 1$; the interior includes the $q = 2, 3, 4, 5, 6, 7, 8$ ray families listed above and all higher reduced denominators. Divisibility crosshatching overlays the rational-slope structure. The exact maximum is $2 \cdot 256^2 = 131072$.

167. Denominator iteration, decimal periods, and useful approximations

Triangular values at rational arguments can be tested on exact reduced fractions. If $\gcd(a, q) = 1$, the reduced denominator of $T_{a/q}$ is

$$Q_1 = \eta(q)q^2, \qquad \eta(q) = \begin{cases} 1, & q \text{ odd} \\ 2, & q \text{ even} \end{cases} \tag{167.1}$$

Indeed both a and $a + q$ are coprime to q. For odd q their product is even and cancels the factor 2; for even q it is odd. Repeating the triangular map on the reduced value therefore gives

$$Q_0 = q, \qquad Q_{m+1} = \eta(Q_m)Q_m^2 \qquad Q_m = \begin{cases} q^{2^m}, & q \text{ odd} \\ (2q)^{2^m}/2, & q \text{ even} \end{cases} \tag{167.2}$$

This is an exact sequence, not a fit to digit patterns. It has the linear logarithmic reading

$$\log_{10} Q_m = \begin{cases} 2^m \log_{10} q, & q \text{ odd} \\ 2^m \log_{10}(2q) - \log_{10} 2, & q \text{ even} \end{cases} \tag{167.3}$$

For a reduced reciprocal with denominator $Q = 2^\alpha 5^\beta d$, $\gcd(d, 10) = 1$, the nonrepeating prefix has length $\max\{\alpha, \beta\}$. If $d > 1$ the period is $\mathrm{ord}_d(10)$; if $d = 1$ the expansion terminates and the period is recorded as zero. The following are exact integer results:

initial q	iteration m	Q_m	prefix length of $1/Q_m$	period
7	$0, 1, 2$	$7, 49, 2401$	$0, 0, 0$	$6, 42, 2058$
31	$0, 1, 2$	$31, 961, 923521$	$0, 0, 0$	$15, 465, 446865$
44	$0, 1, 2$	$44, 3872, 29984768$	$2, 5, 11$	$2, 22, 2662$

For these three rows the period laws are, respectively, $6 \cdot 7^{2^m-1}$, $15 \cdot 31^{2^m-1}$, and $2 \cdot 11^{2^m-1}$. One proof checks the initial orders $6, 15, 2$ and that p^2 does not divide $10^\ell - 1$ for $p = 7, 31, 11$ with the respective order ℓ. Binomial expansion then lifts the order by a factor of p at each higher prime power. For $q = 44$, the power of 2 is $3 \cdot 2^m - 1$, giving the printed prefix lengths. The initial orders and the non-Wieferich lifting checks are included in the exact arithmetic receipt of this Dossier.

Finite approximations can retain exact remainder information

The familiar $1/7$ block expansion and the reciprocal of T_{44} have particularly transparent tails. For $J \geq 1$, define

$$\begin{aligned} P_J &= \sum_{j=0}^{J-1} \frac{14 \cdot 2^j}{100^{j+1}} \qquad \frac{1}{7} - P_J = \frac{1}{7 \cdot 50^J} \\ Q_J^* &= \frac{1}{10} \sum_{j=1}^{J} 100^{-j} \quad \frac{1}{990} - Q_J^* = \frac{1}{990 \cdot 100^J} \end{aligned} \tag{167.4}$$

These are geometric-series identities. The logarithms of the relative errors are $-J \log_{10} 50$ and $-2J$. Thus a decimal approximation can be retained with an exact convergence rate, rather than discarded or mistaken for equality. In particular $1/990 = 0.0\overline{01}$. The symbol Q_J^* here is a partial sum, not the denominator sequence Q_m of (167.2).

The nearby empirical marker $11/4$ also has an exact triangular address:

$$\frac{11}{4} = \frac{T_4 + 1}{4}, \qquad T_{11/4} = \frac{165}{32}, \qquad \frac{1}{T_{11/4}} = \frac{32}{165} = \frac{192}{990} = 0.1\overline{93} \tag{167.5}$$

Thus $T_{44} = 192T_{11/4}$, and the denominator $32 = 2 \cdot 4^2$ agrees with (167.1). Its proximity to another marker has a precise error:

$$\frac{11}{4} - \frac{7\pi}{8} = \frac{22 - 7\pi}{8} = \frac{7}{8}\left(\frac{22}{7} - \pi\right) \approx 0.001106428109 \tag{167.6}$$

This identifies the classical rational approximation to π inside the marker comparison. Whether the marker predicts a gap statistic is the separate empirical question in §168.

168. Counting, unfolded gaps, and their triangular coordinate

The arithmetic identities above offer an exact change of coordinates for zero-spacing measurements. They do not remove the fluctuating term in zero counting. The smooth part of the Riemann–von Mangoldt count [2] is

$$N_0(t) = \frac{t}{2\pi}\left(\log\frac{t}{2\pi} - 1\right) + \frac{7}{8}, \qquad N_0'(t) = \frac{1}{2\pi}\log\frac{t}{2\pi} \tag{168.2}$$

This normalization already connects Gamma, π, and the logarithm. With the logarithm of Gamma chosen continuously from $t = 0$,

$$\begin{aligned} \vartheta(t) &= \Im \log\Gamma\left(\frac{1}{4} + \frac{it}{2}\right) - \frac{t}{2}\log\pi, \\ \vartheta(t) &= \frac{t}{2}\log\frac{t}{2\pi} - \frac{t}{2} - \frac{\pi}{8} + \frac{1}{48t} + O(t^{-3}), \qquad t \to +\infty \end{aligned} \tag{168.3}$$

Thus $1 + \vartheta(t)/\pi = N_0(t) + 1/(48\pi t) + O(t^{-3})$. The coefficient follows from the shifted Stirling expansion [2]: $B_2(1/4) = (1/4)^2 - 1/4 + 1/6 = -1/48$, and its imaginary contribution at $it/2$ is $-B_2(1/4)/t$. This is a quarter-argument Gamma coefficient, not a new estimate for the fluctuating zeta argument. The actual zero count $N(t)$ also contains the argument fluctuation of zeta. The counting formula is unconditional: counting ordinates does not determine the real parts of the zeros. Applying the polynomial T_x gives

$$\begin{aligned} \frac{d}{dt}T_{N_0(t)} &= \left(N_0(t) + \frac{1}{2}\right)N_0'(t), \\ T_{N(t)} - T_{N_0(t)} &= \left(N_0(t) + \frac{1}{2}\right)(N(t) - N_0(t)) + \frac{1}{2}(N(t) - N_0(t))^2 \end{aligned} \tag{168.4}$$

The second equality is exact. In particular the unknown counting fluctuation remains present after triangularization.

For consecutive ordinates above 2π, the usual smooth-unfolded gap $s_n = N_0(\gamma_{n+1}) - N_0(\gamma_n)$ has the exact reading

$$\boxed{s_n = \frac{2\left(T_{N_0(\gamma_{n+1})} - T_{N_0(\gamma_n)}\right)}{N_0(\gamma_{n+1}) + N_0(\gamma_n) + 1}} \tag{168.5}$$

This is the adjacent-product identity $2(T_b - T_a) = (b-a)(a+b+1)$. The denominator is positive in the stated range. It is a difference of cumulative triangular coordinates; it is not T_{s_n}. One may also chart the positive gaps themselves by $s \mapsto T_s$, which is strictly increasing. The two operations have different meanings and should not be interchanged.

What the older enrichment experiment can contribute

The report [62] describes a preceding-window enrichment statistic near small-gap valleys, with a broader follow-up scan from 2.30 to 3.20 and lower controls. Its reported enrichment shelf is approximately 2.70–2.81; $11/4 = 2.75$ lies inside it. The plotted ratios are observed to random-surrogate hit counts. They are not average normalized zero spacing, and the reported record does not establish 2.75 as a unique endpoint of the shelf.

The useful rational marker and the reported interval have exact triangular coordinates:

$$\begin{aligned} T_{11/4} &= \frac{165}{32}, \\ T_{[\,2.70,\,2.81\,]} &= \left[\frac{999}{200}, \frac{107061}{20000}\right], \\ T_{11/4\,\pm\,1/2000} &= \frac{165}{32} \pm \frac{13}{8000} + \frac{1}{8000000} \end{aligned} \tag{168.6}$$

The last line transports a symmetric original tolerance to its exact slightly asymmetric triangular image. In general $T_{s+h} - T_s = (s+1/2)h + h^2/2$. To preserve a finite experiment, transport all thresholds, windows, valley and merging rules, and support conditions through the chosen coordinate map. Transforming only the marker while leaving its window unchanged defines a different statistic.

Part E of this Dossier retains the historical tables and the earlier five-marker figure, and reproduces the broader report pages that supply their context. It also retains the modulus audit [61]. Those empirical outcomes do not alter the exact gcd, totient, or decimal identities in §§98 and 167. Their raw gap arrays and complete randomization replay are not available here, so no new significance level or confirmed shelf boundary is asserted.

For a further test, compare prespecified rational and π-based markers on the same block support, retain the full scan correction, and carry the entire statistic into the triangular chart. The existing arithmetic gives that transport exactly. It does not yet supply a new zero-location theorem.

46. Native TFG nonlinear operator route

The scalar recognizers above provide no distribution estimate. A proposed native operator should retain the unreduced grid and distinguish actual arithmetic from an arbitrary prime mask. The necessary proof obligations are:

1. pairwise or higher interaction, not a weighted scalar prime sum;
2. explicit dependence on ambient denominator and gcd multiplicity;
3. failure under a generic support-preserving prime mask;

4. a proved intertwiner to one of the master positivity objects M_ξ, Q_c, J_c, or $\mathcal{C}_c$;
5. a quantifier-complete forcing theorem.

The rational witness theorem gives the native TFG a rigorous indexing role. It does not yet give it an arithmetic forcing role.

169-172. Worked triangular arithmetic

The four sections that follow develop the reciprocal blocks, decimal carries, gcd reduction, the Pascal/TFG address and the polar shells in full. They are detail rather than argument: nothing in the Reading Volume's continuous argument depends on reading them first. Their identities return in §§9, 84, 98 and 167, in the Reading Volume at §R7 and §R17G, and in the source energy. Equation tags (4A.*), (NR.*), (RP.*) and (AR.*) are unchanged.

169. Reciprocal blocks, doubling, and decimal carries

The reciprocal law gives a particularly simple dyadic-index family:

$$\frac{1}{T_{2^j-1}} = \frac{2^{1-j}}{2^j-1} \quad (j \geq 1) \qquad \frac{1}{T_7} = \frac{1}{28} = \frac{1}{4}\frac{1}{7} \tag{4A.1}$$

For every integer $n \geq 1$, the triangular-to-factorial conversion is $1/n! = [(n+1)/(2(n-1)!)]/T_n$. At $n = 7$ this gives the exact bridge

$$\boxed{\frac{1}{7} \xrightarrow{\div 4} \frac{1}{T_7} = \frac{1}{28} \xrightarrow{\div 180} \frac{1}{7!} = \frac{1}{5040}, \qquad 2T_7 = 56} \tag{4A.1a}$$

The repeated blocks in these reciprocals have an exact algebraic source. Using base 100 to group decimal digits in pairs,

$$\boxed{\frac{1}{7} = \frac{14}{100-2} = \sum_{j\geq 0} \frac{14 \cdot 2^j}{100^{j+1}}} \tag{4A.2}$$

The raw coefficients begin $14, 28, 56, 112, 224, \ldots$. They are not yet base-100 digits: the later coefficients create carries. After removing the first two blocks, the remaining value, multiplied by 100^3, is $56/(1-2/100) = 57 + 1/7$. This explains the carried block 57 and closes the six-digit cycle exactly:

$$\frac{1}{7} = 0.\overline{142857}, \qquad \boxed{\frac{1}{T_7} = T_4^{-4}\left(357 + \frac{1}{7}\right) = 0.0357\overline{142857}, \quad T_4 = 10} \tag{4A.3}$$

The original $1/7$ continues as the tail through successive halvings. Each halving is exactly the midpoint of the preceding value and zero:

$$\boxed{\begin{array}{ll} \dfrac{1}{7} = 0.\overline{142857} & \dfrac{1}{14} = 0.07\overline{142857} \\ \dfrac{1}{T_7} = \dfrac{1}{28} = 0.0357\overline{142857} & \dfrac{1}{2T_7} = \dfrac{1}{56} = 0.017857\overline{142857} \end{array}} \tag{4A.3a}$$

The overbars in this display deliberately preserve the phase of the original six-digit block. There is an exact rule for every halving step:

$$\frac{1}{7 \cdot 2^r} = 100^{-r}\left(A_r + \frac{1}{7}\right), \qquad A_r = \frac{50^r - 1}{7}, \qquad A_{r+1} = 50A_r + 7 \quad r \geq 0 \tag{4A.3b}$$

Indeed $50 \equiv 1 \pmod 7$, so A_r is an integer and the fractional part of $100^r/(7 \cdot 2^r)$ is always $1/7$. The prefix integers $0, 7, 357, 17857, \ldots$ are placed in $2r$ decimal positions, with leading zeros included. Thus the repeated block is carried exactly; its unchanged placement and the minimum length of a nonrepeating prefix are two different readings of the same rational value.

The following table uses the shortest prefixes. For example $0.0357\overline{142857} = 0.03\overline{571428}$: moving the overbar rotates the repeating block without changing the number.

Rational value	Decimal expansion	Minimal prefix length	Period length
$1/7$	$0.\overline{142857}$	0	6
$1/14$	$0.0\overline{714285}$	1	6
$1/T_7 = 1/28$	$0.03\overline{571428}$	2	6
$1/(2T_7) = 1/56$	$0.017\overline{857142}$	3	6
$1/7! = 1/5040$	$0.0001\overline{984126}$	4	6
$7!/990 = 56/11$	$5.\overline{09}$	0	2

For a reduced denominator $q = 2^a 5^b d$ with $\gcd(d, 10) = 1$ and $d > 1$, the minimal prefix length is $\max(a, b)$ and the period length is $\operatorname{ord}_d(10)$. Here $5040 = 2^4 \cdot 5 \cdot 63$, with $\operatorname{ord}_{63}(10) = 6$, while $10 \equiv -1 \pmod{11}$ gives period two for $56/11$. At the factorial scale, $1/5040 = (1/720)(1/7)$ still retains the factor $1/7$, but the additional factor 9 in the reduced recurring denominator 63 changes the block to 984126. That block is not a cyclic rotation of 142857. The shared six-digit length has an order-theoretic explanation even though the repeating blocks differ. Dossier §98 extends this cyclic-order viewpoint; §76 connects the factorial and triangular scales while retaining their different integer conditions.

The positional base and the logarithmic coordinate also fit together exactly. This volume uses $\log = \ln$ unless a base is displayed; decimal plots use $\log_{10}$ when labelled. The conversion is

$$\boxed{v = \log_{10} n = \frac{\ln n}{\ln 10}, \qquad n^{-s} = e^{-s \ln n} = 10^{-sv}} \tag{4A.4}$$

Thus the source shift $u = \ln n$ becomes $u = (\ln 10)v$. In an integral, $du = (\ln 10)\,dv$; in a Fourier phase, $tu = (t \ln 10)v$. Decimal cycles depend on the chosen base through multiplicative order. The analytic identities remain the same after the coordinate, measure, and frequency are converted together.

In the displayed family, $\ln 28 = \ln 7 + 2\ln 2$, $\ln 56 = \ln 7 + 3\ln 2$, and $\ln 5040 = \ln 28 + \ln 180$. The same addition laws hold with $\log_{10}$. They express the reciprocal scalings in logarithmic coordinates; the digit periods are determined separately by the denominator orders above.

The same reciprocal scale also has an exact degree-to-radian rendering:

$$\boxed{\left(\frac{1}{T_7}\right)^\circ = \frac{\pi}{180T_7}\,\mathrm{rad} = \frac{\pi}{7!}\,\mathrm{rad} = \frac{\pi}{5040}\,\mathrm{rad}} \tag{4A.5}$$

Here the angle is assigned the degree measure $1/T_7 = 1/28$, and the conversion factor is $\pi/180$. Its radian measure divided by π is $1/7!$. Grouping π with the angle-conversion factor makes the triangular bridge explicit:

$$\underbrace{\frac{1}{7}\cdot\frac{1}{4}}_{1/T_7}\qquad\underbrace{\frac{\pi}{180}}_{\text{degree-to-radian factor}}\qquad = \frac{\pi}{180T_7} = \frac{\pi}{7!} \tag{4A.6}$$

If the angle is $\theta = (1/T_7)^\circ$, its radian measure is $\pi/5040$, while its fraction of a half-turn is $\theta/(180^\circ) = \theta/(\pi\,\mathrm{rad}) = 1/5040$. The π cancels in this normalized fraction, not in the radian measure itself or its decimal evaluation. A complex quarter-turn is multiplication by i; the displayed product changes an angle's scale and units.

170. A triangle inside a triangle: 990, 496, and reduced rays

The value 990 connects the reciprocal examples to an exact composition of triangular coordinates. Start with $T_2 = 3$, $T_4 = 10$, and $T_{10} = 55$:

$$\boxed{T_{44} = T_2^2 T_4(T_4+1) = 2T_2^2 T_{T_4} = 18T_{10} = 990} \tag{NR.1}$$

Thus the inner product is precisely the triangular product at T_4. Its coefficient is $T_2^2 = 9$; relative to the usual coefficient $1/2$, it multiplies the inner triangle by 18. This is a composition identity, not an inference from the appearance of decimal digits.

The general centered scaling law explains the neighboring perfect number:

$$\begin{aligned} T_{az+(a-1)/2} &= a^2 T_z + T_{(a-1)/2} \\ T_{31} &= T_{3\cdot 10+1} = 9T_{10} + 1 = 496 \\ 2T_{31} &= T_{44} + 2 = 992 \end{aligned} \tag{NR.2}$$

The first line is a polynomial identity for real or complex a, z; odd integer a preserves integer indices. Expanding either side, or using $8T_z + 1 = (2z+1)^2$, proves it. Another useful factorization is

$$T_{ab} = a^2 T_b - bT_{a-1}, \qquad T_{44} = 15T_{11} = T_5 T_{11} = 10^3 - 10 \tag{NR.3}$$

The divisors of $496 = 16 \cdot 31$ come in two finite rows:

power-of-two row	1	2	4	8	16
multiply by 31	31	62	124	248	496
distance to the next power of two	1	2	4	8	16

Indeed $31 \cdot 2^k = 2^{k+5} - 2^k$. Summing these divisors gives $(1+2+4+8+16)(1+31) = 31 \cdot 32 = 992 = 2 \cdot 496$, the classical even-perfect construction [45]. The extension 992 continues the doubling pattern but is not a divisor of 496.

For positive integers n, k, the greatest common divisor $d = \gcd(n, k)$ removes their shared scale: $(n, k) = d(q, a)$ with $\gcd(q, a) = 1$. Euler's totient $\varphi(q)$ counts $1 \leq a \leq q$ coprime to q (with $\varphi(1) = 1$). Thus it counts primitive rational directions at denominator q, while gcd tells how often a direction is repeated in larger triangular rows. The modulus comparison has an exact common scale:

$$\boxed{\varphi(496) = \varphi(990) = 240 = 2T_{15}, \qquad \varphi(992) = 480} \tag{NR.4}$$

This identifies equal counts of reduced residues; it does not identify their arrangements or their decimal periods. Section 162 gives the complete Pell family behind the offset 2, including the stricter modular filter. The tested interval 990 through 1009 remains a useful empirical search window. EVIDENCE Section 168 and Part E of the Dossier state exactly what the reported tests do and do not establish; no result in this volume rests on them.

The distinction is visible in base ten. For $496 = 2^4 \cdot 31$, removing the factors of 2 and 5 leaves 31: $1/496$ has a four-digit nonrepeating prefix and period $\mathrm{ord}_{31}(10) = 15$. For $990 = 2 \cdot 5 \cdot 99$, the remaining denominator is 99: $1/990 = 0.0\overline{01}$ has a one-digit prefix and period two. The same totient 240 therefore coexists with different decimal behavior. Section 167 gives the general valuation and multiplicative-order rule.

From gcd reduction to reciprocal triangular weights

For a native chamber address (n, k), let $d = \gcd(n, k)$, $q = n/d$, and $a = k/d$. The rational direction is a/q, and its denominator weight is

$$\boxed{\frac{1}{T_q} = 2\left(\frac{1}{q} - \frac{1}{q+1}\right) = \frac{2d^2}{n(n+d)}} \tag{NR.5}$$

Thus the gcd and the reciprocal telescope describe the same weight in two coordinates. Among all addresses $1 \leq k \leq n \leq N$, the number having reduced denominator q is

$$C_N(q) = \varphi(q) \left\lfloor \frac{N}{q} \right\rfloor \qquad T_N = \sum_{q \leq N} C_N(q) \tag{NR.6}$$

Consequently the complete weighted chamber sum is $\sum_{q \leq N} C_N(q)/T_q$. This is the bridge to the TFG denominator moments in the Technical Dossier. Here q is an integer denominator; the later $q(s) = s(1-s)$ is an analytic coordinate.

The distinction between a denominator weight and a folded rational value is visible side by side:

$$\frac{1}{T_q} = \frac{2}{q(q+1)}, \qquad T_{a/q} = \frac{a(a+q)}{2q^2}, \qquad \frac{1}{T_{a/q}} = \frac{2q^2}{a(a+q)} \tag{NR.7}$$

The last two formulas use the numerator as well. Section 167 follows their reduced denominators under iteration, with exact decimal periods and $\log_{10}$ scales. These are useful arithmetic coordinates even when a particular spacing experiment fails to detect a modulus effect.

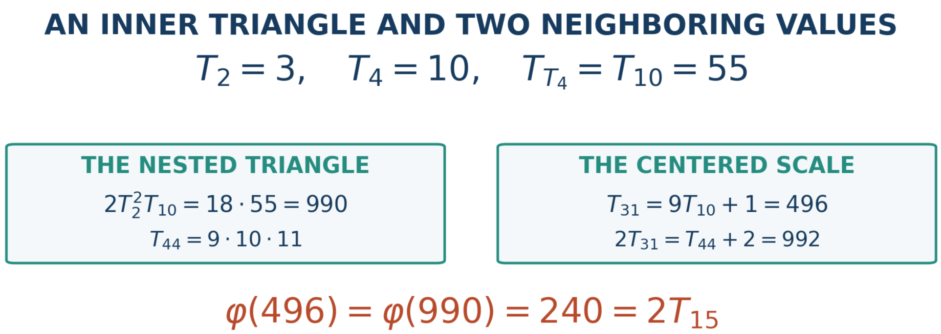

Figure 11: Nested triangular values organize 990 and 496 before either is used as a modulus. The shared totient is a separate exact comparison.

171. Reciprocal folding, Pascal coefficients, and the TFG address

Pascal's triangle already contains the triangular numbers: $\binom{n+1}{2} = T_n$. The row $1, 5, 10, 10, 5, 1$ contains the repeated $10 = T_4$ and pairs naturally when the two inputs are reciprocals. For $z \neq 0$, define

$$y = z + \frac{1}{z}, \qquad \mathcal{P}_m(y) := z^m + z^{-m} \tag{RP.1}$$

Exchanging z and $1/z$ leaves both y and $\mathcal{P}_m$ unchanged. The quadratic relation $z^2 - yz + 1 = 0$ gives a recurrence without a long binomial expansion:

$$\boxed{\mathcal{P}_0 = 2, \quad \mathcal{P}_1 = y, \quad \mathcal{P}_m = y\mathcal{P}_{m-1} - \mathcal{P}_{m-2} \quad (m \geq 2)} \tag{RP.2}$$

The first polynomials and their values at $y = 3$ are

m	reciprocal polynomial $\mathcal{P}_m(y)$	value at $y=3$
0	2	2
1	y	3
2	y^2-2	7
3	y^3-3y	18
4	y^4-4y^2+2	47
5	y^5-5y^3+5y	123

Pascal's fifth row groups exactly as

$$\left(z+\frac{1}{z}\right)^5 = \mathcal{P}_5(y)+5\mathcal{P}_3(y)+10\mathcal{P}_1(y) \tag{RP.3}$$

The unsigned coefficients $1, 5, 10, 10, 5, 1$ are the magnitudes of row 5 of the signed grid. Pairing reciprocal powers yields $1, 5, 10$ in (RP.3). The coefficients inside the reciprocal polynomials themselves have a neighboring-cell formula, for $m \geq 1$:

$$\mathcal{P}_m(y) = \sum_{j=0}^{\lfloor m/2 \rfloor} (c_{m-j,j} - c_{m-j-1,j-1})y^{m-2j}. \tag{RP.3a}$$

It follows by substituting the signed Pascal recurrence into (RP.2). For $m=5$, the coefficients are 1, $-4-1=-5$, and $3-(-2)=5$. The separate initial value $\mathcal{P}_0=2$ counts the two reciprocal powers; the coefficient-grid seed remains 1.

Thus $y=3$ gives $3^5=243=123+5\cdot 18+10\cdot 3$. The literal fifth power of the sum is 243; the recovered sum of fifth powers is 123. Distinguishing them is essential when using a binomial identity as a computational shortcut. The two input branches are $z=(3\pm\sqrt{5})/2$, and reciprocal inversion exchanges them.

This is the same quadratic recurrence mechanism as (4.4b). In general, if $A_m=\alpha^m+\beta^m$, then

$$A_m=(\alpha+\beta)A_{m-1}-\alpha\beta A_{m-2} \qquad A_0=2, \quad A_1=\alpha+\beta \tag{RP.4}$$

For adjacent reciprocals $1/n, 1/(n+1)$, its coefficients are $j_n/(2T_n)$ and $1/(2T_n)$. For $z, 1/z$, they are y and 1. The formulas therefore share an algebraic mechanism while keeping their different products visible.

For a positive reduced TFG value $z=a/q$, $\gcd(a,q)=1$,

$$y=\frac{a^2+q^2}{aq}, \qquad y^2-4=\frac{(a^2-q^2)^2}{a^2q^2} \tag{RP.5}$$

The first fraction is reduced: its numerator is coprime to both a and q. Its denominator is aq, and numerator–denominator exchange implements the reciprocal symmetry. This is an exact map of rational values; it does not assert equality of different TFG aggregate weights.

The analytic return appears in §R7. With $z_C = s/(1-s)$ and $q(s) = s(1-s)$, that section gives

$$y_C = z_C + \frac{1}{z_C} = \frac{1}{q(s)} - 2 \tag{RP.6}$$

Thus the same reciprocal coordinate is already present in the completed fold. Pascal grouping, triangular coefficients, and the recurrence keep the two inverse branches visible through a single invariant. On the unit circle inversion is conjugation; away from it those operations differ. The missing completed-source sign is still a further analytic condition.

This Pascal arithmetic returns in the source energy of §R17G. Its exact matrix has entries $\binom{r+s}{r} = (-1)^r c_{r+s,r}$ of the signed grid. At $r = 2$ these follow the same grid's column $j = 2$: $c_{s+2,2} = T_{s+1}$, giving $1, 3, 6, 10, \ldots$. Dossier §163A displays the matrix, proves its Gram factorization, and identifies the polynomial reflection behind the change of basis.

172. Cyclic sums, polar shells, and the $1/12$ marker

The first arithmetic bridge is built before any zero criterion. For a positive integer q, define the cyclic-order sum

$$\Psi_{\text{cyc}}(q) = \sum_{a=1}^{q} \frac{q}{\gcd(a,q)} = \sum_{d|q} d\varphi(d) \tag{AR.1}$$

The notation Ψ_{cyc} is deliberate: it is an arithmetic function of the integer q and is unrelated to the folded resolvent $S_\xi(x)$. Its Dirichlet series is

$$\boxed{F_{\text{cyc}}(s) = \sum_{q\ge 1} \frac{\Psi_{\text{cyc}}(q)}{q^s} = \frac{\zeta(s)\zeta(s-2)}{\zeta(s-1)} \qquad \Re s > 3} \tag{AR.2}$$

The pole at $s = 3$ has residue $\zeta(3)/\zeta(2)$. First-Riesz smoothing multiplies it by $1/[s(s+1)]$, hence

$$\boxed{D = \frac{1}{s(s+1)}\bigg|_{s=3} \frac{\zeta(3)}{\zeta(2)} = \frac{1}{12}\frac{\zeta(3)}{\zeta(2)} = \frac{1}{2T_3}\frac{\zeta(3)}{\zeta(2)}} \tag{AR.3}$$

This is the exact reason for the positive $1/12$ in the Riesz main term: $3 \cdot 4 = 2T_3 = 12$. The familiar continuation value

$$\zeta(-1) = -\frac{1}{12} = -\frac{1}{2T_3} \tag{AR.4}$$

has the opposite sign but a different owner. Triangular reflection sends $3 \mapsto -4$ and preserves $T_3 = T_{-4}$, so it preserves the positive kernel factor $1/12$; it does not create an automatic reflected coefficient $-D$.

The Polar Shell Renderer supplies a compatible picture, not the proof of (AR.2)–(AR.4). Its reduced shell points are

$$Z_{n,k} = \sqrt{n}\, e^{2\pi i k/n} \qquad (k,n) = 1 \tag{AR.5}$$

and division by the shell radius gives primitive roots of unity. The points k and $n-k$ are conjugates, so a real shell sum never comes from an unpaired complex phase. Combining the angular factor with the Mellin weight gives

$$U_{n,k}(s) = e^{2\pi i k/n} n^{1/2-s} \qquad S_n^{\text{shell}}(s) := \sum_{(k,n)=1} U_{n,k}(s) = \mu(n) n^{1/2-s} \tag{AR.6}$$

For squarefree $n > 1$,

$$\left| S_n^{\text{shell}}(s) \right| = n^{1/2-\sigma} = 1 \iff \sigma = \frac{1}{2} \tag{AR.7}$$

This is an exact critical-line detector, but no source identity here forces a zeta zero to make its value one. At $n = 12$, the reduced shell contains $\varphi(12) = 4$ primitive twelfth roots in two conjugate pairs and sums to $\mu(12) = 0$; it is a clean conjugate-pair example, not a modulus-one detector. The full cyclic/Riesz proof is in §§56–57, and the renderer construction is cited separately in [55].

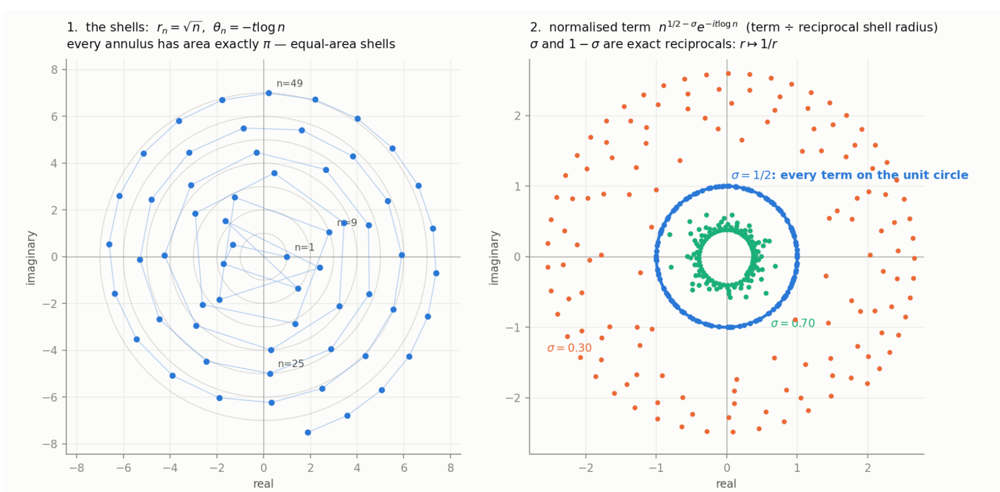

Figure 12: Equal-area polar shells and the $1/\sqrt{n}$ normalization. The angular laws differ, but every complex phase must retain its conjugate partner.

173. The grid's own finite arithmetic: tracks, reflections, collisions

These are properties of the signed coefficient grid itself, collected out of the reading line. They are exact and they are finite. None of them supplies an inequality, and none is used by any positivity argument in either document.

The columns are read as tracks: the edge carries 1, the next counts k, the third is $\binom{k}{2} = T_{k-1}$, and the fourth is $\binom{k}{3} = \sum_{r=1}^{k-2} T_r$ for $k \geq 3$. At $k = 6$ that fourth entry is $20 = 1 + 3 + 6 + 10$, beside the triangular $15 = T_5$. Reflection supplies the other half:

$$\binom{k}{k-j} = \binom{k}{j}, \qquad (-1)^{k-j}\binom{k}{k-j} = (-1)^k(-1)^j\binom{k}{j} \tag{SW.4c}$$

An even row has identical signed coefficients when reversed; an odd row has opposite signed coefficients. This is a reflection of coefficients. The attached terms also change: $x^j Z_{k+j} \mapsto x^{k-j} Z_{2k-j}$. They are not equal functions merely because their coefficient magnitudes agree. Complex conjugation is separately retained by the folded zero sum in (SW.2).

Interior triangular collisions. The third track is triangular by construction. To ask a different, finite question, exclude the edge and count tracks and retain one half of each reflected row. In the exact domain $1 \leq k \leq 20$, $3 \leq j \leq \lfloor k/2 \rfloor$, the complete list is

$$\begin{aligned} &\binom{10}{3} = T_{15}, \qquad \binom{10}{4} = T_{20}, \qquad \binom{14}{6} = T_{77}, \\ &\binom{15}{5} = T_{77}, \qquad \binom{17}{8} = T_{220}, \qquad \binom{19}{5} = T_{152} \end{aligned} \tag{SW.4e}$$

Reflection supplies the matching positions in the right halves. The test is exact: a positive integer v is triangular if and only if $8v + 1$ is an odd square. This finite census makes no classification claim outside the stated domain and does not include the automatic $j = 2$ track.

Row $k = 14$ gives

$$\boxed{\binom{14}{6} = \binom{14}{8} = 3003 = T_{77} = \binom{78}{2}} \tag{SW.4f}$$

The eight positions of 3003 in Pascal's triangle (compare Singmaster's problem [89]) are exactly $(14, 6)$, $(14, 8)$, $(15, 5)$, $(15, 10)$, $(78, 2)$, $(78, 76)$, $(3003, 1)$, and $(3003, 3002)$. To check exhaustiveness, reflect to $j \leq k/2$. For $j \geq 7$ the smallest entry is at least $\binom{14}{7} = 3432 > 3003$. For each $1 \leq j \leq 6$, $\binom{k}{j}$ increases strictly with $k \geq 2j$; checking the neighboring values leaves precisely the four left-half positions listed above. This is an arithmetic multiplicity statement. It gives no source inequality and no additional positivity for W_{14}.

The complete row at $k = 12$ is also explicit:

$$\begin{gathered} (1, -12, 66, -220, 495, -792, 924, \\ \qquad -792, 495, -220, 66, -12, 1), \\ \boxed{(-1)^9\binom{12}{9} = -220} \end{gathered} \tag{SW.4h}$$

The $k = 0$ seed and the reduced-rung boundary. The coefficient grid of the Reading Volume includes the valid coefficient row $[+1]$, as used by $F_{n,0}$ in (SW.3). The differential definition (R.3), the normalized resolvent row (SW.4b), and the criterion (R.4) all require $k \geq 1$. An antiderivative can be added by a separate convention. For a chosen $x_* > 0$, define

$$\mathcal{A}_0(x) := -\int_{x_*}^{x} S_\xi(t)\,dt, \qquad \mathcal{A}_0' = -S_\xi, \qquad -\mathcal{A}_0' - x\mathcal{A}_0'' = W_1 \tag{SW.4g}$$

This verifies the recurrence at the boundary for that convention. It does not extend the rung definition to a negative derivative order or assign a positivity condition to $\mathcal{A}_0$. Adding a constant changes the antiderivative but leaves its displayed recurrence unchanged. The coefficient -1 in this convention and the signed Pascal seed $[+1]$ at $k = 0$ belong to different expressions.

The formal resolvent $Z_0 = \sum_{[\rho]} m_\rho$ diverges, and $(2k-1)! = \Gamma(2k)$ is singular at $k = 0$. Continuing the isolated coefficient ratio gives $\Gamma(2k)/\Gamma(k) \to 1/2$; with a sign continuation tending to -1, that isolated coefficient tends to $-1/2$. It does not define a canonical antiderivative or a rung. Likewise $(-1)^j\binom{-1}{j} = 1$ defines an infinite power-series row, not another finite member of (SW.4b).

The normalization is itself an accumulated triangular product:

$$(2k-1)! = \prod_{r=1}^{k-1} 2T_{2r}, \qquad \frac{(2k+1)!}{(2k-1)!} = 2T_{2k}, \qquad \frac{11!}{9!} = 2T_{10} = 110 \tag{SW.4d}$$

The ratio is twice column $j = 2$ of row $2k+1$ in the same grid: $2T_{2k} = 2c_{2k+1,2}$. For $k = 5$, the entry $c_{11,2} = 55$ therefore gives $11!/9! = 110$.

This is the odd-factorial denominator of the sine series (PR.6), and the Bernstein location is $B_{11,5}(a) = a^5 W_6(a)/(5!6!)$ by (BR.3a).

Technical chapter III. Centered geometry and operator models

The centered product appears in Gamma products, Casimir spectra and finite geometry. Each operator model retains its own space and normalization.

10. Odd-dimensional moment-Casimir rail

Let

$$u(z) = \frac{z(z-1)}{2} \qquad u_d(s) = \frac{(s-1)(s-d+1)}{2}$$

For $j \geq 1$, the difference $u_d(s) - u(s-j)$ is independent of s if and only if

$$\boxed{d = 2j+1}$$

At that dimension,

$$\boxed{u_{2j+1}(s) = u(s-j) - T_{j-1}}$$

At an inherited pole $s = j + \rho$,

$$u_{2j+1}(j+\rho) + T_{j-1} = u(\rho)$$

The split-norm form is

$$\boxed{u_{2j+1}(j+\rho) = \frac{1}{2}\left[\left(\rho - \frac{1}{2}\right)^2 - \left(j - \frac{1}{2}\right)^2\right]}$$

The discrete spherical degree value has the parallel form

$$\lambda_n^{(2j+1)} = \frac{1}{2}\left[\left(n + j - \frac{1}{2}\right)^2 - \left(j - \frac{1}{2}\right)^2\right]$$

Both use the same fixed half-gap $j - 1/2$, but n and ρ live in different spaces. The result is a common coordinate rail, not an operator identification.

For every fixed $j \geq 1$,

$$\text{RH} \iff u_{2j+1}(j+\rho) \in \mathbb{R}_{<0} \quad \text{for every nontrivial zero } \rho$$

This is a coordinate equivalence: the imaginary part is $\gamma(\beta - 1/2)$.

11. Triangular canonical product

Define

$$\Pi_{\triangle}(u) = \prod_{n=1}^{\infty} \left(1 - \frac{u}{T_n}\right)$$

Since $\sum T_n^{-1} = 2$, the product converges locally uniformly. Under

$$u(s) = \frac{s(s-1)}{2}$$

the exact Gamma closure is

$$\boxed{\Pi_{\triangle}(u(s)) = \frac{1}{\Gamma(1+s)\Gamma(2-s)}}$$

At the fixed point $s = 1/2$,

$$u(1/2) = -\frac{1}{8} \qquad \boxed{\Pi_{\triangle}(-1/8) = \frac{4}{\pi}}$$

The factors $1/4$, $1/2$, or 2 that turn this identity into $1/\pi$ or $2/\pi$ are external normalizations and must be declared. Repeated scalar contacts do not identify mechanisms.

One of these contacts is not scalar, and the caution is withdrawn for it alone. The substitution $u = s(s-1)/2$ *is* the fold of §16: with $x = -2u = s(1-s) = q(s)$ and $\nu = \sqrt{x - \frac{1}{4}}$, Γ reflection turns the Gamma closure above into

$$\boxed{\prod_{n\geq 1}\left(1 + \frac{x}{2T_n}\right) = \frac{\sin \pi s}{\pi\, q(s)} = \frac{\cosh \pi\nu}{\pi x}, \qquad \sum_{n\geq 1} \frac{1}{x + 2T_n} = \frac{\pi \tanh \pi\nu}{2\nu} - \frac{1}{x}} \tag{11.1a}$$

the second being the logarithmic derivative of the first. So the fixed-point value is not a numerical coincidence: $u = -1/8$ is $x = q(1/2) = 1/4$, the foot of the critical line, and $\Pi_{\triangle} = 4/\pi$ is the value there. In this form the product is visibly entire of order $\frac{1}{2}$ in x with zeros exactly at $x = -2T_n$, $n \geq 1$; $x = 0$ has removable value one, not a zero. This model and the completed determinant have the same entire order, not the same type; Section 12B proves the difference. Here the model parameter is $x = q(s)$, whereas the completed source parameter is $s(s-1) = -q(s)$. Reader Section R6A keeps these two evaluations separate. The model nodes are real and positive. Section 12 supplies the spherical degree interpretation; Section 12A realizes exactly the multiplicity-one product by a Dirichlet–Neumann interval operator with its zero mode removed. No identification with the completed spectrum is proved.

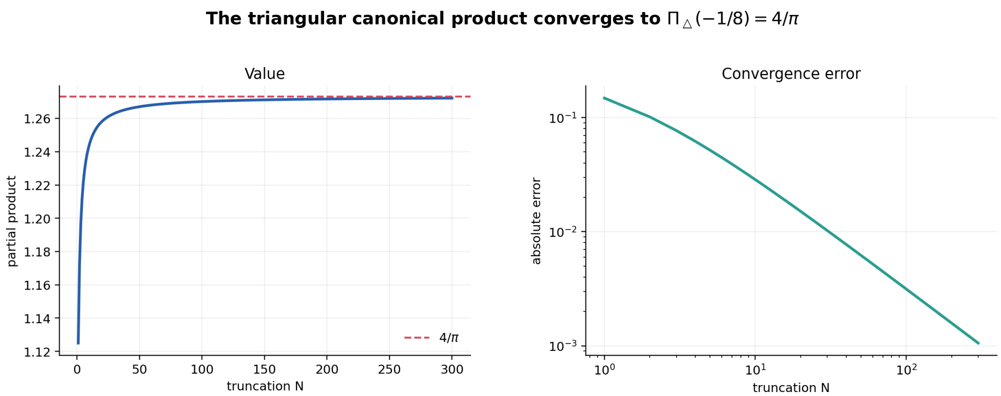

Figure 13: Convergence of the triangular canonical product at the fixed point.

12. Spherical Casimir and positive degree

For $d \geq 2$, set

$$\lambda_n^{(d)} = \frac{n(n+d-2)}{2}$$

Let Λ_d be the Dirichlet-to-Neumann operator of the unit ball. Harmonic extension sends a degree-n spherical harmonic to $r^n Y_n$, so

$$\Lambda_d Y_n = n Y_n$$

Therefore

$$\boxed{-\frac{1}{2}\Delta_{S^{d-1}} = \frac{1}{2}\Lambda_d(\Lambda_d + (d-2)I)}$$

Equivalently,

$$\Lambda_d = \sqrt{-\Delta_{S^{d-1}} + \frac{(d-2)^2}{4} I} - \frac{d-2}{2} I$$

This supplies a canonical positive branch of the reflection-completed degree line. The centered square is

$$\lambda_n^{(d)} + \frac{(d-2)^2}{8} = \frac{1}{2}\left(n + \frac{d-2}{2}\right)^2$$

The dimension-3 spectrum is exactly T_n. The same shifted degree is the Bessel order arising from radial separation.

The dimension-dependent determinant closes as

$$\Pi_d(u_d(z)) = \frac{\Gamma(d-1)}{\Gamma(z)\Gamma(d-z)} \qquad u_d(z) = \frac{(z-1)(z-d+1)}{2}$$

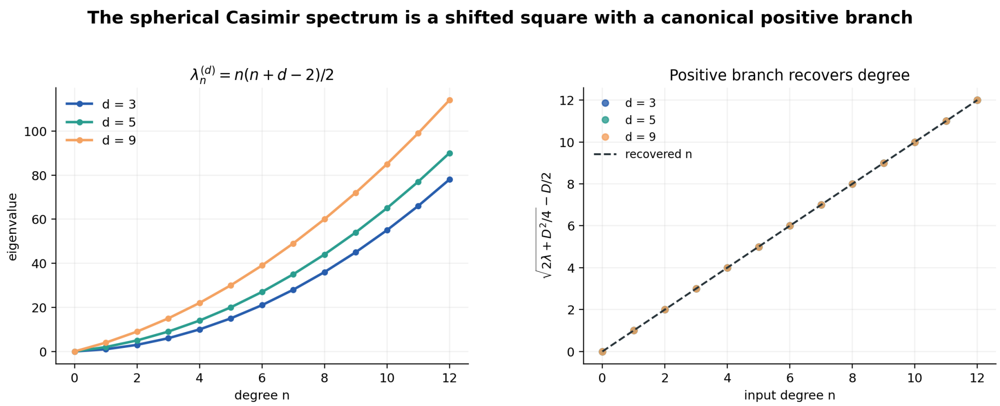

Figure 14: Casimir spectra and recovery of the canonical positive degree branch.

12A. The triangular sine operator and its finite projection

The multiplicity-one triangular product has an explicit interval realization. Use the reflected polynomials of Section 155A, $\mathcal{P}_0 = 1$, $\mathcal{P}_1 = 3 - y$ and $\mathcal{P}_{m+1} = (2-y)\mathcal{P}_m - \mathcal{P}_{m-1}$. Their triangular expansion and finite geometric sum give, with $n = 2m+1$,

$$\begin{aligned} \mathcal{P}_m(y) &= (2m+1)\sum_{j=0}^{m} \frac{(-2y)^j}{(2j+1)!}\prod_{r=0}^{j-1}(T_m - T_r), \\ \mathcal{P}_m(4\sin^2(\theta/2)) &= \sum_{h=-m}^{m} e^{ih\theta} = \frac{\sin(n\theta/2)}{\sin(\theta/2)}. \end{aligned} \tag{12A.1}$$

These are the fourth-kind Chebyshev polynomials in the normalization of [63, equation 18.5.4]. The quotient has its removable interpretations.

Proposition 12A.1 (triangular contraction and finite tent). Locally uniformly for complex z,

$$\boxed{\frac{\mathcal{P}_m(z^2/(2T_m))}{2m+1} \longrightarrow \frac{\sin z}{z}.} \tag{12A.2}$$

Here $m \geq 1$ in the approximants and the value at $z = 0$ is one. Indeed, the jth coefficient is $(-1)^j/(2j+1)!$ times $\prod_{r<j}(1 - T_r/T_m)$. Each retained factor lies in $[0, 1]$, the product tends to one for fixed j, and $R^{2j}/(2j+1)!$ is a summable majorant on $|z| \leq R$. This proves the uniform limit without extrapolating finite computations. Also, directly from (12A.1),

$$\frac{1}{n}\mathcal{P}_m\left(4\sin^2\frac{\pi u}{n}\right) = \frac{\operatorname{sinc}_\pi(u)}{\operatorname{sinc}_\pi(u/n)}, \qquad \operatorname{sinc}_\pi(u) = \frac{\sin \pi u}{\pi u}. \tag{12A.3}$$

For bounded real u the error from $\operatorname{sinc}_\pi(u)$ is $O(n^{-2})$. Squaring the real-angle sum gives the Fejer identity

$$\frac{\mathcal{P}_m(4\sin^2(\theta/2))^2}{n} = \sum_{h=-(n-1)}^{n-1}\left(1 - \frac{|h|}{n}\right)e^{ih\theta}. \tag{12A.4}$$

There are exactly $n - |h|$ pairs with difference h. Positive and negative lags each contribute T_{n-1} pairs; zero lag contributes n. Thus $n + 2T_{n-1} = n^2$ counts the whole square. For odd $n = 2m+1$ this is also $2T_{2m} + 2m + 1 = (2m+1)^2 = 8T_m + 1$. $\square$

The weighted sine identity of Section 95A is compatible with this limit: $g_m(z) = z\mathcal{P}_m(z^2/(2T_m))/(2m+1) \to \sin z$ locally uniformly, so analytic differentiation gives $T_D g_m \to T_D \sin z$. This relates two operations by a limit, not by equality of the finite polynomials.

Theorem 12A.2 (a specified positive comparison operator). On $L^2(0, \pi)$ let

$$A_\triangle = -\frac{d^2}{d\theta^2} - \frac{1}{4}, \qquad \mathcal{D}(A_\triangle) = \{f \in H^2(0,\pi) : f(0) = 0,\ f'(\pi) = 0\}. \tag{12A.5}$$

It is self-adjoint and nonnegative, with a complete orthonormal basis

$$\psi_m(\theta) = \sqrt{\frac{2}{\pi}}\sin((m + \tfrac{1}{2})\theta), \qquad A_\triangle\psi_m = 2T_m\psi_m \quad (m \geq 0). \tag{12A.6}$$

Proof. The separated Dirichlet–Neumann boundary conditions give the regular self-adjoint second-derivative operator. Direct differentiation produces $(m+1/2)^2 - 1/4 = m(m+1)$. Orthonormality is elementary sine integration. For completeness, reflect a function evenly about π into $(0, 2\pi)$; its Dirichlet sine expansion retains exactly the odd modes. The resulting complete spectral resolution also proves nonnegativity. With ω as in (95A.4), the map

$$(Uf)(\theta) = \sqrt{\frac{2}{\pi}}\sin(\theta/2)f(4\sin^2(\theta/2)) \tag{12A.7}$$

is unitary from $L^2(\omega)$ to $L^2(0,\pi)$ and sends $\mathcal{P}_m$ to ψ_m. Differentiation gives the polynomial equation $y(4-y)\mathcal{P}_m''+(6-2y)\mathcal{P}_m'+2T_m\mathcal{P}_m=0$. The unitary images, not the bare polynomials in θ, are the interval eigenfunctions. □

Remove the $m=0$ zero mode and call the restriction A_+. Since $\sum_{m\geq 1}[m(m+1)]^{-1}=1$, its inverse is positive trace class and

$$\boxed{\det(I+xA_+^{-1})=\prod_{m\geq 1}\left(1+\frac{x}{2T_m}\right)=\frac{\cosh(\pi\sqrt{x-1/4})}{\pi x}.} \tag{12A.8}$$

The last equality is Section 11, including the entire continuation and removable value one at zero. These factors have multiplicity one. The full spherical Laplacian has additional angular multiplicities and is not this determinant without a specified restriction.

Theorem 12A.3 (projection and sine-kernel limit). The rank-N orthogonal projection onto $\psi_0,\ldots,\psi_{N-1}$ has kernel

$$\boxed{\Pi_N(\theta,\phi)=\frac{1}{2\pi}\left[\frac{\sin(N(\theta-\phi))}{\sin((\theta-\phi)/2)}-\frac{\sin(N(\theta+\phi))}{\sin((\theta+\phi)/2)}\right].} \tag{12A.9}$$

For every fixed $\theta_0\in(0,\pi)$, uniformly on compact real u,v sets,

$$\frac{\pi}{N}\Pi_N\left(\theta_0+\frac{\pi u}{N},\theta_0+\frac{\pi v}{N}\right)\longrightarrow \operatorname{sinc}_\pi(u-v). \tag{12A.10}$$

Proof. Product-to-sum and the finite cosine sum prove (12A.9), with removable values on the diagonal. In its difference term the denominator is its argument times $1+O(N^{-2})$. In the reflected-sum term it tends to $\sin\theta_0>0$, while the numerator is bounded. The normalization makes that second term $O(N^{-1})$, proving the uniform limit. At the two endpoints the reflected term instead survives:

$$\begin{aligned}\frac{\pi}{N}\Pi_N(\pi u/N,\pi v/N)&\longrightarrow \operatorname{sinc}_\pi(u-v)-\operatorname{sinc}_\pi(u+v),\\ \frac{\pi}{N}\Pi_N(\pi-\pi u/N,\pi-\pi v/N)&\longrightarrow \operatorname{sinc}_\pi(u-v)+\operatorname{sinc}_\pi(u+v).\end{aligned} \tag{12A.11}$$

Both follow by substitution, uniformly on compact positive u,v sets. Removing the zero mode changes the rescaled interior kernel by a term tending to zero; its inclusion here does not change the convention in (12A.8). □

A random-position comparison, not a zeta model. Introduce the density $\det[\psi_{i-1}(\theta_j)]_{i,j=1}^{N}{}^2/N!$ on $(0,\pi)^N$. Expansion of both determinants and orthonormality prove that its integral is one. Integrating all but two variables gives distinct-point intensity

$$\rho_{2,N}(\theta,\phi)=\Pi_N(\theta,\theta)\Pi_N(\phi,\phi)-\Pi_N(\theta,\phi)^2. \tag{12A.12}$$

After the scaling (12A.10) this tends, with the Jacobian factor $(\pi/N)^2$, to $1-\operatorname{sinc}_\pi(u-v)^2$. It is a distribution of random positions, not of the deterministic triangular eigenvalues. The latter unfold to the equally spaced sequence $\sqrt{2T_m+1/4}=m+1/2$. No identification with actual zeta zeros is made. Section 61A supplies the precise ordinate-scale comparison; Section 155C uses a weighted trace of this operator for a different positive measure.

12B. The comparison and completed determinants have different types

Use separate evaluation parameters: $E_\triangle(z)=\prod_{n\ge1}(1+z/[n(n+1)])$ and $E_\xi(x)=X(-x)/X(0)=\xi(s_x)/\xi(1)$. The Gamma/reflection substitution of Section 11 is $z=q(s)$, whereas the completed source uses $x=-q(s)=s(s-1)$. Consequently

$$\begin{aligned} E_\triangle(1/4)&=4/\pi,\\ E_\xi(-1/4)&=X(1/4)/X(0)=\xi(1/2)/\xi(1),\\ E_\xi(1/4)&=X(-1/4)/X(0)=\xi((1+\sqrt{2})/2)/\xi(1).\end{aligned} \tag{12B.1}$$

The first two are centered evaluations in different parameter conventions; the third is the completed determinant at the model's positive numerical comparison parameter. They must not be identified.

Proposition 12B.1 (order does not identify type). As real $x\to\infty$,

$$\begin{aligned} \log E_\triangle(x)&=\pi\sqrt{x}-\log(2\pi x)+O(x^{-1/2}),\\ \log E_\xi(x)&=\frac{\sqrt{x}}{4}\log x-\frac{1+\log(2\pi)}{2}\sqrt{x}+\frac{7}{8}\log x+C_\xi+O\Big(\frac{\log x}{\sqrt{x}}\Big).\end{aligned} \tag{12B.2}$$

Both functions have order one-half. The triangular determinant has finite type π at this order; the completed determinant has infinite type, without assuming RH.

Proof. Expand the closed quotient $\cosh(\pi\sqrt{x-1/4})/(\pi x)$ for the first formula. For the second, $\frac{d}{dx}\log E_\xi=S_\xi$, and integration of (OP.1) gives $\sqrt{x}\log x/4-(1+\log(2\pi))\sqrt{x}/2+(7/8)\log x$. Its remainder is integrable at infinity and leaves a constant plus $O(\log x/\sqrt{x})$. The closed quotient bounds the triangular circle maximum by an algebraic factor times $\exp(\pi\sqrt{r+1/4})$, and its positive axis attains type π. The completed positive-axis growth already makes $\log M(r)/\sqrt{r}$ unbounded; the folded order-one-half statement is established in Section 16. □

RH concerns the negative-real-zero set of E_ξ, not equality of its entire-function type or spectral density with the triangular model. The operator and sine-kernel results of Section 12A remain comparison results with their stated multiplicities.

13. Reciprocal and Cayley uniformization

For $d>2$, put $D=d-2$ and

$$p = \frac{z-1}{D} \qquad r = \frac{p}{1-p}$$

Then reflection $z \mapsto d - z$ becomes

$$p \mapsto 1 - p \qquad r \mapsto r^{-1}$$

For real $0 < p < 1$ (equivalently $r > 0$), the bounded invariant is

$$\boxed{\tau = p(1-p) = \frac{r}{(1+r)^2} = \frac{1}{4}\operatorname{sech}^2 y \qquad r = e^{2y}}$$

The reciprocal $(1+r)^2/r$ is not the bounded variable τ. On the zeta-centered right sheet, $p = 1/2 + c$ and hence

$$\boxed{\tau = \frac{1}{4} - c^2 \qquad r = \frac{1+2c}{1-2c} \qquad y = \operatorname{artanh}(2c)}$$

This is the exact collar coordinate used in the flux synthesis below.

Proposition 13.1 - The self-scaling conic pencil

The triangular-circle relation from the geometric branch can be written

$$T_x = \frac{1}{2}y\left(c + \frac{1}{2}\right) - \frac{1}{2}y^2 - \frac{1}{8}$$

With $X = x + 1/2$, this is exactly

$$\boxed{X^2 + y^2 - \left(c + \frac{1}{2}\right)y = 0}$$

For fixed c, let

$$r_c = \frac{c + 1/2}{2}$$

The locus is the circle

$$X^2 + (y - r_c)^2 = r_c^2$$

For $r_c \neq 0$ it has center $C_c = (0, r_c)$, radius $|r_c|$, passes through $F = (0,0)$, and is tangent there to $L : y = 0$. Its centers satisfy

$$|C_c - F| = \operatorname{dist}(C_c, L)$$

Because the focus lies on the directrix, the center locus is the degenerate focus-directrix parabola $X = 0$. In the original coordinate it is $x = -1/2$.

Now impose a linear selector

$$c = \lambda X + \mu$$

Eliminating c gives

$$\boxed{X^2 - \lambda X y + y^2 - \left(\mu + \frac{1}{2}\right) y = 0}$$

Its conic discriminant is

$$\Delta = \lambda^2 - 4$$

When $\mu \neq -1/2$, the locus is a nondegenerate ellipse, parabola, or hyperbola according as $|\lambda| < 2$, $|\lambda| = 2$, or $|\lambda| > 2$. The exceptional value $\mu = -1/2$ removes the linear term and produces the corresponding homogeneous degeneration.

For the selector $c = X$ $(\lambda = 1, \mu = 0)$, the original coordinates obey

$$x^2 - xy + y^2 + x - y + \frac{1}{4} = 0$$

The center is $(-1/3, 1/3)$. With

$$\xi = x + \frac{1}{3}, \qquad \eta = y - \frac{1}{3}, \qquad u = \frac{\xi + \eta}{\sqrt{2}}, \qquad v = \frac{\xi - \eta}{\sqrt{2}}$$

the ellipse is

$$\boxed{\frac{u^2}{1/6} + \frac{v^2}{1/18} = 1}$$

Its foci are

$$\left(-\frac{1}{3} \pm \frac{1}{3\sqrt{2}}, \frac{1}{3} \pm \frac{1}{3\sqrt{2}}\right)$$

with matching signs. The selected circle has real intersections precisely for $-1/6 \leq c \leq 1/2$.

For $c = 2X$ one obtains the focus-directrix parabola

$$\boxed{\left(x + \frac{1}{2} - y\right)^2 = \frac{y}{2}}$$

with focus and directrix

$$F = \left(-\frac{9}{16}, \frac{1}{16}\right) \qquad L:\ x + y = -\frac{5}{8}$$

For $c = 3X$ the eliminated curve is the hyperbola

$$\left(x + \frac{1}{2}\right)^2 - 3\left(x + \frac{1}{2}\right)y + y^2 - \frac{1}{2}y = 0$$

Finally, the PP74 level circles

$$\left(U + 1 + \frac{1}{2k}\right)^2 + V^2 = \frac{1}{4k^2}$$

form the same focus-directrix center construction after a Euclidean similarity: their centers lie on $V = 0$, every circle passes through $(-1, 0)$, and each is tangent there to $U = -1$. This upgrades the old visual comparison to an exact conic-pencil bridge. It remains geometric; it supplies no zero-discrepancy estimate by itself.

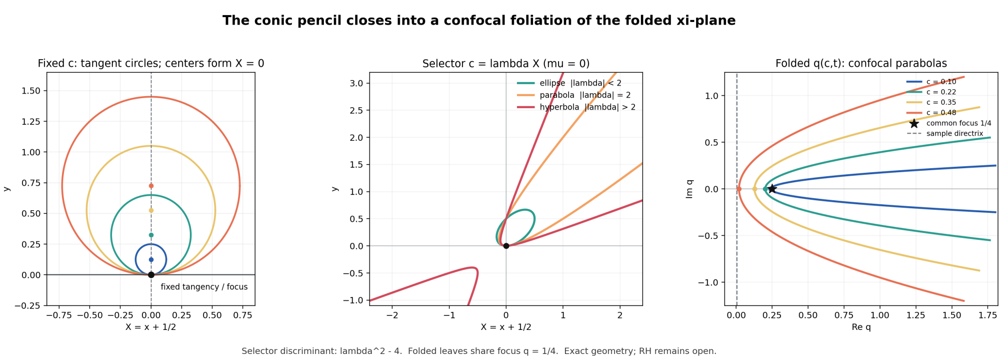

Figure 15: Exact circle-pencil and selector-conic diagnostic.

14. Retained exact operator families

The following families connect the centered coordinate to operator models. Their scalar identities and operator domains have different scopes.

Family	Exact content	Boundary
Higher-simplex products	Root-symmetric Gamma closure; order $1/p$	Entire-type convention merits specialist review
Continuous Pascal row	Gamma interpolation, dimension raising, central splitting	Scalar identities do not create an arithmetic sieve
Cube-sphere lift	Degree/Casimir and Boolean-noise/Poisson-semigroup intertwiners	Different Hilbert spaces; norm multiplier retained
Gaussian-Laguerre	Explicit Fourier eigenmodes in harmonic sectors	No eventual-sign theorem

Family	Exact content	Boundary
Mellin-Fourier	Degree-resolved Gamma multiplier and fixed-line unitarity	Maximal unbounded-operator domains not developed
Sphere/Bessel	Coordinate characteristic functions and Gram positivity	Radial sign observables remain nonlinear
Log-Gamma/Laplace	Determinant amplitude as a characteristic function	Probability law does not imply zeta-zero location
Phase-complement collar	Exact complement, Cayley, rapidity, and τ bookkeeping	Physical-source operators remain independent

77. Cube roots, $A_3 = D_3$, and the twelve-ray theorem

The primary six-cardinal construction fixes the cone-figure cube

$$Q_\pi = \{(\pm\pi/2, \pm\pi/2, \pm\pi/2)\} \tag{77.1}$$

Its twelve edge midpoints are

$$C_\pi = \{(\pm\pi/2, \pm\pi/2, 0) \text{ and permutations}\} \tag{77.2}$$

each of norm $\pi/\sqrt{2}$. This is the cone cube, not the distinct inward $\sqrt{3}$ cube retained elsewhere in the geometry corpus.

Partition Q_π by the sign of xyz. Each four-point class is a regular tetrahedron, and the two classes are negatives of one another. If $v_1, \ldots, v_4$ are the vertices of either class, then

$$\left\{\frac{v_j - v_i}{2} : i \neq j\right\} = C_\pi \tag{77.3}$$

After normalization by $\pi/\sqrt{2}$, (77.2) becomes

$$\boxed{\mathcal{E} = \frac{1}{\sqrt{2}}\{(\pm1, \pm1, 0), (\pm1, 0, \pm1), (0, \pm1, \pm1)\} = \Phi(A_3) = \Phi(D_3)} \tag{77.4}$$

Thus the cube contains the twelve directed tetrahedral edge directions and the cuboctahedral root system. Both parity tetrahedra generate the identical set.

Choose the threefold axis and registered plane basis

$$u = \frac{(1,1,1)}{\sqrt{3}}, \qquad e_1 = \frac{(1,-1,0)}{\sqrt{2}}, \qquad e_2 = \frac{(1,1,-2)}{\sqrt{6}} \tag{77.5}$$

Let P_u be orthogonal projection to $u^\perp$, expressed in this basis. Here u is the perspective or viewing ray. The symbol i enters only after the image plane is identified with $\mathbb{C}$ by $z(v) = (v \cdot e_1) + i(v \cdot e_2)$: multiplication by i is the oriented quarter-turn inside the image, not the viewing ray itself. Replacing i by $-i$ reverses the handedness of the registered view. Direct substitution in the twelve coordinates gives

$$\boxed{P_u(\mathcal{E}) = \mu_6 \ \sqcup \ \frac{1}{\sqrt{3}}\zeta_{12}\mu_6} \tag{77.6}$$

The six roots orthogonal to u form the outer radius-one hexagon. The six remaining roots form the staggered radius-$1/\sqrt{3}$ hexagon. Their twelve rays have exactly the arguments

$$0^\circ, 30^\circ, \ldots, 330^\circ \tag{77.7}$$

Hence radial normalization of the nonzero projected points gives μ_{12}. The projection itself does not.

Theorem 77.1 (radial impossibility). No orthogonal projection of $\mathcal{E}$ onto a plane places all twelve projected points on one circle.

Proof. The normalized roots form the tight frame

$$\sum_{e\in\mathcal{E}} ee^\mathsf{T} = 4I \tag{77.8}$$

If projection along a unit normal n gave equal radii, then $1-|e\cdot n|^2$ would be constant. Taking the trace against nn^T in (77.8) forces

$$|e \cdot n|^2 = \frac{1}{3} \quad \text{for every } e \tag{77.9}$$

Comparing $(1,1,0)/\sqrt{2}$ with $(1,-1,0)/\sqrt{2}$ forces $n_1n_2 = 0$. The analogous pairs force $n_1n_3 = n_2n_3 = 0$. Thus n is a coordinate axis. For a coordinate axis, however, $|e\cdot n|^2$ takes the two values 0 and $1/2$, contradicting (77.9). □

There is also a group-theoretic obstruction. The full root automorphism group is the octahedral group O_h of order 48, isomorphic to a central C_2 extension of S_4. Its element orders divide $1, 2, 3, 4$, or 6; it has no element of order 12. Therefore the geometry induces no intrinsic C_{12} action.

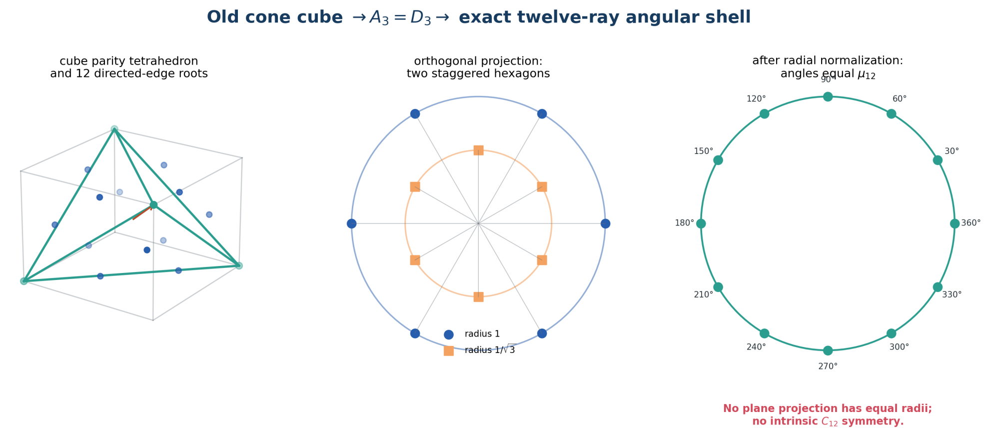

Figure 16: The cone cube yields the A_3 roots and twelve exact rays, but equal radii appear only after a separate radial normalization.

The strongest honest classification is therefore

$$\boxed{\begin{array}{c}\text{geometric } A_3 \text{ skeleton} + \text{ exact twelve-ray angles} \\ + \text{ radial and cyclic no-go}\end{array}} \tag{77.10}$$

The shared value $1/\sqrt{3}$ in the inward cube cascade and in (77.6) is a shared three-coordinate normalization. No intertwiner between the two operators is known. The normalized cube-corner value $\pm 1/8$ and the triangular completed-square correction $-1/8$ have cubic and quadratic homogeneity respectively; they remain an exact normalization contact only.

78. Balanced stabilizers, factorial mid-shells, and the intrinsic D_8

Let $\mathcal{F}_{24}$ be the complete ordered tetrahedral frames. Choosing a reference ordering identifies it with the regular S_4-set. For the directed edge $(1,2)$ and the unoriented edge $\{1,2\}$, the stabilizers are

$$H = \{1, (34)\} \cong C_2 \qquad K = \langle (12), (34) \rangle \cong V_4 \tag{78.1}$$

Therefore

$$\boxed{\mathcal{F}_{24} \cong S_4 \longrightarrow E_{12}^{\to} \cong S_4/H \longrightarrow E_6 \cong S_4/K} \tag{78.2}$$

is a balanced $2:1$ then $2:1$ tower of sets. It follows that

$$\boxed{12^2 = 24 \cdot 6, \qquad 12 = \sqrt{3!4!}} \tag{78.3}$$

The owner of (78.3) is the stabilizer chain, not a factorial-induced map.

More generally, if $1 < H < K < G$ are finite and $|H| = [K : H] = r$, then $|K| = r^2$ and

$$\boxed{|G/H|^2 = |G|\,|G/K|} \tag{78.4}$$

For an n-simplex, the complete frames, directed edges, and edges have sizes

$$(n+1)!, \qquad n(n+1), \qquad \frac{n(n+1)}{2}$$

The first fiber has size $(n-1)!$ and the second has size 2. The tower is balanced binary only when $(n-1)! = 2$, hence uniquely for $n = 3$. This is the structural reason that the tetrahedral $24 \to 12 \to 6$ packet is exceptional.

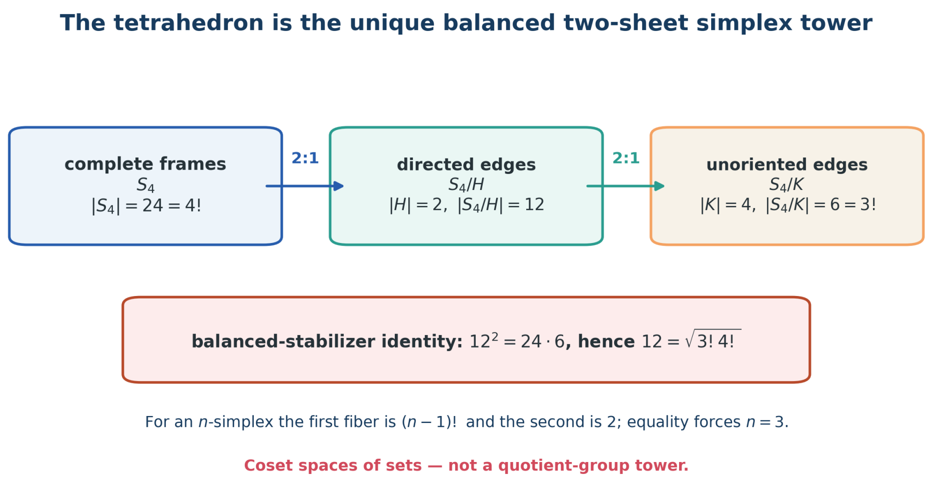

Figure 17: The middle value 12 is the exact cardinal geometric mean because the tetrahedral frame tower has two equal stabilizer fibers.

The number 12 is not, however, the unique factorial mid-shell. From

$$q^2 = n!(n+1)! = (n!)^2(n+1)$$

one obtains

$$\boxed{q \in \mathbb{Z} \iff n+1 = a^2, \qquad q = a\,n!} \tag{78.5}$$

This is an infinite family. The value 12 is uniquely the *doubling* member: $q = 2n!$ and $(n+1)! = 2q$ force $n+1 = 4$, so $n = 3$ and $q = 12$. The Pell identity $17^2 - 2 \cdot 12^2 = 1$ is exact, but no recurrence intertwines the Pell orbit with (78.5); it remains a one-hit shared scale.

78.1 The four-state fiber

Over each unoriented edge sit four complete frames. Two intrinsic involutions act on the fiber:

$$A(i, j; k, l) = (j, i; k, l) \qquad B(i, j; k, l) = (i, j; l, k) \tag{78.6}$$

They commute, are fixed-point-free, and generate a regular $V_4 = \langle A, B\rangle$.
The registered cyclotomic bijection $\Psi : \mathcal{F}_{24} \to \mu_{24}$ transports a quarter-turn L with

$$L^2 = B, \qquad L^4 = 1, \qquad ALA = L^{-1} \tag{78.7}$$

Although choosing L rather than L^{-1} requires an oriented frame, the group it generates with A does not:

$$\boxed{\langle A, L\rangle = C_{\mathrm{Sym}(\mathcal{Q}_{\bar{e}})}(B) \cong D_8} \tag{78.8}$$

Indeed the centralizer of a fixed-point-free double transposition in S_4 has order eight. Both possible quarter-turn orientations generate this same centralizer. Consequently the envelope D_8 is intrinsic, while the regular $C_4 = \langle L\rangle$ and its label $+i$ are registration-relative. On the same four points,

$$V_4 \cap C_4 = \langle B\rangle \cong C_2 \qquad \langle V_4, C_4\rangle = D_8 \tag{78.9}$$

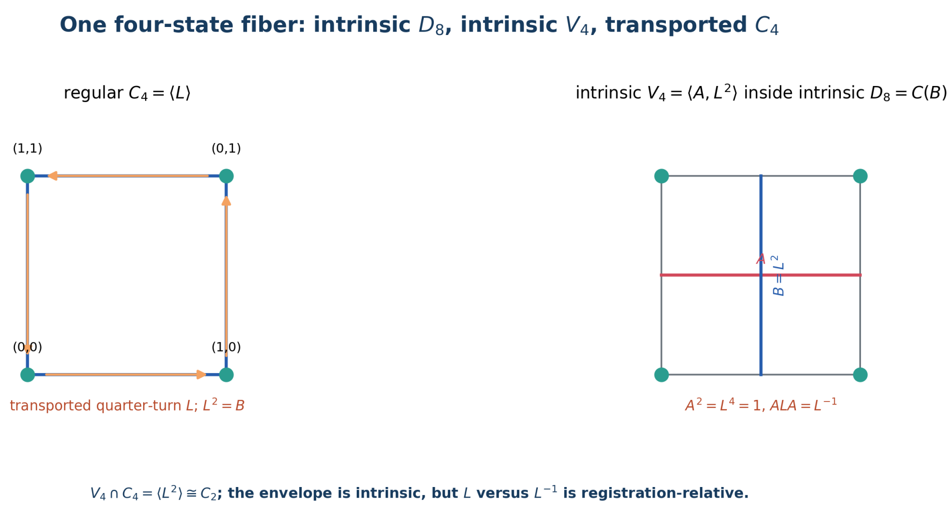

Figure 18: The intrinsic V_4 and transported C_4 sit in one intrinsic dihedral envelope; only the orientation of the quarter-turn is registered.

With the determinant registration, write a top exponent as $K = r + 6q$, $q \in \mathbb{Z}/4$. Then

$$L : q \mapsto q + 1 \qquad B : q \mapsto q + 2 \qquad A : q \mapsto -q - 1 \tag{78.10}$$

On roots, where $y = z^4 = \zeta_6^r$, endpoint reversal is the literal fiber reflection

$$\boxed{A(z) = -i\,\zeta_{12}^r\,\overline{z}} \tag{78.11}$$

The cyclotomic order is constant around the C_4 cycle exactly when r is odd. Geometrically these are the three apex edges incident to the registered threefold-axis vertex; the even-r fibers are the three base-face edges. The primitive eight states are exactly the two complete fibers $r = 1, 5$. This is cyclotomic primitivity, not integer primality.

The tetrahedral tower remains a coset tower of sets. Since H is not normal in S_4, S_4/H is not a quotient group. Likewise $E_6 \simeq A_4/\langle(12)(34)\rangle$ is a homogeneous space, not a quotient group. The root-of-unity tower

$$\mu_{24} \xrightarrow{z^2} \mu_{12} \xrightarrow{z^2} \mu_6$$

is a genuine group tower. Their maximal unregistered common structure is a free C_2-set; stagewise registered maps do not make the ambient groups isomorphic.

The finite-rank statements below specify their certificate geometry and mathematical grade. Sections 92–93 give the global result through order eight; §138 gives the distinct rank-twelve result at one fixed basepoint.

Technical chapter IV. Completion, folded support, and the Gamma source

Completion selects the particular resolvent. Moment and matrix criteria apply to that function; the auxiliary Gamma scaffold is then compared with it.

15. Recognition is not distribution

Wilson's theorem and the successor gate give exact finite prime recognizers. To enter analytic number theory one must pass to prime powers with the von Mangoldt measure

$$\nu = \sum_{m\geq 2} \Lambda(m)\, \delta_{\log m}$$

whose Laplace transform is

$$\mathcal{L}\nu(s) = -\frac{\zeta'(s)}{\zeta(s)} \qquad \Re s = \sigma > 1$$

In the finite-visibility convention used here this means

$$s = \sigma + it, \qquad \Re s = \sigma > 1$$

This closes the finite-to-prime adapter. It does not provide the cancellation or positivity needed beyond $\Re s = 1$.

The polar/Ramanujan bridge is likewise exact:

$$c_n(m) = \sum_{(k,n)=1} e^{2\pi i mk/n} \qquad \sum_{n\geq 1} \frac{c_n(m)}{n^s} = \frac{\sigma_{1-s}(m)}{\zeta(s)}$$

The series identity holds for each fixed positive integer m and $\Re s > 1$. For $m = 1$ it reaches $1/\zeta(s)$ directly. It does not show analyticity in $\Re s = \sigma > 1/2$.

16. Completion and folded coordinate

Use the completed entire function

$$\xi(s) = \frac{1}{2}s(s-1)\pi^{-s/2}\Gamma(s/2)\zeta(s) \qquad \xi(s) = \xi(1-s)$$

Here and in every completion formula,

$$\boxed{s = \sigma + it, \qquad 1-s = (1-\sigma) - it, \qquad \bar{s} = \sigma - it} \tag{16.0}$$

Put

$$q(s) = s(1-s)$$

Functional-equation invariance gives a unique entire function X such that

$$\xi(s) = X(q)$$

For a zero $\rho = \beta + i\gamma$,

$$q_\rho = \rho(1-\rho) = \frac{1}{4} + \gamma^2 - (\beta - \tfrac{1}{2})^2 - 2i\gamma(\beta - \tfrac{1}{2})$$

All folded zeros satisfy $\Re q_\rho > 0$ unconditionally. RH is the stronger statement

$$\boxed{q_\rho \in \mathbb{R}_{>0} \quad \text{for every zero orbit}}$$

Define the folded resolvent

$$M_\xi(q) = -\frac{X'(q)}{X(q)}$$

On the negative real axis, let

$$s(x) = \frac{1+\sqrt{1+4x}}{2} > 1 \qquad S_\xi(x) = M_\xi(-x)$$

Thus the source evaluation is the specialization

$$s(x) = \sigma_x + i0, \qquad \sigma_x = \frac{1+\sqrt{1+4x}}{2} > 1, \qquad x = s(x)(s(x)-1) = 2T_{s(x)-1} \tag{16.1a}$$

Then

$$S_\xi(x) = \frac{1}{\sqrt{1+4x}}\frac{\xi'(s(x))}{\xi(s(x))}$$

The $s > 1$ prime/archimedean formula is

$$\boxed{S_\xi(x) = \frac{1}{\sqrt{1+4x}}\left[\frac{1}{s} + \frac{1}{s-1} - \frac{1}{2}\log\pi + \frac{1}{2}\psi(s/2) - \sum_{n\geq 2}\frac{\Lambda(n)}{n^s}\right]}$$

152. Full $s = \sigma + it$ expansion and the triangular center

Starting from $s = \sigma + it$, direct multiplication gives the entire coordinate chart:

object	Cartesian expansion	critical-line specialization $\sigma = 1/2$
s	$\sigma + it$	$1/2 + it$
$1 - s$	$(1-\sigma) - it$	$1/2 - it = \overline{s}$
$\overline{s}$	$\sigma - it$	$1/2 - it = 1 - s$
s^2	$(\sigma^2 - t^2) + 2i\sigma t$	$(1/4 - t^2) + it$
$q = s(1-s)$	$\sigma(1-\sigma) + t^2 + i\,t(1-2\sigma)$	$1/4 + t^2 \in \mathbb{R}_{>0}$
$x = s(s-1) = -q$	$\sigma^2 - \sigma - t^2 + i\,t(2\sigma - 1)$	$-(1/4 + t^2)$
$T_{s-1} = s(s-1)/2$	$(\sigma^2 - \sigma - t^2)/2 + i\,t(\sigma - 1/2)$	$-1/8 - t^2/2$
centered coordinate $j = 2s - 1$	$(2\sigma - 1) + 2it$	$2it$

Thus

$$\boxed{\begin{aligned} q(s) &= (\sigma + it)(1 - \sigma - it) \\ &= \sigma(1-\sigma) + t^2 + i\,t(1-2\sigma) \\ T_{s-1} &= \frac{\sigma^2 - \sigma - t^2}{2} + i\,t\Big(\sigma - \frac{1}{2}\Big) \end{aligned}} \tag{152.1}$$

Two identities hold without placing s on any line:

$$\boxed{4q(s) = 1 - (2s-1)^2, \qquad 8T_{s-1} + 1 = (2s-1)^2} \tag{152.2}$$

The same centered coordinate therefore owns the fold and the triangular completion. On the real safe axis put $s_x = n + 1$ with $n \geq 0$. Then

$$\boxed{\begin{aligned} s_x &= n + 1 = \sigma_x + i0 \\ x &= s_x(s_x - 1) = n(n+1) = 2T_n \\ R &= 2s_x - 1 = 2n + 1 = j_n = \sqrt{1+4x} \end{aligned}} \tag{152.3}$$

This is the analytic version of $8T_n + 1 = (2n+1)^2$. It does **not** put a nontrivial zeta zero at a triangular point: on the critical line $x = -q < 0$, whereas the source half-line uses $x > 0$ and $t = 0$. The identity is a shared coordinate chart, not a zero-location theorem.

For a zero $\rho = \beta + i\gamma$, (152.1) becomes

$$\boxed{q_\rho = \rho(1-\rho) = \frac{1}{4} + \gamma^2 - \left(\beta - \frac{1}{2}\right)^2 - 2i\gamma\left(\beta - \frac{1}{2}\right)} \tag{152.4}$$

Consequently q_ρ is real for a nonreal zero exactly when $\beta = 1/2$. The omitted $\gamma = 0$ branch is the reason the informal statement $\Im q = 0 \iff \sigma = 1/2$ is false for arbitrary s; the exact real-axis distinction is

$$\Im q = t(1-2\sigma) = 0 \iff t = 0 \text{ or } \sigma = \frac{1}{2} \tag{152.5}$$

The coordinate atlas in Reading Volume §R6 displays this same fold.

153. The self-dual Mellin weight $n^{-1/2} = 1/\sqrt{n}$

For $n > 0$ and $s = \sigma + it$,

$$\boxed{n^{-s} = n^{-(\sigma+it)} = n^{-\sigma}e^{-it\log n} = \frac{\cos(t\log n) - i\sin(t\log n)}{n^\sigma}} \tag{153.1}$$

The modulus and phase separate:

$$|n^{-s}| = n^{-\sigma}, \qquad |n^{-it}| = 1, \qquad \arg(n^{-s}) = -t\log n \pmod{2\pi} \tag{153.2}$$

Reflection and conjugation give two different products:

pairing	expanded calculation	result
functional-equation reflection	$n^{-s}n^{-(1-s)} = n^{-(\sigma+it)}n^{-((1-\sigma)-it)}$	$n^{-1} = 1/n$ for every σ, t
Hermitian conjugation	$n^{-s}\overline{n^{-s}} = n^{-(\sigma+it)}n^{-(\sigma-it)}$	$n^{-2\sigma}$

They agree for every $n > 1$ exactly when $2\sigma = 1$. Equivalently,

$$\boxed{|n^{-s}| = |n^{-(1-s)}| \iff \sigma = \frac{1}{2} \qquad n^{-1/2} = \frac{1}{\sqrt{n}}} \tag{153.3}$$

Thus $1/\sqrt{n}$ is not an arbitrary normalization in the explicit formula. It is the unique pointwise magnitude at which the two functional-equation partners carry the same length. On the critical line,

$$n^{-(1/2+it)} = \frac{e^{-it\log n}}{\sqrt{n}}, \qquad n^{-(1/2-it)} = \frac{e^{it\log n}}{\sqrt{n}} = \overline{n^{-(1/2+it)}} \tag{153.4}$$

The resolvent carrier makes the same equality visible. With $a_x = \sqrt{x + 1/4}$ and $f_x(u) = e^{-a_x|u|}(1/(4a_x) + \frac{1}{2}\operatorname{sgn} u)$, declare $\widehat{f}_x(t) = \int_{\mathbb{R}} f_x(u)e^{-itu}\,du$. The sign of the transform is part of the definition. For real t,

$$\boxed{\widehat{f}_x(t) = \frac{1/2 - it}{t^2 + a_x^2} = \frac{1-s}{x + q(s)}\Big|_{s=1/2+it}, \qquad |\widehat{f}_x(t)|^2 = \frac{q}{(x+q)^2}} \tag{153.5}$$

The opposite convention gives the conjugate numerator:

$$\int_{\mathbb{R}} f_x(u) e^{+itu}\, du = \frac{1/2 + it}{t^2 + a_x^2} = \overline{\widehat{f}_x(t)} \tag{153.5a}$$

The modulus-square equality in (153.5) uses $1 - s = \overline{s}$ and $q = s(1-s) = s\overline{s}$ on the line. Off the line, reflection and conjugation separate, so replacing the holomorphic square by a modulus square would assume the desired zero placement.

The rotation diagram in Reading Volume §R8 displays the conjugate phases.

The Gauss-circle connection is exact only at the level of a coordinate and a weight. For a finite disk and $r_2(n) = \#\{(a,b) \in \mathbb{Z}^2 : a^2 + b^2 = n\}$,

$$\sum_{0 < a^2 + b^2 \le R^2} (a^2 + b^2)^{-w} = \sum_{1 \le n \le R^2} r_2(n) n^{-w} \tag{153.6}$$

At $w = 1/2$, each lattice vector has weight $n^{-1/2} = 1/\sqrt{a^2+b^2} = 1/r$. This is a useful visual and Mellin comparison, but the multiplicity $r_2(n)$ changes the arithmetic object. No Gauss-circle estimate, Dirichlet-divisor estimate, or RH implication is transported by (153.6).

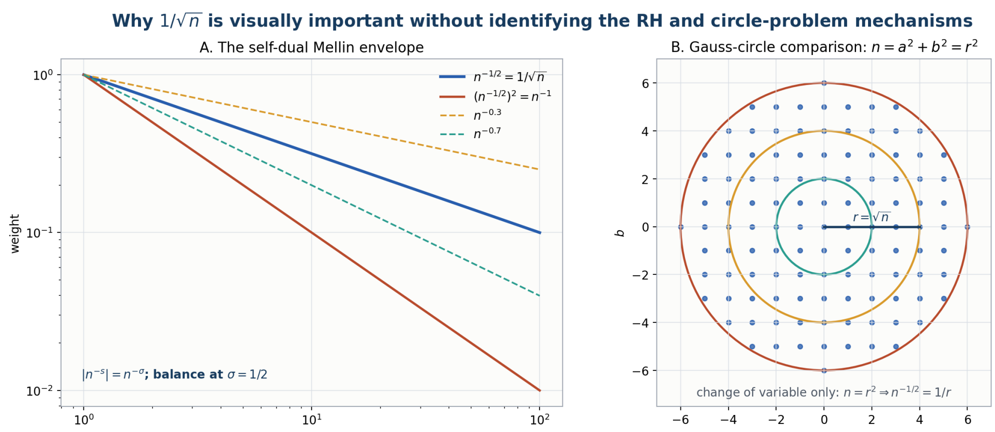

Figure 19: The square-root weight and its lattice-radius reading. The right panel is a comparison model, not an identification of proof mechanisms.

17. Stieltjes, heat, and moment equivalences

The folded moment chain is

$$\begin{aligned} \text{RH} &\iff (\mu_k) \text{ is a Hamburger moment sequence} \\ &\iff [\mu_{i+j}]_{i,j=0}^{N} \succeq 0 \quad \forall N \\ &\iff M_\xi \text{ is Herglotz-Pick} \\ &\iff S_\xi \text{ is Stieltjes} \\ &\iff \Theta_\xi \text{ is completely monotone} \end{aligned}$$

The folded heat trace is

$$\Theta_\xi(u) = \sum_{[\rho]} m_\rho e^{-uq_\rho} \qquad S_\xi(x) = \int_0^\infty e^{-xu}\Theta_\xi(u)\,du$$

The central-Pascal change of basis between folded moments and Li coefficients is (155.3).

Using Gaussian subordination, the prime contribution to the heat trace becomes the explicit log-Gaussian comb

$$-\frac{e^{-u/4}}{2\sqrt{\pi u}} \sum_{n\geq 2} \frac{\Lambda(n)}{\sqrt{n}} \exp\left[-\frac{(\log n)^2}{4u}\right]$$

balanced by an explicit Gamma term.

The full load-bearing PP1 theorem remains:

> Starting only from the $s > 1$ prime/archimedean formula, prove that S_ξ is Stieltjes, that Θ_ξ is completely monotone, or that every prime-side Loewner matrix is positive semidefinite.

The first six reduced-Widder diagonal inequalities are source-certified in §§35–38 and 74–74A; W_1 is analytic and W_2–W_6 are A-CAT from one bundled certificate. Reading Volume §R12 states the controlling rung status. This is genuine finite-order progress inside the criterion, but it does not establish the complete hierarchy required for the Stieltjes class. Ordinary positivity of $S_\xi(x)$ is unconditional and is not the target.

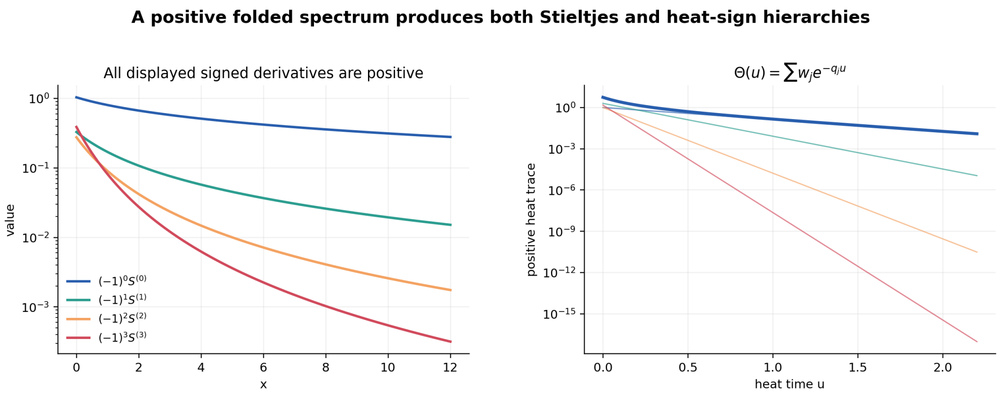

Figure 20: Finite positive folded spectrum illustrating Stieltjes derivative signs and heat decay.

18. Li/transverse defect identity

For $s = 1/2 + u + iv$,

$$s(1-s) = \frac{1}{4} + v^2 - u^2 - 2iuv$$

Thus the adjacent triangular polarization $P(u, v) = 2uv$ is exactly the imaginary folded-zero defect. If $C_\xi e_\rho = q_\rho^{-1} e_\rho$, then

$$\mathcal{E}_\xi = \frac{1}{4}\|C_\xi - C_\xi^*\|_{\mathrm{HS}}^2 = \sum_{[\rho]} m_\rho \frac{P(\beta - \frac{1}{2}, \gamma)^2}{|q_\rho|^4}$$

Consequently

$$\boxed{\mathrm{RH} \iff \sum_{[\rho]} \frac{m_\rho}{|\rho(1-\rho)|^2} = 4\lambda_1 - \lambda_2}$$

This identifies the missing object as a nonholomorphic absolute-square norm. The arithmetic construction of that norm remains open.

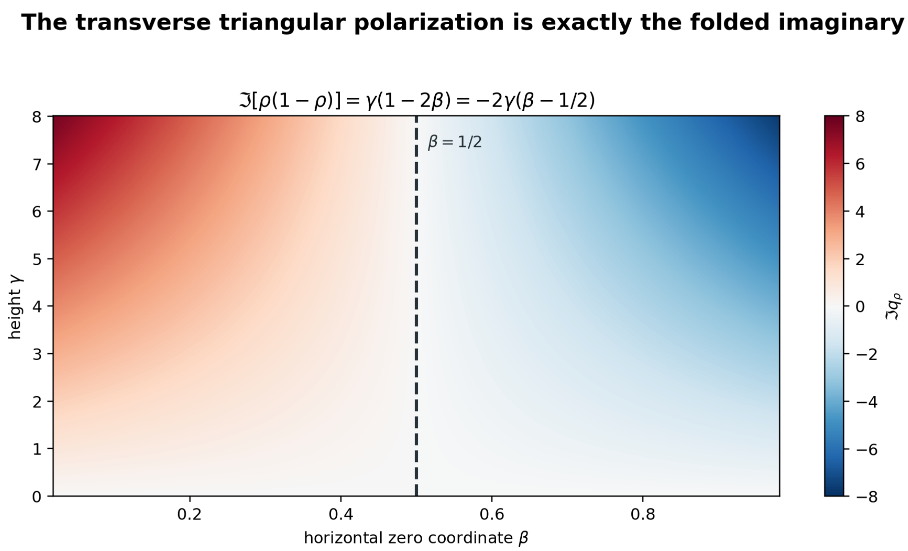

Figure 21: The folded imaginary coordinate is exactly the transverse critical-line defect.

155. Li positivity, PP97, and the Löwner source gate

To keep the analytic variable visible, define the Li coefficients with a dummy differentiation variable z:

$$\boxed{\lambda_n = \frac{1}{(n-1)!}\frac{d^n}{dz^n}\left[z^{n-1}\log\xi(z)\right]\Big|_{z=1}} \tag{155.1}$$

Li's criterion is

$$\boxed{\mathrm{RH} \iff \lambda_n \geq 0 \quad \text{for every } n \geq 1} \tag{155.2}$$

This is an all-order criterion. A long positive finite prefix is not the quantified statement in (155.2). The log-frequency notation $L_n = \log n$ in the Montgomery–Vaughan calculation is unrelated to λ_n.

The folded moments and Li coefficients are joined by the exact central-Pascal transform

$$\boxed{\mu_{k-1} = \sum_{j=1}^{k}(-1)^{j+1}\binom{2k}{k-j}\lambda_j} \tag{155.3}$$

The first rows, printed rather than hidden inside the binomial, are

$$\begin{aligned}
\mu_0 &= \lambda_1 \\
\mu_1 &= 4\lambda_1 - \lambda_2 \\
\mu_2 &= 15\lambda_1 - 6\lambda_2 + \lambda_3 \\
\mu_3 &= 56\lambda_1 - 28\lambda_2 + 8\lambda_3 - \lambda_4 \\
\mu_4 &= 210\lambda_1 - 120\lambda_2 + 45\lambda_3 - 10\lambda_4 + \lambda_5
\end{aligned} \tag{155.4}$$

The second row is the particularly important bridge:

$$\boxed{\mu_1 = 4\lambda_1 - \lambda_2} \tag{155.5}$$

On the folded-zero side this is holomorphic data in $q_\rho = \rho(1-\rho)$. The exact RH-equivalent equality

$$\boxed{\sum_{[\rho]} \frac{m_\rho}{|\rho(1-\rho)|^2} = 4\lambda_1 - \lambda_2} \tag{155.6}$$

compares a nonholomorphic left side with the holomorphic folded moment on the right. A proof of (155.6) must create conjugation through a two-point, sesquilinear, or variational mechanism; scalar holomorphic bookkeeping cannot do so by itself.

Now define

$$S_\xi(x) = \sum_{[\rho]} \frac{m_\rho}{x + q_\rho}, \qquad h(x) = xS_\xi(x), \qquad x > 0 \tag{155.7}$$

Under RH, $q_\rho > 0$ and S_ξ is Stieltjes, so h is complete Bernstein and operator monotone. Conversely, the Pick continuation of h excludes nonreal folded poles and forces RH. For positive nodes x_i define

$$[\mathcal{L}_h]_{ij} = \begin{cases} \dfrac{h(x_i) - h(x_j)}{x_i - x_j}, & i \neq j \\ h'(x_i), & i = j \end{cases} \tag{155.8}$$

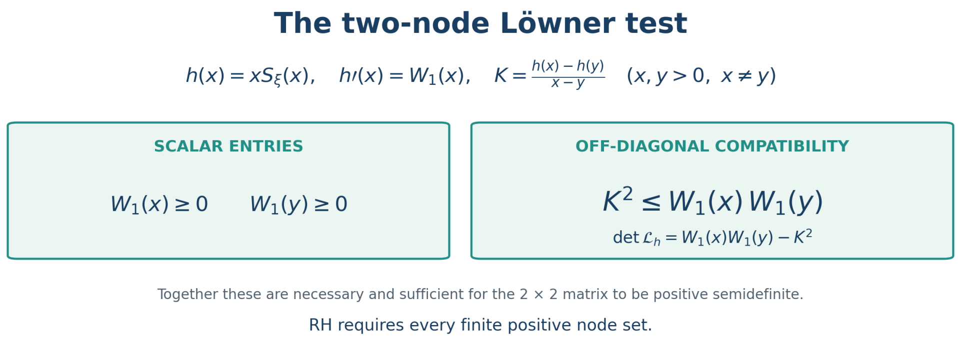

Figure 22: A two-node Löwner matrix tests off-diagonal compatibility as well as scalar signs. With $K = [h(x) - h(y)]/(x - y)$, positive semidefiniteness requires $K^2 \leq W_1(x)W_1(y)$. The global order-eight theorem already includes this two-node test. The all-size quantifier below is the remaining requirement.

Then

$$\boxed{\mathrm{RH} \iff \mathcal{L}_h(x_1, \ldots, x_N) \succeq 0 \quad \text{for every } N \text{ and every positive node set}} \tag{155.9}$$

On the safe source sheet

$$s_x = \sigma_x + i0 = \frac{1 + \sqrt{1 + 4x}}{2} > 1, \qquad R = 2s_x - 1 = \sqrt{1 + 4x} \tag{155.10}$$

the explicit formula splits

$$S_\xi(x) = \frac{1}{x} + G(x) - P(x) \tag{155.11}$$

with

$$G(x) = \frac{\psi((1 + R)/4) - \log \pi}{2R}, \qquad P(x) = \frac{1}{R} \sum_{n \geq 2} \frac{\Lambda_{\mathrm{vM}}(n)}{n^{s_x}} \tag{155.12}$$

Because constants disappear from divided differences,

$$\boxed{\mathcal{L}_h = L_\Gamma - L_P} \tag{155.13}$$

This is PP97's exact source gate. The 1×1 diagonal is

$$h'(x) = S_\xi(x) + xS'_\xi(x) = W_1(x) > 0 \tag{155.14}$$

but the full statement is

$$\boxed{L_\Gamma - L_P \succeq 0 \quad \text{for every rank and every positive node set}} \tag{155.15}$$

Equation (155.15) is equivalent to RH and remains unproved. Its diagonal, finite-rank, and finite-rung shadows must be kept separate:

layer	exact content	present authority
Li sequence	$\lambda_n \geq 0$ for all n	RH-equivalent; all-order sign open
folded moment	$[\mu_{i+j}] \succeq 0$ at all sizes	RH-equivalent; finite minors do not close it
Widder scalar	$W_k(x) \geq 0$ for every k, x	W_1 analytic; W_2–W_6 certified from the source (A-CAT); source-side $W_7 \rightsquigarrow F^{(14)}$ and the hierarchy open
local Dobsch	derivative matrices at one x_0 and all ranks	all-rank statement RH-equivalent
global Löwner	all positive node sets	ranks through eight certified; rank nine/all ranks open
source split	$\mathcal{L}_h = L_\Gamma - L_P$	identity exact; dominance (155.15) open

Reader §§R15–R16 display the Li–moment–matrix dictionary. The proof map in Reading Volume §R24 places its all-size positivity condition alongside the other RH criteria.

The global owner is the completed matrix $\mathcal{L}_h$. Its source-side Gamma and prime pieces are separately signed and nearly cancel. Positive translation-defect representations retain a negative scalar anchor, while compression to the scalar symbol in §159 loses off-line reflection data. These are concrete restrictions on a source proof, not a change of target.

155A. Reflected Li forms and explicit positive-node witnesses

Put $y = q^{-1}$ and $w = 1 - 1/\rho$. Reflection gives $w_{1-\rho} = w_\rho^{-1}$ and $y = 2 - w - w^{-1}$; conjugation is a different operation off the critical line. Define the polynomials $Q_n(y) = 2 - w^n - w^{-n}$ and $\mathcal{P}_m(y) = \sum_{r=-m}^{m} w^r$. They satisfy

$$\mathcal{P}_0 = 1, \quad \mathcal{P}_1 = 3 - y, \quad \mathcal{P}_{m+1} = (2 - y)\mathcal{P}_m - \mathcal{P}_{m-1}. \tag{155A.1}$$

The calligraphic symbol distinguishes these polynomials from the reciprocal polynomials of Section 171 and the source rows of Section 163.

Proposition 155A.1 (triangular coefficients and reflected squares). For $m \geq 0$,

$$\begin{aligned}
\mathcal{P}_m(y) &= \sum_{j=0}^{m} d_{m,j} y^j, \\
d_{m,j} &= (-1)^j (2m+1) \frac{(m+j)!}{(m-j)!(2j+1)!}, \\
\mathcal{P}_m(y) &= (2m+1) \sum_{j=0}^{m} \frac{(-2y)^j}{(2j+1)!} \prod_{r=0}^{j-1} (T_m - T_r), \\
Q_{2m+1}(y) &= y\mathcal{P}_m(y)^2, \\
y\mathcal{P}_r(y)\mathcal{P}_s(y) &= Q_{r+s+1}(y) - Q_{|r-s|}(y).
\end{aligned} \tag{155A.2}$$

Proof. The coefficient formula satisfies (155A.1) and its two initial conditions. The product formula follows from $(m+j)!/(m-j)! = \prod_{r<j}(m-r)(m+r+1) = 2^j \prod_{r<j}(T_m - T_r)$. Multiply $1 - w^{2m+1} = (1-w)w^m \mathcal{P}_m$ by its reciprocal-reflected version to get the square. For the cross identity, put $w = e^{i\theta}$: $\mathcal{P}_m = \sin((m+1/2)\theta)/\sin(\theta/2)$, and use the sine product identity. Polynomial identity extends the result from $0 < y < 4$ to all complex y. □

For the actual folded functional $\mathcal{L}[y^j] = \mu_j$, the fixed-degree sums converge absolutely because $\sum_q m_q/|q| < \infty$. Set $H_N = [\mu_{i+j}]_{0\le i,j<N}$ and $\mathsf{C}_N = [d_{i,j}]_{0\le i,j<N}$, with zero entries above the diagonal. Then

$$\boxed{K_{r,s} = \lambda_{r+s+1} - \lambda_{|r-s|}, \qquad K_N = \mathsf{C}_N H_N \mathsf{C}_N^{\mathsf{T}}, \qquad K_{m,m} = \lambda_{2m+1}.} \tag{155A.3}$$

Here $\lambda_0 = 0$ and $\det \mathsf{C}_N = (-1)^{N(N-1)/2}$, so the leading determinants and inertias agree. In particular $\lambda_3 = 9\mu_0 - 6\mu_1 + \mu_2$ and $\det K_2 = \lambda_1\lambda_3 - (\lambda_2 - \lambda_1)^2 = \mu_0\mu_2 - \mu_1^2$. The diagonal λ_{2m+1} already mixes the original off-diagonal data. These are holomorphic squares, not absolute squares; positive individual moments do not establish their signs.

The even counterpart. Put $\mathcal{B}_r(y) = \sum_{j=0}^{r}(-1)^j\binom{r+j+1}{2j+1}y^j = U_r(1-y/2)$. The same sine calculation gives

$$\begin{aligned} y(4-y)\mathcal{B}_r(y)\mathcal{B}_s(y) &= Q_{r+s+2}(y) - Q_{|r-s|}(y), \\ J_{r,s} &= \lambda_{r+s+2} - \lambda_{|r-s|}, \\ J_N &= \mathsf{B}_N[4\mu_{i+j} - \mu_{i+j+1}]\mathsf{B}_N^{\mathsf{T}}, \qquad J_{r,r} = \lambda_{2r+2}. \end{aligned} \tag{155A.4}$$

The coefficient matrix B_N is triangular with diagonal $(-1)^r$. The extra weight $4-y$ distinguishes the even and odd forms.

The diagonal cases. Putting $r = s = m$ in (155A.2) and $r = s = m-1$ in (155A.4), and using $Q_0 = 0$, prints the square form of every reflected rung in one place:

$$\boxed{Q_{2m+1}(y) = y\,\mathcal{P}_m(y)^2, \qquad Q_{2m}(y) = y(4-y)\,\mathcal{B}_{m-1}(y)^2} \tag{155A.4a}$$

The odd case is the fourth line of (155A.2); the even case is a specialization of (155A.4) and not an independent result. Both weights are nonnegative exactly on $0 \le y \le 4$, the interval that Reading Volume (10C.6) identifies with the critical-line condition for the orbit carrying y. The first rows are $Q_1 = y$, $Q_2 = y(4-y)$, $Q_3 = y(3-y)^2$, $Q_4 = y(4-y)(2-y)^2$ and $Q_5 = y(y^2 - 5y + 5)^2$. Reading Volume §R10C states the same pair as the endpoint of the pole-to-Li dictionary; nothing here constrains where the zeros lie, since λ_n sums Q_n over all orbits.

Theorem 155A.2 (the actual odd-subsequence criterion). For the actual Riemann function, RH is equivalent to eventual nonnegativity of λ_{2m+1}, and hence also to nonnegativity at every odd index.

Proof. Write $F(z) = \xi(1/(1-z))/\xi(1)$ and $D = F'/F$. The parity projection $A(z) = (D(z) + D(-z))/2 = \sum_{m\ge0}\lambda_{2m+1}z^{2m}$ is analytic near every real $0 \le z < 1$, since ξ has no real zeros. Eventual nonnegativity, after subtracting a polynomial, and Pringsheim's theorem force its Taylor radius to be at least one. If RH fails, a zero with $\Re\rho > 1/2$ gives a pole at $z_\rho = 1 - 1/\rho$ inside the disk. Its cancellation by $D(-z)$ would require a zero at $\rho/(2\rho-1)$, but

$$\left|\Im\frac{\rho}{2\rho-1}\right| = \frac{|\Im\rho|}{(2\Re\rho-1)^2 + 4(\Im\rho)^2} \le \frac{1}{4|\Im\rho|} < \frac{1}{4}.$$

This contradicts the low-height zero exclusion already implicit in the volume's first-zero input: every nontrivial zero has $|\Im\rho| > 1$. Thus the pole survives. Under RH, (155A.2) gives the converse term by term. No new low-height certificate is being claimed. □

A stronger version will be useful for a source bound. If RH fails, let $r_0 < 1$ be the least pole modulus of D. For a fixed $R > r_0$ before the next poles, subtraction of the finitely many poles a on $|a| = r_0$ gives

$$\lambda_n = -\sum_{|a|=r_0} m_a a^{-n} + O(R^{-n}). \tag{155A.5}$$

All these actual poles have $\Re a > 0$, by the same low-height exclusion. Simultaneous recurrence of the finitely many phases $2m \arg a$ to zero on their compact torus gives arbitrarily large m with $\sum m_a \cos((2m+1)\arg a)$ bounded below by a positive constant. (Recurrence follows by the pigeonhole principle on equal small torus boxes.) Consequently, for some $c > 0$, $\lambda_{2m+1} \le -cr_0^{-(2m+1)}$ infinitely often. Tied dominant poles have been retained, not replaced by one preferred zero.

Proposition 155A.3 (a constructive source witness). For fixed m, set $x_i = (i+1)\varepsilon$, $0 \le i \le m$, and

$$c_i(\varepsilon) = \frac{(-1)^i}{i!}\sum_{r=i}^{m} \frac{d_{m,r}}{(r-i)!\,\varepsilon^r}. \qquad \boxed{c(\varepsilon)^{\mathsf{T}}(L_\Gamma - L_P)c(\varepsilon) \longrightarrow \lambda_{2m+1}.} \tag{155A.6}$$

Proof. The elementary partial-fraction identity gives

$$\sum_{i=0}^{m} \frac{c_i(\varepsilon)}{q + x_i} = \sum_{r=0}^{m} \frac{d_{m,r}}{\prod_{j=0}^{r}(q + (j+1)\varepsilon)} \longrightarrow q^{-1}\mathcal{P}_m(q^{-1}).$$

The exact divided difference in (155.8) is $\sum_q m_q q/((x_i+q)(x_j+q))$. Thus its quadratic form tends to $\sum_q m_q q^{-1}\mathcal{P}_m(q^{-1})^2$. Since $\Re q > 0$, $|q + x_i| \ge |q|$; the summands for fixed m are bounded by $C_m m_q/|q|$, using the positive minimum of $|q|$. Dominated convergence proves (155A.6). □

A negative odd value therefore gives negative positive-node tests inside every neighborhood of zero. This is a necessary consequence, not a contradiction supplied by the source. At $m = 8$ it tests one rank-nine quadratic form involving moments through μ_{16}, not every rank-nine minor. Large coalescing coefficients require their own numerical error control.

155B. The regularized Li source and its triangular curvature

The preceding identities specify a source inequality at the boundary. Its regularization can be stated explicitly. Put

$$\Psi(X) = \sum_{\ell \le X} \Lambda_{\mathrm{vM}}(\ell), \quad M(u) = \Psi(e^u) - e^u + 1, \quad -\frac{\zeta'}{\zeta}(1+v) = \frac{1}{v} + \sum_{j \ge 0} \eta_j v^j. \tag{155B.1}$$

In particular $\eta_0 = -\gamma_E$. These are coefficients of the local regular part, not an unregularized Euler sum at $s = 1$.

Theorem 155B.1 (reserve and signed prime remainder). For every $n \ge 1$,

$$\begin{aligned} \mathcal{A}_n &= n\lambda_1 + \sum_{\substack{\ell \ge 3 \\ \ell \text{ odd}}} \left[(1 - 1/\ell)^n - 1 + n/\ell\right], \\ \mathcal{E}_n &= \sum_{j=2}^{n} \binom{n}{j} \eta_{j-1} = \int_0^\infty e^{-u} M(u) \left[L_{n-1}^{(2)}(u) - n\right] du, \\ \lambda_n &= \mathcal{A}_n - \mathcal{E}_n, \qquad \mathcal{A}_n \ge n\lambda_1 > 0, \qquad \mathcal{A}_n = \tfrac{1}{2} n \log n + O(n). \end{aligned} \tag{155B.2}$$

The symbols $\mathcal{A}_n, \mathcal{E}_n$ here do not denote the cutoff-row norm A_N or the energy $\mathscr{E}_N$. Nor is this renormalized scalar reserve the separately signed matrix L_Γ.

Proof of the split and reserve. For analytic g at one the Li operation is $\sum_{j=1}^{n} \binom{n}{j} g^{(j)}(1)/(j-1)!$. Apply it to $\log s + \log((s-1)\zeta(s)) - s \log \pi/2 + \log \Gamma(s/2)$. The polygamma series and the regular part in (155B.1) give

$$\lambda_n = 1 - \frac{n}{2}(\gamma_E + \log(4\pi)) + \sum_{j=2}^{n} (-1)^j \binom{n}{j} (1 - 2^{-j}) \zeta(j) - \sum_{j=1}^{n} \binom{n}{j} \eta_{j-1}. \tag{155B.3}$$

Separate η_0 and expand $(1 - 2^{-j})\zeta(j)$ over odd positive integers. The $\ell = 1$ sum is $n - 1$; the binomial theorem gives (155B.2) for the remaining denominators. For $0 \le z \le 1$ and $n \ge 2$,

$$0 \le (1-z)^n - 1 + nz = n(n-1) \int_0^z (z - v)(1 - v)^{n-2} dv \le \min\{nz, n(n-1)z^2/2\}.$$

This proves convergence and positivity. Splitting at $\ell = n$ and using the odd harmonic sum yields $n\lambda_1 \le \mathcal{A}_n \le n\lambda_1 + (n/2)\log n + (n-1)/2$. The lower bound $n/\ell - 1$ on the initial segment supplies the matching asymptotic. The case $n = 1$ is immediate.

Why the boundary integral exists. The classical prime-number-theorem error [3] supplies constants $C, a > 0$ with $|M(u)| \le Ce^{u - a\sqrt{u}}$, after enlargement on a compact interval. This is an unconditional existence bound, not a numerical interval certificate. It justifies every fixed-degree integral and endpoint limit below. For $v > 0$,

$$\int_0^\infty e^{-(1+v)u} dM(u) = -\frac{\zeta'}{\zeta}(1+v) - \frac{1}{v}.$$

Use $L_{n-1}^{(1)}(u)=\sum_{j=1}^{n}\binom{n}{j}(-u)^{j-1}/(j-1)!$ and $(e^{-u}L_{n-1}^{(1)}(u))'=-e^{-u}L_{n-1}^{(2)}(u)$. Integration by parts, followed by right differentiation at $v=0$, gives

$$\begin{aligned}\lim_{T\to\infty}\left[\sum_{\ell\le e^T}\frac{\Lambda_{\mathrm{vM}}(\ell)}{\ell}L_{n-1}^{(1)}(\log\ell)-\int_0^T L_{n-1}^{(1)}(u)du\right]&=\sum_{j=1}^{n}\binom{n}{j}\eta_{j-1}\\&=\int_0^\infty e^{-u}M(u)L_{n-1}^{(2)}(u)du.\end{aligned}\tag{155B.4}$$

The boundary term is $e^{-T}M(T)L_{n-1}^{(1)}(T)\to 0$ and $M(0)=0$. At $n=1$ the integral equals η_0; subtracting $n\eta_0$ proves the $-n$ subtraction in (155B.2). Omitting either subtraction changes the functional. $\square$

Corollary 155B.2 (the accumulated curvature target). Define $\mathcal{A}_0=\mathcal{E}_0=\lambda_0=0$ and $\Delta^2 f_n=f_{n+2}-2f_{n+1}+f_n$. Then

$$\begin{aligned}G_n&:=\Delta^2\mathcal{A}_n=\sum_{\substack{\ell\ge 3\\ \ell\text{ odd}}}\frac{(1-1/\ell)^n}{\ell^2}>0,\\ I_n&:=\Delta^2\mathcal{E}_n=\int_0^\infty e^{-u}M(u)L_{n+1}^{(0)}(u)du,\\ \lambda_N&=N\lambda_1+\sum_{n=0}^{N-2}(N-1-n)(G_n-I_n).\end{aligned}\tag{155B.5}$$

The first equality is a finite difference of the convergent reserve. The Laguerre recurrence $L_r^{(\alpha)}-L_{r-1}^{(\alpha)}=L_r^{(\alpha-1)}$ proves the second; $n=0$ follows from $L_1^{(0)}=1-u$. Twice summing finite differences proves the last line. The positive weights sum to T_{N-1}.

The unproved sign target is $\mathcal{E}_{2m+1}\le\mathcal{A}_{2m+1}$ for every m, equivalently the nonnegativity of (155B.5) at every odd N. An upper bound

$$\forall\epsilon>0\ \exists C_\epsilon<\infty\ \forall m\ge 0:\quad \mathcal{E}_{2m+1}\le C_\epsilon e^{\epsilon(2m+1)}\tag{155B.6}$$

already suffices, by (155A.5) and the growth of $\mathcal{A}_n$. Conversely RH implies $\mathcal{E}_n\le\mathcal{A}_n$, so (155B.6) is RH-equivalent. The constants and the all-rate quantifier matter.

The coefficientwise absolute PNT estimate does not prove (155B.6). It gives

$$|\mathcal{E}_n|\le 2C\left[\frac{n}{a^2}+\sum_{j=0}^{n-1}\binom{n+1}{j+2}\frac{(2j+1)!}{j!a^{2j+2}}\right].\tag{155B.7}$$

Its last summand has nth root asymptotic to $4n/(ea^2)$, so this particular majorant is superexponential. That is not a lower bound on $|\mathcal{E}_n|$. At $n=3$ the actual kernel is $u^2/2-4u+3$, of changing sign. Earlier nonnegative Li coefficients do not control the next triangular weighted sum; cancellation, not the reserve constant, is the missing source estimate.

155C. A compensated positive reserve and the arithmetic defect

Section 155B gives a positive scalar reserve $\mathcal{A}_n \geq n\lambda_1 > 0$. That does not make its reflected matrix positive. The obstruction and its exact repair can both be stated in the same polynomial basis as the actual completed matrix K_N.

Proposition 155C.1 (the original reserve is indefinite). Put $g_j = \sum_{\ell\geq 3,\ \ell \text{ odd}} \ell^{-j}$ for $j = 2, 3$. The first reserve block is

$$\mathsf{A}_2 = \begin{pmatrix} \lambda_1 & \lambda_1 + g_2 \\ \lambda_1 + g_2 & 3\lambda_1 + 3g_2 - g_3 \end{pmatrix}, \qquad (3,-1)\mathsf{A}_2(3,-1)^{\mathsf{T}} = 6\lambda_1 - 3g_2 - g_3 < -\frac{47}{600}. \quad (155\text{C}.1)$$

Proof. Expanding the first three reserves in (155B.2) gives the matrix. For an exact sign bound, the positive atanh series gives $\log 2 > 842/1215$ and $\log 3 > 263/240$. The decreasing sequence $H_n - \log n$ yields $\gamma_E < H_{32} - 5(842/1215) < 3/5$. Also $\pi > 3$ and $\log(4\pi) > \log 12 > 2(842/1215) + 263/240 > 99/40$. The formula $\lambda_1 = 1 + \gamma_E/2 - \log(4\pi)/2$ therefore gives $\lambda_1 < 1/16$. Since $g_2 > 1/9 + 1/25$ and $g_3 > 0$,

$$6\lambda_1 - 3g_2 - g_3 < \frac{3}{8} - 3\left(\frac{1}{9} + \frac{1}{25}\right) = -\frac{47}{600} < 0.$$

For example $\pi > 3$ itself follows by integrating the alternating lower polynomial $\sum_{k=0}^{7}(-1)^k t^{2k}$ for $(1+t^2)^{-1}$ on $[0,1]$. Every comparison used above is rational after these series bounds. Since $3\mathcal{P}_0 - \mathcal{P}_1 = y$, the direction is the y^2 moment of the reserve functional. It is not a counterexample to the actual completed matrix. □

Theorem 155C.2 (sharp linear anchor in the reserve family). For real c and $n \geq 0$ define

$$\begin{aligned} \mathcal{A}_n^{[c]} &= cn + \sum_{\substack{\ell\geq 3 \\ \ell \text{ odd}}} \left[(1-1/\ell)^n - 1 + n/\ell\right], \\ \mathsf{R}_N^{[c]} &= [\mathcal{A}_{r+s+1}^{[c]} - \mathcal{A}_{|r-s|}^{[c]}]_{0\leq r,s<N}. \end{aligned} \qquad (155\text{C}.2)$$

Put

$$\boxed{c_* = \sum_{\substack{\ell\geq 3 \\ \ell \text{ odd}}} \frac{1}{\ell(2\ell-1)} = \frac{\pi}{4} + \frac{\log 2}{2} - 1.} \qquad (155\text{C}.3)$$

Then

$$\boxed{\mathsf{R}_N^{[c]} \succeq 0 \quad \text{for every } N \geq 1 \quad \Longleftrightarrow \quad c \geq c_*.} \qquad (155\text{C}.4)$$

For $c \geq c_*$ every finite block is positive definite. At $c = c_*$ its Gram measure is the following Catalan measure times a resolvent weight:

$$\boxed{d\nu_+(y) = W(y)d\nu_C(y), \qquad W(y) = \sum_{\substack{\ell\geq 3\\ \ell \text{ odd}}} \frac{1}{(2\ell-1)[1+\ell(\ell-1)y]}, \quad 0<y<4.} \tag{155C.5}$$

Here ν_C is the probability measure (95A.4), while the mass of ν_+ is c_*. The sharpness assertion is within the family (155C.2), not an optimization over every possible comparison form.

Reconciliation from the Gamma pole lattice. The quarter-centered repair of the Gamma pole expansion has positive measures $d\sigma_m$. Under the reciprocal pushforward $y = 1/t \in (0,4)$, the sum over $m \geq 1$ is exactly the resolvent measure in (155C.5), while the $m = 0$ term is the Catalan measure itself. The total baseline cost is $\pi/4 + (\log 2)/2$, so after removing the $m = 0$ unit mass one recovers exactly c_* of (155C.3). Thus the pole-derived reserve is the existing compensated reserve in another coordinate, not a new positive owner.

Proof of the positive representation. Set $L = r+s+1$, $d = |r-s|$ and $h = L-d = 2\min(r,s)+1$. Under $y = 4\sin^2(\theta/2)$, the measure η of (95A.4) is $d\theta/\pi$. The cosine representation $\mathcal{P}_r = 1 + 2\sum_{j=1}^{r}\cos(j\theta)$ gives $\int \mathcal{P}_r\mathcal{P}_s\, d\eta = h$. For $0<t<1$ the convergent geometric Poisson kernel is

$$p_t(\theta) = \frac{1-t^2}{1-2t\cos\theta + t^2} = 1 + 2\sum_{j\geq 1} t^j\cos(j\theta).$$

The cross identity $y\mathcal{P}_r\mathcal{P}_s = 2\cos(d\theta) - 2\cos(L\theta)$ therefore gives $\int \mathcal{P}_r\mathcal{P}_s(y/2)p_t\, d\eta = t^d - t^L$. For $t = 1-1/\ell$ and $a_\ell = \ell(\ell-1)$, direct algebra yields

$$\frac{2}{2\ell-1} - \frac{y}{2}\frac{1-t^2}{(1-t)^2+ty} = \frac{4-y}{2(2\ell-1)(1+a_\ell y)}. \tag{155C.6}$$

Multiplying by $\mathcal{P}_r\mathcal{P}_s$ and integrating gives

$$\boxed{\int_0^4 \frac{\mathcal{P}_r(y)\mathcal{P}_s(y)}{(2\ell-1)(1+a_\ell y)}\, d\nu_C(y) = \frac{2h}{2\ell-1} - (t^d - t^L).} \tag{155C.7}$$

The right side equals the reflected difference of the single-ℓ term in (155C.2), plus $h/[\ell(2\ell-1)]$. At $r = s = 0$ it shows that this positive component measure has mass $1/[\ell(2\ell-1)]$. Tonelli and the summability of these masses justify the sum of measures; boundedness of every fixed polynomial on $[0,4]$ justifies every Gram entry. Consequently

$$[\mathsf{R}_N^{[c_*]}]_{r,s} = \int_0^4 \mathcal{P}_r(y)\mathcal{P}_s(y)d\nu_+(y), \qquad \nu_+([0,4]) = c_*. \tag{155C.8}$$

The density is positive on $(0,4)$, so every nonzero polynomial has strictly positive squared integral. This proves positive definiteness. For general c the representing finite signed measure is $\nu_c = \nu_+ + (c-c_*)\eta$, which is positive if $c \geq c_*$.

Sharpness. Near $y = 4$ the terms of W have a uniformly summable $O(\ell^{-3})$ bound, so W is continuous and finite there. The density of ν_c relative to η is $(4-y)W(y)/2 + c - c_*$ and tends to $c - c_*$. If $c < c_*$, it is negative on an interval next to 4. Choose a nonzero continuous squared test supported inside that interval and approximate its square root uniformly by polynomials. Finite total variation passes its negative integral to some polynomial square. Because the $\mathcal{P}_r$ span the polynomials, some finite block then has a negative direction. This proves the reverse implication in (155C.4).

Finally the absolutely convergent sum in (155C.3) equals

$$c_* = \frac{1}{2}\int_0^1 \frac{x^{1/4} - x^{1/2}}{1-x}dx = 2\int_0^1 \frac{t^4}{(1+t)(1+t^2)}dt = \frac{\pi}{4} + \frac{\log 2}{2} - 1. \tag{155C.9}$$

The substitution is $x = t^4$; polynomial division and partial fractions evaluate the last integral. $\square$

A second finite-entry calculation. The Catalan transform is

$$\int_0^4 \frac{d\nu_C(y)}{1+ay} = \frac{2}{1+\sqrt{1+4a}}, \qquad a \geq 0. \tag{155C.10}$$

The substitution of (95A.4) and the elementary integral of $(1 + 2a - 2a\cos\theta)^{-1}$ prove it, with continuity at $a = 0$. At $a = a_\ell$ its value is $1/\ell$, independently checking the component mass in (155C.7). If $M_{j,\ell} = \int y^j/(1+a_\ell y)d\nu_C$, then $M_{0,\ell} = 1/\ell$ and $M_{j,\ell} = (C_{j-1} - M_{j-1,\ell})/a_\ell$ for $j \geq 1$. These exact rational moments give a separate route to every finite entry.

The same weight as an operator trace. Restrict $A_\triangle$ of Section 12A to the closed span of ψ_{2r}, $r \geq 1$, and denote the restriction by A_{e}. Its eigenvalues and odd coordinates are $a_r = 2T_{2r} = (2r)(2r+1)$ and $\sqrt{1+4a_r} = 4r+1$. Substitution $\ell = 2r+1$ in (155C.5) proves

$$\boxed{W(y) = \mathrm{Tr}\big[(I + 4A_{\mathrm{e}})^{-1/2}(I + yA_{\mathrm{e}})^{-1}\big], \qquad y > 0.} \tag{155C.11}$$

The terms are $O_y(r^{-3})$. At $y = 0$ this trace diverges, although $W(y)d\nu_C(y)$ has the finite mass already proved. It is a weighted resolvent trace, not the unweighted resolvent or a bounded endpoint multiplier. It uses exactly the even-triangular indices of Section 133A, but does not identify them with the actual folded zeros.

Corollary 155C.3 (positive reserve minus the complete defect). Put $\delta = c_* - \lambda_1 > 0$, and shift both source channels:

$$\mathcal{A}_n^+ = \mathcal{A}_n + \delta n, \qquad \mathcal{E}_n^+ = \mathcal{E}_n + \delta n, \qquad \lambda_n = \mathcal{A}_n^+ - \mathcal{E}_n^+. \tag{155C.12}$$

The positivity of δ follows from $\lambda_1 < 1/16$ and the first four positive terms of c_*, whose sum exceeds $1/10$. For orientation, $c_* = 0.1319717536774209643\ldots$ and $\delta = 0.1088760447112999305\ldots$; these decimals are not certificates. Define, for $0 \leq r, s < N$,

$$\begin{aligned}
[\mathsf{R}_N]_{r,s} &= \mathcal{A}^+_{r+s+1} - \mathcal{A}^+_{|r-s|}, & \mathsf{R}_N \succ 0,\\
[\mathsf{D}_N]_{r,s} &= \mathcal{E}_{r+s+1} - \mathcal{E}_{|r-s|} + \delta(2\min(r,s)+1), \quad & K_N = \mathsf{R}_N - \mathsf{D}_N.
\end{aligned} \tag{155C.13}$$

The reserve is exactly the Gram matrix (155C.8). For an explicit prime expression set $\Phi_0(u) = 0$ and $\Phi_n(u) = L^{(2)}_{n-1}(u) - n$ for $n \ge 1$. Then

$$[\mathsf{D}_N]_{r,s} = \delta(2\min(r,s)+1) + \int_0^\infty e^{-u} M(u)[\Phi_{r+s+1}(u) - \Phi_{|r-s|}(u)]du. \tag{155C.14}$$

Here $M(u) = \Psi(e^u) - e^u + 1$ is exactly (155B.1). All fixed-degree integrals converge by Theorem 155B.1. The $-n$ subtraction is retained, and Φ_0 is defined separately rather than using $L^{(2)}_{-1}$. Equations (155C.12)–(155C.14) follow by subtraction; omitting the compensation $\delta(2\min(r,s)+1)$ would change the source. □

The remaining comparison is

$$\boxed{\mathsf{D}_N \preceq \mathsf{R}_N \quad \text{for every } N \ge 1.} \tag{155C.15}$$

It is equivalent to requiring the largest eigenvalue of $\mathsf{R}_N^{-1/2}\mathsf{D}_N\mathsf{R}_N^{-1/2}$ to be at most one at every rank. This is a one-sided form bound: it does not require D_N positive or its absolute operator norm bounded by one. By Section 155A's congruence, it is RH-equivalent and remains unproved. Its diagonal condition cancels the adjustment and is precisely $\mathcal{E}_{2m+1} \le \mathcal{A}_{2m+1}$, the existing odd-Li target. Thus the positive reserve has not supplied a hidden sign proof.

This is a boundary comparison. No isometric identification with the full Bernstein–Laguerre row at $a = 2$ is asserted. Section 166F defines and approximates a separate equivalent target directly at scale two. Section 166G reconstructs the actual boundary block from a finite Taylor polynomial of the full cutoff source at two, with a uniform normalized error. Its coupled degree and cutoff are essential; it does not evaluate the raw cutoff at zero or prove the source upper bound.

155D. Reserve growth and the one-sided source criterion

This section keeps the completed reserve/defect problem in the reflected polynomial basis while suppressing the longer conditioning derivation retained in earlier editions. For nonzero p of degree $< N$ let $\mathcal{R}[p]$ be the positive reserve form and $\mathcal{D}[p]$ the actual completed defect. The extremal generalized eigenvalues are

$$\beta_N^+ = \sup_{p\neq 0} \frac{\mathcal{D}[p]}{\mathcal{R}[p]}, \qquad \beta_N^- = \inf_{p\neq 0} \frac{\mathcal{D}[p]}{\mathcal{R}[p]}. \tag{155D.2}$$

Polynomial conditioning of the reserve

With $y = 2 - 2\cos\theta$, the third-kind Chebyshev basis

$$V_j(y) = \frac{\cos((j+\frac{1}{2})\theta)}{\cos(\theta/2)}, \qquad d\nu_C = \frac{2}{\pi}\cos^2(\theta/2)d\theta \tag{155D.4}$$

is orthonormal for the Catalan measure. The reflected basis has Gram matrix

$$(G_N)_{rs} = \begin{cases} 4r+1 & r=s, \\ 4\min(r,s)+2 & r \neq s, \end{cases} \tag{155D.5}$$

and the explicit inverse gives the two-sided conditioning estimate

$$\boxed{\frac{I}{125(2N^2-1)} \preceq \mathsf{R}_N \preceq \frac{c_* N(4N^2-1)}{3} I.} \tag{155D.6}$$

Thus the reserve costs only polynomial factors in N.

Spectral growth and the exact criterion

For $y \notin [0,4]$ write $w + w^{-1} = 2 - y$, $|w| > 1$, and put $r(y) = |w|$; set $r(y) = 1$ on $[0,4]$. At actual folded zeros this is the reciprocal Li coordinate,

$$\chi_\rho = 1 - \rho^{-1}, \qquad \mathfrak{L} = \sup_\rho |\chi_\rho| = \sup_{[\rho]} r(y_\rho) \geq 1. \tag{155D.8}$$

The reserve bounds and the Chebyshev expansion imply

$$\|\mathsf{Z}_N\|_{\mathrm{op}} \leq 1 + 125 M_1 N(2N-1)^2 \mathfrak{L}^{2N-2}. \tag{155D.10}$$

The converse exponential rate is obtained from one maximizing nonreal folded orbit. Hence the actual one-sided source problem is exactly

$$\boxed{\begin{aligned} \mathrm{RH} &\iff \forall \epsilon > 0\ \exists C_\epsilon\ \forall N:\ \mathsf{D}_N \preceq C_\epsilon e^{\epsilon N} \mathsf{R}_N \\ &\iff \exists C, A \geq 0\ \forall N:\ \mathsf{D}_N \preceq C(1+N)^A \mathsf{R}_N \\ &\iff \|\mathsf{Z}_N\|_{\mathrm{op}} = O(N) \iff \|\mathsf{Z}_N\|_{\mathrm{op}} \text{ is polynomially bounded.} \end{aligned}} \tag{155D.11}$$

No inequality in this display is proved for the actual source; the theorem identifies the strength required.

The linear compensation remains controlled. With $d\eta = dy/[\pi\sqrt{y(4-y)}]$ and $\mathcal{H}[p] = \int p^2 d\eta$,

$$0 \leq \delta\mathcal{H}[p] \leq 125\delta N^2 \mathcal{R}[p], \qquad \deg p < N. \tag{155D.13}$$

Thus the open term is the signed arithmetic remainder after this explicit reserve and compensation are retained. The longer basis inversion and extremal-orbit proof are preserved in the edition-4.6 package of the Zenodo version chain.

155E. Curvature, progression filters, and cosine coordinates

Let $M(u) = \Psi(e^u) - e^u + 1$ and

$$I_n = \int_0^\infty e^{-u} M(u) L_{n+1}^{(0)}(u)\,du.$$

For the actual boundary source, $\mathcal{E}_0 = \mathcal{E}_1 = 0$ and

$$\mathcal{E}_N = \sum_{n=0}^{N-2} (N-1-n) I_n. \tag{155E.1}$$

Theorem 155E.1 (one-sided scalar criterion). The following are equivalent:

$$\boxed{\begin{aligned} \mathrm{RH} &\iff \sup_{n\ge 0} I_n < \infty \\ &\iff \exists C, A \ge 0\ \forall n:\ \ I_n \le C(1+n)^A \\ &\iff \forall \epsilon > 0\ \exists C_\epsilon\ \forall n:\ \ I_n \le C_\epsilon e^{\epsilon n}. \end{aligned}} \tag{155E.2}$$

The upper bounds may hold only eventually. Under RH one has the stronger uniform estimate

$$|I_n| \le \frac{\pi^2}{8} - 1 + 2\lambda_1. \tag{155E.3}$$

The proof is short: under RH, second differences of the absolutely grouped Li sum are bounded trigonometric moments; conversely (155E.1) turns any all-rate one-sided upper bound into the odd-index source criterion of §155B.

The generating function and its poles

With $H_{\mathrm{reg}}(s) = -\zeta'(s)/\zeta(s) - 1/(s-1)$,

$$\mathcal{I}(z) = \sum_{n\ge 0} I_n z^n = \frac{H_{\mathrm{reg}}(1/(1-z)) + \gamma_E}{z}. \tag{155E.4}$$

A zero ρ contributes the genuine pole

$$z_\rho = 1 - \rho^{-1}, \qquad \operatorname*{Res}_{z=z_\rho} \mathcal{I}(z) = -\frac{m_\rho}{z_\rho \rho^2} \ne 0. \tag{155E.5}$$

Pringsheim's theorem applied separately to the positive and negative coefficient parts gives the same exponential obstruction on either sign. Admissible arithmetic progressions retain it when the pole angles cannot collide; arbitrary sparse subsequences do not inherit that conclusion.

Cosine-coordinate matrix

After the adjacent-difference basis change the arithmetic defect has the Toeplitz-plus-Hankel form

$$\begin{gathered}\widetilde{\mathsf{D}}_d = \delta I_d + \widetilde{\mathsf{E}}_d,\\ \widetilde{\mathsf{E}}_{00} = 0, \quad \widetilde{\mathsf{E}}_{0r} = J_r/\sqrt{2}, \quad \widetilde{\mathsf{E}}_{rs} = (J_{r+s} + J_{|r-s|})/2.\end{gathered} \tag{155E.14}$$

The reserve obeys

$$\widetilde{\mathsf{R}}_d \succeq \frac{1-\cos(\pi/(2d))}{125} I_d. \tag{155E.15}$$

Therefore a polynomial one-sided bound on either parity of I_n is an explicit sufficient arithmetic target for RH. The detailed progression angle estimate and cosine-basis diagonalization remain in earlier editions.

155F. Direct curvature cutoffs and the envelope obstruction

Section 155E isolates the actual curvature $I_{k-1} = \int_0^\infty e^{-u} M(u) L_k^{(0)}(u)du$, with $M(u) = \Psi(e^u) - e^u + 1$. A finite approximation must retain its regularization. This section gives one directly on the real axis; Section 166G gives a different boundary approximation from completed Taylor data at two. Neither proves the source upper bound.

For $U > 0$ fill the removable quotient at $v = 0$ and define

$$\begin{aligned}\widehat{H}_U(v) &= \sum_{2\le n\le e^U} \frac{\Lambda(n)}{n^{1+v}} - \frac{1-e^{-vU}}{v},\\ \widehat{I}_{k-1}(U) &= \sum_{2\le n\le e^U} \frac{\Lambda(n)}{n} L_k^{(-1)}(\log n) + L_{k+1}^{(-2)}(U), \qquad k \ge 1.\end{aligned} \tag{155F.1}$$

The first function is entire in v and approximates the regular part $H_{\mathrm{reg}}(1+v)$, not the unregularized Euler sum. Negative Laguerre parameters here denote finite polynomial continuations; they do not assert positive-weight orthogonality.

Proposition 155F.1 (finite regularization). For $U > 0$ and $k \ge 1$,

$$\boxed{\int_0^U e^{-u} M(u) L_k^{(0)}(u)du = \widehat{I}_{k-1}(U) - e^{-U} M(U) L_k^{(-1)}(U).} \tag{155F.2}$$

Proof. The polynomial identities $(e^{-u}L_k^{(-1)}(u))' = -e^{-u}L_k^{(0)}(u)$ and $(L_{k+1}^{(-2)}(u))' = -L_k^{(-1)}(u)$ have the required zero endpoint values at $u = 0$. Integrate by parts against $dM = \sum_{n\ge2} \Lambda(n)\delta_{\log n} - e^u du$. The atoms give the finite prime sum; the continuous term gives the polynomial counterterm; the remaining endpoint has the displayed minus sign. At a prime-power cutoff the atom and endpoint jumps cancel. □

For example $\widehat{I}_0(U) = U^2/2 - \sum_{n \le e^U} \Lambda(n)(\log n)/n$. Omitting its $U^2/2$ does not approximate I_0. Omitting the endpoint from (155F.2) is also incorrect; it can be omitted from an approximant only with its error included.

Theorem 155F.2 (uniform direct-boundary remainder). Retain the existence constants $C, c > 0$ in the PNT estimate $|M(u)| \le Ce^{u-c\sqrt{u}}$, enlarged on a compact interval as in Section 155B. For $K \ge 1$, $U \ge K$ and $v = c\sqrt{U}$, set

$$e_K(U) = \frac{Ce^{K^2/U}}{K!}\left[U^K e^{-v} + \frac{2}{c^{2K+2}}\Gamma(2K+2, v)\right]. \qquad \max_{1 \le k \le K} |I_{k-1} - \widehat{I}_{k-1}(U)| \le e_K(U). \tag{155F.3}$$

Here $\Gamma(s, v) = \int_v^\infty t^{s-1}e^{-t}dt$ is the upper incomplete Gamma function. These are not newly certified numerical constants for the primes.

Proof. Reversing the finite coefficients gives $|L_k^{(0)}(u)| \le (u^k/k!)\sum_{r=0}^k k^{2r}/(r!u^r) \le u^k e^{k^2/u}/k!$. The absolute coefficients of $L_k^{(-1)}$ are no larger. For $u \ge U \ge K$ and $k \le K$ both are bounded by $u^K e^{K^2/U}/K!$. Apply the PNT estimate to the endpoint and the remaining integral in (155F.2), using $\int_U^\infty u^K e^{-c\sqrt{u}}du = 2c^{-2K-2}\Gamma(2K+2, c\sqrt{U})$. $\square$

For any fixed $\eta > 0$, a sufficient schedule is

$$U_K = \max\left\{K, \left[\frac{(1+\eta)K\log(K+2)}{c}\right]^2\right\}, \tag{155F.4}$$
$$\log e_K(U_K) = -\eta K \log K + 2K \log\log K + O_{C,c,\eta}(K).$$

Indeed, for $v > 2K+1$ the incomplete Gamma term is between $v^{2K+1}e^{-v}$ and that quantity divided by $1-(2K+1)/v$. Substitute $v = (1+\eta)K\log(K+2)$ and use Stirling's formula. The error is smaller than every fixed exponential in degree, but the prime cutoff is $X = e^{U_K}$, much larger than the exponential-in-rank Taylor cutoff of Section 166G. No necessity or optimality is asserted.

In the cosine coordinates (155E.14), replace each I_n by its approximant, keep $J_0 = 0$, and retain the entire compensation δI_d. For $d \ge 2$ the highest index is $2d-3$. The row-sum bound and (155E.15) give

$$\left\|\widetilde{R}_d^{-1/2}(\widetilde{D}_d - \widehat{\widetilde{D}}_{d,U})\widetilde{R}_d^{-1/2}\right\|_{\mathrm{op}} \le \frac{125d}{1-\cos(\pi/(2d))}\, e_{2d-2}(U). \tag{155F.5}$$

Its prefactor is $O(d^3)$, so (155F.4) controls the full mixed block. This is a second boundary approximant, not an identification with the Taylor polynomial or a sign theorem for either matrix.

What the absolute PNT envelope loses

Put $F_k(c) = 2(2k+1)!/(k!c^{2k+2})$ and $Q_k(c) = \int_0^\infty e^{-c\sqrt{u}}L_k^{(0)}(u)du$. Then

$$\begin{aligned} Q_k(c) &= (-1)^k F_k(c)(e^{-c^2/4}+o(1)), \\ \left(\int_0^\infty e^{-c\sqrt{u}}|L_k^{(0)}(u)|du\right)^{1/k} &\sim \frac{4k}{ec^2}. \end{aligned} \tag{155F.6}$$

To prove both assertions, integrate the finite expansion and reverse its index. The ratio $(-1)^k Q_k/F_k$ is $\sum_{r=0}^k (-1)^r A_{k,r}$, where

$$A_{k,r} = \frac{1}{r!}\prod_{j=0}^{r-1}\frac{c^2(k-j)}{2(2(k-j)+1)} \longrightarrow \frac{(c^2/4)^r}{r!}, \qquad 0 \le A_{k,r} \le \frac{(c^2/4)^r}{r!}. \tag{155F.7}$$

Dominated convergence gives the signed limit. The absolute integral lies between $|Q_k|$ and $F_k e^{c^2/4}$; factorial asymptotics give its root limit. Thus preserving the Laguerre oscillation alone does not repair an estimate that has already replaced the actual remainder by this envelope. It is not a lower bound on the actual I_n.

One fixed positive counting measure shows that the obstruction is also one-sided. Let $F(X) = (X-1)(1-e^{-\sqrt{\log X}})$ for $X \ge 1$ and $\widetilde{\Psi}_s = F$. It is increasing and nonnegative, with remainder $\widetilde{M}_s(u) = -(e^u-1)e^{-\sqrt{u}}$. At $c=1$ the alternating sum in (155F.7) is at least $3/4$. Since $\int_0^\infty e^{-u}|L_k(u)|du \le 2^k$, odd $k = 2m+1$ give

$$\widetilde{I}_{2m,s} \ge \frac{3}{2}\frac{(4m+3)!}{(2m+1)!} - 2^{2m+1}. \tag{155F.8}$$

The integer-supported version $\widetilde{\Psi}_d(X) = F(\lfloor X \rfloor)$ has positive weights $F(n)-F(n-1)$ at $n \ge 2$. Differentiation gives $0 \le F' \le 3/2$ (use $(1-e^{-t})/\sqrt{t} \le 1$). Hence

$$\begin{aligned} |\widetilde{M}_d(u)| &\le (1+\tfrac{3}{2}e^{1/4})e^{u-\sqrt{u}}, \\ \widetilde{I}_{2m,d} &\ge \frac{3}{2}\frac{(4m+3)!}{(2m+1)!} - \frac{5}{2}\,2^{2m+1}. \end{aligned} \tag{155F.9}$$

These are artificial measures, not the von Mangoldt measure or a Gamma-completed zeta function. They show that a PNT-quality envelope, monotonicity, nonnegative weights and integer support do not alone force the curvature upper bound. The next section keeps prime-power support as well, and identifies the arithmetic it still does not retain.

155G. The actual denominator and the limits of positive prime support

Define the disk function

$$\mathcal{B}(z) = z\zeta\left(\frac{1}{1-z}\right) = \sum_{n\ge 0} b_n^{\mathrm{den}} z^n, \qquad \mathcal{B}(0) = 1. \tag{155G.1}$$

Its zeros in $|z| < 1$ are exactly the right-half-strip images $1 - 1/\rho$. Combining $\mathcal{B}$ with the curvature generating function of §155E gives the exact signed recurrence

$$\boxed{\sum_{j=0}^{n} b_j^{\mathrm{den}} I_{n-j} = -(n+2)b_{n+2}^{\mathrm{den}} + (2n + \gamma_E + 1)b_{n+1}^{\mathrm{den}} + (1-n)b_n^{\mathrm{den}}.} \tag{155G.3}$$

It is a convolution identity, not a positivity recurrence. Already $b_1^{\mathrm{den}} = \gamma_E - 1 < 0$, from the Laurent expansion of ζ at $s = 1$. Numerically $b_2^{\mathrm{den}}, \dots, b_{16}^{\mathrm{den}}$ are positive, and a directed Euler–Maclaurin certificate gives $b_{17}^{\mathrm{den}} < 0$, where the sign changes again. Neither sign is a negative Li coefficient or a negative Widder rung.

The coefficients are square summable with the classical normalization

$$\boxed{\sum_{n\geq 0} (b_n^{\mathrm{den}})^2 = \log(2\pi) - \gamma_E.} \tag{155G.6}$$

but not absolutely summable. Thus an unweighted Neumann/Rouche argument is unavailable; finite-radius control additionally needs a lower bound for the truncated denominator. The constant in (155G.6) is the one of Theorem 96A.3: by (96A.5) it is also $\sum_{k\geq 2} \zeta(k)/T_k$ and a weighted mean square of ζ on the critical line.

The prime-supported countermodel retained from earlier editions is deliberately stronger than a cardinality toy model: it keeps positive prime-power weights, a PNT-size envelope, a meromorphic Euler product and an arbitrarily long exact prime prefix, yet introduces a conjugate pair of interior poles. Its role is only to show that those reduced hypotheses do not imply the required one-sided curvature bound. It is not a model of the completed functional equation and is not a counterexample to RH.

The next section therefore restores the exact divisor arithmetic. Full coefficient enclosures, the countermodel Euler product and its pole separation are retained in earlier editions.

155H. Exact divisor arithmetic and a Mellin squared-error target

Here $\mu(d)$ is the Möbius function, not a boundary moment μ_j. The actual primitive factors satisfy $\Lambda * 1 = \log$, $\mu * 1 = \delta_1$ and $\Lambda = \mu * \log$. In particular, for $N = \lfloor X \rfloor$ and $H_N = \sum_{k\leq N} 1/k$,

$$\boxed{\sum_{k=1}^{N} M\left(\log \frac{X}{k}\right) = \log(N!) - XH_N + N.} \tag{155H.1}$$

Finite reordering gives $\sum_{k\leq N} \Psi(X/k) = \sum_{d\leq N} \Lambda(d)\lfloor X/d \rfloor$. Regrouping by the product gives $\sum_{n\leq N} \sum_{d|n} \Lambda(d) = \log(N!)$. Both subtractions in M are retained. The perturbed weights in Section 155G add the discrepancy $\sum_{n\leq N}(\sum_{d|n} \widetilde{\Lambda}_P(d) - \log n)$. Thus (155H.1) uses information absent from that model, but alone supplies no sign for the delayed, correlated Laguerre transforms.

Take finitely supported real coefficients c_d with $\sum_d c_d/d = 0$, and define

$$\begin{aligned} D_c(s) &= \sum_d c_d d^{-s}, & h_c(x) &= 1 - \sum_d c_d \lfloor x/d \rfloor, \\ \mathscr{N}(c) &= \int_1^\infty h_c(x)^2 \frac{dx}{x^2} & &= \sum_{n\geq 1} \frac{(1-\sum_d c_d\lfloor n/d\rfloor)^2}{n(n+1)}. \end{aligned} \tag{155H.2}$$

The scalar D_c is not the defect matrix D_d; this Mellin error is not a Bernstein row energy. Balance gives $h_c = 1 + \sum_d c_d\{x/d\}$ and $|h_c| \leq 1 + \sum |c_d|$, so the norm is finite. Jumps occur at integers, proving the series. The weight $1/[n(n+1)] = 1/(2T_n)$ is exactly the integral of x^{-2} over that unit interval. The square follows the signed divisor sum.

Proposition 155H.1 (Mellin identity). For $\Re s > 0$,

$$\begin{aligned} E_c(s) &:= \int_1^\infty h_c(x) x^{-s-1} dx = \frac{1-\zeta(s)D_c(s)}{s}, \\ \mathscr{N}(c) &= \frac{1}{2\pi}\int_{\mathbb{R}} |E_c(1/2+it)|^2 dt. \end{aligned} \tag{155H.3}$$

Proof. For $\Re s > 1$, each floor integral equals $\zeta(s)d^{-s}/s$. Summing proves the identity there. The bounded error makes its integral holomorphic for $\Re s > 0$; $D_c(1) = 0$ cancels the zeta pole, so continuation proves it throughout. At $x = e^u$, $h_c(e^u)e^{-u/2}$ lies in $L^1 \cap L^2$ on $u \geq 0$; Fourier Plancherel gives the factor $1/(2\pi)$ and the norm. □

If L is a common multiple of the support indices, balance also gives $h_c(n+L) = h_c(n)$. Summing through T has the rigorous tail budget

$$0 \leq \mathscr{N}(c) - \sum_{n=1}^{T} \frac{h_c(n)^2}{n(n+1)} \leq \frac{(1+\sum_d |c_d|)^2}{T+1}. \tag{155H.4}$$

Exact-prefix cancellation and zero detection

Require additionally $c_d = \mu(d)$ for $1 \leq d \leq K$. The inverse-divisor identity gives $\sum_{d\leq n} \mu(d)\lfloor n/d\rfloor = 1$ for every $n \geq 1$; coefficients beyond K cannot affect the first K intervals. Thus $h_c(x) = 0$ for $1 \leq x < K+1$.

Theorem 155H.2. Every actual zero $\rho = \sigma + i\gamma$ with $\sigma > 1/2$ forces, for every balanced exact-prefix family,

$$\boxed{\mathscr{N}(c) \geq \frac{2\sigma-1}{|\rho|^2}(K+1)^{2\sigma-1}.} \tag{155H.5}$$

Proof. At a zero, $E_c(\rho) = 1/\rho$. By the vanishing prefix and Cauchy–Schwarz, $|\rho|^{-2} \leq \mathscr{N}(c)\int_{K+1}^\infty x^{-2\sigma}dx = \mathscr{N}(c)(K+1)^{1-2\sigma}/(2\sigma-1)$. No phase selection or verified height is used.

□

Consequently the following is sufficient for RH, even along one fixed unbounded sequence of actual prefix lengths:

$$\boxed{\forall\epsilon>0\ \exists C_\epsilon<\infty\ \forall K:\quad \mathscr{N}(c^{(K)})\le C_\epsilon(K+1)^\epsilon.} \tag{155H.6}$$

The family must be specified and preserve balance and the exact prefix. No converse is asserted for an arbitrary choice of extensions. A fixed $O(K^a)$ bound, $0\le a<1$, excludes only $\Re\rho>(1+a)/2$, and reflection gives the corresponding symmetric strip. Unlike a polynomial matrix-rank allowance, the prefix-length allowance here must be below every positive power.

One explicit balanced extension is

$$a_K=\sum_{d\le K}\frac{\mu(d)}{d},\quad q=K+1,\qquad D_K(s)=\sum_{d\le K}\mu(d)d^{-s}-q\,a_Kq^{-s},\qquad \mathscr{N}(c^{(K)})\le 4(K+1). \tag{155H.7}$$

Indeed $Ka_K=1+\sum_{d\le K}\mu(d)\{K/d\}$ gives $|a_K|\le 1$. Then $|h_c|\le 2(K+1)$ and its vanishing prefix gives the displayed linear bound. For $\sigma=\Re s>1$ the same family satisfies

$$\left|D_K(s)-\frac{1}{\zeta(s)}\right|\le\frac{K^{1-\sigma}}{\sigma-1}+(K+1)^{1-\sigma}\longrightarrow 0. \tag{155H.8}$$

This is safe-half-plane convergence, not the missing subpower norm estimate. At $K=1$, $D_1(s)=1-2^{1-s}$ and $h_c(n)$ is one for even n, zero for odd n, giving

$$\mathscr{N}(c^{(1)})=\sum_{j\ge1}\frac{1}{2j(2j+1)}=1-\log 2. \tag{155H.9}$$

Why a natural balanced primitive product fails

For integer $P\ge 2$ set $Q_P=\prod_{p\le P}p$ and

$$A_P(s)=\prod_{p\le P}(1-p^{-s})=\sum_{d|Q_P}\mu(d)d^{-s},\quad \alpha_P=A_P(1),\quad D_P^{\mathrm{E}}(s)=A_P(s)-\alpha_P. \tag{155H.10}$$

This uses actual inverse Euler factors. The subtraction enforces balance, but changes the coefficient at one: it is not an exact-prefix family. Although $A_P\to 1/\zeta$ for $\Re s>1$ and $\alpha_P^{-1}\ge H_P\to\infty$, the norm satisfies

$$\boxed{\mathscr{N}(c^{\mathrm{E,P}})\ge\alpha_P^2(P+1-H_{P+1})\ge\frac{P^{1/3}}{18e^2}\longrightarrow\infty\quad(P\ge5).} \tag{155H.11}$$

Proof. Inclusion–exclusion makes $\sum_{d|Q_P}\mu(d)\lfloor n/d\rfloor$ count the integers at most n coprime to Q_P. Only one survives for $1\le n\le P$. The balancing correction therefore makes

$h_{\mathrm{E,P}}(n) = \alpha_P n$. Their contribution to (155H.2) is the first lower bound. For an elementary product bound, adding all integers coprime to six gives $\alpha_P \geq \frac{1}{3}\prod_{5\leq n\leq P,(n,6)=1}(1-1/n)$. Use $-\log(1-1/n) \leq 1/n + 1/[2n(n-1)]$ and pair $6j-1, 6j+1$. Their reciprocal sum through $J = \lceil (P+1)/6 \rceil \leq P$ is at most $(\log P + 1)/3 + 1/70$, since $1/(6j-1) + 1/(6j+1) = 1/(3j) + 1/[3j(36j^2-1)]$. The remaining logarithm error is at most $1/8$, and $1/3+1/70+1/8 < 1$. Thus $\alpha_P \geq e^{-1}/(3P^{1/3})$. Finally $P + 1 - H_{P+1} \geq P/2$. □

Even division by $1-\alpha_P$ to restore the first coefficient leaves the ramp $\alpha_P(n-1)/(1-\alpha_P)$ and a positive multiple of the same $P^{1/3}$ lower bound. This excludes the displayed balancing scheme, not all Euler products or mollifiers. The successful family would need an upper bound such as (155H.6); neither tested construction provides it. The framework is classical Mellin/fractional-part approximation, with no claim of literature priority.

155I. One denominator residual, Mellin norm, and Laguerre expansion

The denominator of Section 155G and the balanced arithmetic approximant of Section 155H are connected by an exact norm identity. Keep the same c_d, D_c, h_c and $\mathscr{N}(c)$; put $s(z) = 1/(1-z)$ and

$$\begin{aligned} \mathcal{C}_c(z) &= D_c(s(z))/z, \qquad \mathcal{C}_c(0) = D_c'(1), \\ \mathcal{F}_c(z) &= 1 - \mathcal{B}(z)\mathcal{C}_c(z) = 1 - \zeta(s(z))D_c(s(z)). \end{aligned} \tag{155I.1}$$

Balance removes the apparent singularity in $\mathcal{C}_c$. The residual at zero is $1 - D_c'(1)$, not 1: treating $\zeta(1)D_c(1)$ as zero would lose the removable product's limit.

Theorem 155I.1 (exact isometry). With the normalized Hardy coefficient norm on $\mathbb{D}$, the residual belongs to $H^2(\mathbb{D})$ and

$$\boxed{\begin{aligned} &\mathcal{F}_c(z) = \sum_{n\geq 0} r_n(c) z^n, \qquad r_n(c) = \int_0^\infty e^{-u} h_c(e^u) L_n^{(0)}(u)\,du, \\ &\|\mathcal{F}_c\|_{H^2}^2 = \sum_{n\geq 0} |r_n(c)|^2 = \mathscr{N}(c). \end{aligned}} \tag{155I.2}$$

Proof. The exact Mellin identity (155H.3), with $g(u) = h_c(e^u)$, becomes

$$\mathcal{F}_c(z) = \frac{1}{1-z}\int_0^\infty e^{-u} g(u) \exp\left(-\frac{uz}{1-z}\right) du. \tag{155I.3}$$

The kernel is the ordinary Laguerre generating function. On a small closed disk $|z| \leq r < 1/2$, its absolute coefficient majorant is $(1-r)^{-1}\exp(ur/(1-r))$. Since g is bounded, termwise integration is justified locally. The Laguerre polynomials are orthonormal in $L^2(e^{-u}du)$ by Rodrigues and integration by parts. They are complete: if f is orthogonal to all polynomials, then $A(t) = \int_0^\infty f(u)e^{-u}e^{tu}du$ is analytic for $\Re t < 1/2$ by Cauchy–Schwarz and all its derivatives at zero vanish. Analytic continuation and Fourier uniqueness on the imaginary axis give $f = 0$. Parseval now proves (155I.2), since $\int |g|^2 e^{-u} du = \mathcal{N}(c)$. The square-summable series defines an H^2 function on the whole disk; identity with (155I.1) follows from local equality. This does not infer a Hardy bound from pointwise boundary values alone. □

For a normalization check, $s(e^{i\theta}) = 1/2 + (i/2)\cot(\theta/2)$ and $|d\theta| = dt/(1/4 + t^2)$. The normalized circle norm is therefore exactly (155H.3), with its single factor $1/(2\pi)$.

The finite Dirichlet polynomial gives explicit multiplier coefficients:

$$\begin{aligned} \mathcal{C}_c(z) &= \sum_{n\geq 0} t_n(c) z^n, & t_n(c) &= \sum_d \frac{c_d}{d} L_{n+1}^{(-1)}(\log d), \\ r_n(c) &= \mathbf{1}_{n=0} - \sum_{j=0}^{n} b_j^{\mathrm{den}} t_{n-j}(c). \end{aligned} \tag{155I.4}$$

Indeed $D_c(s(z)) = \sum_d (c_d/d) \exp[-(\log d)z/(1-z)]$ and $\exp[-az/(1-z)] = \sum_{k\geq 0} L_k^{(-1)}(a) z^k$; its constant term cancels by balance. Each convolution is finite. Thus the same error is

$$\mathcal{N}(c) = \sum_{n\geq 0} \left| \mathbf{1}_{n=0} - \sum_{j=0}^{n} b_j^{\mathrm{den}} \sum_d \frac{c_d}{d} L_{n-j+1}^{(-1)}(\log d) \right|^2 . \tag{155I.5}$$

Signs remain inside the square; absolute summability of b_j^{den} is neither used nor true. Schwarz's lemma applied to the numerator of $\mathcal{C}_c$ gives $\|\mathcal{C}_c\|_\infty \leq \sum |c_d|/\sqrt{d}$. This and (155G.6) do not establish subpower growth for chosen families. For $c_1 = 1, c_2 = -2$, $r_0 = 1 - \log 2$ and $\mathcal{N}(c) = 1 - \log 2$; the constant coefficient contributes only $(1 - \log 2)^2$ to that full squared norm.

Prefix support is the additional analytic information

For $c_d = \mu(d)$ through K, set $T = K + 1$. The support cancellation $h_c = 0$ on $[1, T)$ gives

$$\mathcal{G}_{c,T}(z) = T^{s(z)-1/2} \mathcal{F}_c(z) \in H^2, \qquad \|\mathcal{G}_{c,T}\|_{H^2}^2 = \mathcal{N}(c). \tag{155I.6}$$

To prove this, apply the same isometry to $x \mapsto T^{-1/2} h_c(Tx)$. Its norm is $\int_T^\infty h_c(v)^2 v^{-2} dv = \mathcal{N}(c)$ and its Mellin transform is $T^{s-1/2} E_c(s)$. The prefix is essential: $T^{s(z)-1/2}$ is not a bounded multiplier on arbitrary H^2 functions.

At an actual zero $\rho = \sigma + i\gamma$ with $\sigma > 1/2$, $\mathcal{F}_c(z_\rho) = 1$ and $1 - |z_\rho|^2 = (2\sigma - 1)/|\rho|^2$. The coefficient evaluation inequality $|\mathcal{G}(z)|^2 \leq \|\mathcal{G}\|_{H^2}^2/(1 - |z|^2)$ recovers exactly (155H.5), with the same constant and exponent.

This joins the analytic denominator and exact-divisor error in one residual, not an improved zero lower bound. The remaining sufficient estimate is (155H.6). A finite prefix of coefficients in (155I.5) gives a lower bound on the full norm, not an upper tail certificate. These infinite Laguerre coefficients are not the curvature I_n, the finite Bernstein–Laguerre row at two, or the reserve-normalized boundary matrix. The shared polynomial basis does not identify different inputs or norms.

155J. Fixed plateau exponent, scalar logarithmic target, and proof firewalls

Sections 155H–155I gave a sufficient exact-prefix construction target. For one specified family the exponent can be identified exactly. Define

$$V_N(s) = \sum_{d\le N} \mu(d)\left(1-\frac{d}{N}\right) d^{-s}, \qquad U_N = \int_0^\infty \left|\mathbf{1}_{[1,\infty)}(x) + \sum_{d\le N} \mu(d)\left(1-\frac{d}{N}\right)\{x/d\}\right|^2 \frac{dx}{x^2}. \tag{155J.1}$$

For $K < L$, put

$$A_{K,L} = \frac{LV_L - KV_K}{L-K}, \qquad C_{K,L}(s) = A_{K,L}(s) - (K+1)A_{K,L}(1)(K+1)^{-s}. \tag{155J.2}$$

The coefficients of $A_{K,L}$ equal $\mu(d)$ through K and then taper linearly to zero. The final term balances at the first index after the exact prefix, so it changes no coefficient through K. With $E = \log(2\pi) - \gamma_E$, Minkowski and the exact initial cancellation give

$$\boxed{\mathscr{N}(C_{K,L}) \le E\left(\frac{L\sqrt{U_L} + K\sqrt{U_K}}{L-K}\right)^2}, \qquad \mathscr{N}(C_{K,2K}) \le 9E\max(U_K, U_{2K}). \tag{155J.3}$$

The constant is independent of the prefix length; this is not a constant-cost repair theorem for arbitrary input coefficients.

Theorem 155J.1 (fixed-family exponent). Let $\Theta_\zeta = \sup_\rho \Re\rho$, over nontrivial zeros. Then

$$\boxed{\lim_{N\to\infty} \frac{\log(1+U_N)}{\log N} = 2\Theta_\zeta - 1, \qquad \lim_{K\to\infty} \frac{\log(1+\mathscr{N}(C_{K,2K}))}{\log K} = 2\Theta_\zeta - 1.} \tag{155J.4}$$

Proof. The upper exponent is as before: fix $\sigma_0 > \Theta_\zeta$, use the zero-free-half-plane Möbius estimate quoted in Báez-Duarte [25, Lemma 2.1], and remove the damping by finite Abel summation. This gives $U_N \ll_{\sigma_0,\epsilon} N^{2\sigma_0-1+\epsilon}$. The lower exponent for the *raw taper* needs a bootstrap because V_N does not have an exact Möbius prefix. For a zero $\rho = \sigma + i\gamma$ put $\delta = 2\sigma - 1 > 0$ and $b_\rho = \sqrt{\delta}/(|\rho|\sqrt{E})$. For $K < N$ the exact-prefix plateau relation implies

$$\sqrt{U_N} \ge \left(1-\frac{K}{N}\right) b_\rho (K+1)^{\delta/2} - \frac{K}{N}\sqrt{U_K}. \tag{155J.4a}$$

If $U_K \le DK^a$ with $a > \delta$, choose $K = \lfloor (rN)^{2/(2+a-\delta)} \rfloor$ with $0 < r \le b_\rho/(4\sqrt{D})$. Then, for all sufficiently large N,

$$U_N \ge c_{\rho,a,D} N^{2\delta/(2+a-\delta)}. \tag{155J.4b}$$

Use the global upper exponents $a > 2\Theta_\zeta - 1$, then let the zero real parts approach Θ_ζ and a decrease to that value. The endpoint $\Theta_\zeta = 1$ uses the elementary linear bound; at 1/2 nonnegativity of $\log(1+U_N)$ supplies the lower limit. Equation (155J.3) transfers the exponent to the balanced dyadic plateau. □

Thus, for this specified family,

$$\boxed{\mathrm{RH} \iff \forall\epsilon>0:\ U_N=O_\epsilon(N^\epsilon),} \tag{155J.5}$$

with the estimate allowed on one fixed unbounded set of indices. This is a fixed-family converse; it does not assert boundedness under RH and does not apply automatically to arbitrary exact-prefix extensions.

Write

$$\mathcal{X}_N=2\sum_{d<e\le N}\mu(d)\mu(e)\left(1-\frac{d}{N}\right)\left(1-\frac{e}{N}\right)G(d,e),\qquad G(d,e)=\int_0^\infty \{x/d\}\{x/e\}\frac{dx}{x^2}. \tag{155J.6}$$

The diagonal and linear pieces can be evaluated separately and give

$$\boxed{U_N-\mathcal{X}_N=\kappa\log N+\kappa_0+o(1),\qquad \kappa=\frac{\log(2\pi)-\gamma_E}{\zeta(2)}.} \tag{155J.7}$$

Hence the remaining norm target may be written one-sidedly as $\mathcal{X}_N\le C_\epsilon N^\epsilon$ for every $\epsilon>0$ on one fixed unbounded index set. The signs $\mu(d)\mu(e)$ remain outside the positive Gram kernel; positivity of G does not supply this upper bound.

A second, different scalar target is

$$B_{\log}(x)=1-\sum_{d\le x}\frac{\mu(d)}{d}\log(x/d). \tag{155J.8}$$

Its Mellin transform is $1/s-1/[s^2\zeta(1+s)]$. The same pole/positive-envelope argument gives

$$\boxed{\mathrm{RH} \iff \forall\epsilon>0:\ B_{\log}(n)\le C_\epsilon n^{-1/2+\epsilon}\quad (n\gg_\epsilon 1).} \tag{155J.9}$$

No positivity of $B_{\log}$ is assumed. The eventual-integer form can, however, be replaced by two structured meshes. Put $\mathfrak{M}(x)=\sum_{d\le x}\mu(d)$ and

$$w(t)=\log t+\gamma_E-H_{\lfloor t\rfloor}-(\gamma_E-1)\frac{\{t\}}{t}. \tag{155J.9a}$$

Finite divisor convolutions give

$$\boxed{B_{\log}(x)=\frac{1+(\gamma_E-1)\log x}{x}-\frac{1}{x}\int_1^x \mathfrak{M}(x/t)w(t)dt.} \tag{155J.9b}$$

Here $|w(t)|<1/t$, and the rational interval certificate gives $\int_1^\infty |w(t)|t^{-1/2}dt<0.950760<1$. Hence $|\mathfrak{M}(y)|\le Ay^\theta$ through X, $\theta\ge 1/2$, implies $|B_{\log}(x)|\le(1+A)x^{\theta-1}$ on the same finite range. This is one-way smoothing, not a contraction equation for the same unknown.

In logarithmic coordinates, the exact Dirichlet Green formula yields

$$B_{\log}(x) \le \max\{B_{\log}(a), B_{\log}(b)\} + \frac{1}{4}\log^2(b/a), \qquad a \le x \le b. \tag{155J.9c}$$

Consequently (155J.9) is equivalent to its restriction to all sufficiently large fourth powers $x = k^4$, and also to the squared triangular mesh $x = T_k^2$, with the same arbitrary positive slack. The interpolation costs are $O(x^{-1/2})$. An arbitrary sparse sequence is still insufficient.

The original balanced canonical prefix family has the same sharp power exponent. If J_K is the raw untapered norm and N_K the balanced canonical norm, then $N_K \le EJ_K$ and

$$\boxed{\lim_{K\to\infty}\frac{\log(1+N_K)}{\log K} = \lim_{K\to\infty}\frac{\log(1+J_K)}{\log K} = 2\Theta_\zeta - 1.} \tag{155J.9d}$$

The accepted unconditional Mertens estimate also transfers to the fixed taper:

$$\boxed{U_N \ll N\exp(-c\sqrt{\log N}), \qquad \mathcal{X}_N \ll N\exp(-c\sqrt{\log N})} \tag{155J.9e}$$

for some $c > 0$; the second statement is one-sided. These improve the finite allowance while leaving power exponent one, so neither proves RH.

The arithmetic norm also has the exact sine realization

$$P_c(x) = \frac{\sin(2\pi x)}{\pi} + \sum_d \frac{c_d}{d}\{dx\}, \qquad \boxed{\mathcal{N}(c) = \int_0^\infty P_c(x)^2\frac{dx}{x^2} = \frac{\pi^2}{2}\int_0^1 \frac{P_c(x)^2}{\sin^2(\pi x)}dx.} \tag{155J.10}$$

This is an isometry for the same signed arithmetic residual, not a replacement by the positive sine-comparison measure of Section 12A. It gives no missing upper estimate.

Determinant and topology checks

A Vandermonde on n nodes has scaling degree T_{n-1}. For confluent multiplicities m_i, total n, the degree is $T_{n-1} - \sum_i T_{m_i-1} = \sum_{i<j} m_i m_j$; raw derivative columns also carry $\prod_i \prod_{j=0}^{m_i-1} j!$, removed by Taylor normalization. This explains recurring triangular determinant exponents but identifies no new source operator.

For finite coefficient optimization, if $H > 0$, $Cp = u$, and C has full row rank, the constrained minimum is

$$p_* = H^{-1}C^*(CH^{-1}C^*)^{-1}u, \qquad \min_{Cp=u} p^*Hp = u^*(CH^{-1}C^*)^{-1}u. \tag{155J.11}$$

It is a useful exact solver for prefix/balance constraints, but a minimum over adjustable coefficients is not an upper bound on the fixed taper above. A positive kernel update likewise need not decrease a normalized defect: the reviewed rational counterexample has $K_4 - K_3 \succeq 0$ while $25/99 < 4225/15136$. Finally, completion arguments must retain continuity of the zero observation. Our exact-prefix Mellin route does so through

$$\left|\int_q^\infty h_c(x)x^{-s-1}dx\right| \le \sqrt{\mathcal{N}(c)}\,\frac{q^{1/2-\sigma}}{\sqrt{2\sigma-1}}, \qquad q = K+1,\ \sigma > 1/2. \tag{155J.12}$$

$s = \sigma + it$

These checks close tempting shortcuts; they do not improve the open upper bound in (155J.7) or (155J.9).

53. Complete-Bernstein and operator-monotone owner

The Stieltjes criterion in PP1 has a natural increasing form.

Theorem 53.1. With $h(x) = xS_\xi(x)$,

$$\boxed{\begin{aligned} \mathrm{RH} &\iff S_\xi \text{ is Stieltjes} \\ &\iff h \text{ is a complete Bernstein function} \\ &\iff h \text{ is operator monotone on } (0,\infty) \end{aligned}} \tag{53.1}$$

The middle equivalence is the standard Stieltjes–complete-Bernstein correspondence: a nonnegative f is complete Bernstein precisely when $f(x)/x$ is Stieltjes.

A direct proof is instructive. Under RH,

$$h(x) = \sum_{[\rho]} m_\rho \frac{x}{x + q_\rho} \tag{53.2}$$

For $q > 0$, the map

$$f_q(X) = X(X + qI)^{-1} = I - q(X + qI)^{-1} \tag{53.3}$$

is operator monotone increasing because inversion reverses positive-operator order. The series converges locally in operator norm by (48.1), hence h is operator monotone.

Conversely, Löwner's theorem extends an operator-monotone function on the positive half-line to a Pick function holomorphic in the upper half-plane. The genus-zero continuation of (53.2) has poles at $-q_\rho$. If a folded zero were nonreal, conjugation symmetry would place one of $-q_\rho, -\overline{q_\rho}$ in the upper half-plane. Common-sign multiplicities prevent cancellation, contradicting holomorphy. Thus every q_ρ is positive real and RH follows from (50.12).

For positive nodes $x_1, \dots, x_N$, define the Löwner matrix

$$\mathcal{L}_h(x_1, \dots, x_N) = [\ell_{ij}]_{i,j=1}^N \qquad \ell_{ij} = \begin{cases} \dfrac{h(x_i) - h(x_j)}{x_i - x_j}, & i \neq j \\ h'(x_i), & i = j \end{cases} \tag{53.4}$$

Then

$$\boxed{\mathrm{RH} \iff \mathcal{L}_h(x_1, \dots, x_N) \succeq 0 \quad \text{for every finite positive node set}} \tag{53.5}$$

The 1×1 condition is exactly

$$h'(x) = S_\xi(x) + xS'_\xi(x) = W_1(x) > 0 \tag{53.6}$$

Thus the analytic W_1 theorem is the first diagonal Löwner condition. The higher scalar Widder rungs are local derivative shadows of the full matrix problem; no finite collection of shadows replaces (53.5). Section 48C gives an exact rational rank-two witness showing why the centered Gamma pole terms cannot themselves be split into positive Löwner sublattices; this closes a proposed decomposition route without changing (53.5).

54. Exact Gamma–prime source matrix

On the safe real half-line $s > 1$, put

$$R = \sqrt{1+4x}, \qquad s = \sigma + i0 = \frac{1+R}{2} > 1 \tag{54.1}$$

The explicit source formula separates exactly as

$$\boxed{S_\xi(x) = \frac{1}{x} + G(x) - P(x)} \tag{54.2}$$

where

$$G(x) = \frac{\psi((1+R)/4) - \log\pi}{2R} \qquad P(x) = \frac{1}{R}\sum_{n\geq 2}\frac{\Lambda(n)}{n^s} \tag{54.3}$$

Indeed,

$$\frac{1}{R}\left(\frac{1}{s} + \frac{1}{s-1}\right) = \frac{1}{x} \tag{54.4}$$

Therefore

$$h(x) = 1 + xG(x) - xP(x) \tag{54.5}$$

The constant disappears from divided differences. Define

$$L_\Gamma = \left[\frac{x_iG(x_i) - x_jG(x_j)}{x_i - x_j}\right]_{i,j} \qquad L_P = \left[\frac{x_iP(x_i) - x_jP(x_j)}{x_i - x_j}\right]_{i,j} \tag{54.6}$$

with diagonal entries obtained by differentiation. Then

$$\boxed{\mathcal{L}_h = L_\Gamma - L_P} \tag{54.7}$$

This identifies the principal missing theorem in source-native form.

Open Source Forcing Theorem. Prove directly from the explicit Gamma and von-Mangoldt terms that

$$\boxed{L_\Gamma - L_P \succeq 0} \tag{54.8}$$

for every finite positive node set.

By Theorem 53.1, (54.8) is equivalent to RH. Unlike a zero-side restatement, it keeps all arithmetic on the absolutely convergent real Dirichlet half-line. It is stronger and more coherent than proving $W_4, W_5, \ldots$ one at a time, although finite-rung certificates remain useful local information.

The proof map in Reading Volume §R24 displays this all-node source obligation with its quantifiers. Reader §R15 supplies the moment-to-matrix dictionary.

131. Gamma-triangular analytic scaffold

The triangular fold is the exact invariant-coordinate identity

$$q = s(1-s) = -2\mathsf{T}_{s-1} \tag{131.1}$$

To turn this coordinate identity into an analytic statement about the Gamma factor, antisymmetrize its logarithmic derivative across the two sheets.

Put

$$A_\Gamma(s) = \frac{1}{2}\psi(s/2) - \frac{1}{2}\log\pi \qquad R = 2s-1 \qquad q = s(1-s) \tag{131.2}$$

and define folded antisymmetrization by

$$\mathfrak{F}[A](q) = \frac{A(s) - A(1-s)}{2R} \tag{131.3}$$

The classical digamma partial fraction gives

$$A_\Gamma(s) = -\frac{\gamma_E + \log\pi}{2} + \sum_{m=0}^{\infty}\left(\frac{1}{2(m+1)} - \frac{1}{s+2m}\right) \tag{131.4}$$

For every $m \geq 0$,

$$(s+2m)(1-s+2m) = q + 2m(2m+1) = q + 2\mathsf{T}_{2m} \tag{131.5}$$

whereas

$$-\frac{1}{s+2m} + \frac{1}{1-s+2m} = \frac{R}{q+2\mathsf{T}_{2m}} \tag{131.6}$$

The regularizing terms in (131.4) cancel under (131.3). Local normal convergence away from the pole set follows from $2\mathsf{T}_{2m} = 4m^2 + 2m$.

Theorem 131.1 (Gamma-triangular scaffold). Meromorphically in q,

$$\boxed{\mathfrak{G}_\triangle(q) := \mathfrak{F}[A_\Gamma](q) = \frac{1}{2}\sum_{m=0}^{\infty}\frac{1}{q+2\mathsf{T}_{2m}}} \tag{131.7}$$

Hence the nonpositive even Gamma lattice folds exactly to

$$q = -2\mathsf{T}_{2m} = 0, -6, -20, -42, -72, \ldots \tag{131.8}$$

This is the first explicit analytic intertwiner from the Gamma factor to the triangular lattice in this volume. It is stronger than (131.1), but its weights and spectral orientation remain distinct from the synthetic measure of Section 96.

132. All-order Löwner geometry of the scaffold

For $q > 0$, (131.7) is a Stieltjes transform with measure

$$d\mu_\Gamma(a) = \frac{1}{2}\sum_{m=0}^{\infty}\delta_{2\mathsf{T}_{2m}}(da) \tag{132.1}$$

The Stieltjes integrability condition holds because the positive atoms grow quadratically. Therefore, for every $k \geq 0$,

$$(-1)^k\mathfrak{G}_\triangle^{(k)}(q) = \frac{k!}{2}\sum_{m=0}^{\infty}\frac{1}{(q+2\mathsf{T}_{2m})^{k+1}} > 0 \tag{132.2}$$

Define

$$g_\Gamma(q) = q\mathfrak{G}_\triangle(q) = \frac{1}{2} + \frac{1}{2}\sum_{m=1}^{\infty}\frac{q}{q+a_m} \qquad a_m = 2\mathsf{T}_{2m} \tag{132.3}$$

For distinct positive nodes $q_1, \ldots, q_N$, direct divided differences give

$$\boxed{\mathcal{L}_{g_\Gamma}(q_1,\ldots,q_N)_{ij} = \frac{1}{2}\sum_{m=1}^{\infty}\frac{a_m}{(q_i+a_m)(q_j+a_m)}} \tag{132.4}$$

Every summand is a rank-one Gram atom. Strictness follows because a null vector would make the rational function $\sum_i c_i/(q_i + a)$ vanish at every $a = a_m$; its numerator has degree at most $N - 1$, so infinitely many distinct zeros force every c_i to vanish.

Corollary 132.1 (all-order scaffold Löwner theorem). The function g_Γ is complete Bernstein on $(0, \infty)$, and every finite Löwner matrix in (132.4) is positive definite at distinct positive nodes.

This solves an all-order triangular Gamma model. It does not solve the source matrix (54.7), because g_Γ uses both sheets through $A_\Gamma(s) - A_\Gamma(1-s)$.

133. Completion cancels the scaffold

Write

$$\frac{\xi'(s)}{\xi(s)} = A_0(s) + A_\Gamma(s) + A_\zeta(s) \qquad A_0(s) = \frac{1}{s} + \frac{1}{s-1} \qquad A_\zeta(s) = \frac{\zeta'(s)}{\zeta(s)} \tag{133.1}$$

The completed logarithmic derivative is odd under $s \mapsto 1-s$. Hence

$$M_\xi(q) = \mathfrak{F}[A_0](q) + \mathfrak{G}_\triangle(q) + \mathfrak{F}[A_\zeta](q) \qquad \mathfrak{F}[A_0](q) = -\frac{1}{q} \tag{133.2}$$

For $m \geq 1$, the Gamma term has residue $+1/2$ at $q = -2\mathsf{T}_{2m}$. The simple trivial zero of ζ at $s = -2m$ contributes residue $-1/2$ through the reflected zeta term. At $q = 0$, the elementary, Gamma, and zeta residues are respectively

$$-1, \qquad \frac{1}{2}, \qquad \frac{1}{2} \tag{133.3}$$

Proposition 133.1 (exact trivial-scaffold cancellation). Every pole $q = -2\mathsf{T}_{2m}$ of the Gamma scaffold is removable in the completed folded resolvent. None is a zero or spectral atom of ξ.

Binet's formula supplies a complementary positive-kernel description. For $z > 0$,

$$\log \Gamma(z) = \left(z - \frac{1}{2}\right) \log z - z + \frac{1}{2} \log(2\pi) + \int_0^\infty e^{-zt} K_B(t) \, \frac{dt}{t} \tag{133.4}$$

where

$$K_B(t) = \frac{1}{e^t - 1} - \frac{1}{t} + \frac{1}{2} = \frac{1}{2} \coth(t/2) - \frac{1}{t} > 0 \tag{133.5}$$

Indeed, with $u = t/2$, positivity is equivalent to $u \cosh u - \sinh u > 0$; its derivative is $u \sinh u > 0$. Differentiation gives

$$A_\Gamma(s) = \frac{1}{2} \log \frac{s}{2\pi} - \frac{1}{2s} - \frac{1}{2} \int_0^\infty e^{-st/2} K_B(t) \, dt \tag{133.6}$$

Thus the Binet remainder is completely monotone, but it enters A_Γ with a minus sign. The safe-half-line block cannot be replaced by the positive scaffold. In fact, with G from (54.3) and $h_\Gamma(x) = xG(x)$,

$$\boxed{\lim_{x\downarrow 0} h'_\Gamma(x) = \frac{\psi(1/2) - \log\pi}{2} = -\frac{\gamma_E + \log(4\pi)}{2} < 0} \tag{133.7}$$

Proposition 133.2 (Gamma-only source no-go). The actual source block L_Γ is not positive semidefinite even at order one for all positive nodes. Completion-level Gamma-prime cancellation is necessary.

The scaffold figure in Reading Volume §R17 summarizes these exact cancellations.

133A. Quarter-Gamma products and a positive triangular comparison

The half-sized Gamma argument selects the even triangular ladder. For $a = s/2$, $b = (1-s)/2$, and $q = s(1-s)$,

$$4(m+a)(m+b) = 2T_{2m} + q. \tag{133A.1}$$

On $s = 1/2+it$, the two arguments are conjugates. Set $C(q) = \Gamma(s/2)\Gamma((1-s)/2)$, independent of the selected root of $s(1-s) = q$. The convergent Gamma product gives

$$\begin{aligned}
\frac{\Gamma(1/4)^2}{|\Gamma(1/4+it/2)|^2} &= \prod_{m=0}^{\infty}\left(1 + \frac{t^2}{2T_{2m}+1/4}\right),\\
-\frac{d}{dq}\log C(q) &= \sum_{m=0}^{\infty}\frac{1}{q+2T_{2m}} = 2\mathfrak{G}_\triangle(q),\\
E(q) := \frac{2\sqrt{\pi}}{qC(q)} &= \frac{\Gamma(3/2)}{\Gamma(1+s/2)\Gamma(1+(1-s)/2)} = \prod_{m=1}^{\infty}\left(1+\frac{q}{2T_{2m}}\right).
\end{aligned} \tag{133A.2}$$

Here the logarithmic derivative is for $q > 0$, and $E(0) = 1$ by removal of the zero-point singularity. The normalization follows from $C(q) \sim 2\sqrt{\pi}/q$. Alternatively the finite product equals $\Gamma(N+1+a)\Gamma(N+1+b)\Gamma(3/2)$ divided by $\Gamma(1+a)\Gamma(1+b)\Gamma(N+1)\Gamma(N+3/2)$; the N-dependent ratio tends to one because $a+b = 1/2$. This proves the product and its normal convergence directly.

Consequently $E'(0) = \sum_{m\geq 1}(2T_{2m})^{-1} = 1-\log 2$, recovering (TR.3). Euler's Beta substitution $v = e^x/(1+e^x)$ also gives

$$C(1/4+t^2) = 2\sqrt{2\pi}\int_0^\infty \frac{\cos(ty)}{\sqrt{\cosh y}}dy. \tag{133A.3}$$

The reciprocal sum is the negative logarithmic derivative of this integral, not the integral itself. Differentiating (133A.2) gives $(\log C)''(q) = \sum_{m\geq 0}(q+2T_{2m})^{-2} > 0$ and $(\log E)''(q) = -\sum_{m\geq 1}(q+2T_{2m})^{-2} < 0$. The signed cosine integrand is not a positive measure in the parameter t; the product proves these q-curvature statements.

The reciprocal telescope has a compatible Gaussian difference formula:

$$\frac{1}{T_x} = \frac{2}{\sqrt{\pi}}\int_0^\infty \frac{e^{-x^2u}-e^{-(x+1)^2u}}{\sqrt{u}}du \quad (x>0), \qquad \sum_{n=1}^{N}\frac{1}{T_n} = 2\left(1-\frac{1}{N+1}\right). \tag{133A.4}$$

Scaling Euler's Gamma integral proves the first identity; finite telescoping and monotone convergence give the infinite sum two. With $f_n(t) = n^{-1/2-it}$, the full adjacent product retains the phase:

$$(f_n - f_{n+1})\overline{(f_n+f_{n+1})} = \frac{1}{2T_n} + \frac{2i}{\sqrt{2T_n}}\sin\left(t\log\frac{n+1}{n}\right). \tag{133A.5}$$

Its real parts sum to one; the complex series converges absolutely for fixed t. This is an exact connection to the Mellin weights of Section 153, not a zero-location assertion.

Proposition 133A.1 (all-order Li positivity of the comparison). Define $\mathcal{M}(s) = E(s(s-1))$, explicitly $E(-q(s))$ rather than $E(q(s))$. For $a_m = 2T_{2m}$, let $\cos\theta_m = 1-1/(2a_m)$ and define $\log\mathcal{M}(1/(1-z)) = \sum_{n\geq 1}\ell_n z^n/n$. Then

$$\boxed{\ell_n = 2\sum_{m\geq 1}[1-\cos(n\theta_m)], \qquad 0<\ell_n\leq n^2(1-\log 2).} \tag{133A.6}$$

Proof. Under $s = 1/(1-z)$ each factor of the product becomes $(1-e^{i\theta_m}z)(1-e^{-i\theta_m}z)/(1-z)^2$. Taking its local logarithm gives the coefficient in (133A.6). The bound $4\sin^2(n\theta_m/2)\leq n^2/a_m$ proves convergence; for fixed n, sufficiently small positive θ_m give strictly positive summands. □

Thus $\ell_1 = 1-\log 2$, whereas the actual first Li value is $\lambda_1 = (1-\log 2)+(\gamma_E-\log\pi)/2$. The first correction is already negative. The remaining local logarithm $\log(\xi(s)/(\xi(1)\mathcal{M}(s)))$ needs a separate source estimate. The cancellation in Section 133 still applies; no comparison spectrum is identified with the actual completed spectrum.

For comparison, scalar log-convexity alone is insufficient. The positive real-axis Laplace transform $\mathcal{F}(s) = (2+\cosh(4(s-1/2)))/(2+\cosh 2)$ is reflection symmetric and has $(\log\mathcal{F})'' = 16(2\cosh(4(s-1/2))+1)/(2+\cosh(4(s-1/2)))^2 > 0$ on the real axis. Its zeros nevertheless have real parts $1/2\pm\operatorname{arcosh}(2)/4$ and imaginary parts $(2k+1)\pi/4$. Positivity of the comparison in (133A.6) uses its particular product, not merely scalar convexity.

Technical chapter V. Flux geometry and rational witnesses

One energy gives the collar flux, the parabolic pullback and the rational witness criterion. Its zero-height slice leads to the source-rung calculations.

20. Normalization

Define

$$\Xi(t) = \xi\left(\frac{1}{2} + it\right)$$

and for $c > 0$,

$$E_c(t) = \xi\left(\frac{1}{2} + c - it\right) = A_c(t) - iB_c(t)$$

The Wronskian is

$$\Omega_c(t) = A_c B_c' - A_c' B_c$$

Cauchy-Riemann gives the exact identities

$$\boxed{\Omega_c(t) = \frac{1}{2}\partial_c |E_c(t)|^2 = |E_c(t)|^2 \Re \frac{\xi'}{\xi}\left(\frac{1}{2} + c - it\right)}$$

The canonical normalization in this volume is

$$\boxed{J_c(t) = \frac{\Omega_c(t)}{c}}$$

The division by c makes J_c the derivative with respect to the square coordinate c^2, as proved in §25.

21. Generalized Laguerre hierarchy

For a real entire function f, define

$$L_n[f](t) = \frac{1}{(2n)!} \sum_{k=0}^{2n} (-1)^{n+k} \binom{2n}{k} f^{(k)}(t) f^{(2n-k)}(t)$$

In particular,

$$L_1[f] = f'^2 - f f''$$

The exact generating laws are

$$\boxed{|E_c(t)|^2 = \sum_{n=0}^{\infty} L_n[\Xi](t) c^{2n}}$$

and

$$\boxed{J_c(t) = \sum_{n=1}^{\infty} n L_n[\Xi](t) c^{2n-2}}$$

At the fold,

$$J_0(t) = L_1[\Xi](t) = \Xi'(t)^2 - \Xi(t)\Xi''(t)$$

This series already suggests the correct differentiation variable: c^2, not c.

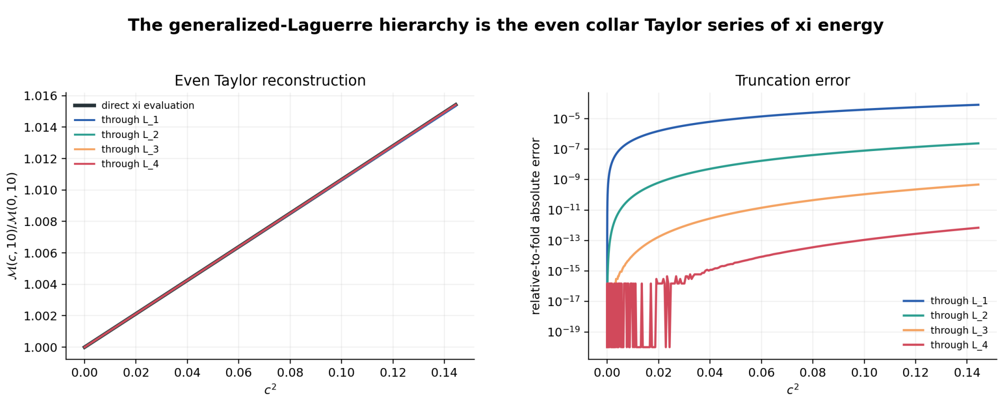

Figure 23: Direct xi evaluation and its even generalized-Laguerre Taylor reconstruction at t equals 10.

22. Energy and flux kernels

Let Φ be the even theta kernel with

$$\Xi(t) = \widehat{\Phi}(t)$$

If $f_c(x) = e^{-cx}\Phi(x)$, then the energy kernel

$$\mathcal{H}_c = f_c * \widetilde{f_c}$$

satisfies

$$\widehat{\mathcal{H}_c}(t) = |E_c(t)|^2 \geq 0$$

Differentiating in the collar direction gives the flux kernel

$$\boxed{\mathcal{C}_c(x) = \frac{1}{2c}\int_{\mathbb{R}} (x-2u)\sinh(c(x-2u))\Phi(u)\Phi(x-u)\,du}$$

It obeys

$$\boxed{J_c(t) = \widehat{\mathcal{C}_c}(t)}$$

Pointwise $\mathcal{C}_c(x) \geq 0$ because $y\sinh(cy) \geq 0$. However,

$$\mathcal{C}_c(x) \geq 0 \not\Longrightarrow \widehat{\mathcal{C}_c}(t) \geq 0$$

The missing statement is positive definiteness of $\mathcal{C}_c$.

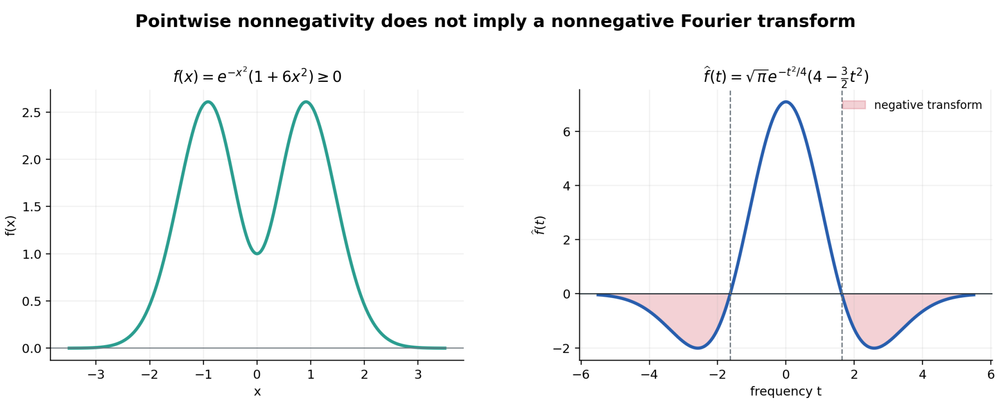

Figure 24: A nonnegative function with a sign-changing Fourier transform: the positive-definiteness firewall.

22A. Every rung test has essential Fourier cancellation

The firewall closing §22 is not a gap in the argument; it is a theorem, and it holds at every order. Fix $x > 0$, put $b = \frac{1}{2}$ and $a = \sqrt{x + \frac{1}{4}} > b$, and let

$$f_{k,x}(t) = \left[\frac{4x(t^2 + b^2)}{(t^2 + a^2)^2}\right]^k, \qquad \widehat{f}_{k,x}(u) = \int_{\mathbb{R}} f_{k,x}(t) e^{-itu}\, dt \tag{22A.1}$$

Here t is an independent real frequency; it is not a substitution for the imaginary part of an off-line zero, and (22A.1) is a scalar test, not the completed Weil form.

Theorem 22A.1. For every $x > 0$ and every integer $k \geq 1$, the real even transform $\widehat{f}_{k,x}$ has at least k sign changes on $u > 0$. Consequently $f_{k,x}$ is not positive definite. For odd k the transform is eventually negative; for even k it is eventually positive and negative on some nonempty interval.

Proof. Parameter differentiation of the elementary rational transform gives $\Phi_m(u; a) = \int_{\mathbb{R}} (t^2 + a^2)^{-m} e^{-itu} dt = \frac{(-1)^{m-1}}{(m-1)!} \partial_{a^2}^{m-1} \left(\frac{\pi}{a} e^{-a|u|}\right)$. Expanding $t^2 + b^2 = (t^2 + a^2) - x$,

$$\widehat{f}_{k,x}(u) = (4x)^k \sum_{j=0}^{k} \binom{k}{j} (-x)^j \Phi_{k+j}(u; a) \tag{22A.2}$$

which for $u \geq 0$ is e^{-au} times a real polynomial of degree $2k - 1$ whose leading coefficient is $(-1)^k 2\pi x^{2k} / [(2k-1)!\, a^{2k}]$. So the transform has finitely many sign changes, exponential moments for $|y| < a$, and $\widehat{f}_{k,x}(0) = \int f_{k,x} > 0$. Analytic inversion in the strip $|\Im t| < a$ gives

$$\frac{1}{2\pi} \int_{\mathbb{R}} e^{yu} \widehat{f}_{k,x}(u)\, du = f_{k,x}(-iy) = \left[\frac{4x(b^2 - y^2)}{(a^2 - y^2)^2}\right]^k \tag{22A.3}$$

whose right side has a zero of order exactly k at each of $y = \pm b$, both strictly inside the strip since $x > 0$.

Now the variation-diminishing step. A continuous real $g \not\equiv 0$ with M sign changes and finite exponential polynomial moments has a bilateral Laplace transform with at most M real zeros, counted with multiplicity, inside the interval of convergence: for $M = 0$ the transform has one strict sign; for the induction step, multiplying g by $(u - u_0)$ at a sign change removes one sign change and replaces F by $F' - u_0 F = e^{u_0 y}\left(e^{-u_0 y} F\right)'$, and Rolle's theorem with multiplicities closes the induction on each compact subinterval. Applied to (22A.3), the $2k$ zeros force at least $2k$ sign changes on the whole axis; evenness and $\widehat{f}_{k,x}(0) > 0$ put at least k of them on $u > 0$. The leading coefficient gives the eventual signs. ☐

The obstruction is already visible at weight zero: the identity

$$\boxed{\int_{\mathbb{R}} \cosh(u/2)\, \widehat{f}_{k,x}(u)\, du = 0} \tag{22A.4}$$

rules out an everywhere nonnegative transform, since a nonzero nonnegative density would have strictly positive weighted integral.

Scope, and the $k = 1$ consistency check. This closes, at all orders, the route that asserts the rung sign by claiming these scalar tests have nonnegative transforms. It does *not* exclude a separate Weil-functional representation, a two-variable positivity construction, or an argument using more of the arithmetic source. For $k = 1$ the transform's unique positive root is exactly the crossover $u_x = (1 + \frac{1}{2x})/a$ recorded at §R11 — at $x = 1, 3, 10$ it is 1.34164079, 0.64715023, 0.32796490 — so Theorem 22A.1 contains the volume's exact first-rung statement as its first case rather than competing with it. A residue computation of (22A.2) for $k \le 4$ at $x = 1, 3, 10$ returns degree $2k - 1$, leading sign $(-1)^k$, and exactly k positive roots in all twelve cases; whether the count is exactly k in general is **open and is not used**.

23. Signed zero blocks

Let an off-axis zero quartet have horizontal displacement $a > 0$. Its paired contribution to the normalized horizontal log-derivative is

$$\boxed{H_{a,c}(u) = \frac{1}{c}\left[\frac{c-a}{(c-a)^2 + u^2} + \frac{c+a}{(c+a)^2 + u^2}\right]}$$

Equivalently,

$$H_{a,c}(u) = \frac{2(c^2 + u^2 - a^2)}{((c-a)^2 + u^2)((c+a)^2 + u^2)}$$

If $a < c$, the block is positive for every u. If $a > c$, it is negative exactly when

$$|u| < \sqrt{a^2 - c^2}$$

Thus

$$b = \sqrt{a^2 - c^2}$$

is the exact negative-core half-width. It is not an optimal smoothing radius.

At a fixed c, a dangerous block can be hidden. If k critical-line blocks are placed at the same ordinate, complete compensation occurs exactly when

$$k(a^2 - c^2) \ge 2c^2$$

This firewall is correct, but it concerns a fixed horizontal line. It does not survive the limit in which c approaches the target zero itself; that limit is the key to Theorem 27.

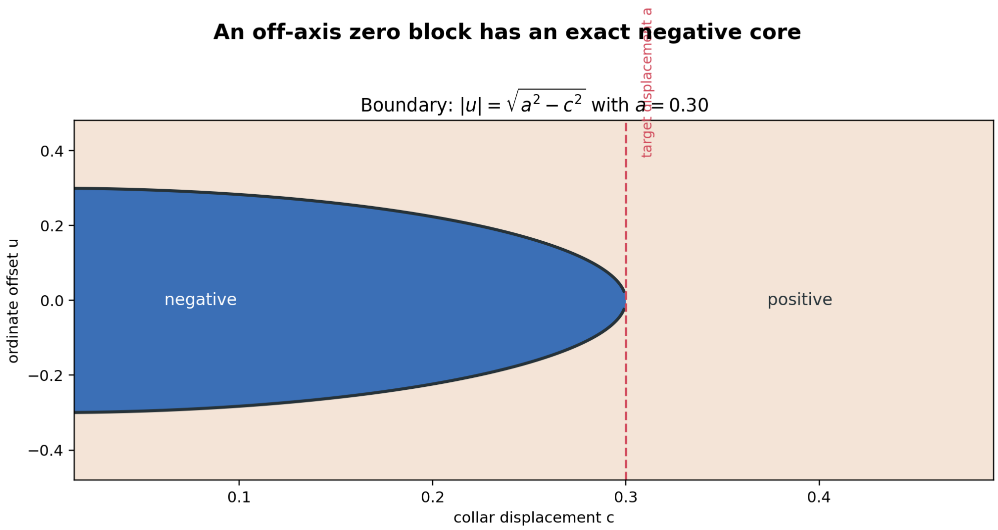

Figure 25: Exact sign region of a synthetic off-axis zero block.

24. Master energy and collar variables

Put

$$\mathcal{M}(c,t) = \left|\xi\left(\frac{1}{2} + c - it\right)\right|^2 \qquad c > 0$$

Functional equation and conjugation imply

$$\mathcal{M}(-c,t) = \mathcal{M}(c,t)$$

Hence $\mathcal{M}$ is analytic in the square variable

$$x = c^2$$

On the complementary collar $0 < c < 1/2$, define

$$p = \frac{1}{2} + c \qquad \tau = p(1-p) = \frac{1}{4} - c^2 \qquad r = \frac{1+2c}{1-2c}$$

The fold is $c = 0$, $p = 1/2$, $\tau = 1/4$, $r = 1$. Moving outward on either sheet increases $|c|$, decreases τ, and sends r away from its fixed radius.

25. Theorem A - Cayley-Laguerre flux identity

For every $c > 0$ and every real t at which the displayed logarithmic derivative is finite,

$$\boxed{\frac{\partial}{\partial(c^2)}\mathcal{M}(c,t) = J_c(t)}$$

and

$$\boxed{\frac{\partial}{\partial(c^2)}\log\mathcal{M}(c,t) = Q_c(t) := \frac{1}{c}\Re\frac{\xi'}{\xi}\left(\frac{1}{2}+c-it\right)}$$

Equivalently,

$$\boxed{J_c(t) = -\frac{\partial}{\partial\tau}\mathcal{M}(\tau,t) \qquad Q_c(t) = -\frac{\partial}{\partial\tau}\log\mathcal{M}(\tau,t)}$$

Proof. By the Wronskian identity,

$$\partial_c\mathcal{M}(c,t) = 2\Omega_c(t) = 2cJ_c(t)$$

Since $\partial_{c^2} = (2c)^{-1}\partial_c$, the first identity follows. Dividing by $\mathcal{M}$ gives the logarithmic identity. Finally $\tau = 1/4 - c^2$, so $\partial_\tau = -\partial_{c^2}$. $\square$

The phase-complement product τ, the generalized Laguerre flux J_c, and the horizontal log-derivative Q_c are linked by these derivatives of one energy. The next theorem identifies its folded-resolvent coordinate.

26. Theorem B - Folded-resolvent parabolic pullback

Let

$$q = s(1-s), \qquad \xi(s) = X(q), \qquad M_\xi(q) = -\frac{X'(q)}{X(q)}$$

For

$$s = \frac{1}{2} + c - it$$

the folded coordinate is

$$\boxed{q(c,t) = \tau + t^2 + 2ict = \frac{1}{4} - c^2 + t^2 + 2ict}$$

The logarithmic derivative factors as

$$\boxed{\frac{\xi'}{\xi}(s) = 2(c - it)M_\xi(q(c,t))}$$

Consequently

$$\boxed{Q_c(t) = \frac{2}{c}\Re[(c - it)M_\xi(q(c,t))]}$$

Proof. Since $dq/ds = 1 - 2s = -2(c - it)$ and $X'/X = -M_\xi$,

$$\frac{\xi'}{\xi}(s) = \frac{X'}{X}(q)\frac{dq}{ds} = 2(c - it)M_\xi(q)$$

Take the real part and divide by c. □

Corollary 26.1 - Fixed-focus parabolic foliation

Write

$$q(c,t) = u + iv$$

For fixed $c > 0$,

$$u = \tau + t^2, \qquad v = 2ct$$

and elimination of t gives

$$\boxed{v^2 = 4c^2(u - \tau) \qquad \tau = \frac{1}{4} - c^2}$$

Thus every fixed-c pullback path is a focus-directrix parabola. Its vertex, focus, and directrix are

$$\boxed{V_c = \left(\frac{1}{4} - c^2, 0\right), \qquad F_* = \left(\frac{1}{4}, 0\right), \qquad L_c: \ u = \frac{1}{4} - 2c^2}$$

The focus F_* is independent of c, the Cayley complement τ is the vertex coordinate, and c^2 is the focal length. Directly,

$$\left|q(c,t) - \frac{1}{4}\right| = c^2 + t^2 = \operatorname{dist}(q(c,t), L_c)$$

At $c = 0$ the leaf degenerates to the real focal ray $[1/4, \infty)$. Hence the folded zero statement admits the exact conic form

$$\boxed{\text{RH} \iff \text{every folded zero lies on the degenerate focal ray,}}$$

whereas a zero $\rho = 1/2 + a + i\gamma$ with $a \neq 0$ lies on the genuine confocal leaf $c = |a|$. This is the analytic focus-directrix bridge described by the shared centered square; it is a reformulation of zero location, not a forcing theorem.

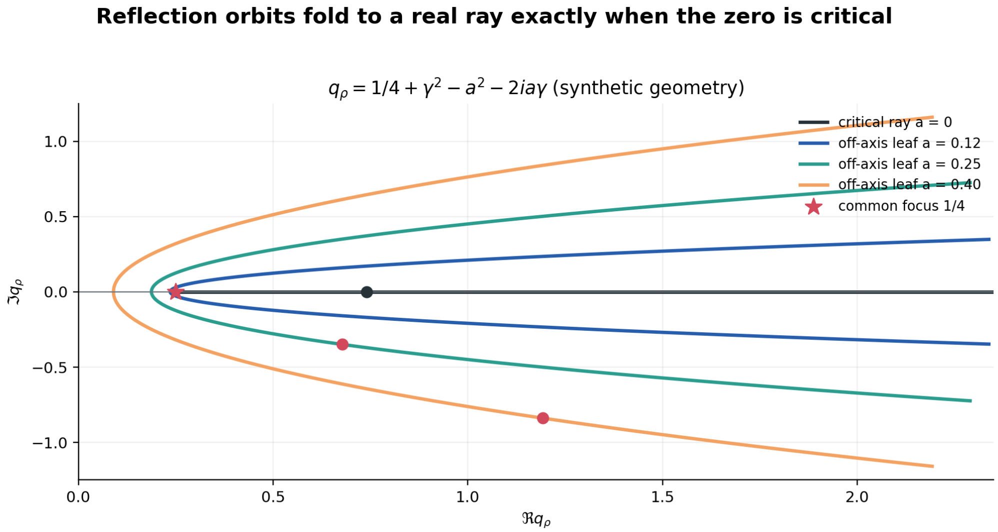

Figure 26: Synthetic reflection orbits in the folded q-plane; critical orbits map to the real ray.

Consequence

PP1 and the signed zero-Poisson program are two coordinate views of one resolvent. PP1 studies M_ξ on the negative real q-axis, where the prime Dirichlet series converges after the $s(x) > 1$ substitution. The HB/Poisson program studies directional real parts of the same function along the parabolas $q(c, t)$.

This is an exact intertwiner, not a new estimate.

Prior-art boundary

The horizontal-modulus core of the next theorem is not claimed as new. Sondow and Dumitrescu proved that $|\xi|$ is horizontally increasing in a zero-free right half-plane and extracted the RH reformulation; Matiyasevich, Saidak, and Zvengrowski gave a related treatment and traced the idea through Jensen/Polya and Lagarias [12-14]. The contribution of this volume is the proof-preserving identification of that known monotonicity criterion with J_c, τ, the folded resolvent, the flux kernel, and the native rational TFG witness system. The proof is repeated to make every normalization and converse quantifier explicit.

27. Theorem C - Outward-modulus criterion in flux coordinates

Let $F(z) = \xi(1/2 + z)$. The following are equivalent.

1. The Riemann hypothesis is true.
2. For every $c > 0$ and $t \in \mathbb{R}$,
$$\Re \frac{F'}{F}(c - it) > 0$$
3. For every $c > 0$ and $t \in \mathbb{R}$,
$$J_c(t) > 0$$
4. For every fixed t, the function
$$c \longmapsto \mathcal{M}(c, t)$$
is strictly increasing on $(0, \infty)$.
5. On $0 < c < 1/2$, the same energy is strictly decreasing as a function of $\tau = 1/4 - c^2$.
6. For every $c > 0$, the flux kernel $\mathcal{C}_c$ is positive definite.

The strict inequalities may be replaced by nonnegative/nondecreasing inequalities without changing the equivalence.

Proof that RH implies outward positivity

Under RH the zeros of F are $\pm i\gamma$, with multiplicity. The paired Hadamard product is

$$F(z) = F(0) \prod_{\gamma > 0} \left(1 + \frac{z^2}{\gamma^2}\right)^{m_\gamma}$$

Because $\sum \gamma^{-2} < \infty$, its logarithmic derivative has the absolutely convergent real-part expansion

$$\frac{F'}{F}(z) = \sum_{\gamma > 0} m_\gamma \left(\frac{1}{z - i\gamma} + \frac{1}{z + i\gamma}\right)$$

At $z = c - it$,

$$\Re \frac{F'}{F}(c - it) = \sum_{\gamma > 0} m_\gamma \left[\frac{c}{c^2 + (t + \gamma)^2} + \frac{c}{c^2 + (t - \gamma)^2}\right] > 0$$

Theorem A then gives strict outward monotonicity and $J_c > 0$.

Proof that outward nonnegativity implies RH

If RH fails, functional-equation symmetry supplies a zero

$$z_0 = a - i\gamma$$

of F with $a > 0$. Let its multiplicity be m. In a disk containing no other zero,

$$\frac{F'}{F}(z) = \frac{m}{z - z_0} + h(z)$$

where h is analytic. For $d > 0$ small, put

$$w = z_0 - d = (a - d) - i\gamma$$

Then

$$\Re \frac{F'}{F}(w) = -\frac{m}{d} + O(1) < 0$$

Thus $J_{a-d}(\gamma) < 0$ for all sufficiently small d. This contradicts nonnegativity. Hence all zeros lie on the critical line.

Positive-definiteness equivalence

The kernel $\mathcal{C}_c$ is continuous and rapidly decreasing, and $\widehat{\mathcal{C}_c} = J_c$. Bochner's theorem therefore identifies $J_c \geq 0$ with positive definiteness of $\mathcal{C}_c$. This completes the equivalence. □

28. Quantitative local witness theorem

The preceding converse has a useful quantitative form.

Let $z_0 = a - i\gamma$ be an off-axis zero of multiplicity m. Choose $r > 0$ so that z_0 is the only zero in $|z - z_0| \leq r$, after multiplicity is absorbed into the target factor. Put

$$h(z) = \frac{F'}{F}(z) - \frac{m}{z - z_0} \qquad B = \sup_{|z - z_0| \leq r/2} |\Re h(z)|$$

For

$$0 < d < \min\left\{a, \frac{r}{2}, \frac{m}{2B}\right\}$$

with the last bound omitted if $B = 0$, one has

$$\boxed{d \Re \frac{F'}{F}(z_0 - d) \leq -\frac{m}{2}}$$

Indeed,

$$d \Re \frac{F'}{F}(z_0 - d) = -m + d \Re h(z_0 - d) \leq -m + dB \leq -\frac{m}{2}$$

Therefore every off-axis zero creates an **open** negative flux region in the (c,t) plane. Fixed-c compensation cannot remove that region because the target pole diverges as $c \uparrow a$ while all non-target contributions remain bounded locally.

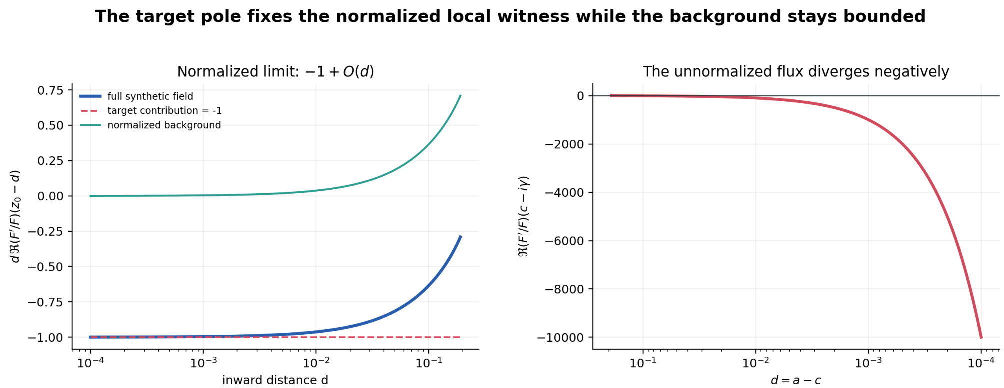

Figure 27: Synthetic local-pole scaling: the normalized witness tends to minus the target multiplicity.

29. Theorem D - Native TFG rational witness criterion

Let

$$\mathcal{C}_{\triangle} = \mathbb{Q} \cap (0, 1/2)$$

be represented by centered native cells as in Proposition 8.1. Independently, address rational heights by unreduced integer pairs:

$$\mathcal{T}_{\mathbb{Q}} = \left\{ \frac{p}{q} : p \in \mathbb{Z},\ \ q \in \mathbb{N} \right\} = \mathbb{Q}$$

Then RH is equivalent to the countable family of inequalities

$$\boxed{\mathcal{M}(c_2, t) \geq \mathcal{M}(c_1, t) \quad \text{for all } t \in \mathcal{T}_{\mathbb{Q}} \quad c_1, c_2 \in \mathcal{C}_{\triangle} \quad c_1 < c_2}$$

Equivalently, for all finite indices satisfying

$$c_i = \frac{|2k_i - n_i|}{2n_i} \qquad 0 < |2k_i - n_i| < n_i$$

and all rational heights $t = p/q$, the outward finite difference is nonnegative.

Proof. RH implies strict monotonicity for every real c, t by Theorem C, so it implies the displayed rational inequalities. Conversely, if RH fails, the quantitative local witness theorem produces an open rectangle on which $\partial_c \mathcal{M} < 0$. Choose rational t in its height projection and rational $c_1 < c_2$ in its horizontal projection. Then

$$\mathcal{M}(c_2, t) < \mathcal{M}(c_1, t)$$

and Proposition 8.1 supplies finite native-cell indices for both c_i. $\square$

Interpretation

The exact rational coverage in §8 turns any open negative-flux region into a finite, rationally addressed witness cell. No literature-priority claim is made. A finite witness can refute the full criterion; proving it still requires a uniform mechanism that orders every addressed cell.

30. Synthetic diagnostic

The following figure compares two exact finite zero models. It is a diagnostic of the theorem, not data about unknown zeta zeros.

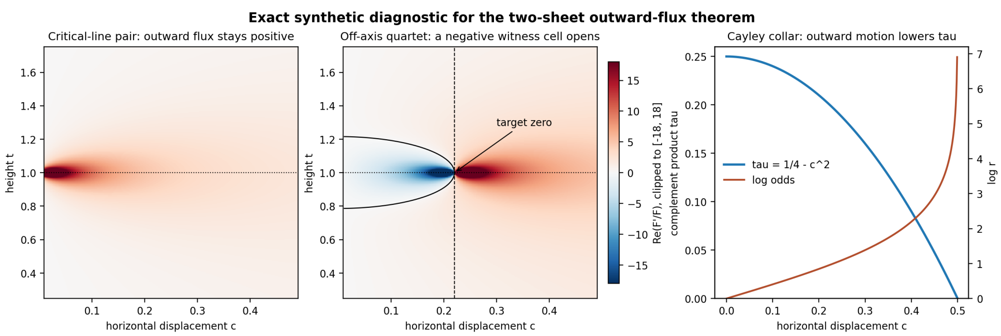

Figure 28: Synthetic critical-line and off-axis flux fields, together with the Cayley collar coordinate.

The left panel uses a polynomial with a critical-line pair $\pm i\gamma$; the outward logarithmic flux is positive. The middle panel uses the symmetric off-axis quartet $\pm a \pm i\gamma$; a blue negative cell opens immediately to the left of the target. The right panel shows that outward motion in c decreases the complement product τ and increases log odds.

31. Theorem E - Axial flux-Widder identity

The parabolic pullback contains the negative-axis folded resolvent as its zero-height slice. Thus the reduced-Widder hierarchy is the axial derivative ladder of the same master flux object, not a second analytic program.

For $x > 0$, set

$$c(x) = \sqrt{x + \frac{1}{4}} \qquad s(x) = \frac{1}{2} + c(x) = \frac{1 + \sqrt{1 + 4x}}{2}$$

Then $c > 1/2$, and at $t = 0$ the folded coordinate of Theorem B is

$$q(c, 0) = \frac{1}{4} - c^2 = -x$$

Consequently,

$$\boxed{Q_{c(x)}(0) = 2M_\xi(-x) = 2S_\xi(x)} \tag{31.1}$$

Since $x = c^2 - 1/4$, differentiation in x agrees with differentiation in c^2 along this slice. Theorem A therefore also gives

$$\boxed{\frac{d}{dx} \log \left| \xi\left(\frac{1 + \sqrt{1 + 4x}}{2} \right) \right|^2 = 2S_\xi(x)} \tag{31.2}$$

Define the reduced-Widder diagonal

$$W_k(x) = (-1)^{k-1} D_x^{2k-1} [x^k S_\xi(x)] \qquad k \geq 1$$

Substitution of (31.1) gives the exact axial-flux formula

$$\boxed{W_k(x) = \frac{(-1)^{k-1}}{2} D_x^{2k-1} \left[x^k Q_{\sqrt{x+1/4}}(0) \right]} \tag{31.3}$$

Thus the hierarchy measures alternating higher differential curvature of the outward logarithmic flux, with the collar parameter and the folded negative-axis parameter related by $x = c^2 - 1/4$.

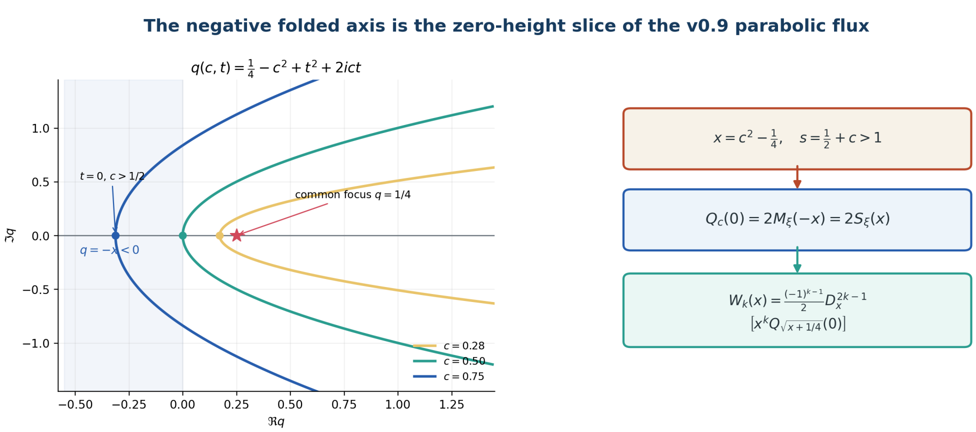

Figure 29: The negative folded axis is the zero-height slice of the confocal parabolic flux, and its axial flux generates every reduced-Widder rung.

42. One master object, several renderings

The exact coordinate relationships are

$$\boxed{\begin{matrix} X(q) \\ \downarrow\ -\partial_q \log \\ M_\xi(q) \end{matrix}} \xrightarrow{q=s(1-s)} \boxed{Q_c(t) = \frac{1}{c}\Re\frac{\xi'}{\xi}(s)} \xrightarrow{\times\mathcal{M}} \boxed{J_c(t)} \xleftrightarrow{\mathcal{F}} \boxed{\mathcal{C}_c(x)}$$

The coordinate collar

$$c^2 = \frac{1}{4} - \tau \qquad \tau = p(1-p) = \frac{r}{(1+r)^2}$$

turns J_c into the negative τ-derivative of the energy. The Laguerre hierarchy is its Taylor expansion at the fold. The signed Poisson blocks are its zero-side partial fractions. The PP1 Stieltjes problem is its folded analytic-class statement. Each rendering retains the same completed resolvent; a sign theorem still requires its full domain and quantifiers.

43. Mesoscopic localization and rational witness size

For a hypothetical target $z_0 = a - i\gamma$, choose $0 < c < a$ and write

$$d = a - c \qquad D = a + c \qquad b = \sqrt{dD} \qquad w = c - i\gamma$$

The target contributes exactly

$$d\Re\frac{m_0}{w - z_0} = -m_0$$

The PP76 mesoscopic owner is

$$M_{\text{meso}} = d\Re \sum_{Cd<|\lambda - z_0|<b} \frac{m_\lambda}{w - \lambda}$$

Current every-target counting gives a crowding scale $C \asymp \log\gamma$. Proving $C = o(\log\gamma)$ would be genuine progress; an $O(\sqrt{\log\gamma})$ result would be major.

The local witness theorem fixes the role of this mesoscopic estimate:

1. **It is not needed to prove the equivalence.** Near a fixed off-axis zero, the target pole dominates automatically.
2. **It remains useful for fixed-line propagation.** If positivity is known at selected c values and one wants to force a neighboring zero or propagate control between scales, the signed discrepancy is the least-lossy owner.
3. **A sublog bound alone is not RH.** The local sign hypothesis, global coverage in c, and an iteration or termination theorem are still needed.
4. **The signed field is primary.** Counts, quadratic energy, second harmonics, and fixed finite-Weil compressions lose directional information.

The recommended successor problem is therefore two-pronged:

Source question — collar monotonicity. Prove $-\partial_\tau \log \mathcal{M} \geq 0$ from the explicit prime/Gamma source, equivalently prove the PP1 Stieltjes/Pick/Loewner property.

Quantitative question — witness localization. Develop validated bounds for the size of the negative rational witness box around a hypothetical off-axis zero and determine what zero-spacing input would make a finite mesh certificate possible up to height T.

The source question is RH-equivalent. The quantitative localization question controls witness size; it is not by itself a proof of RH.

Technical chapter VI. Widder source proofs and their asymptotic limits

The full derivative identity fixes the normalization. The first four source proofs appear together, followed by fixed-rung tails and the limits of phase-based detection.

32. Theorem F - Full Widder-zero-heat identity

For integers $n, k \geq 0$, define the full Widder functional

$$\mathcal{F}_{n,k}[S](x) = (-1)^n D_x^{n+k}[x^k S(x)]$$

The notation $\mathcal{F}_{n,k}$ here is the same functional denoted by $F_{n,k}$ in reader (13.2). The reduced diagonal is

$$W_k = \mathcal{F}_{k-1,k}$$

Because X has order $1/2$, its folded canonical product has genus zero:

$$X(q) = X(0) \prod_{[\rho]} \left(1 - \frac{q}{q_\rho}\right)^{m_\rho} \qquad q_\rho = \rho(1-\rho)$$

There is one factor per functional-equation orbit. An off-line quartet folds to a conjugate pair $q_\rho, \overline{q_\rho}$; it must not be counted four times. Logarithmic differentiation on $q = -x$ yields

$$S_\xi(x) = \sum_{[\rho]} \frac{m_\rho}{x + q_\rho} \tag{32.1}$$

Polynomial division, or $n + k$ direct differentiations, gives the one-pole identity

$$(-1)^n D_x^{n+k} \frac{x^k}{x+q} = (n+k)! \frac{q^k}{(x+q)^{n+k+1}}$$

Hence

$$\boxed{\mathcal{F}_{n,k}[S_\xi](x) = (n+k)! \sum_{[\rho]} m_\rho \frac{q_\rho^k}{(x+q_\rho)^{n+k+1}}} \tag{32.2}$$

Now introduce the folded heat trace

$$\Theta_\xi(u) = \sum_{[\rho]} m_\rho e^{-uq_\rho} \qquad u > 0$$

For fixed $u > 0$, this series and all of its u-derivatives converge absolutely. The zero-counting estimate and $q_\rho \asymp \gamma^2$ also give absolute convergence after the weighted Laplace integration below. Since

$$\frac{(n+k)!}{(x+q)^{n+k+1}} = \int_0^\infty e^{-(x+q)u} u^{n+k}\, du$$

Tonelli-Fubini applied to absolute values gives

$$\boxed{\mathcal{F}_{n,k}[S_\xi](x) = \int_0^\infty e^{-xu} u^{n+k} (-1)^k \Theta_\xi^{(k)}(u)\, du} \tag{32.3}$$

In particular,

$$\boxed{W_k(x) = (2k-1)! \sum_{[\rho]} m_\rho \frac{q_\rho^k}{(x+q_\rho)^{2k}} = \int_0^\infty e^{-xu} u^{2k-1} (-1)^k \Theta_\xi^{(k)}(u)\, du} \tag{32.4}$$

This proves the heat bridge directly from the spectral expansion. No integration by parts is used, so there are no unverified endpoint terms. It also explains the universal completion cancellation. The Laplace transform of the completion term $1/x$ is the constant heat mode 1; every $k \geq 1$ heat derivative annihilates it.

Folded multiplicity and preserved information

Here $[\rho]$ is the reflection pair $\{\rho, 1-\rho\}$, and m_ρ is its common zero multiplicity. For an off-line quartet, the two factors in the product are $(1-q/q_\rho)^{m_\rho}$ and $(1-q/\bar{q}_\rho)^{m_\rho}$. On the critical line there is one such factor, not two copies of it. No assumption of simplicity is made.

The factorization $q(s_1) - q(s_2) = (s_1 - s_2)(1 - s_1 - s_2)$ proves that the only identification made by the fold is $s \sim 1-s$. Since nontrivial zeros have nonzero imaginary part, q_ρ is real exactly when $\Re\rho = 1/2$; in that case $q_\rho = 1/4 + (\Im\rho)^2 > 1/4$. Reciprocal and sign changes of q_ρ are invertible, whereas a real-part observation is a further map. Any probability construction made from these data must declare its own atoms and multiplicity convention; none is needed for Theorem F.

32A. The Widder array as a Laguerre transform of the heat trace

Theorem F places the derivatives on the heat trace. Moving them onto the kernel instead turns the whole array $F_{n,k}$ into a single integral transform against Θ_ξ, with a scalar kernel whose sign pattern is explicit at every index.

Theorem 32A.1. For all integers $n, k \geq 0$ and every $x > 0$,

$$\boxed{F_{n,k}[S_\xi](x) = k! \int_0^\infty e^{-xu} u^n L_k^{(n)}(xu)\, \Theta_\xi(u)\, du} \tag{32.14}$$

with $L_k^{(n)}(t) = \sum_{j=0}^{k} (-1)^j \binom{n+k}{k-j} t^j / j!$. In particular, for every $k \geq 1$,

$$\boxed{W_k(x) = k! \int_0^\infty e^{-xu} u^{k-1} L_k^{(k-1)}(xu)\, \Theta_\xi(u)\, du} \tag{32.15}$$

and for $k \geq 1$ the scalar kernel in (32.14) has exactly k simple sign changes on $u > 0$.

Proof. Leibniz's rule gives the kernel identity directly:

$$(-1)^n D_x^{n+k}\left[x^k e^{-xu}\right] = k!\, e^{-xu} u^n L_k^{(n)}(xu) \tag{32.16}$$

Differentiating the absolutely convergent heat representation under the integral is justified term by term, since after expansion each contribution is dominated by $\sum_{[\rho]} m_\rho \int_0^\infty e^{-(x+\Re q_\rho)u} u^{n+j} du = (n+j)! \sum_{[\rho]} m_\rho (x + \Re q_\rho)^{-(n+j+1)} < \infty$, including the least-decaying case $n = j = 0$, because $\Re q_\rho \asymp \gamma^2$ against a zero count $O(T \log T)$. No sign for Θ_ξ and no hypothesis is used. Setting $n = k-1$ gives (32.15), which requires $k \geq 1$; this is consistent with $W_k = F_{k-1,k}$ and introduces no reduced W_0.

For the sign count, Rodrigues' formula makes $L_k^{(n)}$ orthogonal to every polynomial of degree below k against the positive weight $t^n e^{-t} dt$; the k integrations by parts have vanishing boundary terms because $n \geq 0$. If there were fewer than k positive sign changes, multiplying by the polynomial with those points as roots would give a nonzero one-sign integrand of degree below k, contradicting orthogonality. Degree k then forces exactly k simple positive roots, and every other kernel factor is positive for $u > 0$. ☐

What the two placements identify, and what neither creates. Nonnegativity of an undifferentiated heat trace cannot force these signs: at any prescribed x, a smooth nonnegative function supported where $L_k^{(n)}(xu) < 0$ gives a negative functional. That is an abstract countermodel to the inference, not a statement about the actual Riemann heat trace. Keeping the derivatives on the heat trace instead, as in Theorem F, requires exactly the complete-monotonicity signs already equivalent to RH (§33). **The two exact placements of the derivatives name the missing information from either side; neither supplies it.** This is the same firewall as §22A in the Laguerre basis rather than the Fourier one.

33. The reduced-Widder criterion and its firewall

Reader (12.1)–(12.4) prints the first six differential rows and their common recurrence. Here the full family supplies the criterion.

Widder's real-variable characterization, in the concise form restated and proved by Sokal, says that a smooth real function S on $(0, \infty)$ is Stieltjes if and only if

$$S(x) \geq 0 \quad \text{and} \quad \mathcal{F}_{k-1,k}[S](x) \geq 0 \quad (k \geq 1, x > 0)$$

For S_ξ, the baseline $S_\xi(x) > 0$ is unconditional: the positive theta-kernel representation makes $\xi(1/2 + y)$ increasing for $y > 0$. Combining Widder's theorem with the folded Stieltjes equivalence gives

$$\boxed{\text{RH} \iff W_k(x) \geq 0 \quad \text{for every } k \geq 1 \text{ and every } x > 0} \tag{33.1}$$

This is an exact RH criterion. Its quantifiers are load-bearing. Positivity of W_1, W_2, W_3, or of any other currently verified finite prefix, does not supply the complete diagonal hypothesis in Widder's theorem. Nothing in the present work promotes a finite prefix to the full Stieltjes class.

34. Theorem G - General source-jet ladder

On the negative axis write

$$x = s(s-1), \qquad s = \sigma + i0 > 1, \qquad R = 2s - 1 = \sqrt{1 + 4x}$$
$$L(s) = \frac{\xi'(s)}{\xi(s)}, \qquad S_\xi(x) = \frac{L(s)}{R}$$

Then $D_x = R^{-1} D_s$. The elementary Jacobian satisfies

$$D_x R^{-p} = -2pR^{-p-2}, \qquad D_x^r R^{-1} = (-1)^r 2^r (2r-1)!! R^{-2r-1} \quad (r \geq 0) \tag{34.0a}$$

where $(-1)!! = 1$. Each differentiation of the inverse Jacobian advances its denominator exponent by two. At the Widder derivative order $r = 2k - 1$, this gives $2r + 1 = 4k - 1$: the successive clearing powers are $R^3, R^7, R^{11}, R^{15}, R^{19}$. The coordinate value $R = 2n + 1$ and the derivative index r have separate roles, joined by this explicit differential law. For every $k \geq 1$ there are polynomials $C_{k,j}(x, R)$ such that

$$\boxed{R^{4k-1} W_k = \sum_{j=0}^{2k-1} C_{k,j}(x, R) L^{(j)}(s)} \tag{34.1}$$

The top coefficient is

$$\boxed{C_{k,2k-1}(x,R) = (-1)^{k-1}x^k R^{2k-1}} \tag{34.2}$$

These source-jet coefficients come from the factorially weighted signed-grid rows in (SW.6), followed by $S = L/R$ and $D_x = R^{-1}D_s$. The product rule introduces the additional Jacobian factors in (34.0a). In particular the top coefficient reads the right-hand grid edge: $C_{k,2k-1} = -c_{k,k}x^k R^{2k-1}$. The lower polynomial coefficients include derivatives of the Jacobian and are not unweighted grid entries.

Indeed, before differentiation the coefficient of L in $x^k L/R$ has one power of R in the denominator. Each application of $D_x = R^{-1}D_s$ can increase the denominator exponent by at most two, so R^{4k-1} clears the $2k-1$ differentiations. The term $L^{(2k-1)}$ arises only when every D_s differentiates L; before clearing it has coefficient $(-1)^{k-1}x^k/R^{2k}$, proving (34.2).

Regularize the zeta pole by

$$F(s) = (s-1)\zeta(s) > 0 \qquad g(s) = \frac{F'(s)}{F(s)}$$

Then

$$L(s) = \frac{1}{s} - \frac{1}{2}\log\pi + \frac{1}{2}\psi(s/2) + g(s)$$

which is regular at $s = 1$. Define the polynomialized owner

$$\mathfrak{N}_k = F^{2k}R^{4k-1}W_k$$

Because $g^{(2k-1)}$ contains $F^{(2k)}/F$ with coefficient 1, the coefficient of the highest regularized source jet in $\mathfrak{N}_k$ is

$$\boxed{(-1)^{k-1}x^k R^{2k-1}F^{2k-1}} \tag{34.3}$$

It never vanishes for $x > 0$. Thus

$$\boxed{W_k \rightsquigarrow F^{(2k)}} \tag{34.4}$$

is a genuine source-control ladder, not merely bookkeeping notation.

Rung	Cleared owner	Highest L derivative	Highest prime moment	Highest F jet	Status
W_1	R^3W_1	L'	P_1	$F^{(2)}$	Analytic, global
W_2	R^7W_2	L'''	P_3	$F^{(4)}$	A-CAT, global
W_3	$R^{11}W_3$	$L^{(5)}$	P_5	$F^{(6)}$	A-CAT, global
W_4	$R^{15}W_4$	$L^{(7)}$	P_7	$F^{(8)}$	A-CAT, global
W_5	$R^{19}W_5$	$L^{(9)}$	P_9	$F^{(10)}$	A-CAT, global
W_6	$R^{23}W_6$	$L^{(11)}$	P_{11}	$F^{(12)}$	A-CAT, global

One scalar ladder, two proof channels

rung	boundary / $(2k-1)!$	source jet	global sign	independent source
W_1	μ_0	$F^{(2)}$	PROVED	analytic
W_2	μ_1	$F^{(4)}$	PROVED	A-CAT
W_3	μ_2	$F^{(6)}$	PROVED	A-CAT
W_4	μ_3	$F^{(8)}$	PROVED	A-CAT
W_5	μ_4	$F^{(10)}$	PROVED	A-CAT
W_6	μ_5	$F^{(12)}$	PROVED	A-CAT

source frontier: the next independent rung is $W_7 \to F^{(14)}$.

Figure 30: The same source-depth dictionary as Reading Volume §R12. Independent Gamma–prime source certificates now reach W_6 and $F^{(12)}$; the next source rung is $W_7 \rightsquigarrow F^{(14)}$.

35. The first rung - an analytic theta proof

Direct differentiation gives

$$\boxed{R^3 W_1 = (1+2x)L + xRL'} \tag{35.1}$$

There is a more revealing proof of its sign. Put

$$y = s - \frac{1}{2} = \frac{R}{2} > \frac{1}{2} \qquad f(y) = \xi\left(\frac{1}{2} + y\right)$$

The classical theta representation can be normalized as

$$f(y) = \int_0^\infty \Phi(u)\cosh(yu)\,du \qquad \Phi(u) > 0$$

Let $\ell = f'/f$. Then $\ell(y) > 0$. After writing the cosh integral as a bilateral exponential integral against a positive symmetric measure, $(\log f)'' = \ell'$ is the variance of u under the exponentially tilted probability measure. Hence $\ell'(y) \geq 0$.

Since $x = y^2 - 1/4$ and $S = \ell/(2y)$,

$$xS(x) = \left(\frac{y}{2} - \frac{1}{8y}\right)\ell(y) = a(y)\ell(y)$$

where $a(y) > 0$ and $a'(y) > 0$ for $y > 1/2$. Therefore

$$W_1(x) = \frac{1}{2y}\left[a'(y)\ell(y) + a(y)\ell'(y)\right] > 0$$

Thus

$$\boxed{W_1(x) > 0 \quad (x > 0)} \tag{35.2}$$

This proof is unconditional, source-theta-side, and uses no nontrivial-zero location data.

36. Theorem H - Global positivity of the second rung

Write

$$b = 1 + 2x \qquad c = 2x^2 + 2x + 1$$

Three applications of $D_x = R^{-1} D_s$ give the exact owner

$$\boxed{R^7 W_2 = 12cL - 6RcL' - 6xR^2bL'' - x^2R^3L'''} \tag{36.1}$$

The completion part $L_{\text{pole}} = R/x$ gives $S_{\text{pole}} = 1/x$, so $-D_x^3[x^2 S_{\text{pole}}] = 0$. For

$$P_j(s) = \sum_{n \geq 2} \Lambda(n)(\log n)^j n^{-s}$$

the arithmetic block is

$$T_2 = -12cP_0 - 6RcP_1 + 6xR^2bP_2 - x^2R^3P_3 \tag{36.2}$$

The negative coefficient of P_3 is retained; no termwise positivity is asserted. With $g = F'/F$, singular cancellation gives the regular owner

$$T_2 = 6(b + 2) + 12cg - 6Rcg' - 6xR^2bg'' - x^2R^3g''' \tag{36.3}$$

Multiplication by F^4 produces the polynomialized owner $\mathfrak{N}_2 = F^4R^7W_2$ and retains the load-bearing term $-x^2R^3F^{(4)}F^3$.

Computer-assisted theorem H. For every $x > 0$,

$$\boxed{W_2(x) > 0}$$

Finite continuum certificate

The primary MPFR implementation certifies $1 \leq s \leq 10$ with 44 complete continuum cells, not a point grid. It uses a common-δ Taylor model for the correlated F-jet, 256-bit directed rounding, Euler–Maclaurin cutoff $N = 30$, order $M = 12$, and Taylor degree 6. The weakest standard cell is

$$[1, 1.05] \qquad \mathfrak{N}_2 > 1.7722913290995005 \times 10^{-4}$$

The adversarial replay changes simultaneously to 512 bits, $N = 60$, $M = 16$, and degree 8, and gives

$$\mathfrak{N}_2([1, 1.05]) > 1.7722971519681892 \times 10^{-4}$$

A materially separate directed-Decimal implementation covers $1 \leq s \leq 40$ with 40 differently partitioned cells. Its weakest cell is

$$[1, 1.0625] \qquad \mathfrak{N}_2 > 1.4504105013872846170863250\,89 \times 10^{-4}$$

It uses 70 decimal digits in the standard run and 120 digits in its adversarial run. The independent replay reproduced every standard cell, adversarial cell, and exact analytic-tail field in the published Decimal receipt.

Analytic outer theorem

For $s \geq 10$, one-sided positive-real digamma and polygamma asymptotics give

$$A_{\Gamma,2}(s) \geq A_L(s) \qquad A_L(10) > 72975.29282199671$$

After replacing the positive logarithmic coefficient by $\log(5/\pi) > 23/50$, differentiation yields

$$A_L'(s) \geq \frac{(2s-1)Q_2(s)}{525s^{10}}$$

where

$$\begin{aligned} Q_2(s) = {} & 13146s^{12} - 19446s^{11} + 9723s^{10} - 2100s^9 + 525s^8 \\ & + 13440s^7 + 17360s^6 - 325280s^5 + 2515160s^4 \\ & - 6609920s^3 + 7797440s^2 - 4596480s + 1088640 \end{aligned}$$

Every coefficient of $Q_2(10+t)$ is positive, so A_L is increasing. On the prime side, $\Lambda(n) \leq \log n$, integral comparison, and $\log 2 < 7/10$ give

$$|T_2(s)| < \frac{15826993}{2460375} s^7 2^{-s} < 62986$$

Thus $R^7 W_2 > 72975 - 62986 > 9989$ for $s \geq 10$, overlapping the finite certificate.

Artifact classification

The unmodified MPFR source hash is

`923ead8447dd2ba48841b3e8a8325397a62f8261dd4b8dbb60c6018f67f6ba40`

and the independent Decimal source hash is

`6beed41c4644be8ab539fba3995bc6e85f0e174073d08e57c6df9e897fdec7c3`

The theorem is unconditional in its mathematical assumptions, computer-assisted on a finite interval, Gamma/prime analytic outside it, independent of zero data, and classified **A-CAT**. Section 74A proves the same sign again on the uniform partition and tail it shares with $W_3, \ldots, W_6$, in the certificate bundled with this edition.

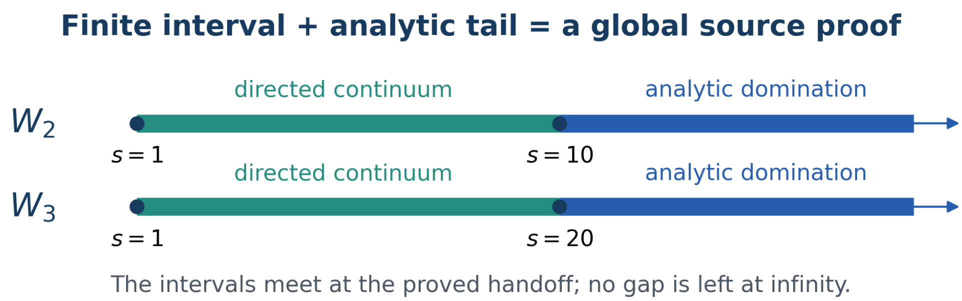

Figure 31: A global source certificate covers the entire $s > 1$ branch: directed finite intervals meet proved analytic tails. The handoffs are $s = 10$ for W_2 and $s = 20$ for W_3; the drawing compresses the unbounded axis.

37. Theorem I - Global positivity of the third rung

Five differentiations give

$$\boxed{R^{11} W_3 = \sum_{j=0}^{5} C_j L^{(j)}} \tag{37.1}$$

where

$$\begin{aligned}
C_0 &= 720(x+1)(2x^2+x+1) \\
C_1 &= -360R(x+1)(2x^2+x+1) \\
C_2 &= -60R^2(4x^3+3x^2-1) \\
C_3 &= 60xR^3(3x^2+3x+1) \\
C_4 &= 15x^2R^4(2x+1) \\
C_5 &= x^3R^5
\end{aligned}$$

Again the completion contribution is annihilated exactly. The source decomposition is

$$R^{11} W_3 = A_{\Gamma,3} + T_3$$

with

$$A_{\Gamma,3} = \frac{C_0}{2}[\psi(s/2) - \log\pi] + \frac{C_1}{4}\psi_1(s/2) + \frac{C_2}{8}\psi_2(s/2) + \frac{C_3}{16}\psi_3(s/2) + \frac{C_4}{32}\psi_4(s/2) + \frac{C_5}{64}\psi_5(s/2)$$

and

$$T_3 = -C_0P_0 + C_1P_1 - C_2P_2 + C_3P_3 - C_4P_4 + C_5P_5 \tag{37.2}$$

The mixed signs are retained. Singular regularization gives

$$\boxed{T_3 = 240(3x^2 + 5x + 5) + \sum_{j=0}^{5} C_j g^{(j)}} \tag{37.3}$$

If $G_0 = F'$ and

$$G_{j+1} = FG_j' - (j+1)F'G_j$$

then $g^{(j)} = G_j/F^{j+1}$ and

$$\boxed{\mathfrak{N}_3 := F^6R^{11}W_3 = F^6A_{\Gamma,3} + 240(3x^2 + 5x + 5)F^6 + \sum_{j=0}^{5} C_jG_jF^{5-j}} \tag{37.4}$$

The coefficient of $F^{(6)}$ is $C_5F^5 = x^3R^5F^5 > 0$, so the sixth source jet is genuinely load-bearing.

Computer-assisted theorem I. For every $x > 0$,

$$\boxed{W_3(x) > 0}$$

Finite continuum certificate

The directed MPFR artifact certifies $1 \le s \le 20$ in 135 continuum cells at 256 bits. It uses a common-variable degree-6 Taylor model, with center Euler–Maclaurin parameters $(N, M) = (24, 9)$ and uniform-remainder parameters $(12, 7)$. The weakest cell is

$$[1, 1.01] \qquad \mathfrak{N}_3 > 1.6950218693828748 \times 10^{-5}$$

The adversarial replay changes to 512 bits, Taylor degree 8, center parameters $(40, 12)$, and remainder parameters $(24, 10)$. It gives

$$1.6951786515869995 \times 10^{-5} < \mathfrak{N}_3([1, 1.01]) < 2.2185472840400943 \times 10^{-5}$$

Analytic outer theorem

For $s \geq 20$, elementary polygamma series bounds and $\log(s/(2\pi)) > 23/20$ yield

$$A_{\Gamma,3} > \frac{3Q_3(s)}{s^3}$$

where

$$\begin{aligned} Q_3(s) = 324s^9 - 5652s^8 + 23266s^7 - 47632s^6 + 58430s^5 \\ - 46350s^4 + 24055s^3 - 8052s^2 + 1519s - 120 \end{aligned}$$

Every coefficient of $(Q_3(s) - 93s^9)|_{s=20+t}$ is positive; consequently

$$A_{\Gamma,3} > 279s^6$$

On the arithmetic side, $\Lambda(n) \leq \log n$ and exact log-moment integration give

$$|T_3| < 14s^{11}2^{-s}$$

Since

$$14\frac{20^5}{2^{20}} = \frac{21875}{512} < 279$$

and $s^5/2^s$ decreases for $s \geq 20$,

$$|T_3| < 279s^6 < A_{\Gamma,3}$$

This closes the analytic tail with no zero-location input.

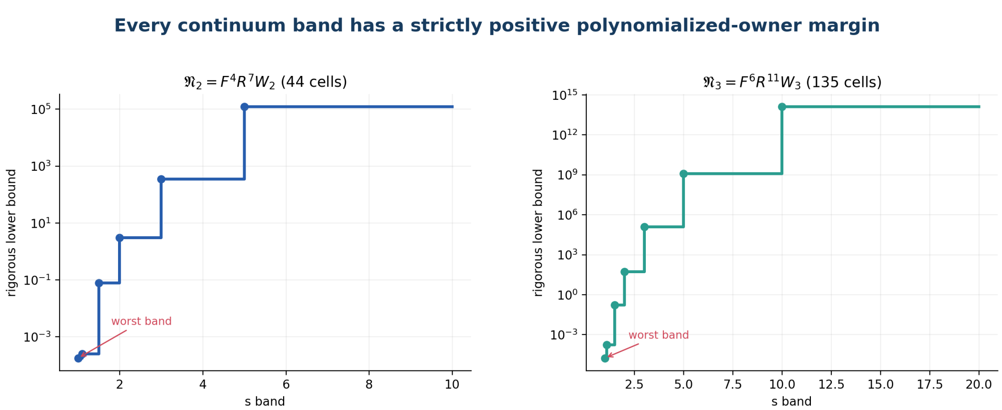

Figure 32: The finite W_2 and W_3 continuum certificates have positive lower bounds on every band; the two panels show different polynomialized owners and should not be compared in absolute scale.

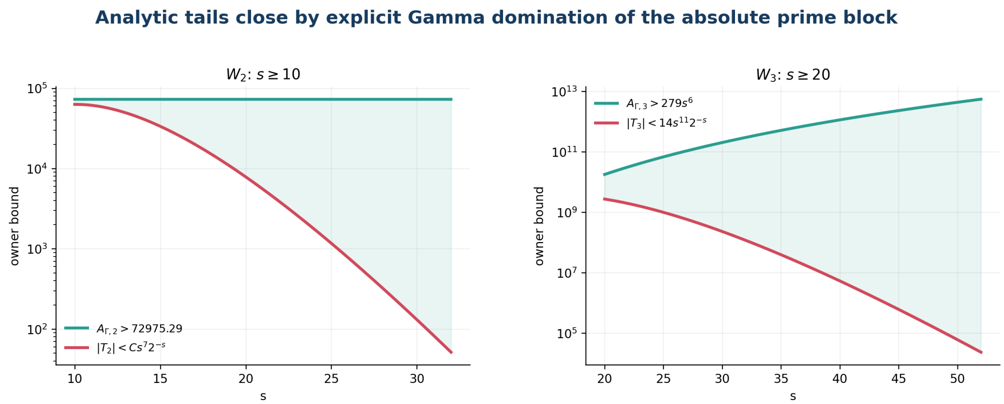

Figure 33: The explicit analytic tails: an Archimedean lower bound dominates the complete absolute von-Mangoldt block beyond the stated handoff.

Reproducible source certificate

The certificate uses exact rational Bernoulli data and outward-rounded interval arithmetic on 135 continuum cells, and its adversarial replay reproduced every cell and every analytic-tail constant. Together with the tail theorem this proves the global result with grade A-CAT. Section 74A proves the same sign again on the uniform partition and tail it shares with the other certified rungs, in the certificate bundled with this edition.

38. The fourth owner and the non-raising recurrence

The next reduced rung is

$$W_4(x) = -D_x^7[x^4 S_\xi(x)]$$

Exact differentiation gives

$$\boxed{R^{15} W_4 = \sum_{j=0}^{7} D_j L^{(j)}} \tag{38.1}$$

where, with

$$A(x) = 10x^4 + 20x^3 + 18x^2 + 10x + 5$$

the coefficients are

$$\begin{aligned}
D_0 &= 20160A(x)\\
D_1 &= -10080RA(x)\\
D_2 &= -10080R^2(x+1)(2x^3-1)\\
D_3 &= 840R^3(22x^4+32x^3+18x^2+4x-1)\\
D_4 &= -840xR^4(x+1)(2x^2+2x+1)\\
D_5 &= -84x^2R^5(10x^2+10x+3)\\
D_6 &= -28x^3R^6(2x+1)\\
D_7 &= -x^4R^7
\end{aligned}$$

The array $D_0, \ldots, D_7$ is row $k = 4$ of the signed-grid construction after the factorial and Jacobian operations in (SW.6) and §34. Its top entry $D_7 = -x^4R^7$ uses $c_{4,4} = +1$. An exact rational differentiator independently reproduces every one of these coefficients and verifies the general top coefficient through $k = 8$. The highest prime moment is P_7 and the highest regularized source jet is $F^{(8)}$.

There is an exact recurrence between successive rungs:

$$\boxed{W_{k+1} = -j_kW_k' - xW_k'' = -x^{-2k}D_x[x^{2k+1}W_k'], \qquad j_k = 2k+1} \tag{38.2}$$

To prove it, write $x^{k+1}S = x(x^kS)$ and use $D_x^m(xf) = xD_x^m f + mD_x^{m-1}f$ with $m = 2k+1$. The recurrence is not a positivity-raising operator: knowing only $W_k \geq 0$ gives no control over the two derivatives on the right. An independent source-side continuum certificate and analytic tail close the sign, as proved in Theorem 74.1:

$$\boxed{W_4(x) > 0 \qquad (x > 0)}$$

38A. Positive descent, not positive raising

For the actual completed rungs the non-raising recurrence (38.2) has a positive inverse in the downward direction:

$$\boxed{W_k(x) = \frac{1}{2k}\left[x^{-2k}\int_0^x t^{2k}W_{k+1}(t)dt + \int_x^\infty W_{k+1}(t)dt\right], \qquad k \geq 1.} \tag{38A.1}$$

Proof. The recurrence is $(x^{2k+1}W_k')' = -x^{2k}W_{k+1}$. Analyticity at zero removes the first integration constant. Each fixed rung tends to zero at infinity by its folded expansion and dominated convergence. Integrating twice, and interchanging the order, gives (38A.1). This interchange is absolute: for $\Re q > 0$, $|t+q|^2 \geq (t+|q|)^2/2$, so the integral of the absolute value of one $(k+1)$-st rung is at most $C_k|q|^{-k}$, summable over the folded zeros. □

Both kernels are nonnegative. Thus $W_{k+1} \geq 0$ on the full positive axis implies $W_k \geq 0$ there. Positivity on that axis at every index in any unbounded set implies the whole Widder criterion;

odd indices are one example. This does not raise a finite prefix, and values at $x = 0$ alone do not satisfy its hypotheses. The separate odd Li criterion is Theorem 155A.2.

74. Global fourth-rung theorem

This section proves the fourth scalar rung directly from the source. It is a source-side theorem: the finite certificate evaluates the regularized zeta/Gamma source on the real half-line $s > 1$, and the analytic tail uses only polygamma inequalities and the absolutely convergent von-Mangoldt series. It does not use a zeta zero table, a verified RH height, or RH.

Put

$$x = s(s-1), \qquad R = 2s-1, \qquad s > 1$$

and

$$L(s) = \frac{\xi'(s)}{\xi(s)}$$

Section 38 proved the exact owner

$$R^{15}W_4 = \sum_{j=0}^{7} D_j L^{(j)} \tag{74.1}$$

with the displayed polynomial coefficients $D_0, \ldots, D_7$. Regularize the pole of ζ at 1 by

$$F(s) = (s-1)\zeta(s) > 0$$

and define

$$\boxed{\mathfrak{N}_4(s) = F(s)^8 R^{15} W_4(x(s))} \tag{74.2}$$

Since F and R are positive on $s > 1$, $\mathfrak{N}_4$ and W_4 have the same sign.

Theorem 74.1 (global fourth source rung). For every $x > 0$,

$$\boxed{W_4(x) > 0} \tag{74.3}$$

The accepted classification is **A-CAT / SOURCE-SIDE**, as recorded in §R12.
This is the source-side A-CAT fourth-rung theorem, established by a finite continuum certificate and a separate analytic tail. The section keeps the original proof, with its own handoff at $s = 40$ and its own constants; §74A proves the same sign again inside the bundled certificate that covers $W_2, \ldots, W_6$ on one partition. The independent verified-height theorem also includes this scalar sign. No finite positive prefix establishes the

all-order RH criterion.

Finite continuum $1 \le s \le 40$

The regular source identity is

$$L(s) = \frac{1}{s} - \frac{1}{2}\log\pi + \frac{1}{2}\psi\left(\frac{s}{2}\right) + \frac{F'(s)}{F(s)} \tag{74.4}$$

Substituting (74.4) in (74.1), multiplying by F^8, and performing every operation in one common Taylor variable preserves the correlations among $F, F', \ldots$. This point matters: independent interval substitution for the jets is far too wide near $s = 1$.

The standard replay uses GNU MPFR directed rounding at 256 bits. It covers $[1, 40]$ by the following exact schedule:

band	cell width	cells
$[1, 1.1]$	0.01	10
$[1.1, 1.3]$	0.02	10
$[1.3, 1.5]$	0.025	8
$[1.5, 2]$	0.02	25
$[2, 3]$	0.05	20
$[3, 5]$	0.1	20
$[5, 10]$	0.25	20
$[10, 20]$	0.5	20
$[20, 40]$	1	20

Thus 153 complete continuum cells are certified. Taylor degree eight, center Euler–Maclaurin parameters $(N, M) = (24, 9)$, and remainder parameters $(12, 7)$ require correlated center jets through $F^{(16)}$ and a remainder through $F^{(17)}$. Bernoulli numbers are exact rationals; every arithmetic operation, including the Euler–Maclaurin remainder, is rounded outward.

The weakest standard cell is the endpoint cell:

$$s \in [1, 1.01], \qquad \mathfrak{N}_4(s) > 3.2148256503423557 \times 10^{-6} \tag{74.5}$$

An independent adversarial replay changes all material numerical parameters at once: 512 bits, Taylor degree ten, center $(N, M) = (40, 12)$, and remainder $(24, 10)$. It gives

$$\mathfrak{N}_4([1, 1.01]) > 3.2149708080858507 \times 10^{-6} \tag{74.6}$$

The two lower endpoints need not coincide; each is a rigorous enclosure from a different Taylor/Euler–Maclaurin model. Their agreement at the displayed scale comes from an adversarial replay, not from an assumption.

Analytic tail $s \geq 40$

Completion annihilation separates

$$R^{15}W_4 = A_{\Gamma,4} + T_4 \tag{74.7}$$

where

$$A_{\Gamma,4} = \frac{D_0}{2}\left[\psi(s/2) - \log\pi\right] + \sum_{j=1}^{7} \frac{D_j}{2^{j+1}}\psi^{(j)}(s/2) \tag{74.8}$$

and T_4 is the von-Mangoldt source. Integral comparison in the classical polygamma series gives, for $m \geq 1$ and $z > 0$,

$$(m-1)!z^{-m} \leq (-1)^{m+1}\psi^{(m)}(z) \leq (m-1)!z^{-m} + m!z^{-m-1} \tag{74.9}$$

together with $\psi(z) \geq \log z - z^{-1}$. Substitution with the signs of the D_j yields a rational lower function $B_4(s)$. After clearing s^8,

$$s^8\left(B_4(s) - 25000s^8\right) = P_4(s) \tag{74.10}$$

and every coefficient of $P_4(40+t)$ is a strictly positive integer. Consequently

$$\boxed{A_{\Gamma,4} > 25000s^8 \qquad (s \geq 40)} \tag{74.11}$$

For the prime source, $x < s^2$, $R < 2s$, and $\Lambda(n) \leq \log n$ give

$$|T_4| < Ks^{15}2^{-s} \qquad K = \frac{147272517786042096363168 19}{5937162272960256000000000} < 25 \tag{74.12}$$

Since

$$\frac{40^7}{2^{40}} = \frac{78125}{524288} < 1$$

and $s^7/2^s$ decreases for $s \geq 40$,

$$\boxed{|T_4| < 25s^8 \qquad (s \geq 40)} \tag{74.13}$$

Equations (74.11)–(74.13) imply

$$R^{15}W_4 > 24975s^8 > 0 \qquad (s \geq 40) \tag{74.14}$$

The finite continuum and the analytic tail overlap at $s = 40$, proving Theorem 74.1. This is the original fourth-rung argument, in its own coordinates: a directed finite certificate on

$1 \le s \le 40$ and the analytic tail (74.11)–(74.14) beyond it. Section 74A proves $W_4 > 0$ again, on the uniform partition and tail shared by $W_2, \dots, W_6$, with a bundled certificate that the v5.0 build re-executed; the two arguments are independent of each other in partition, threshold and handoff point. Independently of both, the verified-height theorem in Reading Volume §R13 includes $W_4 > 0$ in its finite zero-assisted prefix.

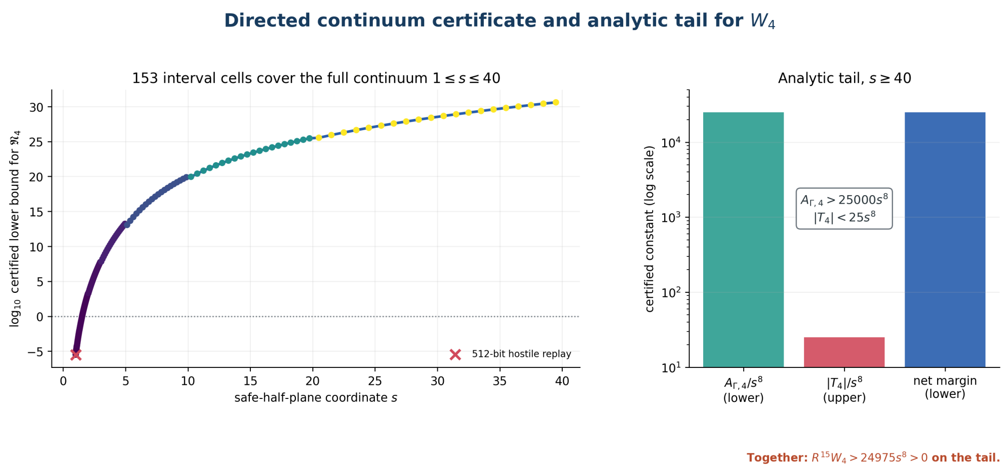

Figure 34: Every cell lower bound is positive; the separate analytic tail leaves a factor-999 source margin.

What the fourth rung does and does not establish

The fourth-rung theorem itself established the inherited source prefix

$$\boxed{W_1, W_2, W_3, W_4 > 0 \quad \text{globally}} \tag{74.15}$$

Section 74A extends the independent source prefix to $W_1, \dots, W_6 > 0$, proving the four certified rungs above the first on one partition and one tail. The non-raising recurrence (38.2) is unchanged, and the next independent owner is $W_7 \rightsquigarrow F^{(14)}$. A finite source prefix is not a zero-location theorem and does not imply the full Widder hierarchy.

74A. One certificate for the source rungs $W_2, \dots, W_6$

The five certified source rungs are proved together, by one certificate: one partition of a finite s-interval, one exact analytic tail beyond it, and two programs that share no arithmetic. No zero table, verified height or RH assumption enters anywhere.

Theorem 74A.1 (global source rungs). For every $x > 0$,

$$\boxed{W_k(x) > 0 \qquad (k = 2, 3, 4, 5, 6).} \tag{74A.1}$$

The classification is **A-CAT / SOURCE-SIDE**. The owners reach $F^{(4)}$ at the second rung and $F^{(12)}$ at the sixth, for $F(s) = (s-1)\zeta(s)$.

Use $x = s(s-1)$, $R = 2s-1$, $D_x = R^{-1}D_s$ and $L = \xi'/\xi$, so that $W_k(x) = (-1)^{k-1}D_x^{2k-1}[x^k L/R]$. On $1 \le s \le 128$ the regularization

$$F(s) = 1+(s-1)\left(\zeta(s) - \frac{1}{s-1}\right), \qquad \log\xi(s) = \log s + \log F(s) + \log\Gamma(s/2) - \frac{s}{2}\log\pi - \log 2 \tag{74A.2}$$

removes the pole at one. The certified quantity is

$$\mathcal{W}_k(s) = \frac{s^{2k-1}}{(2k-1)!} W_k(s(s-1)), \tag{74A.3}$$

which is positive exactly where W_k is, because $s^{2k-1}/(2k-1)! > 0$ and $s \mapsto s(s-1)$ carries $[1,\infty)$ onto $[0,\infty)$.

The finite continuum, $1 \le s \le 128$

A complete rational partition into continuum cells proves

$$\boxed{\mathcal{W}_k(s) > \theta_k \quad (1 \le s \le 128)}, \qquad \begin{array}{c|ccccc} k & 2 & 3 & 4 & 5 & 6 \\ \hline \theta_k & 10^{-5} & 10^{-8} & 10^{-10} & 10^{-12} & 10^{-15} \end{array} \tag{74A.4}$$

Each cell is accepted from a bound that holds on the whole interval, never from a point grid. With m the midpoint of a cell and r its radius, p_j an enclosure of $\mathcal{W}_k^{(j)}(m)/j!$, and Q_D an enclosure of $\mathcal{W}_k^{(D)}(\sigma)/D!$ for every σ in the cell, Taylor's theorem with Lagrange remainder gives

$$\mathcal{W}_k(s) \;\ge\; p_0 - \sum_{j=1}^{D-1} |p_j| r^j - \sup|Q_D|\, r^D \qquad (|s-m| \le r). \tag{74A.5}$$

Every operation is outward rounded, the endpoints are exact dyadic rationals, adjacency and both ends of $[1, 128]$ are verified exactly, and a cell whose bound does not clear θ_k is bisected and retried.

The thresholds in (74A.4) are deliberately far below the certified values. The smallest enclosures occur at the left endpoint, where (12.4a) identifies $\mathcal{W}_k(1) = \mu_{k-1}$, the folded boundary moment:

k	2	3	4	5	6
$\mu_{k-1} = \mathcal{W}_k(1)$	3.71006×10^{-5}	1.43678×10^{-7}	6.59828×10^{-10}	3.19389×10^{-12}	1.57589×10^{-14}
θ_k	10^{-5}	10^{-8}	10^{-10}	10^{-12}	10^{-15}

The exact tail, $s \ge 128$

Generate the source polynomials recursively by

$$P_j^{(r+1)} = R(P_j^{(r)})' - 2(2r+1)P_j^{(r)} + RP_{j-1}^{(r)}, \qquad P_0^{(0)} = x^k, \tag{74A.6}$$

which is the product rule for $R^{-1}D_s$ applied to $P(s)L^{(j)}(s)R^{-m}$ at $m = 1, 3, \dots, 4k-3$. With $C_{k,j} = (-1)^{k-1}P_j^{(2k-1)}$ this gives the exact identity

$$R^{4k-1}W_k = \sum_{j=0}^{2k-1} C_{k,j}(s)L^{(j)}(s), \qquad C_{k,2k-1} = (-1)^{k-1}x^k R^{2k-1}. \tag{74A.7}$$

Completion annihilates the elementary $1/s + 1/(s-1)$ terms, which is checked as a polynomial identity, and the recurrence is checked against the closed-form x-Leibniz values of $D_x^{2k-1}[x^{k+m}]$. Separating the Gamma and von-Mangoldt pieces and using $0 < (1-e^{-t})^{-1} - t^{-1} - 1/2 < t/12$ gives an exact rational lower function B_k for the Gamma part; with $\alpha_k = \frac{1}{4}\,\mathrm{lead}(B_k)$ and $\Lambda(n) \le \log n$ with integral comparison for the complete prime part,

$$A_{\Gamma,k}(s) > \alpha_k s^{2k}, \qquad |T_k(s)| < \tfrac{1}{2}\alpha_k s^{2k} \qquad (s \ge 128), \tag{74A.8}$$

both by exact rational checks: every coefficient of $s^{2k+1}(B_k(s) - \alpha_k s^{2k})$, expanded at $s = 128 + t$, is nonnegative with a positive constant term, and the endpoint ratio of the prime bound to the Gamma margin is a rational number below 1/2, after which it decreases because $s^{2k-1}2^{-s}$ does. Hence

$$\boxed{W_k(s(s-1)) > \frac{\alpha_k}{2} \cdot \frac{s^{2k}}{(2s-1)^{4k-1}} \qquad (s \ge 128)} \tag{74A.9}$$

with the exact constants

k	2	3	4	5	6
α_k	7	396	54,000	13,406,400	5,258,131,200
prime/Gamma ratio at $s = 128$	1.9×10^{-33}	1.2×10^{-30}	3.3×10^{-28}	5.1×10^{-26}	5.2×10^{-24}

The finite continuum and the exact tail overlap at $s = 128$, so (74A.4) and (74A.9) prove Theorem 74A.1.

Two arithmetics, one statement

The certificate is executed twice, by programs that share no arithmetic, no special-function implementation and no computer-algebra system:

- `qa/source_rungs/source_rungs_arb.py` evaluates the jets in FLINT/Arb ball arithmetic through python-flint, with SymPy for the exact tail. It generalizes the fifth- and sixth-rung certificate of the 4.5 edition to all five rungs; the evaluator, the cell test and the tail argument are the same, with θ_k and α_k as parameters.
- `qa/source_rungs/source_rungs_decimal.py` uses the Python standard library alone. Arithmetic is `decimal` (libmpdec) with directed rounding on every operation; the ζ jet is Euler–Maclaurin (DLMF 25.2.9) with Lehmer's bound on the periodic Bernoulli function and Cauchy estimates for the Taylor coefficients of the remainder; the ψ jet is the recurrence with the Stirling series (DLMF 5.11.2) and the classical remainder bound $|R_m(w)| \le |B_{2m}|/(2m(\mathrm{Re}\, w)^{2m})$; the source polynomials and the whole tail are exact `Fraction` arithmetic. It imports neither FLINT/Arb nor MPFR, SymPy or mpmath.

Each program also checks the repeated s-operator against a second formulation of the same quantity: the x-Leibniz formula in the first, the polynomial identity (74A.7) in the second. Both are run a second time with every material parameter changed at once – precision, Taylor order and partition, and in the standard-library program the Euler–Maclaurin and Stirling truncations as well. `qa/source_rungs/cross_backend_check.py` compares the runs: the exact tail data agree digit for digit, including the source polynomials, the signs, α_k, the prime bound and the endpoint ratio, and the sampled enclosures of $\mathcal{W}_k$ overlap. The receipts record every accepted cell, and the build re-executes both programs.

Thus the source-side prefix is $W_1, \ldots, W_6 > 0$: the first rung analytically (§35), the next five by this certificate. The recurrence (38.2) remains non-raising. The next independent source sign is $W_7 = -x^{-12}(x^{13}W_6')' > 0$, whose owner reaches $F^{(14)}$, and it is open. No finite prefix establishes the all-order Widder criterion.

Pole-sublattice calibration at the next rung

A Gamma-pole analysis supplies an auxiliary NO-GO, not a completed W_7 sign. For a centered pole term f_m let $d\sigma_{f_m}$ be the signed measure of f_m/x. Its density changes sign once, at $u = m + 1/2$, and

$$\int u^{-k}\, d\sigma_{f_m}(u) < 0 \qquad (k \geq 2). \tag{74A.10}$$

The publication label is important: because $h = xE_\xi'/E_\xi$ already contains the factor x,

$$\boxed{\frac{W_k[f_m](0)}{(2k-1)!} = \int u^{-k}\, d\sigma_{f_m}(u),} \tag{74A.11}$$

not $W_k[f_m/x]$. For $m = 0$,

$$\frac{W_k[f_0](0)}{(2k-1)!} = -\binom{2k-2}{k-2}, \qquad k \geq 2, \tag{74A.12}$$

so the complementary centered pole channel contributes at most -792 to the normalized seventh rung at the boundary. This is an obstruction to treating the unused Gamma poles as a hidden positive reserve. It is **not** a negative statement about completed W_7, whose Gamma and prime pieces nearly cancel and whose all-x source sign remains open.

55. Fourth-rung theorem and fixed-rung asymptotics

The fourth reduced-Widder owner is

$$W_4(x) = -840S_\xi'''(x) - 840xS_\xi^{(4)}(x) - 252x^2S_\xi^{(5)}(x) - 28x^3S_\xi^{(6)}(x) - x^4S_\xi^{(7)}(x) \tag{55.1}$$

and

$$W_4 = -7W_3' - xW_3'' \tag{55.2}$$

Its denominator-cleared source owner reaches $F^{(8)}$ for $F(s) = (s-1)\zeta(s)$. Direct source-side $W_4(x) > 0$ for all $x > 0$ is an A-CAT theorem. Section 74A carries the same source-side classification for $W_2, \ldots, W_6$ in one bundled certificate, reaching $F^{(12)}$ at the sixth rung. The original fourth-rung proof remains in §74.

A complementary unconditional outer theorem controls every fixed rung.

Theorem 55.1 (eventual positivity of every fixed rung). For every fixed integer $k \geq 1$,

$$\boxed{W_k(x) = \kappa_k x^{1/2-k} \log x + O_k(x^{1/2-k})} \tag{55.3}$$

where

$$\boxed{\kappa_k = \frac{(2k-1)!!(2k-3)!!}{2^{2k+2}} > 0} \tag{55.4}$$

Hence $W_k(x) > 0$ for all sufficiently large x, with the threshold allowed to depend on k.

Proof. The explicit source formula and the differentiated Stirling–polygamma expansion imply, for each fixed $m \geq 0$,

$$D_x^m S_\xi(x) = D_x^m \left(\frac{\log x}{8\sqrt{x}} \right) + O_m(x^{-m-1/2}) \tag{55.5}$$

To justify differentiation, note that $s \asymp \sqrt{x}$ and $D_x s = 1/R = O(x^{-1/2})$; every fixed derivative of the von-Mangoldt series is exponentially small in s, while the differentiated polygamma remainder is a classical symbol of the required order. Thus (55.5), not merely an undifferentiated big-O estimate, is available.

Now

$$x^k S_\xi(x) = \frac{1}{8} x^{k-1/2} \log x + O_k(x^{k-1/2}) \tag{55.6}$$

with the same differentiated-symbol control through order $2k-1$. The coefficient of $\log x$ after $2k-1$ derivatives is

$$\frac{1}{8} \left(k - \frac{1}{2} \right)_{\underline{2k-1}} x^{1/2-k} \tag{55.7}$$

The falling factorial has sign $(-1)^{k-1}$ and magnitude

$$\left| \left(k - \frac{1}{2} \right)_{\underline{2k-1}} \right| = \frac{(2k-1)!!(2k-3)!!}{2^{2k-1}} \tag{55.8}$$

Multiplication by the Widder sign gives (55.3)–(55.4). □

For $k = 4$,

$$\boxed{W_4(x) = \frac{1575}{1024}x^{-7/2}\log x + O(x^{-7/2})} \tag{55.9}$$

This reduces any fixed-rung proof to a compact interval plus an effective tail. It does not solve RH because the constants and thresholds are not uniform in k.

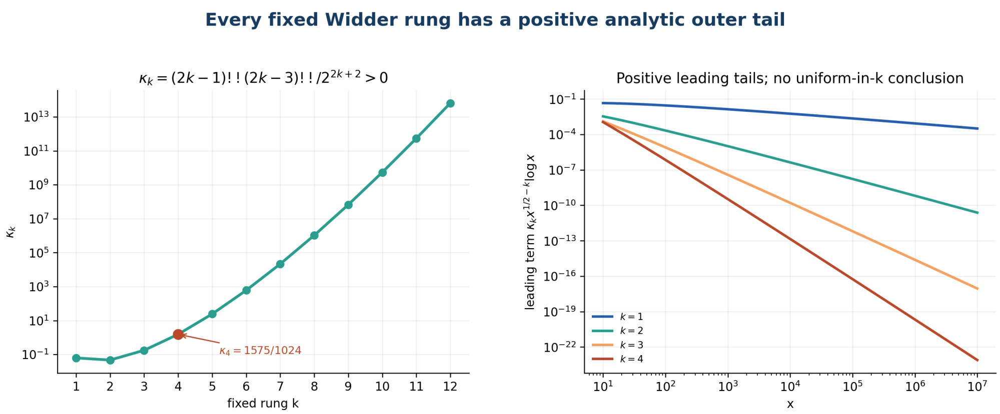

Figure 35: The positive fixed-rung asymptotic constants and the decay of the first four leading tails.

75. Exact reserve phase transition and all-rung shifted handoff

This section audits the triangular coefficient proposed for logarithmic jets of the same regular source $F(s) = (s-1)\zeta(s)$. For $m \geq 1$ put

$$P_{m-1}(s) = \sum_{n\geq 2} \frac{\Lambda(n)(\log n)^{m-1}}{n^s}$$

$$\rho_m(s) = \frac{(s-1)^m P_{m-1}(s)}{(m-1)!} \qquad \mathcal{R}_m(s) = 1 - \rho_m(s) \tag{75.1}$$

Termwise differentiation of the Euler product on $s > 1$ gives the exact identity

$$\boxed{\mathcal{R}_m(s) = (-1)^{m-1}(\log F)^{(m)}(s)\frac{(s-1)^m}{(m-1)!}} \tag{75.2}$$

Fix a rung k and the minimal termwise-positive handoff

$$s_k = 1 + \frac{2k}{\log 2} \tag{75.3}$$

If $1 \le m \le 2k$ and $s \ge s_k$, every source atom has $y = (s-1)\log n \ge m$. Since $y^m e^{-y}$ decreases for $y \ge m$, $\rho_m(s)$ decreases with s. At fixed s_k, the atom ratio from order m to order $m+1$ equals $y/m \ge 1$, so $\rho_m(s_k)$ increases with m. Both monotonicity reductions are therefore exact, and

$$\boxed{\inf_{\substack{s\ge s_k\\ 1\le m\le 2k}} \mathcal{R}_m(s) = \mathcal{R}_{2k}(s_k) = 1 - A_k} \tag{75.4}$$

Writing $Y = 2k + \Delta$ and $\lambda = \log_2(p^a)$ gives the prime-power owner

$$A_k(\Delta) = \frac{1}{(2k-1)!}\sum_{p^a} \frac{(Y\lambda)^{2k} e^{-Y\lambda}}{ap^a} \tag{75.5}$$

The proposed triangular margin is

$$c_k = \frac{1}{kT_k} = \frac{2}{k^2(k+1)} \tag{75.6}$$

It holds on the minimal shell precisely when $A_k(0) < 1 - c_k$.

Theorem 75.1 (exact minimal-shell ladder). The inequality

$$(-1)^{m-1}(\log F)^{(m)}(s) > c_k \frac{(m-1)!}{(s-1)^m} \tag{75.7}$$

for every $s \ge s_k$ and $1 \le m \le 2k$ holds exactly for

$$\boxed{2 \le k \le 11} \tag{75.8}$$

It fails at $k = 1$ and at every $k \ge 12$.

The finite values $1 \le k \le 12$ are enclosed by directed MPFR evaluation of (75.5) through prime powers $p^a \le 20000$, followed by an explicit incomplete-gamma tail. At $k = 12$, the two atoms $n = 2, 3$ already give

$$A_{12}(0) > 1.00660782373417 > 1 \tag{75.9}$$

so the first failure is independent of the rest of the prime source. For $k \ge 13$, the $n = 2$ atom

$$B_k = \frac{(2k)^{2k} e^{-2k}}{2(2k-1)!} \tag{75.10}$$

is increasing and $B_{13} > 1.01385265607324$. Thus one atom proves every later failure. Stirling explains the transition:

$$B_k = \sqrt{\frac{k}{4\pi}}\, e^{-\theta_{2k}} \qquad 0 < \theta_{2k} < \frac{1}{24k} \tag{75.11}$$

so the obstruction scale is 4π, not a triangular number.

At the fourth rung, the sharp reserve is

$$0.28687152864220360 < C_4^* = 1 - A_4 < 0.28687152864220367 \tag{75.12}$$

and therefore

$$\frac{2}{7} < C_4^* < \frac{3}{10}$$

The rational value 1/40 is also a valid lower margin; it is not the optimal constant.

Theorem 75.2 (all-rung shifted handoff). For every integer $k \geq 2$, if

$$s \geq 1 + \frac{2k + \sqrt{2k \log k}}{\log 2} \qquad 1 \leq m \leq 2k \tag{75.13}$$

then

$$\boxed{(-1)^{m-1} (\log F)^{(m)}(s) > \frac{2}{5} \frac{(m-1)!}{(s-1)^m}} \tag{75.14}$$

For completeness, let $B_k(\Delta)$ be the $n = 2$ atom and let E_k be the relative contribution of all remaining atoms. Atom-ratio monotonicity gives

$$A_k(\Delta) \leq (1 + E_2) B_k(\Delta) \qquad 1 + E_2 < \frac{8}{5} \tag{75.15}$$

With $\Delta_k = \sqrt{2k \log k}$, Stirling and $\delta - \log(1 + \delta) \geq \delta^2/2 - \delta^3/3$ give

$$B_k(\Delta_k) \leq \frac{1}{2\sqrt{\pi}} \exp\left(\frac{(\log k)^{3/2}}{3\sqrt{2k}} \right) \tag{75.16}$$

The function $(\log k)^{3/2}/\sqrt{k}$ is maximized at $k = e^3$. Its explicit Stirling majorant has maximum $U_* = (2\sqrt{\pi})^{-1} \exp(\sqrt{3/(2e^3)})$. Numerical evaluation gives

$$B_k(\Delta_k) \leq U_* < \frac{3}{8}, \qquad U_* \approx 0.37074729122661467 \tag{75.17}$$

Therefore

$$A_k(\Delta_k) < \frac{8}{5} \frac{3}{8} = \frac{3}{5}$$

which proves (75.14). No zeros and no RH enter either reserve theorem.

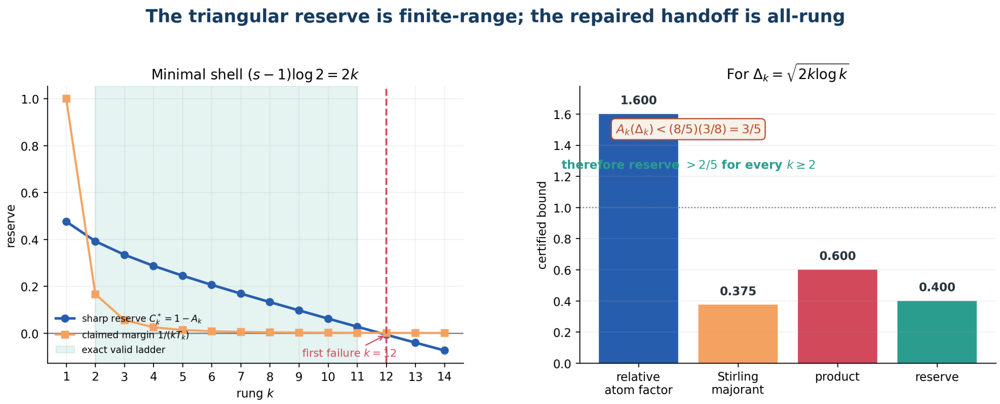

Figure 36: The minimal triangular margin survives exactly through rung 11; moving the handoff by $\sqrt{2k\log k}$ restores an absolute reserve for every rung.

39. Theorem J - Conjugate-block phase and the blind radius

Let $q = a + ib$ with $b \neq 0$ be a nonreal folded zero, paired with $\bar{q}$. Its contribution to the reduced rung is

$$\boxed{W_k^{\{q,\bar{q}\}}(x) = 2(2k-1)!\left(\frac{|q|}{|x+q|^2}\right)^k \cos(k\,[\arg q - 2\arg(x+q)])} \tag{39.1}$$

This follows immediately from (32.4) by adding a term to its conjugate. Define

$$\phi_q(x) = \arg q - 2\arg(x+q)$$

Direct calculation gives

$$\operatorname{Im}\frac{q}{(x+q)^2} = \frac{b(x^2 - |q|^2)}{|x+q|^4} \tag{39.2}$$

Hence $x = |q|$ is the unique positive **blind radius** at which $\phi_q(x) = 0$ and the isolated conjugate block is positive for every k. For every $x \neq |q|$, the phase is nonzero modulo 2π. If $\phi_q(x)/(2\pi)$ is rational, its finite rotation orbit contains negative cosines and repeats them forever; if it is irrational, the orbit is dense. Therefore the isolated block is negative for infinitely many Widder orders.

A useful conditional detection statement follows. Put

$$A_q(x) = \frac{|q|}{|x+q|^2}$$

If at some $x \neq |q|$ a nonreal pair has a strict spectral gap

$$A_q(x) > \sup_{p \neq q, \bar{q}} A_p(x)$$

then the remaining absolutely summable blocks are exponentially smaller along a subsequence for which $\cos(k\phi_q(x)) \leq -1/2$. Consequently $W_k(x) < 0$ for infinitely many k. This is an exact conditional high-order detector. The strict-gap hypothesis is sufficient for this orbitwise argument. Theorem 49.1 supplies a stronger general conclusion without it: an RH failure gives infinitely many negative rungs on an open interval of scales. That converse is proved; the independent source sign remains open.

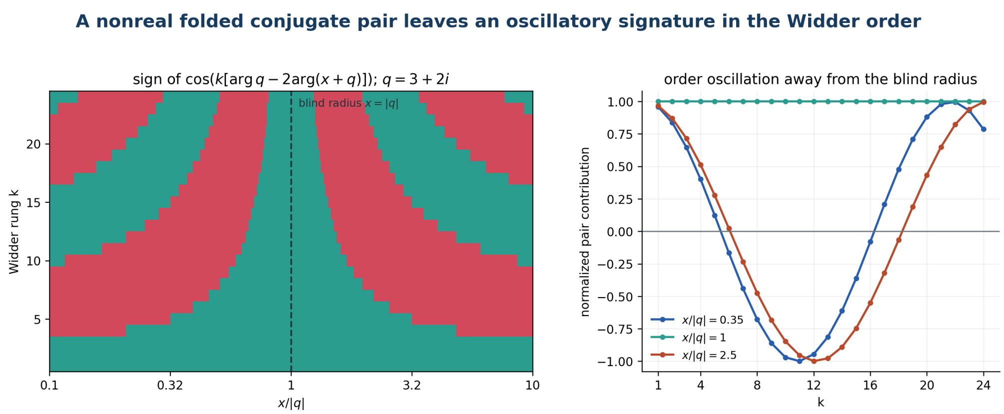

Figure 37: For a synthetic nonreal folded pair, the normalized Widder contribution oscillates in the rung index away from the unique blind radius.

Theorem J.1 - Secondary Cayley spectrum and the critical barrier

The order index k itself carries an exact folded spectrum. Define

$$A_x(q) = \frac{q}{(x+q)^2} \qquad a_k(x) = \frac{W_k(x)}{(2k-1)!}$$

Equation (32.4) becomes the power-sum identity

$$\boxed{a_k(x) = \sum_{[\rho]} m_\rho A_x(q_\rho)^k} \tag{39.3}$$

The scaled eigenvalue is precisely the Cayley complement already present in the triangular collar. With $r = q/x$ and $p = r/(1+r)$,

$$\boxed{\alpha_x(q) := xA_x(q) = \frac{r}{(1+r)^2} = p(1-p)} \tag{39.4}$$

Consequently

$$\boxed{A_x(q) = A_x\left(\frac{x^2}{q}\right)} \tag{39.5}$$

Thus the same reciprocal-complement involution that organized the original Cayley geometry also organizes the Widder-order spectrum. At the blind radius $x = |q|$, the reciprocal image x^2/q is exactly $\bar{q}$; the conjugate pair therefore collapses to one positive secondary eigenvalue. Because $\sum_{[\rho]} m_\rho |A_x(q_\rho)| < \infty$, the genus-zero product

$$\mathcal{D}_x(z) = \prod_{[\rho]} (1 - zA_x(q_\rho))^{m_\rho}$$

converges locally uniformly. Its logarithmic derivative is the generating resolvent of the complete reduced-Widder ladder:

$$\boxed{\mathcal{G}_x(z) := \sum_{k\geq 1} \frac{W_k(x)}{(2k-1)!} z^{k-1} = \sum_{[\rho]} m_\rho \frac{A_x(q_\rho)}{1 - zA_x(q_\rho)} = -\frac{\mathcal{D}_x'(z)}{\mathcal{D}_x(z)}} \tag{39.6}$$

The poles are

$$Z_x(q) = \frac{1}{A_x(q)} = \frac{(x+q)^2}{q} = 2x + q + \frac{x^2}{q} \tag{39.7}$$

If $q > 0$, then the arithmetic-geometric mean inequality gives

$$0 < \alpha_x(q) \leq \frac{1}{4} \qquad Z_x(q) \geq 4x$$

with equality exactly at $q = x$. If $q = |q|e^{i\theta}$ is nonreal, then $\Re q > 0$ for a folded zeta zero, so $0 < |\theta| < \pi/2$. At its blind radius $x = |q|$,

$$\boxed{\alpha_x(q) = \frac{1}{2(1+\cos\theta)} = \frac{1}{4\cos^2(\theta/2)} > \frac{1}{4}, \quad Z_x(q) = 2x(1+\cos\theta) \in (2x, 4x)} \tag{39.8}$$

The blind radius is therefore blind only to phase: it is **supercritical in amplitude**. Every off-line folded zero forces a positive real pole of $\mathcal{G}_x$ strictly below the critical barrier $4x$ at its own scale. Conversely, critical-line folded zeros give only poles in $[4x, \infty)$. Hence the moving-scale secondary-pole criterion

$$\boxed{\text{RH} \iff \text{Pole}(\mathcal{G}_x) \subset [4x, \infty) \quad \text{for every } x > 0} \tag{39.9}$$

is exact. It is a zero-side reorganization, not a source-side proof, but it sharpens the research target: the oscillatory detector away from the blind circle and the strict amplitude-barrier crossing on the blind circle are complementary signatures of one nonreal folded orbit.

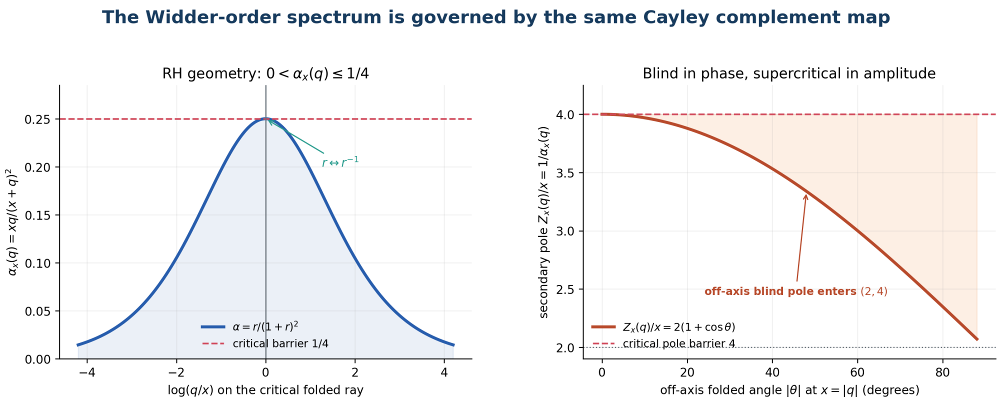

Figure 38: The normalized Widder spectrum uses the same reciprocal Cayley complement: the critical folded ray stays below the one-quarter amplitude barrier, while an off-axis blind pole enters the forbidden interval.

40. Source competition in heat variables

The source-side heat decomposition is

$$\Theta_\xi(u) = 1 + \Theta_\Gamma(u) - \Theta_P(u)$$

where the prime comb is the pointwise-positive function

$$\Theta_P(u) = \frac{e^{-u/4}}{2\sqrt{\pi u}} \sum_{n \geq 2} \frac{\Lambda(n)}{\sqrt{n}} \exp\left[-\frac{(\log n)^2}{4u}\right]$$

It enters with a minus sign. For $k \geq 1$, Theorem F gives

$$W_k(x) = \int_0^\infty e^{-xu} u^{2k-1} (-1)^k \left[\Theta_\Gamma^{(k)}(u) - \Theta_P^{(k)}(u)\right] du \tag{40.1}$$

Thus the exact cancellation of $1/x$ is the heat-side annihilation of the constant completion mode. The W_2 and W_3 theorems establish positivity of the weighted global Gamma/prime assembly; they do not establish pointwise positivity of $(-1)^k \Theta_\xi^{(k)}$. The latter for every k would be complete monotonicity of the heat trace and hence RH.

The recurrence (38.2) is also the Laplace shadow of heat differentiation. Writing $H_k = (-1)^k \Theta_\xi^{(k)}$ and integrating the derivative of $e^{-xu} u^{2k+1}$, with the boundary terms vanishing termwise by the folded spectral sum, gives

$$\int e^{-xu} u^{2k+1} H_{k+1}(u)\, du = -(2k+1) W_k'(x) - x W_k''(x).$$

Technical chapter VII. One-scale moment and derivative criteria

Noncancelling poles give negative-rung witnesses. Hausdorff and Beta–Hankel arguments reduce the full criterion to one prescribed scale, still at every order.

48. Meromorphic completion of the secondary Cayley spectrum

Let $q_\rho = \rho(1-\rho)$, one representative per folded orbit. The zero count gives the genus-zero summability

$$\sum_{[\rho]} \frac{m_\rho}{|q_\rho|} < \infty. \tag{48.1}$$

For fixed $x > 0$ put $A_x(q) = q/(x+q)^2$ and $a_k(x) = \sum m_\rho A_x(q_\rho)^k$. Then

$$\mathcal{G}_x(z) = \sum_{k\geq 1} a_k(x) z^{k-1} = \sum_{[\rho]} m_\rho \frac{A_x(q_\rho)}{1 - zA_x(q_\rho)}, \tag{48.4}$$

with secondary poles

$$z_x(q) = A_x(q)^{-1} = 2x + q + \frac{x^2}{q}. \tag{48.5}$$

For nonreal $q = a + ib$, $r = |q|$, the phase of $A_x(q)$ changes sign only at $x = r$, where

$$A_r(q) = \frac{1}{4r\cos^2(\arg q/2)} > \frac{1}{4r}. \tag{48.13}$$

Thus every nonreal folded point has an open supercritical interval around its blind radius. The full derivation of its reciprocal endpoints and the shifted Joukowski form of $z_x(q)$ is retained in earlier editions; only the consequences used later are kept here.

48A. Exact radius deficit

For an off-line zero write $d = 2\beta - 1$, $v = \gamma^2$, $a = v + (1 - d^2)/4$, $r = |q|$ and $w = r - a$. The exact remainder is

$$\boxed{d^2 - D(q) = \frac{w[w^2 + c(3r - a)]}{vr} > 0,} \tag{48.29}$$

and therefore

$$\boxed{\frac{4\gamma^2}{4\gamma^2 + 1} d^2 < 2w < D(q) < d^2.} \tag{48.30}$$

For fixed x the secondary-pole radius is attained. With $\Delta = \sup_x(4x - R_x)$ and $d_* = \sup_\rho |2\Re\rho - 1|$,

$$0 \le \Delta \le d_*^2 \le 1, \tag{48.31}$$

$$\boxed{\Delta < 1 \iff d_* < 1, \qquad \Delta = 0 \iff \text{RH}.} \tag{48.32}$$

The high-scale statistic is weaker:

$$\boxed{\limsup_{x\to\infty}(4x - R_x) = \limsup_{|\Im\rho|\to\infty}(2\Re\rho - 1)^2.} \tag{48.33}$$

It cannot detect finitely many off-line exceptions. At verified height H, the corresponding two-sided comparison differs by at most $(4H^2 + 1)^{-1}$; this is a conditional error estimate, not a source proof. The whole rung ladder at fixed x is one angular profile: with $w = z/(4x)$ and $\cos\varphi = 1 - 2w$,

$$4xw\, \mathcal{G}_x(4xw) = 2\tan\frac{\varphi}{2}\, \Im h(xe^{i\varphi}), \qquad h(z) = zS_\xi(z). \tag{48.28}$$

This is the exact bridge from the scalar W_k coefficients to the Pick/Löwner owner. Product rewrites do not change the sign obligation: Euler products, finite prime-power products, and the completed zero product encode different cutoffs, and none by itself implies that the folded poles are positive real.

48C. Gamma pole-index sublattices do not absorb the prime source

An adversarial Gamma-pole analysis tested the idea that the regular Gamma pole lattice might dominate the prime-power sublattice. Use the completion-centered terms

$$f_m(x) = \frac{x}{R_x}\left(\frac{1}{2m+1} - \frac{1}{2m + s_x}\right), \qquad m \ge 0. \tag{48.40}$$

At the two positive nodes $x_1 = 5/16$, $x_2 = 3/4$ and $v = (1, -1)^T$, every single term has the same negative Löwner direction. With $a = 4m + 1$,

$$\boxed{v^T L_{f_m} v = -\frac{388a^3 + 2140a^2 + 2473a + 624}{1512(a+1)(a+2)^2(2a+3)^2} < 0.} \tag{48.41}$$

For $m = 0$ alone,

$$L_{f_0} = \begin{pmatrix} 5/27 & 4/21 \\ 4/21 & 3/16 \end{pmatrix}, \qquad \det L_{f_0} = -\frac{11}{7056}. \tag{48.42}$$

So neither the prime-power-indexed nor complementary centered Gamma sublattice is a positive matrix reserve. After the exact baseline repair $f_m = g_m - c_m b$, the g_m have positive Stieltjes measures; §166B identifies that repaired reserve with the already-published Catalan reserve. For a set A of retained indices, let B be its complement and put $F_{A,c} = cb + \sum_{m \in A} g_m - h_P$. On the upper bank $x = -u + i0$, with $u > 1/4$ and $y = \sqrt{4u - 1}$, the continuation gives

$$\boxed{\Im F_{A,c}(-u + i0) = \frac{u}{y}\left[c - a_\Gamma - \sum_{m \in B} \frac{2y^2}{(4m+1)((4m+1)^2 + y^2)}\right].} \tag{48.43}$$

If $\sum_{m \in B}(4m+1)^{-1} = \infty$, monotone convergence makes the bracket negative for all sufficiently large y. Löwner's theorem therefore rules out positive-node Löwner matrices of every rank for any finite real c. This applies both when A is the prime-power sublattice and when A is its complement. It is an all-rank NO-GO for the proposed absorber, not a counterexample to the completed source. The first unsupported line remains the signed prime-error estimate.

49. Pringsheim no-dominance theorem

Theorem 49.1 (open-interval negative-rung theorem). If RH is false, there is a nonempty open interval $J \subset (0, \infty)$ such that, for every $x \in J$,

$$W_k(x) < 0 \quad \text{for infinitely many } k \tag{49.1}$$

Proof. Choose a nonreal folded zero q_0. Its supercritical interval I_{q_0} is nonempty. Remove the locally finite set of blind radii of all nonreal folded zeros and choose a nonempty open subinterval $J \subset I_{q_0}$ disjoint from that set.

Fix $x \in J$. A pole associated with q_0 has modulus below $4x$, so the radius of convergence R_x of (48.4) satisfies

$$R_x < 4x \tag{49.2}$$

The minimum pole modulus is attained: by (48.5), pole moduli tend to infinity with $|q|$, while only finitely many folded zeros lie in any bounded region. The common-sign residue lemma prevents cancellation, so this minimum is the actual power-series radius.

There is no positive-real singularity in $(0, 4x)$. Indeed, for a positive folded zero p,

$$z_x(p) = 2x + p + \frac{x^2}{p} \geq 4x \tag{49.3}$$

and for a nonreal folded zero, $A_x(q)$ is nonreal because x is not a blind radius. Normal convergence away from the locally finite pole set shows that there are no other singularities.

Suppose $a_k(x) \geq 0$ for every sufficiently large k. Removing finitely many initial terms does not change R_x. The remaining power series has nonnegative real coefficients and finite radius R_x. The Vivanti–Pringsheim theorem forces a singularity at the positive point $z = R_x$. This contradicts the absence of positive singularities below $4x$. Hence the real sequence $a_k(x)$ is negative infinitely often. Since $(2k-1)! > 0$, the same is true of $W_k(x)$. □

This strictly strengthens the conditional dominant-orbit detector. It uses neither a largest unique amplitude nor a gap between secondary eigenvalues.

Corollary 49.2 (dense-countable eventual positivity). For every dense set $D \subset (0, \infty)$,

$$\boxed{\mathrm{RH} \iff \forall x \in D\ \exists K_x\ \forall k \geq K_x : W_k(x) \geq 0} \tag{49.4}$$

Under RH every rung is nonnegative. If RH fails, Theorem 49.1 supplies an open interval J; density gives $D \cap J \neq \varnothing$, where eventual positivity fails. In particular, $D = \mathbb{Q}_{>0}$ is sufficient.

50. One prescribed Hausdorff sequence

The preceding criterion still uses a dense family of scales. A stronger normalization compresses the full problem to any one scale chosen in advance. Fix $x_0 > 0$ and define

$$\boxed{h_n(x_0) = (4x_0)^n \frac{W_{n+1}(x_0)}{(2n+1)!}} \tag{50.1}$$

Set

$$t_x(q) = 4xA_x(q) = \frac{4xq}{(x+q)^2} \tag{50.2}$$

Then

$$h_n(x) = \sum_{[\rho]} m_\rho A_x(q_\rho) t_x(q_\rho)^n \tag{50.3}$$

Theorem 50.1 (fixed-scale Hausdorff criterion). For every prescribed $x_0 > 0$,

$$\boxed{\text{RH} \iff (h_n(x_0))_{n\geq 0} \text{ is a Hausdorff moment sequence on } [0,1]} \tag{50.4}$$

RH implies the moment property. Under RH, every q_ρ is positive. The arithmetic–geometric mean inequality gives

$$0 < t_x(q_\rho) \leq 1 \tag{50.5}$$

The finite positive measure

$$d\mu_x(t) = \sum_{[\rho]} m_\rho A_x(q_\rho)\delta_{t_x(q_\rho)}(dt) \tag{50.6}$$

has finite mass by (48.1), and

$$h_n(x) = \int_0^1 t^n \, d\mu_x(t) \tag{50.7}$$

The moment property implies RH. Suppose (50.7) holds at the prescribed $x = x_0$ for some finite positive measure on $[0,1]$. Its Markov transform

$$H_x(z) := \sum_{n\geq 0} h_n(x)z^n = \int_0^1 \frac{d\mu_x(t)}{1-tz} \tag{50.8}$$

is holomorphic on $\mathbb{C} \setminus [1,\infty)$. On a neighborhood of the origin, the secondary expansion gives

$$H_x(z) = \sum_{[\rho]} m_\rho \frac{A_x(q_\rho)}{1-4xzA_x(q_\rho)} \tag{50.9}$$

Normal convergence gives a meromorphic continuation. Every candidate pole

$$z_\rho = \frac{1}{4xA_x(q_\rho)} \tag{50.10}$$

has residue $-m_\rho/(4x)$; coincident poles cannot cancel. Uniqueness of analytic continuation therefore forces every z_ρ onto $[1,\infty)$. Equivalently,

$$A_x(q_\rho) \in \left(0, \frac{1}{4x}\right] \tag{50.11}$$

If q_ρ were nonreal, (48.12) would force $x = |q_\rho|$, while (48.13) would give the strict reverse inequality. Hence all folded zeros are positive real. For $\rho = \beta + i\gamma$,

$$\Im(\rho(1-\rho)) = \gamma(1-2\beta) \tag{50.12}$$

Nontrivial zeros have $\gamma \neq 0$, so $\beta = 1/2$. This is RH. $\square$

The scale is not selected after inspecting zeros. The theorem holds for every arbitrary scale, including $x_0 = 1$:

$$\boxed{\text{RH} \iff \left(4^n \frac{W_{n+1}(1)}{(2n+1)!}\right)_{n\geq 0} \quad \text{is Hausdorff}} \tag{50.13}$$

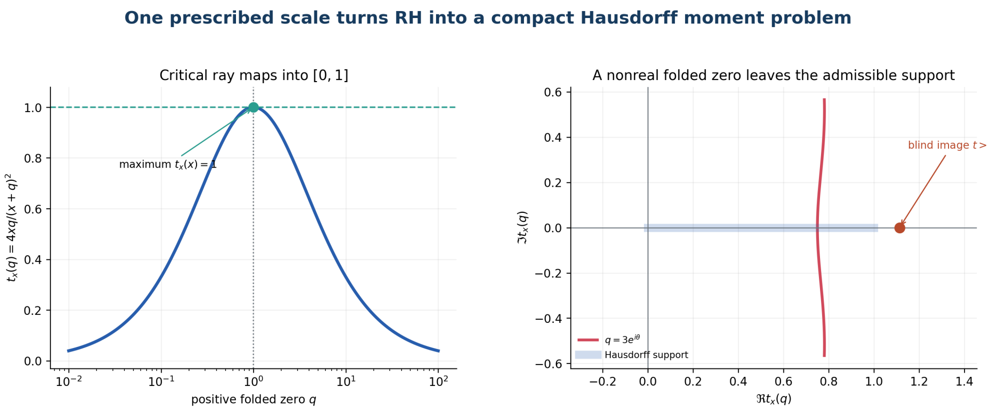

Figure 39: At one prescribed scale, the critical folded ray maps into the compact Hausdorff support, while a nonreal folded zero cannot remain there.

51. Finite witnesses and a positive contraction

Hausdorff's theorem states that a real sequence is a moment sequence on $[0, 1]$ exactly when all forward differences are completely monotone. Thus Theorem 50.1 is equivalent to

$$\boxed{(-1)^r \Delta^r h_n(x_0) \geq 0 \qquad (n, r \geq 0)} \tag{51.1}$$

In the original rungs this becomes

$$\boxed{\sum_{j=0}^{r} (-1)^j \binom{r}{j} (4x_0)^{n+j} \frac{W_{n+j+1}(x_0)}{(2n+2j+1)!} \geq 0} \tag{51.2}$$

Consequently the negation has the strong quantifier order

$$\boxed{\neg\text{RH} \Longrightarrow \forall x_0 > 0 \; \exists n, r \geq 0 : (-1)^r \Delta^r h_n(x_0) < 0} \tag{51.3}$$

At every fixed scale, an off-line zero therefore has a finite Hausdorff witness, even if no individual late rung at that same scale has yet been isolated.

The same theorem has a canonical operator realization.

Theorem 51.1 (positive-contraction criterion). For every fixed $x_0 > 0$, RH is equivalent to the existence of a Hilbert space $\mathcal{H}$, a vector $v \in \mathcal{H}$, and a positive contraction $0 \le T \le I$ such that

$$h_n(x_0) = \langle v, T^n v \rangle \quad (n \ge 0) \tag{51.4}$$

Under RH, take $\mathcal{H} = L^2([0,1], \mu_{x_0})$, let T be multiplication by t, and let $v = 1$. Conversely, the spectral theorem for a positive contraction supplies a positive measure supported on $[0,1]$, and Theorem 50.1 applies.

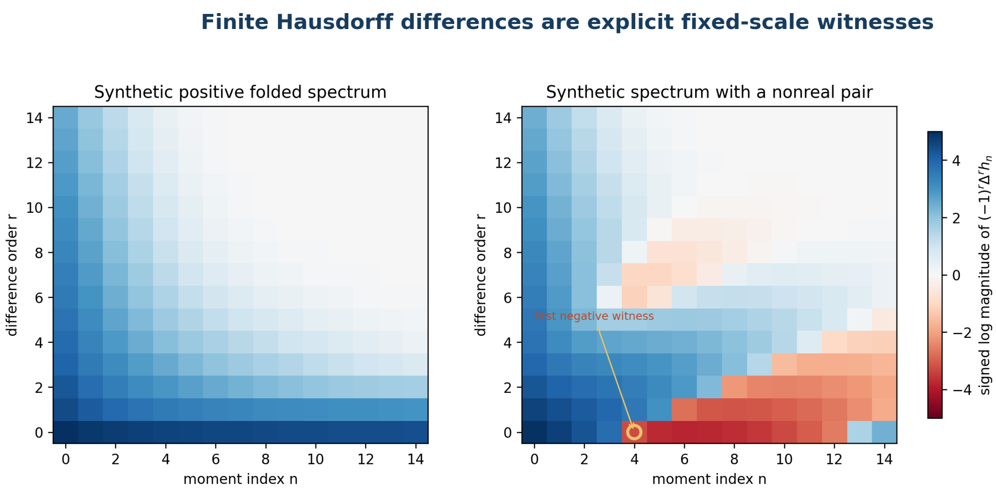

Figure 40: Finite Hausdorff differences in a positive synthetic spectrum and a synthetic off-axis spectrum; the latter exhibits a finite negative witness.

52. Cayley–Bernstein and Markov divided differences

The normalized secondary eigenvalue has a square-complement form. Define

$$c_x(q) = \frac{q - x}{q + x} \tag{52.1}$$

Then

$$\boxed{1 - t_x(q) = c_x(q)^2} \tag{52.2}$$

Under RH, $c_x(q) \in (-1, 1)$ and $t_x(q) = 1 - c_x(q)^2 \in (0, 1]$. The finite Hausdorff differences have the exact zero-side form

$$(-1)^r \Delta^r h_n(x) = \sum_{[\rho]} m_\rho A_x(q_\rho) t_x(q_\rho)^n (1 - t_x(q_\rho))^r \tag{52.3}$$

This is a compact Cayley–Bernstein basis: $t^n(1-t)^r$ is nonnegative on the critical support.

The Markov function is also a reciprocal divided difference of the single owner

$$h(w) = wS_\xi(w) \tag{52.4}$$

Choose u, v so that

$$uv = x^2, \qquad u + v = 2x(1 - 2z) \tag{52.5}$$

Then

$$(q + x)^2 - 4xzq = (q + u)(q + v) \tag{52.6}$$

and termwise

$$\frac{u/(u + q) - v/(v + q)}{u - v} = \frac{q}{(u + q)(v + q)} \tag{52.7}$$

Summing the normally convergent folded expansion yields

$$\boxed{H_x(z) = \frac{h(u) - h(v)}{u - v}} \tag{52.8}$$

For $z = \sin^2(\theta/2)$ one may take $u = xe^{i\theta}$ and $v = xe^{-i\theta}$, so

$$\boxed{H_x\left(\sin^2\frac{\theta}{2}\right) = \frac{\Im h(xe^{i\theta})}{x\sin\theta}} \tag{52.9}$$

The fixed-scale moment problem is therefore a circular Pick-sign problem for the folded resolvent.

Under RH, (50.8) also gives the positive Pick kernel

$$K_x(z, w) = \frac{H_x(z) - \overline{H_x(w)}}{z - \overline{w}} = \int_0^1 \frac{t\,d\mu_x(t)}{(1 - tz)(1 - t\overline{w})} \tag{52.10}$$

Every finite matrix $[K_x(z_i, z_j)]$ is positive semidefinite.

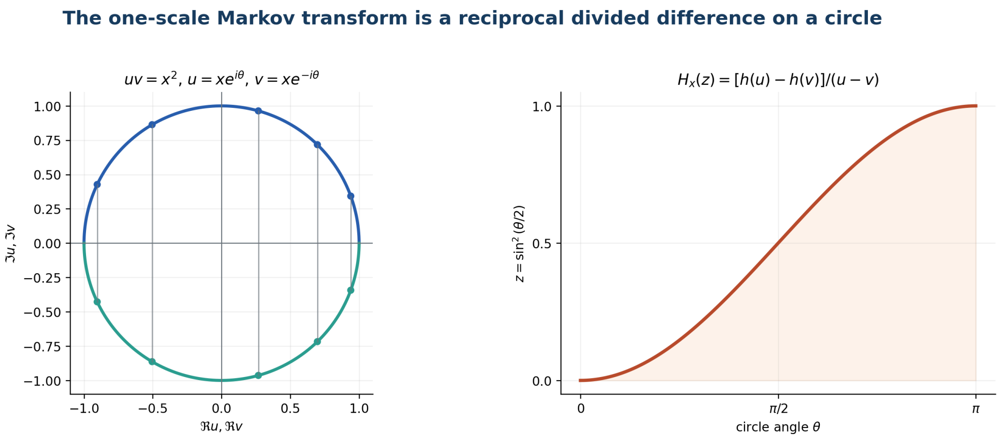

Figure 41: The reciprocal pair u, v runs on a circle, and the Markov parameter is $z = \sin^2(\theta/2)$.

104. The one-point Beta–Hankel and Hausdorff theorem

Put

$$k(u) = -\Theta'_\xi(u)$$

The congruenced local Dobsch matrix is

$$\widehat{H}_N(x)_{ij} = \frac{1}{(i+j+1)!}\int_0^\infty e^{-xu}u^{i+j+1}k(u)\,du \qquad 0 \le i, j < N \tag{104.1}$$

The beta integral

$$\frac{1}{(i+j+1)!} = \frac{1}{i!\,j!}\int_0^1 t^i(1-t)^j\,dt \tag{104.2}$$

turns its quadratic form, for $P_c(z) = \sum_{j<N} c_j z^j/j!$, into

$$\begin{aligned} c^*\widehat{H}_N(x)c &= \int_0^\infty e^{-xu}u\,k(u)\int_0^1 \overline{P_c(ut)}P_c(u(1-t))\,dt\,du \\ &= \int_{a,b>0} e^{-x(a+b)}k(a+b)\overline{P_c(a)}P_c(b)\,da\,db \end{aligned} \tag{104.3}$$

This exposes the additive Hankel kernel

$$K_x(a,b) = e^{-x(a+b)}k(a+b) \tag{104.4}$$

Theorem 104.1 (one prescribed basepoint). For every prescribed $x_0 > 0$,

$$\widehat{H}_N(x_0) \succeq 0 \quad \text{for every } N \iff -\Theta'_\xi \text{ is completely monotone} \tag{104.5}$$

Proof. Complete monotonicity gives $k(u) = \int_0^\infty e^{-\lambda u}\, d\mu(\lambda)$ with $d\mu \geq 0$. Substitution into (104.3) produces

$$\int_0^\infty \left| \int_0^\infty e^{-(x_0+\lambda)a} P_c(a)\, da \right|^2 d\mu(\lambda) \geq 0 \tag{104.6}$$

Conversely, the actual completed source obeys, for every $3/2 < \beta < 2$,

$$|k(a+b)| \leq C_\beta \big(1 + a^{-\beta/2}\big)\big(1 + b^{-\beta/2}\big) \tag{104.7}$$

The exponential-polynomial core $e^{-x_0 a}\mathbb{C}[a]$ is dense in the corresponding weighted L^1 space. Positivity on every finite polynomial core therefore extends to compactly supported tests. Approximating point masses gives $[k(a_r + a_s)] \succeq 0$ for every finite positive node set. Thus k is exponentially convex and has a bilateral Laplace representation by a positive measure. The unconditional decay $k(u) \to 0$ rules out support on $(-\infty, 0]$, leaving a Bernstein–Widder measure on $(0, \infty)$. Therefore k is completely monotone. □

Since $\Theta_\xi(u) \to 0$,

$$-\Theta'_\xi \text{ completely monotone} \iff \Theta_\xi \text{ completely monotone} \tag{104.8}$$

Combining this with the source criterion above gives an exact reorganization, not an RH proof:

$$\boxed{\mathrm{RH} \iff \widehat{H}_N(x_0) \succeq 0 \quad \text{for every } N} \qquad (x_0 > 0 \text{ prescribed}) \tag{104.9}$$

Define

$$a_n(x_0) = \frac{(-1)^n}{(n+1)!} h^{(n+1)}(x_0) \qquad b_n(x_0) = x_0^n a_n(x_0) \tag{104.10}$$

Then $\widehat{H}_N(x_0) = [a_{i+j}(x_0)]$, and under the positive Bernstein measure,

$$b_n(x_0) = \int_0^1 r^n\, d\rho_{x_0}(r) \qquad r = \frac{x_0}{x_0 + \lambda} \tag{104.11}$$

Hausdorff's theorem now gives

$$\boxed{\mathrm{RH} \iff G_{n,k}(x_0) := (-1)^k \Delta^k b_n(x_0) \geq 0 \quad \text{for every } n, k \geq 0} \tag{104.12}$$

The grid recursion is

$$G_{n,k+1} = G_{n,k} - G_{n+1,k} \tag{104.13}$$

On the zero side it has the exact closed form

$$\boxed{G_{n,k}(x) = x^n \sum_{[\rho]} m_\rho \frac{q_\rho^{k+1}}{(x+q_\rho)^{n+k+2}}} \tag{104.14}$$

Under RH, the representing measure is explicitly

$$\rho_{x_0} = \sum_{[\rho]} m_\rho \frac{q_\rho}{(x_0+q_\rho)^2} \delta_{x_0/(x_0+q_\rho)} \tag{104.15}$$

The qd/S-fraction object in PP145 and the canonical moments in PP152 use the same algorithm on different moment sequences. The first is zero-side Stieltjes data; the second is source-side Hausdorff data. They are not one sequence; their different moment measures must be retained.

The one-point theorem is exact only at infinite order. Every usable certificate is finite, and the PP153 scans show that the one-point prefix can lose spectral reach relative to optimizing x. The fixed-scale bound must retain every order, as in (104.12).

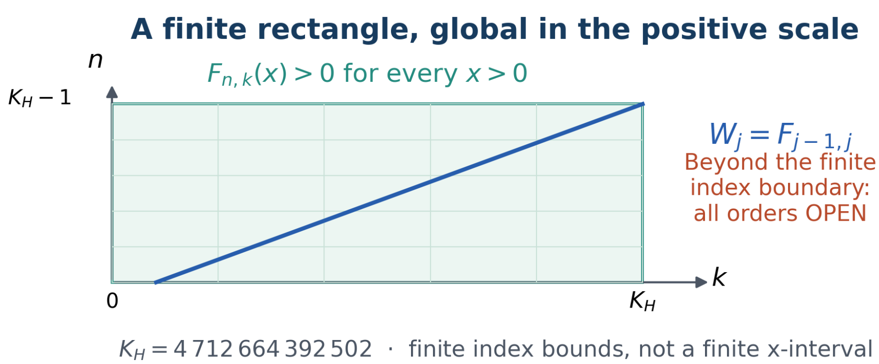

Figure 42: The height-to-sector theorem certifies a finite rectangle at every $x > 0$. Its diagonal $W_j = F_{j-1,j}$ shares the same certified height input. The open continuation lies beyond a finite index boundary, not at the fifth rung.

104A. Fixed-depth filtering, weighted recovery, and triangular damping

This section averages the boundary moments before forming a determinant or Li form. It is different from the positive-scale moments in (104.10) and from multiplying an already computed Li coefficient by a positive scalar. Put

$$b_j = \frac{4^j (j!)^2}{(2j+1)!} = \int_0^1 u^j \frac{du}{2\sqrt{1-u}}, \qquad H_N^{[k]} = [b_{i+j}^k \mu_{i+j}], \quad D_N(k) = \det H_N^{[k]}. \tag{104A.1}$$

The measure is a probability measure, and depth k is multiplication of the support coordinate by k independent variables of this law. The matrix size, filter, and underlying moment array stay fixed; the depth of each observation is identified when outputs are compared.

The exact rank-two test. With $A = \mu_0\mu_2$ and $B = \mu_1^2$,

$$\begin{aligned} D_2(k) &= (8/15)^k A - (4/9)^k B, \\ D_2(k+2) &= \tfrac{44}{45} D_2(k+1) - \tfrac{32}{135} D_2(k), \\ D_2(0) &= \tfrac{33}{8} D_2(1) - \tfrac{135}{32} D_2(2). \end{aligned} \tag{104A.2}$$

For $(\mu_0, \mu_1, \mu_2) = (1, 4/5, 3/5)$ the three values are $-1/25, 8/225, 448/10125$. Thus two positive observations recover a negative unfiltered determinant. If each observation has absolute error at most η, the recovered error is at most $267\eta/32$. A single observation does not suffice: $(1, 0, 1/15)$ has the same $D_2(1)$ and a positive $D_2(0)$.

The triangular curvature law. The ratio $b_{j+1}/b_j = (2j+2)/(2j+3)$ gives

$$\begin{aligned} &\frac{b_{j+1}^2}{b_j b_{j+2}} = 1 - \frac{1}{T_{2j+3}}, \qquad \Delta^2 \log b_j = -\log\left(1 - \frac{1}{T_{2j+3}}\right) > 0, \\ &\prod_{j=0}^{n-1}\left(1 - \frac{1}{T_{2j+3}}\right) = \frac{2n+3}{3(n+1)}, \\ &\prod_{i=0}^{\infty}\left(1 - \frac{1}{T_{4i+3}}\right) = \frac{4\Gamma(3/4)}{\sqrt{\pi}\,\Gamma(1/4)}. \end{aligned} \tag{104A.3}$$

The last finite product is $(1/2)_n(5/4)_n/((3/4)_n(1)_n)$, so the Gamma-ratio limit proves the infinite product. In particular, the squared normalized adjacent entry at $(i, i+1)$ is multiplied by $(1 - 1/T_{4i+3})^k$. These are specified triangular indices, not prime Euler factors.

Theorem 104A.1 (fixed-rank smoothing). For any real array with $\mu_{2i} > 0$, $0 \le i < N$, the matrix $H_N^{[k]}$ is positive definite for all sufficiently large integer k, even if H_N is indefinite.

Proof. Diagonal normalization leaves off-diagonal entry

$$\frac{\mu_{i+j}}{\sqrt{\mu_{2i}\mu_{2j}}}\left(\frac{b_{i+j}}{\sqrt{b_{2i}b_{2j}}}\right)^k.$$

Strict Cauchy–Schwarz in the nondegenerate Beta measure makes the ratio strictly between zero and one for $i \ne j$. For fixed N the normalized matrix tends to I_N; a maximum off-diagonal absolute row sum below one already proves positivity. The normalization is a nonsingular real congruence. □

Theorem 104A.2 (fixed depth retains the complete criterion). For the actual folded moments, and each one fixed finite integer $k \ge 0$,

$$\boxed{\mathrm{RH} \iff H_N^{[k]} \succeq 0 \quad \text{for every } N \geq 1.} \tag{104A.4}$$

Proof. Under RH, push the positive measure $\sum_q (m_q/q)\delta_{1/q}$ through multiplication by the k Beta variables. Conversely, all Hankel matrices positive semidefinite give a positive real representing measure ν by the Hamburger moment theorem. Put $C = \sum_q m_q/|q|$ and $Y = \max_q |q|^{-1}$. Since $b_j \leq 1$, $|b_j^k \mu_j| \leq CY^j$. The even moments then give $\nu(|t| > Y + \epsilon)(Y+\epsilon)^{2n} \leq CY^{2n}$, so $\operatorname{supp}\nu \subset [-Y, Y]$. The function $G_k(z) = \int (1-zt)^{-1} d\nu(t)$ is therefore holomorphic at every nonreal z.

Let V be the product of the k Beta variables, with $V = 1$ at depth zero. Then

$$B_k(z) = \mathbb{E}(1 - zV)^{-1} = \sum_{j \geq 0} b_j^k z^j, \qquad G_k(z) = \sum_q \frac{m_q}{q} B_k(z/q) \tag{104A.5}$$

near zero. B_k is holomorphic off $[1, \infty)$ and singular at one. For $k = 0$ it has a pole; for $k \geq 1$, the asymptotic $b_j^k \sim (\sqrt{\pi}/2)^k j^{-k/2}$ makes its derivative of order $\lceil k/2 \rceil$ diverge along $z \uparrow 1$.

If a nonreal folded point exists, choose one, q_*, of least modulus among such points and approach it along $z = tq_*$, $0 < t < 1$. Its term becomes nonanalytic there. No distinct cut $q[1, \infty)$ contains q_*: a real cut cannot, and a nonreal one would require a smaller modulus. Coincident values have already been combined into positive multiplicities. All other finite terms are analytic near q_*; the infinite tail is normally convergent there, with majorant a constant times $m_q/|q|$. They cannot cancel the distinguished singularity. This contradicts the holomorphy of G_k at q_*. Thus every folded point is real, and $\Im q_\rho = \Im\rho(1 - 2\Re\rho)$, with $\Im\rho \neq 0$, gives RH. □

Fixing depth before imposing all ranks is essential. Theorem 104A.1 can make $\forall N\ \exists k(N)$ positivity automatic; it does not establish (104A.4).

Proposition 104A.3 (signed finite-mode recovery). For known distinct positive rates $\mathcal{R}$, $M = |\mathcal{R}|$, define weights by

$$1 - \prod_{r \in \mathcal{R}} (1 - z/r) = \sum_{\ell=1}^{M} w_\ell z^\ell. \quad F(k) = \sum_{r \in \mathcal{R}} A_r r^k \implies F(0) = \sum_{\ell=1}^{M} w_\ell F(\ell). \tag{104A.6}$$

Evaluation at each $z = r$ proves the result. For independent errors bounded by η, the exact worst-case amplifier is $\kappa = \sum |w_\ell| = \prod_{r \in \mathcal{R}}(1 + 1/r) - 1$. The weights alternate in sign.

For determinants, expand over permutations and group equal nonzero monomial/rate contributions: $D_N(k) = \sum_\pi \operatorname{sgn}(\pi) \prod_i \mu_{i+\pi(i)} (\prod_i b_{i+\pi(i)})^k$. The multiplicities ν_j in each monomial obey $\sum \nu_j = N$ and $\sum j\nu_j = N(N-1) = 2T_{N-1}$. The exact enumerated rate counts for ranks 1 through 9 are $1, 2, 5, 16, 58, 225, 980, 4520, 22244$. This is finite enumeration, not an all-rank count theorem. A geometric filter would give a single common factor; the strict curvature in (104A.3) separates the rates.

For one odd Li form the problem is much smaller. Put $c_{m,j} = [y^j]\mathcal{P}_m(y)^2$, $J = 2m$, and $\Lambda_m(k) = \sum_{j=0}^{J} c_{m,j} b_j^k \mu_j$. Use rates $b_0, \ldots, b_J$ in (104A.6). Then $\lambda_{2m+1} = \sum_{\ell=1}^{2m+1} w_\ell \Lambda_m(\ell)$:

λ_{17} uses 17 observations, not 22,244 determinant modes. The independent-error amplifier satisfies $\log\kappa_m = \frac{1}{2}(2m+1)\log(2m+1) + O(m)$.

A mandatory negative control. Take $q_0 = 17/4$ of multiplicity two and $q_\pm = 147/16 \pm 3i/2$ of multiplicity one. Every model moment $\mu_j^* = 2q_0^{-j-1} + 2\Re(q_+^{-j-1})$ is positive, since $|q_+| > q_0$. Exact rational evaluation gives 37 positive observations $\Lambda_{18}^*(1), \dots, \Lambda_{18}^*(37)$ but recovers $-0.598 < \lambda_{37}^* < -0.597$. The separate directed-error ledger reproduces this negative sign. This is a polynomial comparison model, not an actual-zeta counterexample. The actual source still has to prove the signed comparison between the odd- and even-depth terms in (104A.6). Section 166E treats common, rather than independent, errors.

136. The completed-source Pascal owner

Let

$$h(x) = \frac{x}{R}\Phi(s), \qquad x = s(s-1), \qquad R = 2s-1$$

and let $G_{n,r}$ be the completed Widder/Pascal cells defined in (104.14). They satisfy the exact addition law

$$\boxed{G_{n,r} = G_{n+1,r} + G_{n,r+1}} \tag{136.1}$$

Whenever $G_{n,r} > 0$, define the branch ratios

$$p_{n,r} = \frac{G_{n+1,r}}{G_{n,r}}, \qquad q_{n,r} = \frac{G_{n,r+1}}{G_{n,r}}$$

Then $p_{n,r} + q_{n,r} = 1$. Differentiating (104.14) gives $x\partial_x G_{n,r} = nG_{n,r} - (n+r+2)G_{n+1,r}$. Where both adjacent cells $G_{n+1,r}$ and $G_{n,r+1}$ are nonnegative, the division-free flow corridor is

$$\boxed{-(r+2)G_{n,r} \le x\partial_x G_{n,r} \le nG_{n,r}} \tag{136.2}$$

Equation (136.2) requires the two adjacent signs, but no division by $G_{n,r}$. Where the denominator is positive, those signs also put both branch ratios in $[0,1]$. PP186 certifies all 81 cells with $0 \le n, r \le 8$ at $x = 56$ by directed rational intervals. PP187 certifies the directed confluent rank-eleven block

$$\boxed{\mathfrak{B}_{11}^{\mathrm{conf}}(56) \succ 0} \tag{136.3}$$

These are finite source certificates. By the finite-rank camouflage theorem, no finite prefix proves the first unsupported one-point line without additional completed-source structure:

$$\boxed{G_{n,r}(56) \ge 0 \qquad (n, r \ge 0)} \tag{136.4}$$

Technical chapter VIII. Finite Löwner certificates and spectral reach

The normalized determinant and quartet signature precede the certificate details. Global matrix order and rank at a single basepoint remain distinct.

85. Finite determinant gates through rank six

Throughout the finite-gate sections, put $h = xS_\xi$ and, for $r \geq 2$,

$$M_r(x) = \frac{(-1)^r h^{(r-1)}(x)}{(r-1)!}, \qquad \Delta_N^{\mathrm{L}}(x) = \det[M_{i+j}(x)]_{i,j=1}^N$$

The alternating-sign diagonal congruence identifies this determinant with that of the normalized confluent Löwner matrix. In particular $M_2 = h' = W_1$. This fixes the normalization used in (85.1) and (93.1).

The PP98–PP111 certificate chain establishes, without assuming RH,

$$\boxed{\Delta_N^{\mathrm{L}}(x) > 0 \quad (x > 0), \qquad N = 1, 2, 3, 4, 5, 6} \tag{85.1}$$

The ranks $4, 5, 6$ are classified **A-CAT**: exact symbolic owners are joined to directed interval or exact zero-box compact certificates and analytic source tails. The finite-zero lanes use authenticated zero boxes only in their declared ranges; the source tails use no zero ordinates. Equation (85.1) is a finite leading-minor statement, not the all-order source theorem.

102. Off-line quartet signature, determinant factorization, and reach

Let an off-line zero be

$$\rho = \frac{1}{2} + \delta + i\gamma \qquad 0 < \delta < \frac{1}{2}$$

Its functional-equation and conjugation orbit gives two folded values

$$a = \frac{1}{4} - \delta^2 + \gamma^2 - 2i\delta\gamma \qquad \bar{a} \tag{102.1}$$

For $t = a/x$ define

$$v_N(t) = \sqrt{t}\,\big((1+t)^{-1}, \ldots, (1+t)^{-N}\big)^{\mathsf{T}} \tag{102.2}$$

Write $v = u + iz$. The conjugate pair contributes

$$vv^{\mathsf{T}} + \bar{v}\bar{v}^{\mathsf{T}} = 2uu^{\mathsf{T}} - 2zz^{\mathsf{T}} \tag{102.3}$$

Theorem 102.1 (quartet signature). For $N \geq 2$, every off-line quartet contributes a real rank-two form of signature $(1,1)$: one positive and one negative direction.

Proof. The vectors u and z are independent. Otherwise v would be a complex scalar times a real vector, so every consecutive ratio $v_{j+1}/v_j = (1+t)^{-1}$ would be real. This is impossible because t is nonreal. On the plane spanned by u, z, the determinant of $2(uu^{\mathsf{T}} - zz^{\mathsf{T}})$ is

$$-4(\|u\|^2\|z\|^2 - \langle u, z\rangle^2) < 0$$

The two nonzero eigenvalues therefore have opposite signs. □

Collect the on-line atoms and the positive halves of all off-line quartets in $P_N \succeq 0$, and let W_N contain the negative vectors. Whenever P_N is invertible, the matrix determinant lemma gives

$$\boxed{\Delta_N^{\mathsf{L}}(x) = x^{-N^2} \det P_N(x) \det\Big(I - W_N^{\mathsf{T}} P_N(x)^{-1} W_N\Big)} \tag{102.4}$$

For one quartet, with negative vector w,

$$\nu_N(x) = w_N^{\mathsf{T}} P_N(x)^{-1} w_N \qquad \Delta_N^{\mathsf{L}}(x) > 0 \iff \nu_N(x) < 1 \tag{102.5}$$

The rank monotonicity is exact:

$$\nu_N = \max_{y \in \mathbb{R}^N} \Big(2y^{\mathsf{T}} w_N - y^{\mathsf{T}} P_N y\Big) \tag{102.6}$$

Embedding $y \mapsto (y, 0)$ preserves the objective, hence

$$\boxed{\nu_{N+1}(x) \geq \nu_N(x)} \tag{102.7}$$

Thus the failure ranks form an up-set. This proves that the finite ladder is ordered; it does not prove how high a fixed rank can see.

The PP133 scan reported that rank eight becomes blind to a maximally displaced quartet above approximately $\gamma = 27$. That statement remains **C**: PP134 was assigned to replace the 45-point x scan by a rational cover using

$$\nu_N \le \|w_N\|^2 \operatorname{tr}(P_N^{-1}) \tag{102.8}$$

but no PP134 certificate occurs in the recorded trace. Likewise, the finite-ladder zero-localization conclusion remains a **proposed no-go**, not a replayed theorem. Neither limitation affects the proved global eighth gate (92.1).

86. Rank seven: global certificate and overlap

PP112 gives a three-lane global certificate with low range $0 < x \le 92116$, a $d = 1/20$ analytic middle lane, and a safe-half-plane source tail. PP113 supplies an independent $d = 1/28 = 1/T_7$ alternate with exact zero-box bridge $92116 \le x \le 157976$, an unsplit middle-core ratio $1.08765547236\ldots$, and a 128-box backup ratio $2.4012758008\ldots$.

The PP113 package hashes and terminal, bridge, splice, and cap receipts have been reproduced twice byte-identically after direct extraction of the canonical dependency. A separate full PP112 producing replay then reproduced the middle, low, source-tail, coordinate, and splice receipts byte-for-byte. Therefore

$$\boxed{\Delta_7^{\mathrm{L}}(x) > 0 \ (x > 0): \quad \textbf{A-CAT}} \tag{86.1}$$

The canonical receipt hashes are:

middle: `2a90a75aca94fb4adee1177ef5e7124a4575f3a4c36a252335ca28059b09908c`

low: `4c8f04809c8ea7a0fd358a35587f27d023c3f4b8ae1423112b33af272db6dadb`

tail: `c5b6a3c5db3bfb5b2e72e0ec36569bdadf3ecd3c61ac2e42d8691cbd54a45ec8`

coordinate: `b884ac47b2ce7d7ac0c271f88928e3739de98a0c53f69003fc888fb9d56974b3`

splice: `317de1f7a05a16ce7fe8f42a9a83eedad2373b4e4b23cceb9116be6db9463e12`

The exact identity $x(x-1) = 2T_{x-1}$ and the repetend/triangular observations may be retained as coordinate mnemonics. They do not select the optimal band width and are not proof owners.

87. Rank eight: the $q = 57$ certificate geometry

PP114 constructs a four-lane rank-eight splice. Its $q = 56, L = 6$ adaptive cover has weakest ratio

$$1.000006691152949\ldots \tag{87.1}$$

only 6.7 parts per million above one. The same exact receipt contains a strictly stronger $q = 57, L = 6$ cover:

$$\begin{aligned}
&729 \text{ leaves}, \qquad 11{,}649 \text{ corner evaluations} \\
&\text{weakest ratio } 1.0001919333825133\ldots \\
&250000 \le x \le 750081 \quad \text{for the finite bridge} \\
&75 \text{ bridge cells}, \qquad 861 \text{ authenticated boxes} \\
&x \le \frac{5040589135423290823270400000}{457} \quad \text{for the analytic middle lane} \\
&\text{middle/tail overlap } \frac{180421979233767077267426}{457} > 0
\end{aligned} \tag{87.2}$$

Every one of the 729 exact rational leaves and all 75 bridge cells has passed an independent Fraction recomputation. The recorded Rail G and Rail L receipts replay byte-identically; Rail T agrees in every mathematical field and differs only in a recorded path string. The completed global proof in §92 supplies the theorem authority for this certificate geometry:

$$\boxed{\Delta_8^{\mathrm{L}}(x) > 0 \ (x > 0): \quad \textbf{A-CAT} \ (\S 92)} \tag{87.3}$$

For comparison, the $q = 80, L = 7$ ratio $1.100576995062874\ldots$ uses one midpoint split in each of eight coordinates, hence $2^8 = 256$ rational subboxes. The unsplit ratios are 0.8253553988179236 for $L = 7$ and 0.9432633129347698 for $L = 8$; the first passing unsplit multiplicity is $L = 9$, ratio 1.0611712270516161. Moreover, the proposed sparse bridge fails at $x = 250000$. The $q = 80$ lane is therefore reconnaissance, not a theorem or preferred certificate.

Section 92 joins the low, bridge, middle, tail, and splice kernels into the global eighth-gate proof. The arithmetic parameter $q = 57$ alone does not establish any determinant sign.

92. Global eighth local determinant

Theorem 92.1 (`D8-GLOBAL`, A-CAT). For every real $x > 0$,

$$\boxed{\Delta_8^{\mathrm{L}}(x) > 0} \tag{92.1}$$

Put

$$X_{\mathrm{cap}} = \frac{5040589135423290823270400000}{457} \tag{92.2a}$$

The authenticated PP131 splice is the gap-free union

$$\begin{array}{rl}
0 < x \le 250000 & \text{actual-node low theorem} \\
250000 \le x \le 337267 & \text{exact-box bridge} \\
337267 \le x \le X_{\mathrm{cap}} & q = 57, L = 6 \text{ ray and uniform core} \\
x \ge 1102578756155569617614382 & \text{analytic source tail}
\end{array} \tag{92.2}$$

The provenance substitution is explicit in PP133 Section C.2: PP117's independent clean-room replay occurs byte-for-byte inside PP131 as lane `D8-Q57-L6-UNIFORM-CORE`. Thus PP131 consumes, rather than replaces, the named PP117 rederivation.

The cap overlaps the tail by the exact positive amount

$$\boxed{\frac{1804219792337670772674 26}{457} > 0} \tag{92.3}$$

The independent replays reproduced all declared dependencies. The full package and replay hashes are held with the certificate archive, not here.

The finite verified-height input $H = 3000175332800$ is an unconditional Platt–Trudgian theorem, not an RH assumption. The archived exact-box chain and declared `zeros_14.dat` MD5 are authenticated, but the raw `.dat` bytes were not mounted for a fresh rehash or decode. This provenance limitation is stated rather than hidden.

93. Fixed-order Dobsch–Löwner consequence

Let $h(x) = xS_\xi(x)$ and $W = h'$. With

$$\mathcal{H}_8(x) = \left[\frac{h^{(i+j-1)}(x)}{(i+j-1)!}\right]_{i,j=1}^{8}$$

the fixed alternating-sign congruence gives

$$\mathcal{H}_8(x) = D[M_{i+j}(x)]_{i,j=1}^{8} D \qquad D = \operatorname{diag}(1, -1, \ldots, -1) \tag{93.1}$$

The global positivity of all leading determinants through rank eight and Sylvester's criterion give $\mathcal{H}_8(x) \succ 0$. The audited Dobsch–Donoghue theorem and Löwner characterization therefore yield:

Theorem 93.1 (`DD-ORDER8` / `SRC-LOEWNER-N8`, A-CAT). The folded owner h is matrix monotone of order eight on $(0, \infty)$. Consequently,

$$\boxed{L_\Gamma - L_P \succeq 0} \tag{93.2}$$

for every positive node tuple of size at most eight.

The conclusion is positive semidefinite, not universal strict positive definiteness. The complete dependency digest is held with the certificate archive. Order nine, arbitrary finite order, and the operator intertwiner remain open.

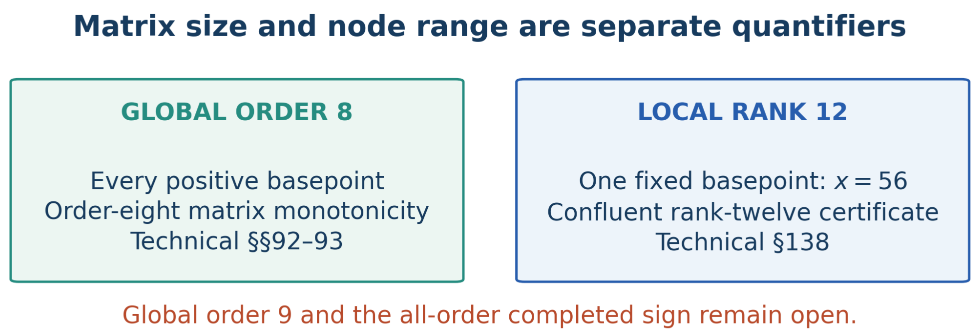

Figure 43: Global order and fixed-node rank are distinct directions. Order eight is certified globally; rank twelve is certified at $x = 56$. The fixed-node certificate does not fill the global order-nine region. See §§92–93 and 138.

138. Rank twelve at its exact finite authority

PP190-T replaces the failed entrywise Gershgorin tail bound by a correlation-preserving one-measure Schur argument. The controlling manifest-bound production branch uses the exact rational unit-lower preconditioner selected from its finite anchor. Its terminal polynomial satisfies

$$q_z(2+u) = \sum_{k=0}^{23} a_k u^k \qquad a_k \in \mathbb{Q}_{\geq 0}, \qquad a_0 > 0 \tag{138.1}$$

Hence $q_z(t) > 0$ for $t \geq 2$. The prime atoms themselves remain indefinite; the positivity occurs only after their common-source correlation is retained. At cutoff 120,750,000, the certified Schur margin is

$$\boxed{\operatorname{Schur}(\mathfrak{B}_{12}^{\mathrm{conf}} \mid \mathfrak{B}_{11}^{\mathrm{conf}}) \geq 1.2252441364765957718 \times 10^{-41} > 0} \tag{138.2}$$

Therefore

$$\boxed{\mathfrak{B}_{12}^{\mathrm{conf}}(56) \succ 0} \tag{138.3}$$

Equation (138.3) is a finite rank-twelve interval certificate at one basepoint, with the cutoff and margin in (138.2). Equation (138.3) proves neither global matrix monotonicity of order nine (meaning global in x), the all-node Löwner inequality, nor RH.

Technical chapter IX. Cyclic arithmetic, Riesz smoothing, and zero frontiers

Cyclic denominator counts enter the zeta quotient through an Euler product. Smoothing controls arithmetic jumps and exposes the zero-frontier exponent.

56. Cyclic arithmetic before zeta

To avoid collision with S_ξ, define

$$\Psi_{\mathrm{cyc}}(q) = \sum_{a=1}^{q} \frac{q}{\gcd(a,q)} \tag{56.1}$$

Grouping residues by their order in the cyclic group gives

$$\boxed{\Psi_{\mathrm{cyc}}(q) = \sum_{d\mid q} d\varphi(d)} \tag{56.2}$$

For a prime power,

$$\Psi_{\mathrm{cyc}}(p^k) = 1 + (p-1)\sum_{j=1}^{k} p^{2j-1} = \boxed{\frac{p^{2k+1}+1}{p+1}} \tag{56.3}$$

Therefore the local Dirichlet factor is

$$\sum_{k\geq 0} \Psi_{\mathrm{cyc}}(p^k)p^{-ks} = \frac{1-p^{1-s}}{(1-p^{-s})(1-p^{2-s})} \tag{56.4}$$

and only then does the Euler product package the arithmetic:

$$\boxed{F_{\text{cyc}}(s) := \sum_{q\geq 1} \frac{\Psi_{\text{cyc}}(q)}{q^s} = \frac{\zeta(s)\zeta(s-2)}{\zeta(s-1)}} \tag{56.5}$$

Singularity classification

The quotient has:

1. a simple pole at $s = 3$ with residue $\zeta(3)/\zeta(2)$;
2. a simple pole at $s = 1$ with residue $1/6$;
3. for every nontrivial zero ρ, a pole at $s = 1 + \rho$ whose order is the multiplicity of ρ;
4. no other poles in $\Re s > 1$.

The inherited pole cannot cancel. At $s = 1+\rho$, the numerator factors are $\zeta(1+\rho)$ and $\zeta(\rho-1)$. The first lies in the zero-free half-plane $\Re s > 1$; the second is neither a nontrivial zero nor a negative even integer. Thus both are nonzero.

Sharp-cutoff no-go

Let

$$A(X) = \sum_{q\leq X} \Psi_{\text{cyc}}(q), \qquad C = \frac{\zeta(3)}{3\zeta(2)} \tag{56.6}$$

and

$$E(X) = A(X) - CX^3 - \frac{X}{6} \tag{56.7}$$

For every prime p, $\Psi_{\text{cyc}}(p) = p^2 - p + 1$, so

$$\boxed{E(p) - E(p-1) = \left(1 - \frac{\zeta(3)}{\zeta(2)}\right)(p^2 - p) + \frac{5}{6} - C} \tag{56.8}$$

The quadratic coefficient is positive. For each prime, at least one of $|E(p)|$ and $|E(p-1)|$ is at least half the jump. Since there are infinitely many primes,

$$\boxed{E(X) = \Omega(X^2), \qquad \limsup_{X\to\infty} \frac{|E(X)|}{X^2} \geq \frac{1}{2}\left(1 - \frac{\zeta(3)}{\zeta(2)}\right)} \tag{56.9}$$

The unsmoothed $O_\varepsilon(X^{3/2+\varepsilon})$ target is therefore impossible, regardless of RH.

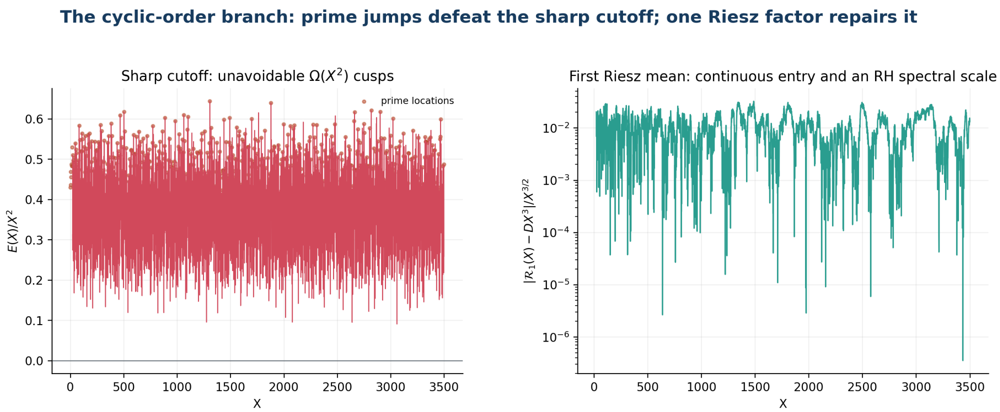

Figure 44: Finite cyclic data show the quadratic sharp-cutoff cusps and the continuous entry created by the first Riesz weight.

57. First-Riesz cyclic criterion

Define the first Riesz mean

$$\boxed{\mathcal{R}_1(X) = \sum_{q \le X} \Psi_{\mathrm{cyc}}(q) \left(1 - \frac{q}{X}\right)} \tag{57.1}$$

Mellin inversion gives, initially for $c > 3$,

$$\boxed{\mathcal{R}_1(X) = \frac{1}{2\pi i} \int_{(c)} F_{\mathrm{cyc}}(s) \frac{X^s}{s(s+1)}\, ds} \tag{57.2}$$

The residue at $s = 3$ is

$$DX^3, \qquad D = \frac{\zeta(3)}{12\zeta(2)} \tag{57.3}$$

The denominator has an exact adjacent-triangular reading:

$$\boxed{\left.\frac{1}{s(s+1)}\right|_{s=3} = \frac{1}{3 \cdot 4} = \frac{1}{12} = \frac{1}{2T_3}, \qquad D = \frac{1}{2T_3} \frac{\zeta(3)}{\zeta(2)}} \tag{57.3a}$$

The continuation value $\zeta(-1) = -1/12$ has the opposite sign but a different analytic owner. The triangular reflection $3 \mapsto -4$ keeps $T_3 = T_{-4}$ and therefore keeps the kernel factor positive; it does not produce a separate identity $-D$. The polar-shell picture of [55] uses the same reciprocal-radius vocabulary but is not the proof of this residue.

Theorem 57.1 (first-Riesz RH equivalence).

$$\boxed{\text{RH} \iff \mathcal{R}_1(X) = DX^3 + O_\varepsilon(X^{3/2+\varepsilon}) \quad \text{for every } \varepsilon > 0} \tag{57.4}$$

RH implies the estimate. Fix $0 < \delta < 1/2$ and write $s = 3/2 + \delta + it$. Since $\Re s > 1$, $\zeta(s) = O_\delta(1)$. The functional equation gives

$$\zeta\left(-\frac{1}{2} + \delta + it\right) \ll_\delta (1 + |t|)^{1-\delta} \tag{57.5}$$

Under RH, Littlewood's reciprocal-zeta estimate in every fixed half-plane to the right of the critical line gives, for every $\eta > 0$,

$$\frac{1}{\zeta(1/2 + \delta + it)} \ll_{\delta,\eta} (1 + |t|)^\eta \tag{57.6}$$

Consequently

$$F_{\text{cyc}}(3/2 + \delta + it) \ll_{\delta,\eta} (1 + |t|)^{1-\delta+\eta} \tag{57.7}$$

After the Riesz kernel, the vertical integrand is $O(|t|^{-1-\delta+\eta})$, which is absolutely integrable when $0 < \eta < \delta$. The same fixed-strip bounds make the horizontal integrals vanish. Shifting from $c > 3$ to $\Re s = 3/2 + \delta$ crosses only $s = 3$ and proves

$$\mathcal{R}_1(X) = DX^3 + O_\delta(X^{3/2+\delta}) \tag{57.8}$$

The estimate implies RH. For $\Re s > 3$, Tonelli's theorem and a direct beta integral give

$$\boxed{\int_1^\infty \mathcal{R}_1(X) X^{-s-1}\, dX = \frac{F_{\text{cyc}}(s)}{s(s+1)}} \tag{57.9}$$

Therefore

$$\int_1^\infty (\mathcal{R}_1(X) - DX^3) X^{-s-1}\, dX = \frac{F_{\text{cyc}}(s)}{s(s+1)} - \frac{D}{s-3} \tag{57.10}$$

The assumed error makes the left side holomorphic in every half-plane $\Re s > 3/2 + \varepsilon$. An off-line zero with $\Re\rho > 1/2 + \varepsilon$ would create an uncancelled inherited pole at $s = 1 + \rho$ inside that half-plane. This is impossible. Letting $\varepsilon \downarrow 0$ and applying functional-equation symmetry gives RH. $\square$

The $s = 1$ residue would contribute $X/12$ only after a contour shift below $\Re s = 1$. It is below the stated error and is not crossed in the RH proof.

58. Fractional Riesz threshold and prime cusp

For $\lambda > 0$, define

$$\mathcal{R}_\lambda(X) = \frac{1}{\Gamma(\lambda+1)} \sum_{q \le X} \Psi_{\mathrm{cyc}}(q) \left(1 - \frac{q}{X}\right)^\lambda \tag{58.1}$$

Its Mellin kernel is

$$\boxed{\frac{\Gamma(s)}{\Gamma(s+\lambda+1)}} \tag{58.2}$$

The $s = 3$ residue gives

$$D_\lambda X^3, \qquad D_\lambda = \frac{2\zeta(3)}{\zeta(2)\Gamma(\lambda+4)} \tag{58.3}$$

On $\Re s = 3/2 + \delta$, Stirling's formula combines with (57.7) to give an integrand of order

$$|t|^{-\lambda-\delta+\eta} \tag{58.4}$$

Thus the direct absolute-contour proof closes for every $\lambda \ge 1$. Conversely, for every $\lambda > 0$, an error $O_\varepsilon(X^{3/2+\varepsilon})$ would continue the Mellin transform past all inherited poles and hence imply RH.

For $0 < \lambda < 1$, a separate arithmetic obstruction appears. Fix $0 < h < 1/2$ and take the central second difference at a prime p. The new prime term occurs only at $p + h$ and equals

$$\frac{\Psi_{\mathrm{cyc}}(p)}{\Gamma(\lambda+1)} \left(\frac{h}{p+h}\right)^\lambda \asymp_\lambda h^\lambda p^{2-\lambda} \tag{58.5}$$

For terms already present at $p - h$, Taylor's theorem and $\Psi_{\mathrm{cyc}}(n) \le n^2$ give

$$\sum_{n \le p-1} \Psi_{\mathrm{cyc}}(n) \left| \Delta_h^2 \left(1 - \frac{n}{X}\right)^\lambda_{X=p} \right| \le C_\lambda h^2 p^{2-\lambda} \tag{58.6}$$

The summable factor is $\sum_{r \ge 1} r^{\lambda-2} < \infty$. Lower-order differentiated factors and the second difference of the cubic main term are $O_\lambda(h^2 p)$. Choose $h = h(\lambda)$ so small that the h^λ entering cusp dominates the h^2 terms. Along every sufficiently large prime,

$$\boxed{\left| \Delta_h^2 (\mathcal{R}_\lambda - D_\lambda X^3)(p) \right| \gg_\lambda p^{2-\lambda}} \tag{58.7}$$

If $\lambda < 1/2$, choose $0 < \varepsilon < 1/2 - \lambda$. Then $2 - \lambda > 3/2 + \varepsilon$, contradicting the proposed RH-scale error.

The rigorous phase diagram is

$$\boxed{\begin{array}{c|c} 0<\lambda<1/2 & \text{RH-scale estimate impossible} \\ 1/2\le\lambda<1 & \text{estimate implies RH; converse open} \\ \lambda\ge 1 & \text{RH-equivalent by the absolute-contour proof} \end{array}} \tag{58.8}$$

The natural next boundary is $\lambda = 1/2$, not the unsmoothed cutoff.

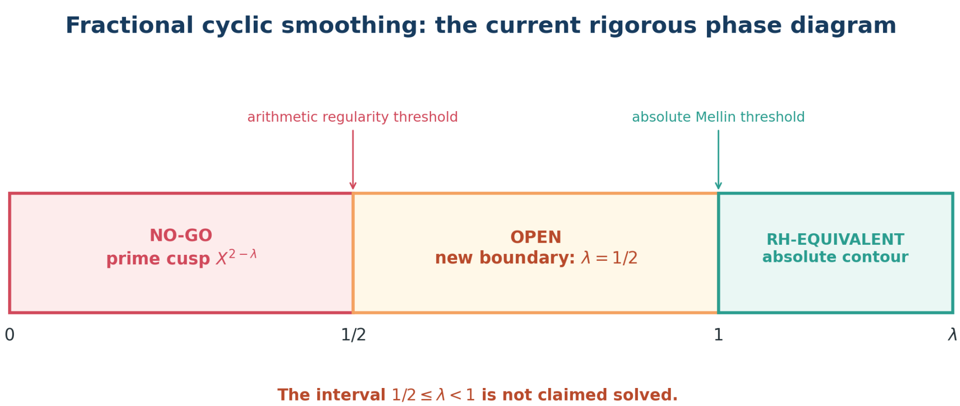

Figure 45: The fractional Riesz phase diagram separates the prime-cusp no-go region, the open middle interval, and the direct RH-equivalent range.

59. Denominator-moment hierarchy

For each integer $j \ge 1$, define

$$\Psi_j(q) = \sum_{d|q} d^j \varphi(d) \tag{59.1}$$

The local factor and global quotient are

$$\sum_{k\ge 0} \Psi_j(p^k)p^{-ks} = \frac{1-p^{j-s}}{(1-p^{-s})(1-p^{j+1-s})} \tag{59.2}$$

and

$$\boxed{F_j(s) = \sum_{q\ge 1} \frac{\Psi_j(q)}{q^s} = \frac{\zeta(s)\zeta(s-j-1)}{\zeta(s-j)}} \tag{59.3}$$

Every nontrivial zero ρ creates an uncancelled pole at $s = j+\rho$. The main pole at $s = j+2$ has residue $\zeta(j+2)/\zeta(2)$.

Define

$$\mathcal{R}_{j,1}(X) = \sum_{q\le X} \Psi_j(q)\left(1-\frac{q}{X}\right) \tag{59.4}$$

The proof of Theorem 57.1 translates without loss: on $\Re s = j + 1/2 + \delta$, the two critical factors are again $\zeta(-1/2+\delta+it)$ and $1/\zeta(1/2+\delta+it)$, while $\zeta(s)$ is bounded. Hence:

Theorem 59.1 (cyclic moment hierarchy). For every integer $j \ge 1$,

$$\boxed{\mathrm{RH} \iff \mathcal{R}_{j,1}(X) = \frac{\zeta(j+2)}{\zeta(2)(j+2)(j+3)}X^{j+2} + O_{\varepsilon,j}(X^{j+1/2+\varepsilon})} \tag{59.5}$$

The half-power gap between the raw prime jump X^{j+1} and the RH spectral scale $X^{j+1/2}$ is universal across the hierarchy.

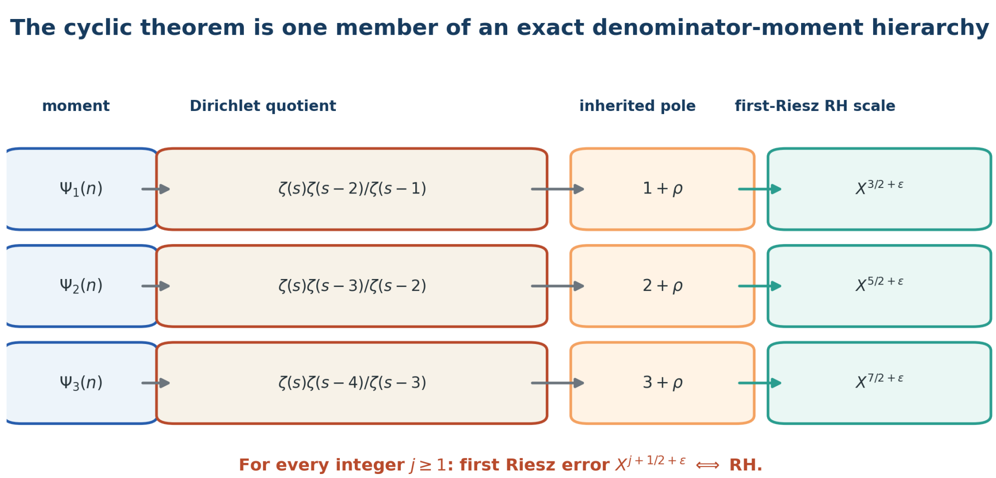

Figure 46: The $j = 1$ cyclic theorem is the first member of a full denominator-moment family with inherited poles $j + \rho$.

60. The zero-frontier exponent

Let

$$\beta_* = \sup_\rho \Re\rho \tag{60.1}$$

and define

$$\alpha_1 = \inf\left\{\alpha : \mathcal{R}_1(X) - DX^3 = O_\varepsilon(X^{\alpha+\varepsilon}) \text{ for every } \varepsilon > 0\right\} \tag{60.2}$$

The inherited poles give the unconditional lower bound

$$\boxed{\alpha_1 \geq 1 + \beta_*} \tag{60.3}$$

Any smaller exponent would analytically continue (57.10) across a pole $1 + \rho$ with real part arbitrarily close to $1 + \beta_*$. The reverse inequality follows from Littlewood's classical reciprocal-zeta estimate in each fixed zero-free half-plane, combined with the same first-Riesz contour argument. Thus, with that standard cited input,

$$\boxed{\alpha_1 = 1 + \beta_*} \tag{60.4}$$

This is a spectral-frontier identity, not a proof that $\beta_* = 1/2$. It explains exactly why first Riesz smoothing measures the rightmost zeta zeros.

61. Cayley–Montgomery bridge: structural only

Under RH, $q_\gamma = 1/4 + \gamma^2$. At a large reference height T, set

$$x_T = T^2 + \frac{1}{4} \qquad c_T(\gamma) = \frac{q_\gamma - x_T}{q_\gamma + x_T} = \frac{\gamma^2 - T^2}{\gamma^2 + T^2 + 1/2} \tag{61.1}$$

For $\gamma = T + \delta$ with $\delta = o(T)$,

$$c_T(\gamma) = \frac{\delta}{T} + O\left(\frac{\delta^2}{T^2} + \frac{|\delta|}{T^3}\right) \tag{61.2}$$

Define

$$\eta_T(\gamma) = \frac{T \log(T/2\pi)}{2\pi} c_T(\gamma) \tag{61.3}$$

For bounded offsets $\gamma - T$ and $\gamma' - T$ (in particular at the local spacing scale $O(1/\log T)$), the nearby ordinates satisfy

$$\eta_T(\gamma) - \eta_T(\gamma') = \frac{\log(T/2\pi)}{2\pi}(\gamma - \gamma') + o(1) \tag{61.4}$$

which is the conventional local spacing normalization.

Both the sine kernel and the Postmaster Markov object admit divided-difference forms, but no limit from the completed-source Pick kernel to the sine kernel is proved here. Section 61A proves a limit for the specified comparison projection of Section 12A. The present statement remains a coordinate bridge, not a proof of pair correlation.

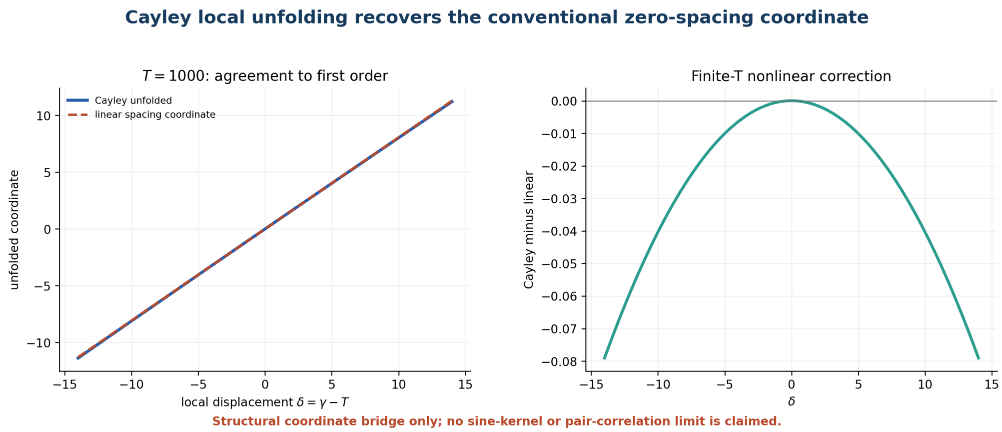

Figure 47: At large T, the local Cayley coordinate agrees to first order with the conventional zero-spacing coordinate.

61A. A comparison sine kernel at the ordinate scale

The sine kernel of Section 12A can be matched to a specified high-height coordinate. This is a theorem about that comparison projection, not the missing completed-source Pick-kernel limit in Section 61.

With Fourier convention $\widehat{f}(t) = \int_{\mathbb{R}} f(u)e^{-2\pi itu}du$, interval integration, convolution and Plancherel give respectively

$$\operatorname{sinc}_\pi(u) = \int_{-1/2}^{1/2} e^{2\pi itu}dt, \qquad \widehat{\operatorname{sinc}_\pi^2}(t) = (1-|t|)_+, \qquad \int_{\mathbb{R}} \operatorname{sinc}_\pi(u)^2 du = 1. \tag{61A.1}$$

The continuous tent measures interval overlap. Its finite counterpart (12A.4) counts pair differences exactly. Montgomery's original paper [79] uses the corresponding distinct-point density $1-\operatorname{sinc}_\pi(u)^2$ in its pair-correlation conjecture. Its theorem assumes RH and treats a restricted Fourier range. The density is not the nearest-neighbor gap distribution; retaining self-pairs adds a delta mass at zero. No conjectured pair-correlation law is used as a proved arithmetic estimate here.

On the critical-line chart $\rho = 1/2 + i\gamma$, $\gamma > 0$,

$$y_\gamma = \frac{1}{\gamma^2+1/4} = 4\sin^2\frac{\theta(\gamma)}{2}, \qquad \theta(\gamma) = 2\arctan\frac{1}{2\gamma}, \qquad \theta'(\gamma) = -\frac{1}{\gamma^2+1/4}. \tag{61A.2}$$

These are algebraic identities. Using a real ordinate in this chart is not the same as using the actual folded coordinate of an off-line zero.

Theorem 61A.1 (joint bandwidth and height limit). Put, for $T > 2\pi$,

$$L_T = \log\frac{T}{2\pi}, \qquad N_T = \left\lfloor \frac{(T^2+1/4)L_T}{2} \right\rfloor, \qquad \gamma_T(u) = T + \frac{2\pi u}{L_T}. \tag{61A.3}$$

For each fixed U and sufficiently large T, uniformly for $|u|, |v| \le U$,

$$\boxed{\frac{\pi}{N_T}\Pi_{N_T}(\theta(\gamma_T(u)), \theta(\gamma_T(v))) = \operatorname{sinc}_\pi(u-v) + O_U((TL_T)^{-1}).} \tag{61A.4}$$

Proof. Taylor's theorem applied to (61A.2), including the floor error, gives $N_T[\theta(\gamma_T(u)) - \theta(T)] = -\pi u + O_U((TL_T)^{-1})$. Here $\theta''(\gamma) = 2\gamma/(\gamma^2+1/4)^2 = O(T^{-3})$ on the required interval. In the difference term of (12A.9), writing $z = N_T(\theta(\gamma_T(u)) - \theta(\gamma_T(v)))$ gives $\sin z/[2N_T \sin(z/(2N_T))]$; the removable quotient converges uniformly to $\sin z/z$. In the reflected term the denominator is asymptotic to $\sin\theta(T) \sim 1/T$, uniformly in u, v. Its normalized magnitude is $O(T/N_T) = O((TL_T)^{-1})$. Together these estimates prove (61A.4). □

The relevant projection dimension is therefore $N \sim (T^2 + 1/4)\log(T/(2\pi))/2$. Fixed degree cannot resolve arbitrarily high microscopic spacing in this coordinate. This N is not automatically a Widder rung index or a count of zeta zeros.

The source comparison retains a different functional. In $\ell = r + s + 1$, $d = r - s$ coordinates, Section 155A gives

$$K_{r,s} = \lambda_\ell - \lambda_{|d|}, \qquad y\mathcal{P}_r(y)\mathcal{P}_s(y) = 2\cos(d\theta) - 2\cos(\ell\theta). \tag{61A.5}$$

The same product-to-sum operation creates (12A.9), but the summation data are different. The actual functional is $\mathcal{L}[f] = \sum_{[\rho]} m_\rho y_\rho f(y_\rho)$, and its identity $\lambda_{2m+1} = \mathcal{L}[\mathcal{P}_m^2]$ uses holomorphic squares, not absolute squares. Neither ω nor ν_C is identified with this functional. The all-rank condition does not occupy only $d = 0$; it constrains the mixed entries. Section 155C supplies an explicit positive reserve and retains its entire adjustment in the arithmetic defect.

Why a limiting spacing law is insufficient by itself. Consider a locally finite multiset of real ordinates and a bounded compactly supported pair test of $(\gamma - \gamma')\log T$, divided by a normalization of order $T\log T$. Adding or removing finitely many fixed ordinates changes its numerator by $O(1)$: each fixed altered point meets only finitely many unchanged points in the shrinking support window. Its normalized limit is unchanged. Thus an abstract finite off-line quartet can coexist with the same limiting ordinate statistic. This is not a counterexample about zeta. It shows why the actual-source inequality $\mathcal{E}_{2m+1} \le \mathcal{A}_{2m+1}$ or the all-rank defect bound must still be proved. The finite negative control of Section 104A remains valid after this sine reformulation.

Technical chapter X. Prime wave packets and the cancellation problem

The moving shell leads to prime oscillation. Exact Bessel coefficients improve the diagonal model; remaining correlation and uniformity assumptions are stated at the end.

45. Gate Z and the Lindelof firewall

The finite octagon identity

$$\omega = e^{2\pi i 7/8} \qquad \sum_{j=0}^{7} \omega^j = 0$$

is exact. Its transfer to n^{-it} is not exact because

$$\log(N+h) = \log N + \frac{h}{N} - \frac{h^2}{2N^2} + \cdots$$

Any exponent-pair submission must retain uniformity in t, M, N, endpoints, integer-derivative danger blocks, and stationary phases. No such new pair is proved here.

Lindelöf controls growth on the critical line. No argument here turns that growth bound into exclusion of sparse off-line zeros. Gate Z is useful analytic infrastructure, not the shortest zero-exclusion route.

105. From the grid to the moving critical shell

For each fixed $x > 0$ and fixed n, PP157 obtains the RH-independent asymptotic

$$\boxed{\begin{aligned} G_{n,k}(x) = \frac{(1/2)_n}{8\sqrt{\pi x}}\, k^{-n-1/2} \left[\log \frac{kx}{\pi^2} + \gamma_E - (2H_{2n} - H_n)\right] \\ + O_{n,x}(k^{-n-1} \log k) \end{aligned}} \tag{105.1}$$

Thus every fixed n row is eventually positive. This is insufficient for the full grid because the threshold is not uniform in n.

The verified-height route gives a very large but finite A-CAT rectangle:

$$G_{n,k}(56) > 0 \qquad (0 \le n \le 6{,}901{,}269{,}318,\ k \ge 0) \tag{105.2}$$

Its size is not a logical substitute for all n. The unresolved owner moves with k.

Put

$$K = k+1, \qquad N = n+1, \qquad \lambda = \frac{N}{\sqrt{K}} \qquad \Gamma^2 + \frac{1}{4} = \frac{xK}{N} \tag{105.3}$$

In the critical scaling $\lambda \to \lambda_0 \in (0,\infty)$, a zero $\rho = \frac{1}{2} + \delta + i(\Gamma + c)$ contributes, after normalization,

$$\exp\left[\frac{2\lambda_0^2}{x}\left(\rho - \frac{1}{2} - i\Gamma\right)^2\right] \tag{105.4}$$

Horizontal pairing gives

$$2e^{-2\lambda_0^2 c^2/x + 2\lambda_0^2\delta^2/x}\cos\frac{4\lambda_0^2\delta c}{x} \tag{105.5}$$

The flat-density Gaussian integral is independent of δ:

$$\int_{\mathbb{R}} e^{-2\lambda^2 c^2/x + 2\lambda^2\delta^2/x}\cos\frac{4\lambda^2\delta c}{x}\,dc = \sqrt{\frac{\pi x}{2\lambda^2}} \tag{105.6}$$

This is why isolated off-line displacement does not control the moving shell; the prime oscillation does.

The even Gaussian test

$$g_{\Gamma,\lambda}(u) = e^{-2\lambda^2(u-\Gamma)^2/x} + e^{-2\lambda^2(u+\Gamma)^2/x} \tag{105.7}$$

has Fourier transform

$$\widehat{g}(y) = \frac{\sqrt{2\pi x}}{\lambda}e^{-\pi^2 x y^2/(2\lambda^2)}\cos(2\pi\Gamma y) \tag{105.8}$$

The exact explicit formula therefore isolates the prime cosine statistic

$$P_x(\lambda,\Gamma) = \sum_{m\ge 2}\frac{\Lambda(m)}{\sqrt{m}}e^{-x(\log m)^2/(8\lambda^2)}\cos(\Gamma\log m) \tag{105.9}$$

PP160 proves unconditionally that, for every fixed $\varepsilon > 0$,

$$\lambda^2 \leq 2x(1-\varepsilon)\log\log\Gamma \quad \Longrightarrow \quad G_{n,k}(x) > 0 \tag{105.10}$$

for all sufficiently large admissible pairs. A convenient k-form is

$$n < (\sqrt{2x} - o(1))\sqrt{k \log\log k} \tag{105.11}$$

The transition beyond this region is the first infinite part of the grid not already covered by fixed-row asymptotics or source-side absolute estimates.

106. Fourier-saddle collision and the first-return exponent

Let

$$A_x(\lambda) = \sum_{m\geq 2} \frac{\Lambda(m)}{\sqrt{m}} e^{-x(\log m)^2/(8\lambda^2)} \tag{106.1}$$

For $\eta > 0$, define the first positive near-return

$$R_x^+(\lambda,\eta) = \inf\{\Gamma \geq 1 : P_x(\lambda,\Gamma) \geq (1-\eta)A_x(\lambda)\} \tag{106.2}$$

With $\eta_\lambda = c_x/\lambda^2$, the return exponent is

$$\boxed{\Theta_x = \liminf_{\lambda\to\infty} \frac{x}{\lambda^2} \log\log R_x^+(\lambda,\eta_\lambda)} \tag{106.3}$$

For each fixed λ, unique factorization makes the prime logarithms rationally independent, so Kronecker approximation gives

$$\limsup_{\Gamma\to\infty} \frac{P_x(\lambda,\Gamma)}{A_x(\lambda)} = 1 \tag{106.4}$$

Fixed-dimensional recurrence is therefore unavoidable. It is harmless at fixed λ, where $A_x(\lambda)$ is fixed and the Archimedean main grows like $\log\Gamma$. The moving dimension is the owner.

Truncating the active primes at

$$\log p \leq 2s + 6\sqrt{s\log\lambda} \qquad s = \lambda^2/x \tag{106.5}$$

leaves $d_\lambda = \exp(2s + o(s))$ phases. Simultaneous Dirichlet approximation gives

$$\log\log R_x^+ \leq 2s + o(s) \tag{106.6}$$

On every bounded Γ interval the normalized cosine statistic tends to zero, so $R_x^+ \to \infty$. Hence the sharp proved interval is only

$$\boxed{0 \leq \Theta_x \leq 2} \tag{106.7}$$

The Postmaster branch needs

$$\boxed{\Theta_x > \frac{1}{2}} \tag{106.8}$$

The analytic reason absolute values stop at this coefficient is visible in the exact rational test

$$H(t) = x^{N-1} \frac{(t^2 + 1/4)^K}{(x + t^2 + 1/4)^{K+N}} \tag{106.9}$$

At its positive saddle,

$$f''(\Gamma) = -\frac{4\lambda^2}{x} + O_x\left(\frac{\lambda^2}{\Gamma^2}\right) \tag{106.10}$$

For Fourier frequency L, the complex shift is

$$\sigma_F(L) = \frac{xL}{4\lambda^2} \tag{106.11}$$

The phase-blind prime-density exponent

$$\Phi(L) = \frac{L}{2} - \frac{xL^2}{8\lambda^2} \tag{106.12}$$

is maximized at

$$L_* = \frac{2\lambda^2}{x} \qquad \boxed{\sigma_F(L_*) = \frac{1}{2}} \tag{106.13}$$

The prime coefficient $m^{-1/2}$ and the saddle shift $m^{-1/2}$ collide exactly on $\Re s = 1$. Absolute convergence can reach the boundary but cannot supply the missing sign. The surviving task is an additive wave-packet anti-resonance theorem.

107. The loose diagonal is exactly self-limiting

A loose version of the moment method bounds the diagonal by a loose expression of the shape $r!S_2^r$. Write

$$\log T = \exp(cs + o(s)) \qquad 0 < c < 1 \tag{107.1}$$

The largest product length compatible with clean orthogonality is

$$r_{\max} \sim \frac{e^{cs}}{2s} \tag{107.2}$$

while exclusion of one derivative-width near-L^1 return requires

$$r_{\text{req}} \sim \frac{e^{cs}}{(1-c)s} \tag{107.3}$$

Therefore

$$\boxed{\frac{r_{\text{req}}}{r_{\max}} \longrightarrow \frac{2}{1-c}} \tag{107.4}$$

Equivalently, with $r = \beta \log T/(2s)$, the method needs

$$\beta > \frac{2}{1-c} \tag{107.5}$$

The same central peak used in the upper bound forces

$$\beta \leq \frac{2}{1-c} \tag{107.6}$$

Theorem 107.1 (loose-diagonal no-go). The diagonal-quality moment architecture cannot prove a strict return exponent larger than c for any $0 < c < 1$. Its reach and its failure are the same exponent equality.

The endpoint can have separate bookkeeping, but it cannot yield the strict crossing (106.8). The exact-diagonal route uses the interior saddle relation (108.9).

118. Gaussian prime energy and the visibility comparison

The following source lemma separates an exact prime-energy asymptotic from the still-unproved comparison between collar width and finite-rank reach.

Lemma 118.1 - Gaussian prime energy

For fixed $s > 0$, let

$$a_p = \frac{\log p}{\sqrt{p}} \exp\left(-\frac{(\log p)^2}{8s}\right)$$

Then

$$\boxed{\mathcal{S}(s) := \sum_p a_p^2 = \sum_p \frac{(\log p)^2}{p} \exp\left(-\frac{(\log p)^2}{4s}\right) < \infty} \tag{118.1}$$

Moreover, as $s \to \infty$, the prime number theorem and partial summation give

$$\boxed{\mathcal{S}(s) = 2s + o(s)} \tag{118.2}$$

For convergence, the Gaussian in $\log p$ eventually dominates every fixed negative power of p. For the asymptotic, $d\pi(t)$ may be replaced at main order by $dt/\log t$; with $u = \log t$ the resulting main integral is

$$\int_0^\infty u e^{-u^2/(4s)}\, du = 2s$$

The integral is exactly $2s$; the discrete prime sum is only asymptotic to it. Consequently the square-root and tilted peak locations inferred from this density replacement are asymptotic diagnostics, not exact finite-s identities.

The exact aperture formula from Section 48 survives PP175 unchanged. The proposed comparison with PP133 does not receive theorem grade: PP133 reports an empirical rank threshold whose zero-count scale grows roughly like $\gamma \log \gamma$, whereas the Lill half-aperture shrinks like $1/\gamma$ for fixed horizontal displacement. Both say that high zeros are harder to see, but no map from collar width to ν_N has been proved.

108. The exact-diagonal theorem and its closure geometry

Set

$$D_s(t) = \sum_p a_p p^{it} \qquad a_p = \frac{\log p}{\sqrt{p}} e^{-(\log p)^2/(8s)} \tag{108.1}$$

and expand

$$D_s(t)^r = \sum_n b_r(n) n^{it} \tag{108.2}$$

The exact diagonal is

$$E_r = \sum_n b_r(n)^2 \tag{108.3}$$

Theorem 108.1 (Bessel-product diagonal).

$$\boxed{E_r = (r!)^2[z^r]\prod_p I_0(2a_p\sqrt{z})} \tag{108.4}$$

Proof. For $n = \prod_p p^{k_p}$ with $\sum_p k_p = r$,

$$b_r(n) = \frac{r!}{\prod_p k_p!}\prod_p a_p^{k_p}$$

Since

$$I_0(2a\sqrt{z}) = \sum_{k\geq 0}\frac{a^{2k}z^k}{(k!)^2}$$

coefficient extraction in the Euler product gives exactly the sum of $b_r(n)^2/(r!)^2$. □

Relation to classical pseudomoments. The quantity E_r is a Gaussian-weighted all-prime pseudomoment, within the classical framework of Conrey–Gamburd and subsequent work [30,32,38]. The local identity is

$$\sum_{k\geq 0}\frac{a_p^{2k}z^k}{(k!)^2} = I_0(2a_p\sqrt{z}) \tag{108.4a}$$

Wahl's prime product uses J_0 factors [31, equation (1.4)], related by $I_0(u) = J_0(iu)$. Theorem 108.1 is an exact coefficient dictionary; the weight and growing-order remainder distinguish the later analytic task. No priority claim is made for the Bessel local-factor mechanism.

The first-order cancellation behind Wahl's renormalizer is explicit: with $a_p = p^{-1/2}$ and $z = -u^2/4$, $I_0(2a_p\sqrt{z}) = J_0(u/\sqrt{p})$, and the divergent p^{-1} term in $\log J_0$ is cancelled by $(1-1/p)^{-u^2/4}$.

The packet weight in (108.1) is an all-prime Gaussian weight. For each fixed s its square is summable,

$$\sum_p a_p^2 = \sum_p \frac{(\log p)^2}{p}e^{-(\log p)^2/(4s)} < \infty \tag{108.4b}$$

so the bare local product converges, while its mass becomes concentrated in a moving logarithmic packet as $s\to\infty$. This damping distinguishes the global object from Wahl's undamped product; the match is at the Bessel local factor, not at the full weighted model.

Growing-order pseudomoment asymptotics occur in the literature; see Bondarenko–Brevig–Saksman–Seip–Zhao [38]. The result below concerns the stated Gaussian-weighted, coupled (r, s) regime. Its theorem is specific to that weight and uniform remainder; no general novelty or priority claim for growing-order pseudomoment saddles is made.

The exact diagonal: factorials retain prime multiplicities

1. One prime: multiplicity j

$$I_0(2a_p\sqrt{z}) \qquad = \qquad \sum_{j=0}^{\infty} \frac{a_p^{2j} z^j}{(j!)^2}$$

2. Extract total degree r from the prime product

$$[z^r]\prod_p I_0(2a_p\sqrt{z}) \qquad = \qquad \sum_{\substack{(j_p)_p\,;\ j_p\ge 0\\ \sum_p j_p = r}} \prod_p \frac{a_p^{2j_p}}{(j_p!)^2}$$

3. Restore the multinomial factor

$$E_r \qquad = \qquad (r!)^2[z^r]\prod_p I_0(2a_p\sqrt{z}) \qquad = \qquad \sum_n b_r(n)^2$$

The Gaussian weights in (108.1) make $\sum_p a_p^2$ finite at each fixed $s > 0$.

Figure 48: The exact Bessel coefficient dictionary keeps the factorial square in each local prime multiplicity. Forming the product and extracting z^r enforces total multiplicity r; it does not control the off-diagonal prime contribution.

The packet-specific analytic statement begins with the following saddle estimate and its uniform remainder, not with (108.4).

If

$$c_r = \frac{\log r}{s}$$

stays in a compact subinterval of $(0, 2)$, the symbolic saddle and local central-limit argument give

$$\boxed{\log E_r = r\left(c_r - \frac{c_r^2}{4}\right)s + O(r\log s)} \tag{108.5}$$

Also

$$\log A_s^{2r} = rs + O(r\log s) \qquad A_s = \sum_p a_p \tag{108.6}$$

Thus

$$\log \frac{A_s^{2r}}{E_r} = r\left(1 - \frac{c_r}{2}\right)^2 s + O(r\log s) \tag{108.7}$$

At

$$r = \frac{\beta \log T}{2s} \qquad \frac{\log r}{s} \to c \tag{108.8}$$

an exact-diagonal translated bound of size $T^{1+o(1)}E_r$ would rule out a return whenever

$$\boxed{\frac{\beta}{2}\left(1 - \frac{c}{2}\right)^2 > 1 \quad \text{equivalently} \quad \beta > \frac{2}{(1 - c/2)^2}} \tag{108.9}$$

Solving the equality for c gives the exact-diagonal closure map

$$\boxed{c_{\mathrm{ED}}(\beta) = 2\left(1 - \sqrt{\frac{2}{\beta}}\right)} \tag{108.10}$$

At $c = 1/2$ the threshold is $32/9$. Two margins are important:

$$\frac{4}{2}\left(\frac{3}{4}\right)^2 - 1 = \frac{1}{8} \tag{108.11}$$

and

$$\frac{11/3}{2}\left(\frac{3}{4}\right)^2 - 1 = \frac{1}{32} \tag{108.12}$$

At the rational pilot

$$\boxed{\beta_0 = \frac{11}{3} \qquad c_{\mathrm{ED}}(\beta_0) = 2\left(1 - \sqrt{\frac{6}{11}}\right) = 0.5229021082\ldots > \frac{1}{2}} \tag{108.13}$$

This shows exponent room. It does not supply the translated theorem or its uniformity in c.

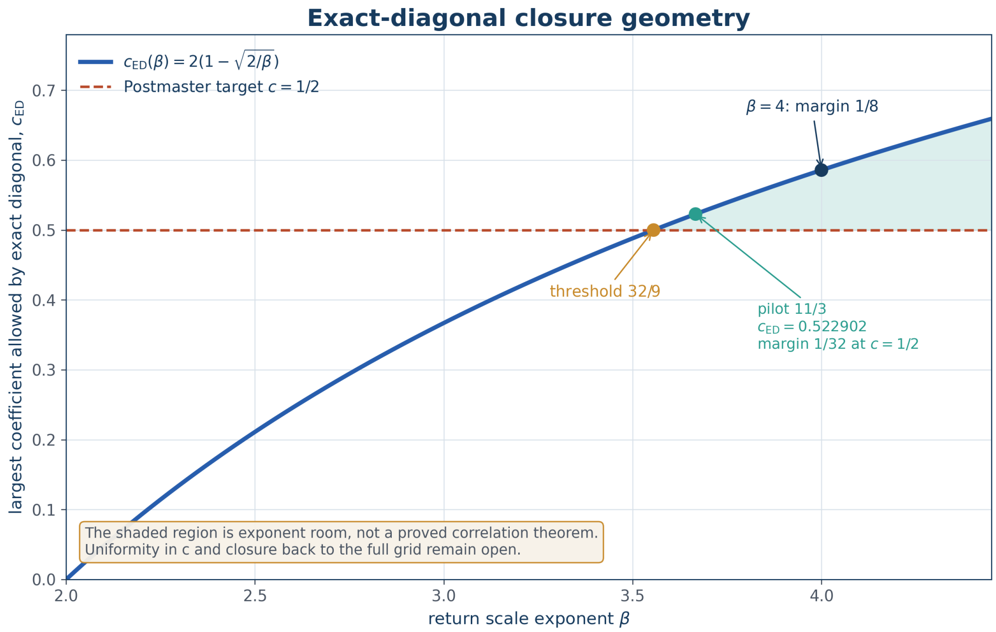

Figure 49: The exact diagonal permits coefficients above one half at the rational pilot, but the shaded region is conditional exponent room.

The inherited rigorous exact-diagonal frontier remains $\beta_{\mathrm{ED}} \geq 32/17$ in supremum sense. The pilot $\beta_0 = 11/3$ is a target, not an attained return theorem.

109. Tilted diagonal, size owner, and the engineered kernel

Define

$$E_r(\theta) = \sum_n n^\theta b_r(n)^2 \qquad \frac{\log r}{s} \to c \in (0,1) \tag{109.1}$$

PP168 proves

$$\boxed{\frac{\log E_r(\theta)}{rs} = \begin{cases} (1+\theta)c - c^2/4, & 0 \leq \theta \leq c/2 \\ c + \theta^2, & \theta \geq c/2 \end{cases} + O\left(\frac{\log s}{s}\right)} \tag{109.2}$$

The value and first derivative agree at $\theta = c/2$, while the second derivatives are 0 and 2. The phase is C^1 but not C^2. Its audited right-tail rate is

$$\boxed{I_c(\alpha) = \frac{\alpha^2 - c^2}{4} \qquad \alpha \geq c} \tag{109.3}$$

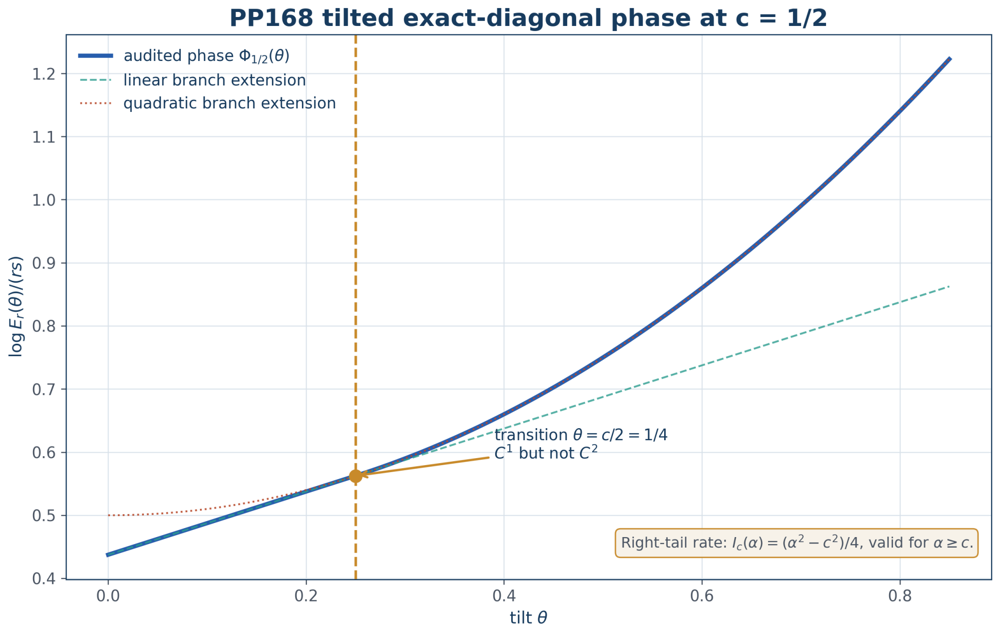

Figure 50: The two tilted branches meet with one derivative but not two. The rate formula is asserted only on its audited right-tail domain.

At $c = 1/2$, with $r = \beta \log T/(2s)$,

$$\frac{E_r[n \asymp T^a]}{E_r} = T^{-a^2/(2\beta)+\beta/32+o(1)} \tag{109.4}$$

is valid for

$$a \geq \frac{\beta}{4} \tag{109.5}$$

After the weighted Montgomery–Vaughan penalty, the exponent is

$$F_\beta(a) = a - 1 - \frac{a^2}{2\beta} + \frac{\beta}{32} = \frac{17\beta}{32} - 1 - \frac{(a-\beta)^2}{2\beta} \tag{109.6}$$

Theorem 109.1 (Montgomery–Vaughan owner and the internal gap). At $c = 1/2$, assume the tilted asymptotic (109.2) in the regime $r = \beta \log T/(2s)$. Then

$$\int_0^T |D_s(t)^r|^2 \, dt = TE_r(0) + O(E_r(1)) \tag{109.6a}$$

and

$$\boxed{\frac{E_r(1)}{TE_r(0)} = T^{17\beta/32-1+o(1)}} \tag{109.6b}$$

Consequently the classical mean-value theorem certifies a diagonal asymptotic when $\beta < 32/17$ and ceases to be main-term quality when $\beta > 32/17$. Since exact-diagonal return at $c = 1/2$ requires $\beta > 32/9$, the classical mean-value range and the return range are disjoint.

Proof. Apply the Montgomery–Vaughan mean-value theorem first to finite truncations of (108.2). Its error is bounded by $\sum_n nb_r(n)^2 = E_r(1)$. The tilted formula gives

$$\frac{\log E_r(0)}{rs} = \frac{7}{16} + O\left(\frac{\log s}{s}\right) \qquad \frac{\log E_r(1)}{rs} = \frac{3}{2} + O\left(\frac{\log s}{s}\right)$$

Thus

$$\log\frac{E_r(1)}{E_r(0)} = \frac{17}{16}rs + O(r\log s) = \left(\frac{17\beta}{32} + o(1)\right)\log T$$

which proves (109.6b). The Gaussian weight makes $E_r(1) < \infty$ for fixed s, so the finite truncations converge in the required weighted ℓ^2 norms and (109.6a) follows by passage to the limit. Finally $32/17 < 32/9$. □

This is a no-overlap theorem for the **classical mean-value estimate**, not a lower bound on the true off-diagonal error. When $\beta > 32/17$, the theorem's allowance may dominate even if the actual signed correlation is smaller. At the rational pilot,

$$\frac{E_r(1)}{TE_r(0)} = T^{91/96+o(1)} \qquad \beta = \frac{11}{3} \tag{109.6c}$$

This quantifies why a correlation theorem, rather than another use of the unmodified mean-value bound, is required.

It has one maximizer:

$$\boxed{a = \beta, \qquad X = T^{\beta+o(1)}} \tag{109.7}$$

The active additive shifts satisfy

$$\boxed{L = \frac{X}{T} = X^{1-1/\beta}} \tag{109.8}$$

The missing relative saving is independent of β in X units:

$$\boxed{T^{-\beta/4} = X^{-1/4}} \tag{109.9}$$

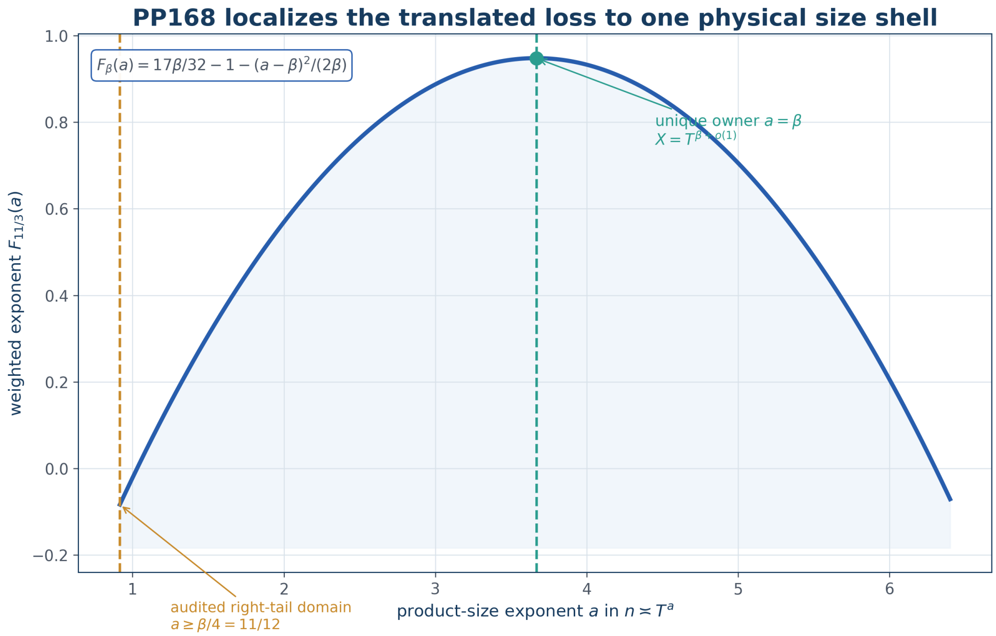

Figure 51: The weighted exponent is a strict parabola whose unique owner is the shell $X = T^\beta$.

On this tilted owner a typical prime factor obeys

$$\log p = 2s + O_{\mathbb{P}}(\sqrt{s}) \qquad p = (\log X)^{4+o(1)} \tag{109.10}$$

The typical factor scale is not a hard whole-product cutoff. The extreme factor for $1 - o(1)$ of the tilted mass reaches

$$\log P^+(n) = (2 + \sqrt{2} + o_{\mathbb{P}}(1))s \tag{109.11}$$

or polylogarithmic exponent $4 + 2\sqrt{2}$. Repeated factors are negligible in the independent tilted product owner, but this does not imply shifted-gcd independence.

For $W \in C_c^\infty([-1,1])$ use

$$\widehat{W}(\xi) = \int_{\mathbb{R}} W(t)e^{i\xi t}\,dt \qquad K_\pi(x) = \cos(\pi x)\widehat{W}(x) \tag{109.12}$$

The Fourier transform of K_π is supported away from the origin, so all of its derivatives vanish there. Equivalently,

$$\boxed{\int_{\mathbb{R}} x^j K_\pi(x)\,dx = 0 \qquad (j = 0, 1, 2, \ldots)} \tag{109.13}$$

Every finite smooth Taylor jet of a local shift density is invisible. What remains must be nonsmooth arithmetic structure, lattice structure, or a boundary term.

110. The rational pilot and the exact local factor

At $\beta_0 = 11/3$,

$$\boxed{X = T^{11/3}, \qquad H = T = X^{3/11}, \qquad L = X/T = X^{8/11}} \tag{110.1}$$

The nonlinear-log and boundary collar is

$$T^{-1} = X^{-3/11} = X^{-1/4} X^{-1/44} \tag{110.2}$$

Thus it has a strict spare power $X^{-1/44}$ relative to the target.

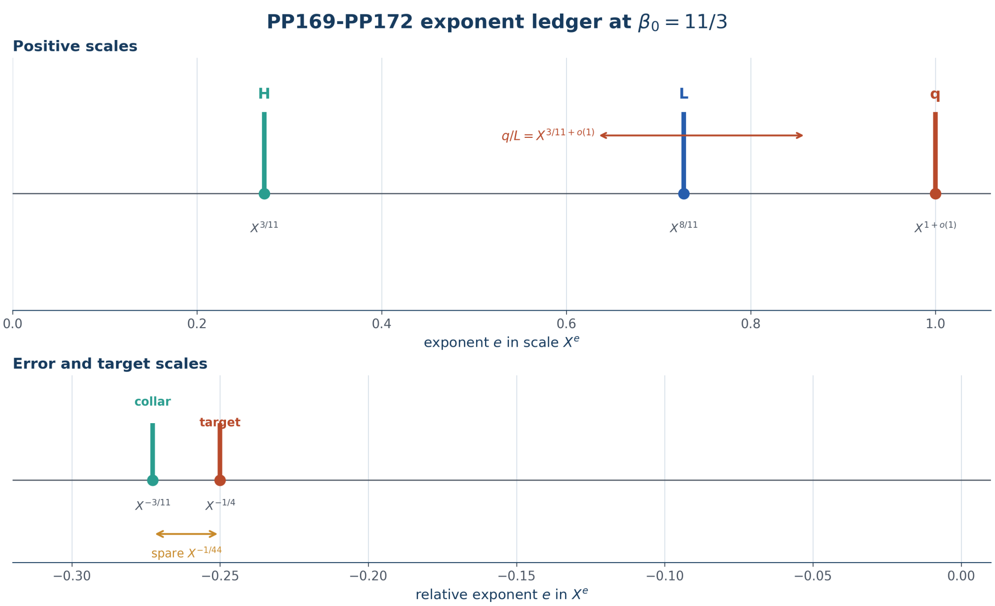

Figure 52: The pilot separates the window, shift, modulus, collar, and target exponents on one common X scale.

The generating-function lift has an exact local p-adic owner. Put

$$A_k = \frac{(za_p)^k}{k!} \qquad B_k = \frac{(wa_p)^k}{k!} \qquad \mu_k = (1-p^{-1})p^{-k} \tag{110.3}$$

For $v = v_p(h) < \infty$,

$$\boxed{\begin{aligned} L_{p,v}(z,w) = &\sum_{k=0}^{v-1} \mu_k A_k B_k \\ &+ p^{-v}\left[(1-2/p)A_v B_v + \sum_{j\geq 1} \mu_j \left(A_{v+j}B_v + A_v B_{v+j}\right)\right] \end{aligned}} \tag{110.4}$$

Proof. If $v_p(n) = k < v$, then $v_p(n+h) = k$, giving the first sum. On the remaining set write $n = p^v m$ and $h = p^v h'$ with $p \nmid h'$. The two classes $m \equiv 0$ and $m \equiv -h' \pmod p$ are distinct. With Haar probability $1 - 2/p$ both are units; otherwise exactly one has positive valuation j, with measure μ_j. Multiplication by p^{-v} gives (110.4). □

In the symmetric squarefree truncation with activity λ,

$$L_{p,1} - L_{p,0} = \frac{(1-\lambda)(1-(1-2/p)\lambda)}{p} \qquad L_{p,2} - L_{p,1} = \frac{\lambda^2}{p^2} \tag{110.5}$$

The sign change at $\lambda = 1$ does not improve an absolute coefficient tail. The correct marginal Mellin activity is

$$\boxed{\lambda_p = z a_p p^{-\sigma}} \tag{110.6}$$

At the pilot saddle,

$$\sigma_* = o(1) \qquad z_* = \frac{11}{3s}[1 + o(1)] \tag{110.7}$$

and on the owner-prime shell,

$$\lambda_p = e^{-3s/2+o(s)} = (\log X)^{-3+o(1)} \longrightarrow 0 \tag{110.8}$$

The Mellin factor in (110.6) is essential to this small-activity regime.

For reciprocal smooth-modulus counting, the modeled tail exponent is only $1/4$ at the typical factor scale and $1/(4 + 2\sqrt{2})$ at the whole-mass cutoff, while the pilot needs

$$\delta > \frac{11}{32} \tag{110.9}$$

Because $\lambda_p \to 0$, the first local coefficient is divisor-normalized like $1/p$; a bounded sign or weight improvement is only subpower over $r \asymp \log X / \log\log X$. The smoothness-counting subroute is therefore closed. This is not a no-go for every possible signed extracted coefficient theorem.

The first missing global line inside this factorization route is

$$R_{r,X}(h) = M_{r,X}\mathfrak{S}_{r,s}(h) + \mathcal{E}_{r,X}(h) \tag{110.10}$$

with a kernel-tested error at relative scale $X^{-1/4+o(1)}$ after both growing-order coefficient extractions.

111. The block owner and the total/off-diagonal Poisson decomposition

Let

$$f_X(n) = b_r(n)\phi(n/X) \qquad P_X(t) = \sum_n f_X(n)n^{it} \tag{111.1}$$

and define

$$B_X = \sum_n f_X(n) \qquad E_X = \sum_n f_X(n)^2 \qquad M_X = \frac{B_X^2}{X} \tag{111.2}$$

Expanding the smoothed moment gives

$$\mathcal{M}_X(U,H) = HK_\pi(0)E_X + H\sum_{h\neq 0} R_X(h)K_{\pi,n}(h) \tag{111.3}$$

where

$$R_X(h) = \sum_n f_X(n)f_X(n+h) \tag{111.4}$$

and $K_{\pi,n}(h)$ retains the exact logarithm $H\log(1+h/n)$. The diagonal is the block quantity E_X, not the global E_r.

The recorded exponent calculations give

$$E_X = A_s^{2r}X^{-3/4+o(1)} \qquad A_s^{2r} = X^{1/2+o(1)} \tag{111.5}$$

No ℓ^1 localization at X has been proved. Positivity gives the sufficient inequality

$$B_X \leq \sum_n b_r(n) = A_s^r \tag{111.6}$$

Therefore

$$\boxed{\frac{E_X}{M_X} = \frac{E_X X}{B_X^2} \geq \frac{E_X X}{A_s^{2r}} = X^{1/4+o(1)}} \tag{111.7}$$

Equality is conditional on the separate localization $B_X = A_s^r X^{o(1)}$.

For the linearized divisor lattice put $u = q/L$. Poisson summation yields

$$\boxed{A^{\text{tot}}(u) = \frac{\pi}{u}\sum_{k\in\mathbb{Z}}[W(2\pi k/u-\pi) + W(2\pi k/u+\pi)]} \tag{111.8}$$

The off-diagonal action is

$$\boxed{A^{\times}(u) = A^{\text{tot}}(u) - K_\pi(0)} \tag{111.9}$$

Let

$$u_0 = \frac{2\pi}{\pi + 1} \qquad u_1 = \frac{2\pi}{\pi - 1} \tag{111.10}$$

For $0 < u < u_0$,

$$\boxed{A^{\text{tot}}(u) = 0 \qquad A^{\times}(u) = -K_\pi(0)} \tag{111.11}$$

Thus the engineered hole annihilates the total lattice action. It does not annihilate the $h \neq 0$ correlation by itself.

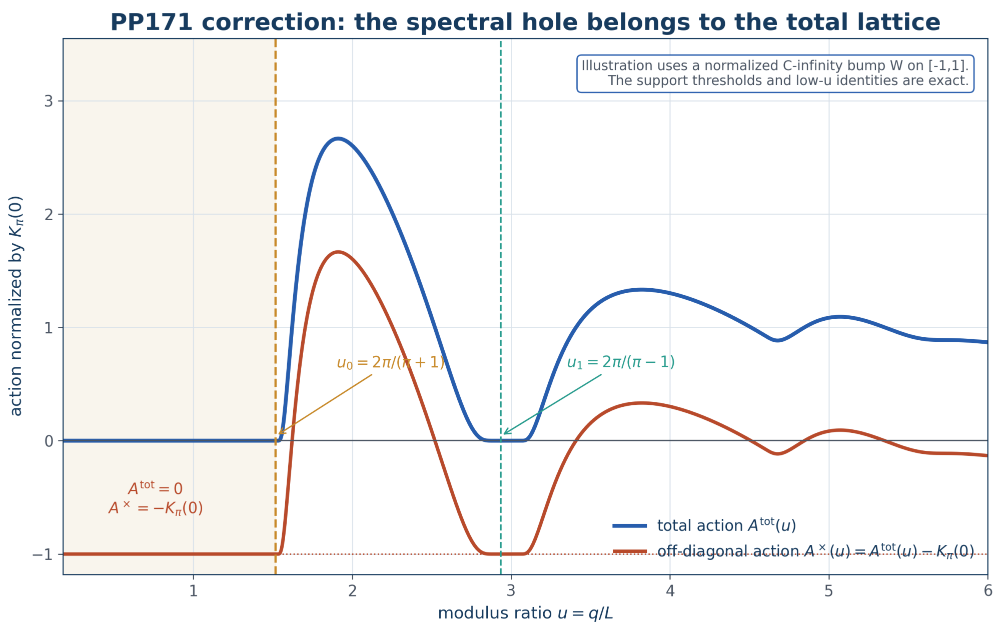

Figure 53: For a representative smooth nonnegative bump, the exact low-modulus identities and the distinction between total and off-diagonal actions are visible directly.

For $W \geq 0$, $A^{\text{tot}}(u) \geq 0$, while as $u \to \infty$,

$$A^{\text{tot}}(u) = K_\pi(0) + O_N(u^{-N}) \qquad A^{\times}(u) = O_N(u^{-N}) \tag{111.12}$$

The high-modulus diagonal channel can therefore reconstruct the explicit diagonal in total action while becoming invisible off diagonal.

112. The matched high-modulus channel and the large-sieve no-go

In the squarefree local specialization, the matched joint monomial has

$$[\alpha\gamma](L_{p,1} - L_{p,0}) = \frac{p-2}{p^2} \qquad [\alpha\gamma](L_{p,\infty} - L_{p,1}) = \frac{1}{p^2} \tag{112.1}$$

Their sum is the positive diagonal coefficient $(p-1)/p^2$. A matched prime is assigned modulus exponent one with relative probability $1-1/(p-1)$ and exponent two with relative probability $1/(p-1)$. Because

$$p = (\log X)^{4+o(1)} \qquad r \sim \frac{\log X}{4\log\log X} \qquad \sum_{j\le r} \frac{1}{p_j - 1} = o(1) \tag{112.2}$$

the positive matched squarefree local channel lies at

$$\boxed{q = \operatorname{rad}(n) = n = X^{1+o(1)} \qquad \frac{q}{L} = X^{3/11+o(1)}} \tag{112.3}$$

This is A for the local matched channel and only candidate A for a global extracted singular series. Other signed channels and their total variation are not controlled.

For prime $p \asymp L$, let

$$F_p(a) = \sum_{n\equiv a \pmod p} f_X(n) \qquad B^*_{X,p} = \sum_{(n,p)=1} f_X(n) \tag{112.4}$$

Character orthogonality gives exactly

$$\boxed{\sum_{a\in(\mathbb{Z}/p\mathbb{Z})^\times} \left| F_p(a) - \frac{B^*_{X,p}}{p-1} \right|^2 = \frac{1}{p-1} \sum_{\chi\ne\chi_0} \left| \sum_n f_X(n)\chi(n) \right|^2} \tag{112.5}$$

The classical multiplicative large sieve yields

$$\sum_{p\asymp L} \operatorname{Var}_p(f_X) \ll X^{o(1)} L E_X \tag{112.6}$$

The unsigned short-shift owner is

$$\mathcal{U}_X = L\frac{B_X^2}{X} = LM_X \tag{112.7}$$

The desired absolute allowance is

$$X^{-1/4}\mathcal{U}_X \tag{112.8}$$

Using inequality (111.7),

$$\frac{LE_X}{X^{-1/4}\mathcal{U}_X} = X^{1/4}\frac{E_X}{M_X} \geq X^{1/2+o(1)} \tag{112.9}$$

Theorem 112.1 (large-sieve normalization no-go). The classical blockwise character large sieve misses the kernel-tested short-shift target by at least $X^{1/2+o(1)}$. Equality in the exponent requires the unproved ℓ^1 block localization; failure of that localization only worsens the miss.

The additive identity itself is exact. With

$$F_X(\alpha) = \sum_n f_X(n)e(n\alpha) \qquad e(t) = e^{2\pi it} \tag{112.10}$$

one has

$$\boxed{\sum_h K_\pi(h/L)R_X(h) = \int_0^1 |F_X(\alpha)|^2 \sum_h K_\pi(h/L)e(-h\alpha)\,d\alpha} \tag{112.11}$$

For the Fourier convention

$$\mathcal{F}K(\xi) = \int_{\mathbb{R}} K(x)e^{-2\pi ix\xi}\,dx \tag{112.12}$$

$$\mathcal{F}K_\pi(\xi) = \pi\left[W(2\pi\xi-\pi) + W(2\pi\xi+\pi)\right] \tag{112.13}$$

Poisson summation therefore selects, modulo one, two windows centered at

$$\alpha = \pm\frac{1}{2L} \tag{112.14}$$

with half-width $1/(2\pi L)$. Controlling the energy in these windows after the correct diagonal/off-diagonal subtraction is the direct surviving branch owner.

129. Nonlinear logarithmic spectral-hole persistence

The exact short-shift kernel is evaluated at

$$H\log(1+h/n)$$

whereas the exact Poisson hole in Section 111 uses the linearized coordinate Hh/n. PP178 determines what finite-order nonlinearity does inside the factorized total-lattice model.

Let

$$\Phi_{H,v}(x) = H\log\left(1+\frac{x}{Hv}\right) \qquad 1\le v\le 2 \tag{129.1}$$

where v is the smooth dyadic n/X variable. Let ρ be smooth and supported in $[1,2]$, and let χ equal one near zero and be smoothly supported where $1+x/(Hv)$ stays uniformly positive. The factorized nonlinear total-lattice action is

$$\mathcal{A}_H^{\mathrm{tot}}(u) = \sum_{m\in\mathbb{Z}}\int_1^2 \rho(v)\chi(mu/H)K_\pi(\Phi_{H,v}(mu))\,dv \tag{129.1a}$$

This is not the coefficient-weighted correlation $R_X(h)$. For this section use the angular-frequency transform $\widehat{K}_{\mathrm{ang}}(\omega)=\int_{\mathbb{R}}K(x)e^{-i\omega x}dx$, so $\widehat{K}_{\mathrm{ang}}(\omega)=\mathcal{F}K(\omega/(2\pi))$ under (112.12). If $K=K_\pi$ is defined by (109.12), then

$$\operatorname{supp}\widehat{K}_{\mathrm{ang}} \subset [-\pi-1,-\pi+1]\cup[\pi-1,\pi+1] \tag{129.2}$$

Writing $y=x/v$, the cutoff composition through order three is

$$\chi(x/H)K(\Phi_{H,v}(x)) = \sum_{j=0}^{3} H^{-j}\mathcal{D}_jK(y) + \mathcal{R}_{4,H,v}(x) \tag{129.3}$$

with

$$\begin{aligned}
\mathcal{D}_0K(y) &= K(y)\\
\mathcal{D}_1K(y) &= -\frac{y^2}{2}K'(y)\\
\mathcal{D}_2K(y) &= \frac{y^3}{3}K'(y)+\frac{y^4}{8}K''(y)\\
\mathcal{D}_3K(y) &= -\frac{y^4}{4}K'(y)-\frac{y^5}{6}K''(y)-\frac{y^6}{48}K'''(y)
\end{aligned} \tag{129.4}$$

Every higher coefficient has the same form: a finite sum of polynomial multiples of derivatives of K. Polynomial multiplication and differentiation preserve Fourier support. Scaling by v replaces the bands by their contractions by $1/v$; smooth integration over $1\le v\le 2$ leaves the outer edge at $\pi+1$ and does not fill the central hole.

Here exact support belongs to the full jets $\mathcal{D}_jK(x/v)$, not to their products with $\chi(x/H)$. Replacing a cut-off jet by its full jet costs $O_{A,N}(H^{-A}(1+|x|)^{-N})$ for every A,N, because the difference is supported where $|x|\asymp H$ and every jet is Schwartz. This cutoff discrepancy is absorbed into $\mathcal{R}_{J,H,v}$ before Poisson summation.

Consequently, with

$$u_0=\frac{2\pi}{\pi+1}$$

Poisson summation annihilates every finite smeared jet for $0 < u < u_0$:

$$\boxed{\sum_{m\in\mathbb{Z}} \int_1^2 \rho(v)\mathcal{D}_j K(mu/v)\, dv = 0 \qquad (j \geq 0)} \tag{129.5}$$

A smooth dyadic cutoff therefore changes only the outer Schwartz tail. For every fixed J, N, after choosing the cutoff-tail order at least J, the combined composition-and-cutoff remainder satisfies

$$|\mathcal{R}_{J,H,v}(x)| \leq C_{J,N} H^{-J}(1 + |x|)^{-N} \tag{129.6}$$

uniformly for $v \in [1, 2]$. Since the lattice sum of the right side is $O_N(H^{-J}(1 + u^{-1}))$, PP178 gives

Theorem 129.1 (nonlinear persistence of the factorized total hole). For $0 < u < u_0$,

$$\boxed{\mathcal{A}_H^{\mathrm{tot}}(u) = O_J\Big(H^{-J}(1 + u^{-1})\Big)} \tag{129.7}$$

and, after removing the zero lattice point,

$$\boxed{\mathcal{A}_H^{\times}(u) = -K_\pi(0) \int_1^2 \rho(v)\, dv + O_J\Big(H^{-J}(1 + u^{-1})\Big)} \tag{129.8}$$

At the pilot, $u \geq L^{-1}$, $H = X^{3/11}$, and $L = X^{8/11}$. Keeping four jets gives

$$H^{-4}(1 + u^{-1}) \ll H^{-4}L = X^{-4/11} = X^{-1/4}X^{-5/44} \tag{129.9}$$

Thus truncation at $J = 4$ is the first one whose remainder clears the required relative power, with spare $X^{-5/44}$.

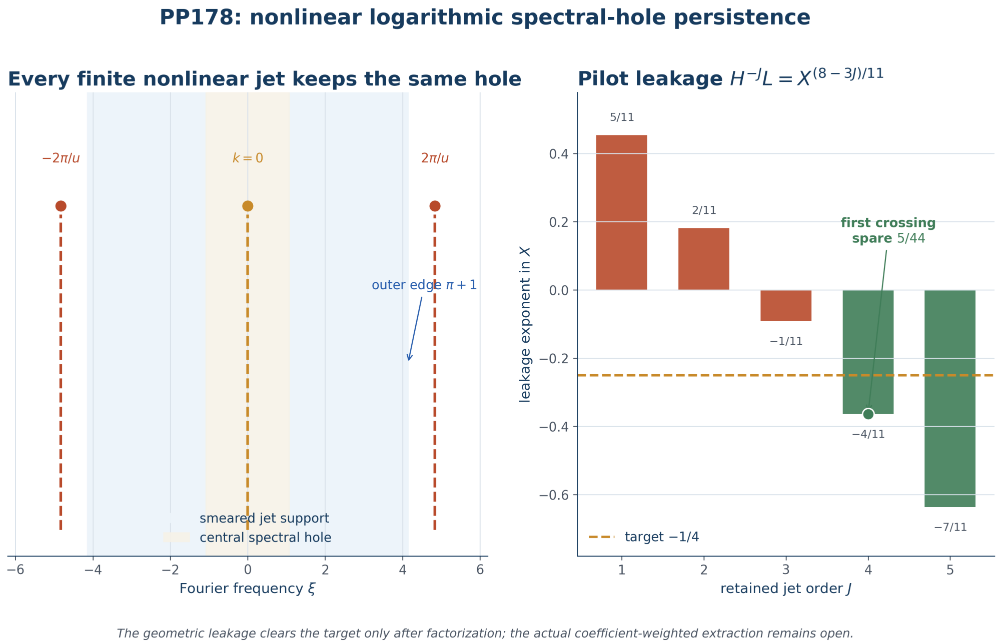

Figure 54: Every nonlinear logarithmic jet preserves the two Fourier bands; at the rational pilot, the fourth remainder is the first to cross below the target scale.

The scope is essential. Theorem 129.1 applies after factorization to the unweighted total lattice, with smooth v-smearing and a harmless dyadic cutoff. It does not replace $R_X(qm)$ by a constant, construct $c_X(q)$, or control the growing-order factorization error. It proves that finite-order kernel geometry is not the missing power. The surviving obstruction is strictly arithmetic transport and extraction.

113. The closure contract

The branch can advance only after the following conditions are met.

Arrow	Direction	Status	Missing uniformity or theorem
all-rank folded positivity $\leftrightarrow -\Theta'_\xi$ CM	equivalence	exact	none
$-\Theta'_\xi$ CM $\leftrightarrow$ one-point Hausdorff grid	equivalence	exact	none
full grid $\Rightarrow$ every moving shell	necessary	exact	converse not automatic
PP157–PP160 source region $\Rightarrow G_{n,k} > 0$ there	sufficient	proved	transition shell remains
$\Theta_x > 1/2 \Rightarrow$ transition-shell positivity	intended sufficient	partial	one uniform theorem must be mounted
additive-window saving $\Rightarrow$ return exclusion	conditional sufficient	branch-open	extraction, nonlinear kernel, and coefficient uniformity

Arrow	Direction	Status	Missing uniformity or theorem
return exclusion only at $c = 1/2 \Rightarrow \Theta_x > 1/2$	false without more	open	needs a c-neighborhood or stability theorem
transition-shell positivity $\Rightarrow$ full grid	conditional sufficient	open	all complementary regimes must be joined

Two owners must therefore remain named.

GLOBAL-OWNER. Prove all-order folded complete monotonicity, equivalently the complete one-point Hausdorff grid, by a positive source transport or another all-order source theorem.

BRANCH-OWNER. Construct the extracted finite-X object, or bypass it, and prove the kernel-tested selected-window saving

$$X^{-1/4+o(1)} \tag{113.1}$$

with the uniformity needed by the return problem.

The exact-diagonal map makes the needed neighborhood plausible but does not provide it. If the translated theorem held uniformly for

$$\frac{1}{2} \le c \le \frac{1}{2} + \varepsilon < c_{\mathrm{ED}}(11/3) \tag{113.2}$$

then returns through that coefficient interval would be excluded with a positive power margin, yielding a strict lower return exponent. A theorem only at $c = 1/2$ gives a boundary statement unless a quantitative stability lemma transports the $1/32$ margin to an interval.

Even after $\Theta_x > 1/2$, one final theorem must state that the return bound closes every cell in the transition shell and that Sections 105–106 cover the complement. Only then does (104.12) return the argument to the RH-facing criterion.

Conditional closure proposition 113.1. Assume:

1. the selected additive-window estimate holds uniformly on a nontrivial c-interval above $1/2$ at $\beta_0 = 11/3$;
2. continuous return exclusion transfers uniformly to the integer Postmaster saddles;
3. the resulting strict return exponent makes every transition-shell cell positive; and
4. the proved fixed-row, finite-prefix, and source regions cover all remaining cells.

Then the full grid is nonnegative, hence the complete-monotonicity criterion holds. None of assumptions 1, 3, or the complete coverage in 4 is proved in the present corpus.

This proposition records the proof contract. It is not an RH theorem.

External-normalization firewall

The symbol β in this branch is defined internally by

$$r = \frac{\beta \log T}{2s} \tag{113.3}$$

PP174 supplies a useful **partial internal dictionary**. The unique Montgomery–Vaughan error owner in (109.6)–(109.7) satisfies

$$\boxed{X = T^{\beta+o(1)} \qquad \beta = \frac{\log X}{\log T} + o(1)} \tag{113.4}$$

Thus β is the logarithmic length coordinate of the dominant $\theta = 1$ coefficient shell. This identifies the internal physical owner and explains the threshold 32/17 in Theorem 109.1.

It does **not** yet identify the full packet with every standard external length parameter. The distinction is theorem-level:

1. $D_s(t)^r$ is an infinite Gaussian-weighted Dirichlet series, whereas a published large-value theorem is normally stated for a hard block $N < n \leq 2N$;
2. passing from the global series to the block f_X requires quantitative ℓ^2 localization, and any ℓ^1 normalization remains separately open;
3. coefficient hypotheses such as $|b_n| \leq 1$, value normalization, spacing, and the relation between N and T must be checked theorem by theorem;
4. Guth–Maynard's condition $N \leq T^{5/6-\varepsilon}$ describes one regime where their new estimate improves earlier bounds. It is not a universal definition of a literature parameter α and does not prove that all large-value methods are irrelevant when $X > T$.

Accordingly, the firewall is narrow but remains necessary. No claim is made that Guth–Maynard barriers, density-hypothesis exponents, or their numerical improvements apply directly to (108.9). Conversely, the internal exact-diagonal geometry is not advertised as an improvement to those external records. The absence of 32/9 from a search is expected for an internal threshold, but is not itself a novelty theorem.

Guth–Maynard arXiv:2405.20552 must be read at v2 (7 April 2026), and Chen–Gupta–Li arXiv:2507.08296 at v2 (27 July 2026) proves the 7/3 zero-density exponent for Dirichlet L-functions by an adaptation of that method. These are current background inputs, not lemmas in the Postmaster proof.

Technical chapter XI. Finite Weil models and controlled limits

Finite dictionaries and positive cutoff tails have precise scope. Ground-state and joint-limit hypotheses needed for spectral recovery remain separate.

19. The actual-Weil ground-state criterion

Let A_λ represent the full global Weil form, with bottom eigenvalue ϵ_0, next eigenvalue ϵ_1, gap $\Delta_\lambda = \epsilon_1 - \epsilon_0$, and normalized proxy $v_\lambda = k_\lambda / \|k_\lambda\|_2$. Define the closed-form Rayleigh excess

$$r_\lambda = q_{A,\lambda}[v_\lambda] - \epsilon_0$$

If the bottom eigenvalue is simple, then

$$1 - |\langle v_\lambda, \phi_\lambda \rangle|^2 \leq \frac{r_\lambda}{\Delta_\lambda}$$

Because the proxy is even, $r_\lambda / \Delta_\lambda < 1$ forces the simple ground state to be even. A sufficient scale is

$$\boxed{\frac{\|k_\lambda\|_2^2 r_\lambda}{\Delta_\lambda} \leq C(1 - \chi_2(\lambda))}$$

Together with bottom simplicity, proxy convergence, the published real-zero theorem, and Hurwitz passage, this would imply RH. Bottom simplicity and the gap-normalized estimate are open.

Every fixed finite Li/Hankel/localizing suite can be passed by a synthetic off-line quartet. Therefore no fixed finite stopping point is an RH certificate.

44. Two-channel finite-Weil sampling

The coarse one-channel sampling cannot distinguish $y = \log n$ from $L - y$. The two-channel construction samples

$$T + kh \qquad \text{and} \qquad T + \left(k + \frac{1}{2}\right) h$$

or uses two polyphase classes on the fine lattice. The de-aliased prime frequency is

$$\frac{\pi \log n}{L}$$

Necessary attainable-weight constraints include

$$w_j \leq \frac{1}{2} \qquad \sum_{j \text{ even}} w_j = \sum_{j \text{ odd}} w_j = \frac{1}{2}$$

and, at the cubic endpoint,

$$\sum_j (-1)^j j^r w_j = 0 \qquad r = 0, 1, \ldots, 6$$

The construction has the following exact structure:

- seven-jet ownership $J_0, \ldots, J_6$;
- individual overlap order seven and operator endpoint order six;
- Newton/central-factorial coordinates;
- finite center/difference Weyl and Wigner identities;
- scoped deep-packet safety with the stated frequency normalization.

The open seats are sharp attainable-range characterization, multiplicative A_T/A_0 comparison, full edge recombination, and uniform bulk coercivity.

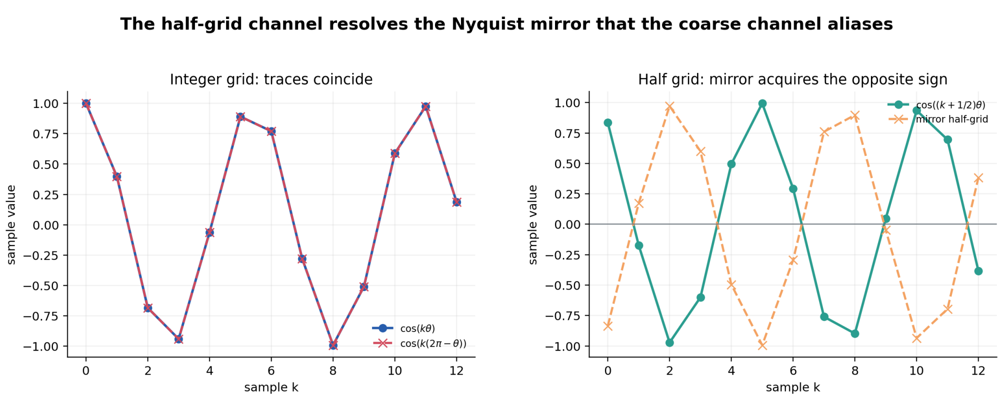

Figure 55: Integer-grid aliasing and its exact half-grid/polyphase separation.

123. Exact finite Guinand–Weil dictionary

This section restates and checks the fixed-rank theorem of Groskin arXiv:2607.02828v3. The attribution is load-bearing: no novelty claim is made for the external theorem. To avoid collision with this volume's Loewner order, write M for the external Galerkin band.

Fix $c > 1$ and put

$$L = \log c \qquad \Delta = \frac{L}{2\pi} \qquad \rho = \frac{2\pi}{L} \tag{123.1}$$

For $v = (v_0, \dots, v_M) \in \mathbb{R}^{M+1}$, use the isometric symmetric embedding

$$u_0 = v_0 \qquad u_k = u_{-k} = \frac{v_k}{\sqrt{2}} \quad (1 \le k \le M) \tag{123.2}$$

and define

$$T_v(t) = \sum_{m=-M}^{M} u_m e^{2\pi imt} \qquad K_v(\omega) = 2\int_0^{\omega} T_v(t)T_v(\omega - t)\,dt \tag{123.3}$$

The associated Fourier weight and test function are

$$\widehat{g}_v(\xi) = \begin{cases} \pi K_v(1 - |\xi|/\Delta), & |\xi| \le \Delta \\ 0, & |\xi| > \Delta \end{cases} \qquad g_v(z) = \int_{-\Delta}^{\Delta} \widehat{g}_v(\xi) e^{2\pi iz\xi}\,d\xi \tag{123.4}$$

The finite source calculus can be checked before invoking any explicit formula. For

$$\psi_{\alpha,\omega}(x) = \frac{\alpha}{\pi}\sin(2\pi\omega x)$$

the divided-difference matrix satisfies

$$\boxed{\langle v, Q_{\alpha,\omega} v\rangle = \alpha K_v(\omega)} \tag{123.5}$$

Indeed, the off-diagonal coefficient is

$$\alpha\frac{\sin(2\pi\omega m) - \sin(2\pi\omega n)}{\pi(m - n)}$$

the diagonal coefficient is $2\alpha\omega\cos(2\pi\omega m)$, and expansion of (123.3) reproduces both; the imaginary contributions cancel under $u_{-m} = u_m$. By linearity the source-to-form map factors through the exact $2M + 1$ coordinates

$$\int \omega\,d\mu \qquad \int \sin(2\pi k\omega)\,d\mu \qquad \int \omega\cos(2\pi k\omega)\,d\mu \quad (1 \le k \le M) \tag{123.6}$$

The entries $(0,0)$, $(k,0)$, and (k,k) recover these coordinates, proving that the quotient dimension is exact.

Theorem 123.1 (Groskin's finite dictionary, audited). For fixed $c > 1$, fixed $M \geq 0$, and every real even Galerkin vector v,

$$\boxed{\langle v, Q_\infty^{(c,M)} v\rangle = \sum_{z:\,\zeta(1/2+iz)=0} g_v(z)} \tag{123.7}$$

with multiplicity and absolute convergence.

The proof is the Guinand–Weil explicit formula applied to (123.4). Its Fourier support is $[-L/(2\pi), L/(2\pi)]$, so every prime power $q > c$ drops out exactly. The prime, pole, and archimedean terms are then precisely those of the fixed-(c, M) truncated matrix.

Three qualifications are part of the theorem statement in this volume.

1. The map is coefficient vector to test function. It does not realize an arbitrary Guinand–Weil test function.
2. The theorem is finite in M and fixed in c.
3. The zero sum ranges over the actual complex zero multiset. No reality of the parameters z and hence no RH assumption is used.

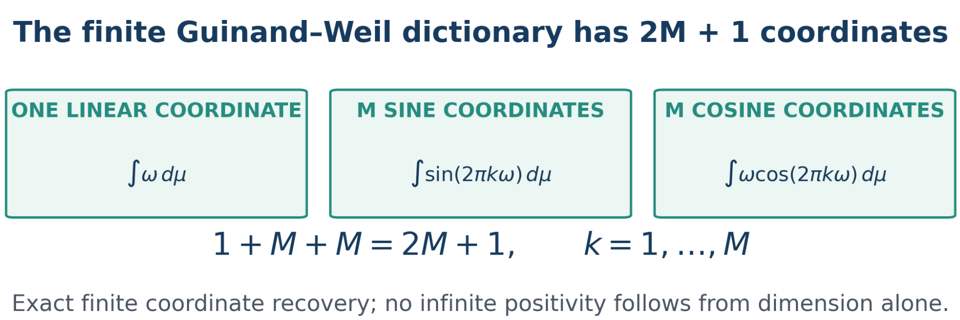

Figure 56: At finite band M, one linear coordinate and two families of M trigonometric coordinates give the exact $2M+1$-dimensional Guinand–Weil dictionary. Finite coordinate recovery is distinct from positivity of an infinite operator.

124. Positive archimedean tail and the cutoff certificate

For $T > \rho M$, put $a_T = T/\rho$ and, for $n \in I_M = \{-M, \ldots, M\}$,

$$p_T(n) = \frac{1}{a_T - n} \qquad q_T(n) = \frac{1}{a_T + n} \tag{124.1}$$

The algebraic hinge is

$$\frac{\dfrac{m}{a^2-m^2}-\dfrac{n}{a^2-n^2}}{m-n}=\frac{1}{2}\left(\frac{1}{(a-m)(a-n)}+\frac{1}{(a+m)(a+n)}\right) \tag{124.2}$$

with diagonal limit $(a^2+n^2)/(a^2-n^2)^2$. Direct integration of the true archimedean source gives at each integer node

$$\mathcal{S}(T,n,L)=\frac{2\sin^2(LT/2)}{\rho}\frac{n}{a_T^2-n^2} \tag{124.3}$$

and differentiation before node evaluation gives exactly the same diagonal limit. Thus the divided-difference matrix is formed from the true source, not merely an integer-node interpolant.

Set

$$h_+(T)=\Re\psi\left(\frac{1}{4}+\frac{iT}{2}\right)-\log\pi \tag{124.4}$$

Its derivative has the positive partial-fraction expansion

$$h_+'(T)=\frac{T}{2}\sum_{k=0}^{\infty}\frac{k+1/4}{((k+1/4)^2+(T/2)^2)^2}>0 \tag{124.5}$$

and $h_+(7)>0$.

Theorem 124.1 (Groskin's archimedean tail order, audited). If $T_2>T_1>\max(\rho M,7)$, then

$$\boxed{Q_{\mathrm{arch},T_2}-Q_{\mathrm{arch},T_1}=\frac{1}{\pi^2}\int_{T_1}^{T_2}h_+(T)\frac{\sin^2(LT/2)}{\rho}\left(p_Tp_T^{\mathsf{t}}+q_Tq_T^{\mathsf{t}}\right)dT} \tag{124.6}$$

The increment is positive definite, and every ordered minor in the natural node order is strictly positive.

Positive definiteness follows without a compactness guess. If a vector annihilates (124.6), the rational function $\sum_{n\in I_M}x_n/(a-n)$ vanishes on an interval. It therefore vanishes identically, and every residue x_n is zero. For ordered minors, the pushed measure lies on two intervals exterior to every node. Andreief's identity expresses a minor as an integral of two Cauchy determinants. Their signs depend on the same number of left-interval samples and cancel; positivity on open sets makes the minor strict.

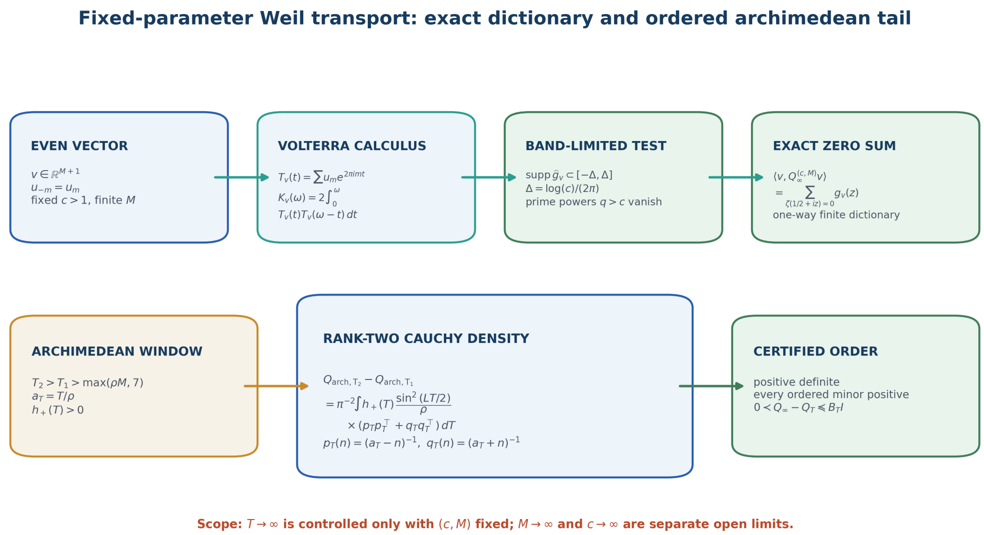

Figure 57: At fixed prime cutoff and Galerkin band, the coefficient vector has an exact zero-sum image and the omitted archimedean tail is an ordered integral of rank-two Cauchy Gram atoms.

For the total fixed-(c, M) matrix define

$$B_T = \frac{1}{\pi^2}\int_T^\infty h_+(r)\frac{\sin^2(Lr/2)}{\rho}\left(\|p_r\|_2^2 + \|q_r\|_2^2\right)dr \tag{124.7}$$

Then

$$0 \prec Q_\infty^{(c,M)} - Q_T^{(c,M)} \preceq B_T I \tag{124.8}$$

and hence

$$\lambda_j(Q_T) < \lambda_j(Q_\infty) \le \lambda_j(Q_T) + B_T \tag{124.9}$$

This produces the exact two-sided decision rule:

finite-T reading	cutoff-free conclusion at fixed (c, M)
$\lambda_j(Q_T) \ge 0$	$\lambda_j(Q_\infty) > 0$
$\lambda_j(Q_T) < -B_T$	$\lambda_j(Q_\infty) < 0$
$-B_T \le \lambda_j(Q_T) < 0$	inconclusive

For $M \ge 1$,

$$B_T \le \frac{2(2M+1)\rho}{\pi^2}\left[\frac{\log T}{T - \rho M} + \frac{1}{\rho M}\log\frac{T}{T - \rho M}\right] \tag{124.10}$$

and, at fixed (c, M),

$$B_T = \frac{(2M+1)\rho}{\pi^2 T}\left(\log\frac{T}{2\pi}+1\right)(1+o(1)) \tag{124.11}$$

At $(c, M, T) = (100, 200, 800)$, direct arithmetic gives

$$\begin{aligned} \rho M &= 272.875270768\ldots \\ \text{bound (124.10)} &= 1.5754527435\ldots \\ \text{leading (124.11)} &= 0.4051372811\ldots \end{aligned} \tag{124.12}$$

The sharper interval value reported by Groskin is not promoted because that ancillary certificate is not mounted here.

Three-limit firewall

The tail theorem removes exactly one regulator:

$$\boxed{T \to \infty \text{ at fixed } (c, M) \text{ is controlled} \qquad M \to \infty \text{ and } c \to \infty \text{ remain open}} \tag{124.13}$$

It does not answer the general one-dimensional Putinar interpolation question: it constructs one explicit positive Cauchy–Stieltjes tail rather than a universal moment-extension theorem. Nor does it prove this volume's all-order source inequality. The external M is a Fourier/Galerkin band, not the matrix order in Δ_N^{L}; moreover the external prime and pole blocks are not made positive by the archimedean increment.

125. Connes–Suzuki theorem and limit audit

The direct technical sources clarify why spectacular finite spectra do not yet form an RH proof.

object	established result	missing identification
Connes–van Suijlekom, Prop. 5.10	finite real-root polynomial under simple spectrum and a one-dimensional even kernel	applicability requires the kernel hypotheses
Connes–van Suijlekom, Thm. 6.1	$\widehat{\xi}$ has only real zeros when the lower-bounded operator has a simple isolated even ground state	those spectral hypotheses must be proved for the target Weil form
CCM, *Zeta Spectral Triples*	self-adjoint rank-one perturbations and high-accuracy finite spectra	simple/even ground state and a zero-carrying joint limit are explicitly missing
Suzuki, Thms. 1.3–1.5	continuity of λ_a; small-a simple even ground state; real zeros of $W(a, \theta; z)$	$a \to \infty$ recovery of zeta ordinates is conjectural
Groskin numerical v4	16-cutoff computation and reported 307–329-digit recovery at the largest cell	fixed-M bias and continuum limit are not bounded

CCM Section 8 states the two essential missing steps: prove that the localized Weil ground state is simple and even, then prove that the proposed k_λ approximates that eigenvector strongly enough to carry its zeros to the zeta-zero limit. This is the controlling statement, not the expository letter's inaccessible continuation.

Suzuki's finite/local results do not require RH. Spectral recovery remains a conjecture, and Section 7 is explicitly heuristic, begins by assuming RH, and introduces A_∞ only as a formal symbol. Real zeros of the finite characteristic function follow from self-adjointness; their identification with zeta zeros does not.

The high-precision numerical paper considered here is arXiv:2605.20224v4. It states that fixed-M Galerkin bias is not independently measurable, labels its classifier verdict intermediate, and makes no proof claim. At $T = 1200$, the $c = 100$ negative block rearranges rather than disappears. These computations do not bound the continuum limit.

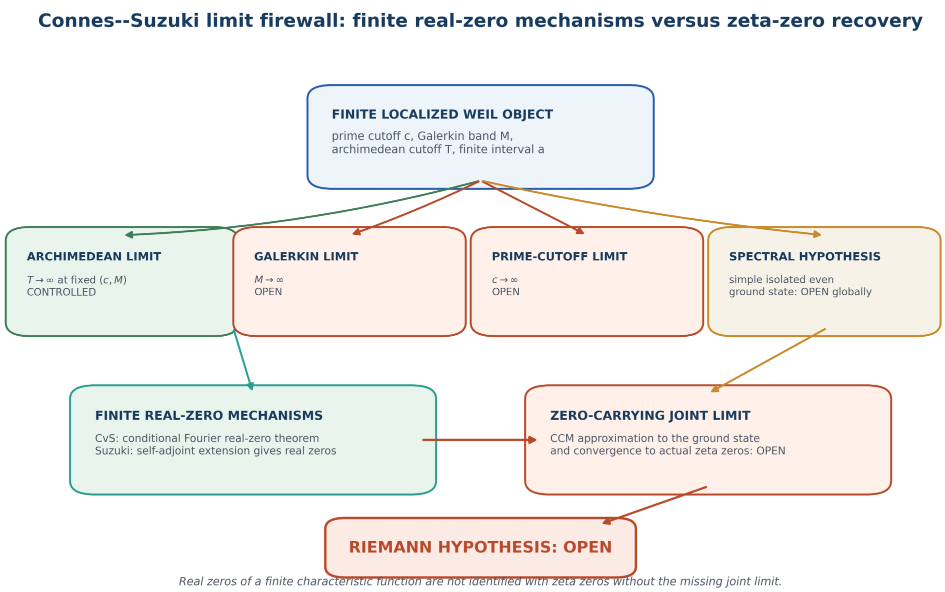

Figure 58: The finite Weil-form results close the archimedean cutoff at fixed parameters; simple-even control and the Galerkin/prime-cutoff limits remain distinct open bridges before any zeta-zero identification.

Technical chapter XII. Dilation, cyclic resolvents, and source carriers

Finite dilation complements fail a Stieltjes sign. The sharp dilation frontier and cyclic-resolvent theorem identify the full conditions, followed by source carrier formulas.

139. Universal finite-dyadic Stieltjes obstruction

Normalize

$$\mathscr{D}^N h(x) = \frac{x}{2^N R}\Phi(2^N s) \qquad B_N = h - \mathscr{D}^N h$$

and

$$G_N(z) = \frac{B_N(z)}{z} = \frac{1}{R}\left[\Phi(s) - 2^{-N}\Phi(2^N s)\right] \tag{139.1}$$

On the upper lip of the folded cut, write

$$z_v = -\frac{1+v^2}{4} + i0, \qquad R_+(z_v) = iv$$

Functional reflection gives the exact boundary identity

$$\boxed{\Im G_{N,+}(z_v) = \frac{2^{-N}}{v}\Re\Phi\Big(2^{N-1}(1+iv)\Big)} \tag{139.2}$$

The positive Ξ kernel proves $\Phi(\sigma) > 0$ for every real $\sigma > 1/2$. Hence the right side of (139.2) is positive for sufficiently small $v > 0$. A Stieltjes function must map the upper half-plane into the closed lower half-plane. Consequently

$$\boxed{\forall N \geq 1 : \quad G_N \text{ is not Stieltjes and } B_N \text{ is not complete Bernstein}} \tag{139.3}$$

This does not contradict preservation of the complete-Bernstein cone by $\mathscr{D}$: cone preservation by $\mathscr{D}$ does not make $I - \mathscr{D}^N$ positive.

The moving terminal has the exact triangular coordinate

$$s_N = 2^{N-1}, \qquad n_N = 2^{N-1} - 1 \qquad x_N = 2T_{2^{N-1}-1} \tag{139.4}$$

For six scales, $(s_6, n_6, x_6) = (32, 31, 992)$ and $992 = 2T_{31}$. The forbidden trace coefficient is

$$\lim_{v\downarrow 0} v\Im G_{N,+}(z_v) = 2^{-N}\Phi(2^{N-1}) > 0 \tag{139.5}$$

It tends to zero as $O(N2^{-N})$ but never vanishes at finite N. This is the precise finite/infinite boundary layer.

140. Holomorphy, positivity, and the surviving equivalence

Let $\Sigma = \mathbb{C} \setminus (-\infty, 0]$ with the principal square root. For every finite N, the terminal term $\Phi(2^N s)$ is Euler-safe on Σ and cannot cancel an off-cut pole of the first term. Therefore

$$\boxed{G_N \text{ holomorphic on } \Sigma \iff \text{RH}} \tag{140.1}$$

Equation (140.1) is an exact equivalence, not a resolution. PP190-IH proves that Stieltjes positivity is strictly stronger than this holomorphy statement for every finite block and fails unconditionally.

The joint conclusions are:

1. ranks through twelve can be certified at the fixed completed-source node;
2. no finite dyadic telescoping block can be the global CBF seed;
3. Gamma and prime contributions must couple before positivity is taken;
4. the required owner is infinite, nonlocal, or exactly completion-compensated.

The dilation and cyclic-resolvent theorems below refine the current proof map in Reading Volume §R24; their exact identities retain the all-order source obligation.

142. Dilation innovations, reflection, and no-gain gates

The following exact statements organize the sharp dilation frontier. The proof map in Reading Volume §R24 places their all-order quantifiers beside the completed source sign. Numerical cutoffs and proof grades are stated at their theorem owners.

142.1 Divisor-square inversion and innovation

The divisor-square carrier and its exact dyadic inversion are

$$D(s) = \frac{\zeta(s)^4}{\zeta(2s)}, \qquad J(s) = 4A(s) - 2A(2s)$$

$$\boxed{A(s) = \sum_{k\geq 0} 2^{-k-2} J(2^k s)} \tag{142.1}$$

The coefficient positivity and derivative-level convergence proved in the source package justify (142.1) in its stated half-plane. The normalized forward lift preserves the complete-Bernstein cone in its proved domain, but its inverse difference does not. For the completed innovation $k = h - \mathscr{D}_2 h$ the directed endpoint enclosure is

$$\boxed{-0.011543 < k'(0) < -0.011392 < 0} \tag{142.2}$$

The exact reconstruction

$$\boxed{h = \sum_{j\geq 0} \mathscr{D}_2^j k} \tag{142.3}$$

is convergent but signed. The finite Euler-prefix/counterterm and fixed prime-translation tests likewise fail. Thus a positive forward lift neither makes its difference positive nor licenses inversion of the cone.

142.2 PP190-T reflection, inertia, and no-gain gates

For a nonreal folded shell $q = |q|e^{i\theta}$, write

$$\frac{e^{i\theta/2}}{x+q} = A_x + iB_x$$

The conjugate pair contributes

$$\boxed{K_q(x,y) + K_{\bar{q}}(x,y) = 2|q|\big(A_x A_y - B_x B_y\big)} \tag{142.4}$$

This is the exact reflection/Krein difference of squares. Every nonreal folded pair has shell-local real signature $(1,1)$; inertia is invariant under invertible congruence, so no shell-local change of basis can turn that pair into a positive atom. The negative-channel contraction formulation is exact, but a Schur lift is a no-gain tautology unless the larger completed block is independently proved positive. The zero-tail member has both a certified negative direction and an independent positive b_0 direction and is therefore genuinely indefinite.

142.3 PP190-IH continuous strengthening

For every finite real $\lambda > 1$, put

$$G_\lambda^{(0)}(z) = \frac{1}{R(z)}\left[\Phi(s(z)) - \lambda^{-1}\Phi(\lambda s(z))\right]$$

The source package proves

$$\boxed{\lambda > 1 \Longrightarrow G_\lambda^{(0)} \text{ is not Stieltjes}} \tag{142.5}$$

The printed dyadic theorem is the specialization $\lambda = 2^N$. Independent positive-axis witnesses include $G_6^{(0)}(30) > G_6^{(0)}(12)$ and $(G_6^{(0)})'(12) > 0$. There is no contradiction with $B_6'(0) > 0$: the latter is a physical-axis derivative, whereas (142.5) is forced by the opposite orientation on the folded upper cut.

143. Exact Stieltjes and complete-Bernstein dilation frontier

Let

$$R(z) = \sqrt{1+4z}, \qquad s(z) = \frac{1+R(z)}{2}$$

$$S_\lambda(z) = \frac{\Phi(\lambda s(z))}{\lambda R(z)} \qquad T_\lambda(z) = zS_\lambda(z) \qquad \lambda > 0$$

and define the horizontal zero frontier

$$\beta_* = \sup_\rho \Re\rho$$

Theorem 143.1

For every $\lambda > 0$, the following are equivalent:

1. S_λ is a Stieltjes function;
2. T_λ is a complete Bernstein function;
3. S_λ is holomorphic on the principal slit plane;
4. $\lambda \geq 2\beta_*$.

Consequently,

$$\boxed{\{\lambda > 0 : T_\lambda \in \mathrm{CBF}\} = [2\beta_*, \infty)} \tag{143.1}$$

Proof. Write $\Xi(w) = \xi(1/2 + w)$ and retain each reflected zero pair. The genus-zero paired logarithmic derivative is

$$\Phi(1/2 + w) = \sum_{\{\pm\alpha\}} m_\alpha \left(\frac{1}{w-\alpha} + \frac{1}{w+\alpha} \right) \tag{143.2}$$

Here m_α is the multiplicity of the paired zeros. The pairing is essential: each paired summand is $O(|\alpha|^{-2})$, while the two separated reciprocal-zero series need not converge absolutely. If $\Re\sigma > \beta_*$, both reflected denominators in (143.2) have positive real part, so $\Re\Phi(\sigma + it) > 0$.

For $\lambda > 2\beta_*$ the principal upper half-plane maps strictly into that positive half-plane. On the upper folded lip,

$$\Im S_{\lambda,+}(-r) = -\frac{\Re\Phi\Big(\frac{\lambda}{2}(1 + i\sqrt{4r-1})\Big)}{\lambda\sqrt{4r-1}} < 0 \tag{143.3}$$

The keyhole maximum principle then gives the Stieltjes property. Locally uniform closure gives the endpoint $\lambda = 2\beta_*$.

For necessity, if $\rho = \beta + i\gamma$ and $\lambda s(z_\rho) = \rho$, then

$$z_\rho = \frac{\rho(\rho-\lambda)}{\lambda^2} \qquad \Im z_\rho = \frac{\gamma(2\beta-\lambda)}{\lambda^2} \tag{143.4}$$

If $\beta > \lambda/2$, the pole lies in the principal upper half-plane. Whenever $\lambda < 2\beta_*$ such a zero exists, contradicting slit-plane holomorphy. The standard Stieltjes/complete-Bernstein quotient equivalence finishes the proof. □

The source-normalized density is

$$\boxed{\omega_\lambda(r) = \frac{\Re\Phi\Big(\frac{\lambda}{2}(1 + i\sqrt{4r-1})\Big)}{\pi\lambda\sqrt{4r-1}}} \tag{143.5}$$

In the strict range,

$$S_\lambda(x) = \int_{1/4}^{\infty} \frac{\omega_\lambda(r)}{x+r}\,dr \qquad \omega_\lambda(r) > 0 \tag{143.6}$$

At the frontier, a zero of multiplicity m at $\rho = \lambda/2 + i\gamma$ maps to

$$r_\rho = \frac{1}{4} + \frac{\gamma^2}{\lambda^2}$$

and contributes the positive atom

$$\boxed{\frac{m/\lambda^2}{x + r_\rho}} \tag{143.7}$$

The exact RH implication chain is therefore

$$\boxed{\begin{aligned} \mathrm{RH} \iff{} & \beta_* = \frac{1}{2} \\ \iff{} & \inf\{\lambda : T_\lambda \in \mathrm{CBF}\} = 1 \\ \iff{} & T_\lambda \in \mathrm{CBF} \quad (\lambda > 1) \\ \iff{} & T_{\lambda_j} \in \mathrm{CBF} \quad \text{for some } \lambda_j \downarrow 1 \end{aligned}} \tag{143.8}$$

Unconditionally, the frontier lies in $[1, 2]$, T_2 is complete Bernstein, and every $\lambda > 2$ lies in the strict range. No sequence approaching 1 has been forced independently of RH.

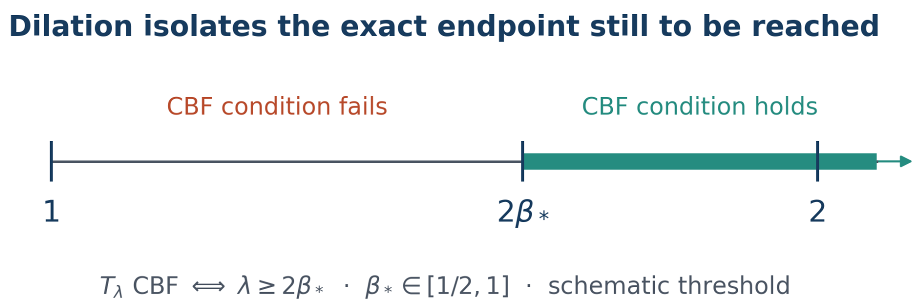

Figure 59: The exact dilation threshold is $\lambda = 2\beta_*$, where $\beta_* = \sup_\rho \Re\rho$. A CBF sequence with $\lambda_j \downarrow 1$ forces $\beta_* = 1/2$. The axis is schematic: the threshold value itself remains unknown.

144. Origin dilation and critical-line-centered dilation

Dilation about the origin and dilation about the critical-line center have different pole geometry. Keep their basepoints explicit.

144.1 Origin-dilation complement

Define

$$T_\lambda^{(0)}(z) = \frac{z}{\lambda R(z)} \Phi(\lambda s(z)) \qquad B_\lambda^{(0)} = h - T_\lambda^{(0)} \tag{144.1}$$

On $\Omega = \mathbb{C} \setminus (-\infty, -1/4]$,

$$\boxed{B_\lambda^{(0)} \text{ is holomorphic on } \Omega \iff \begin{cases} \text{false}, & 0 < \lambda < 1 \\ \text{true}, & \lambda = 1 \\ \text{RH}, & \lambda > 1 \end{cases}} \tag{144.2}$$

For $0 < \lambda < 1$, every zero with $\Re\rho \geq 1/2$ produces a terminal preimage at $s = \rho/\lambda$ in the principal domain. Cancellation would force an outward zero orbit and eventually leave the critical strip. At $\lambda = 1$, $B_1^{(0)} = 0$. For $\lambda > 1$, RH moves both relevant pole families off the principal domain or onto the removed cut; conversely, an off-line zero would require the impossible outward orbit $\rho, \lambda\rho, \lambda^2\rho, \ldots$.

For $\lambda \geq 2$, the terminal is Euler-safe throughout the principal domain. For every $\lambda > 1$, the positive source value near the cut endpoint gives the wrong Stieltjes orientation. For $0 < \lambda < 1$, the orientation reverses but the terminal poles enter the domain. This is the origin-dilation dichotomy. It does not settle arbitrary positive continuous mixtures, whose moving singularity curves may collide and require a separate analysis.

144.2 Critical-line-centered complement

Define instead

$$\widetilde{T}_\lambda(z) = \frac{z}{\lambda R(z)}\Phi\left(\frac{1}{2} + \lambda\left(s(z) - \frac{1}{2}\right)\right) \qquad \widetilde{B}_\lambda = h - \widetilde{T}_\lambda \tag{144.3}$$

The upper folded lip stays on the critical line for every $\lambda > 0$. Hence the terminal cut contribution has zero imaginary part. The precise holomorphy theorem is

$$\boxed{\widetilde{B}_1 = 0, \qquad \widetilde{B}_\lambda \text{ holomorphic on } \Omega \iff \text{RH} \quad (\lambda \neq 1)} \tag{144.4}$$

To see the converse, write each zero as $\rho = 1/2 + \alpha$. Holomorphic cancellation for $\lambda \neq 1$ would make the nonreal zero multiset invariant under scaling $\alpha \mapsto \lambda\alpha$. If $\lambda > 1$, the orbit leaves the critical strip; if $0 < \lambda < 1$, the orbit accumulates at $\alpha = 0$, impossible for the discrete zero set. Under RH, every centered preimage remains on the removed cut.

Equation (144.4) gives the centered-dilation geometry but supplies no forcing sign. The same critical-line reality that removes the cut obstruction also removes the boundary leverage.

145. Cyclic resolvents and finite visibility of every off-line shell

Let $q_\rho = \rho(1-\rho)$, combine equal folded shells with multiplicity M_q, and write

$$h(x) = \sum_q M_q \frac{x}{x+q} \qquad L_h(x,y) = \sum_q M_q \frac{q}{(x+q)(y+q)} \tag{145.1}$$

On the weighted shell space

$$\mathscr{K} = \ell^2(\mathcal{Q}, M_q|q|) \qquad r_x(q) = \frac{1}{x+q} \tag{145.2}$$

the positive-node resolvents are cyclic.

Theorem 145.1

For every nonempty open interval $I \subset (0,\infty)$,

$$\boxed{\overline{\operatorname{span}_{\mathbb{C}}\{r_x : x \in I\}} = \mathscr{K}} \tag{145.3}$$

Proof. If $a \in \mathscr{K}$ is orthogonal to every r_x, then the meromorphic Cauchy transform

$$F_a(z) = \sum_q \frac{M_q|q|\overline{a(q)}}{z+q} \tag{145.4}$$

vanishes on I. Normal convergence gives a meromorphic function on the complement of its poles. The identity theorem and the residues at $z = -q$ force every coordinate of a to vanish.

Conjugation symmetrization gives the corresponding real totality statement. □

If $q_0 \notin \mathbb{R}$, choose a conjugation-real vector supported on $q_0, \bar{q}_0$ whose phase makes

$$\mathcal{E}(f) = \sum_q M_q q f(q)^2$$

strictly negative. Approximation by (145.3) then yields

$$\boxed{\begin{array}{c}\text{RH false} \Longrightarrow \\ \text{a negative finite ordinary Löwner witness exists} \\ \text{inside every positive node interval}\end{array}} \tag{145.5}$$

At any fixed $x_0 > 0$, the powers $(x_0 + q)^{-k-1}$ are likewise total: orthogonality makes every derivative of (145.4) vanish at x_0. Therefore

$$\boxed{\text{RH false} \Longrightarrow \forall x_0 > 0\ \exists N < \infty : \mathfrak{D}_N(h; x_0) \not\succeq 0} \tag{145.6}$$

There is no rank bound in (145.5)–(145.6). Positive rank-nine, rank-eleven, rank-twelve, and fifth-rung point certificates are fully compatible with a later finite failure.

For a fixed finite node set X and a safe terminal,

$$L_{h-T_\lambda}(X) = L_h(X) - L_{T_\lambda}(X) \qquad L_{T_\lambda}(X) \succ 0$$

while $L_{T_\lambda}(X) \to 0$ as $\lambda \to \infty$. Hence

$$\boxed{\exists \lambda \geq 2 : L_{h-T_\lambda}(X) \succeq 0 \iff L_h(X) \succ 0} \tag{145.7}$$

The identical statement holds for a fixed confluent block. This rank-adaptive complement is a strictness reformulation, not an escape from the global gate.

Combining the inherited one-point theorem with (143.8) and (145.3) gives the exact implication chain

$$\boxed{\begin{aligned} \text{RH} &\iff h \text{ is complete Bernstein} \\ &\iff L_h(X) \succeq 0 \quad \text{for every finite positive } X \\ &\iff \mathfrak{D}_N(h; x_0) \succeq 0 \quad \text{for all } N \text{ at any one prescribed } x_0 > 0 \\ &\iff T_{\lambda_j} \in \text{CBF} \quad \text{for some } \lambda_j \downarrow 1 \end{aligned}} \tag{145.8}$$

None of the arrows in (145.8) supplies the missing premise.

146. All-rank probability and common-carrier identities

At a fixed $x_0 > 0$, let

$$b_n(x_0) = x_0^n \frac{(-1)^n}{(n+1)!} h^{(n+1)}(x_0)$$

Taylor's theorem gives the exact all-rank generating function

$$\boxed{\sum_{n\geq 0} b_n(x_0) z^{n+1} = \frac{h(x_0) - h(x_0(1-z))}{x_0}} \tag{146.1}$$

At $x_0 = 56$,

$$R(z) = \sqrt{225 - 224z} \qquad s(z) = \frac{1 + R(z)}{2}$$

$$\boxed{H_{56}(z) = \frac{\Phi(8)}{15} - (1-z)\frac{\Phi(s(z))}{R(z)}} \tag{146.2}$$

The terminal exponential has probability generating function

$$\boxed{\Pi_t(z) = \frac{1}{R(z)} \exp\left[-\frac{R(z)-1}{2}t\right] = \sum_{n\geq 0} \pi_n(t) z^n \qquad \Pi_t(1) = 1} \tag{146.3}$$

Let $\beta_k(t)$ be the PP189 source polynomials in their controlling normalization. Coefficient extraction from $(1-z)\Pi_t(z)$ gives, for every $k \geq 0$,

$$\boxed{e^{-8t}\beta_k(t) = e^{-t}\big(\pi_{k+1}(t) - \pi_k(t)\big)} \tag{146.4}$$

The exact replay reconstructs (146.4) through β_{23}, including the degree-23 controlling range. With

$$\alpha = \frac{224}{225} \qquad c = \frac{15t}{2}$$

$$\pi_n(t) = \frac{e^{-7t}}{15} \frac{\alpha^n}{2^n n!} \theta_n(c) \qquad \theta_n = (2n-1)\theta_{n-1} + c^2\theta_{n-2} \tag{146.5}$$

The Bessel recurrence is the analytic return of the same quadratic Jacobian used in §R1 and technical §34. For $x > 0$ and $t \geq 0$, put $K_t(x) = e^{-ts(x)}/R(x)$, with $s(x) = (1 + R(x))/2$. Then

$$\boxed{(-1)^r D_x^r K_t(x) = \frac{2^r e^{-ts(x)}}{R(x)^{2r+1}} \theta_r\left(\frac{tR(x)}{2}\right), \qquad r \geq 0} \tag{146.5a}$$

For completeness its polynomial normalization is

$$\theta_r(v) = \sum_{j=0}^{r} \frac{(2r-j)!}{2^{r-j}(r-j)!j!} v^j \qquad \theta_{r+1} = (v+2r+1)\theta_r - v\theta_r' \tag{146.5b}$$

The last identity follows by coefficient comparison. Since $D_x R = 2/R$ and $D_x(tR/2) = t/R$, differentiating (146.5a) gives exactly (146.5b), proving (146.5a) by induction from $r = 0$. The same coefficients give $\theta_{r+1} = (2r+1)\theta_r + v^2\theta_{r-1}$ for $r \geq 1$, which is the shifted recurrence in (146.5). Finally $\Pi_t(z) = e^t K_t(x_0(1-z))$; Taylor extraction at $x_0 = 56$ recovers the coefficient formula in (146.5), including every scale factor.

All coefficients of θ_r are positive, so K_t is completely monotone. The multiplication by x in the completed source must still be carried through:

$$\frac{d}{dx}[xK_t(x)] = \frac{e^{-ts(x)}}{R(x)^3}\bigl(1 + 2x - txR(x)\bigr) \tag{146.5c}$$

For fixed $x > 0$ this changes sign as t increases. The exact root-to-derivative connection therefore preserves the source problem: positivity of the elementary kernel does not prove the completed matrix sign.

The ratio recurrence proves that each β_{n-1} has exactly one positive zero. Individual prime cells therefore change sign; completion, not atomwise positivity, remains necessary.

The same law has the mixed-Poisson density

$$\boxed{f_t(\ell) = \frac{e^{t/2}}{2\sqrt{\pi x_0 \ell}} \exp\left[-\frac{\ell}{4x_0} - \frac{x_0 t^2}{4\ell}\right] \qquad t \geq 0} \tag{146.6}$$

At $x_0 = 56$,

$$\mathbb{E}_t N = 56(t+2) \qquad \mathrm{Var}_t\, N = 6328t + 25200 \tag{146.7}$$

The endpoint estimates at $\ell = 0$ justify the Rodrigues formula at $t = 0$ as well as $t > 0$:

$$(-1)^r \Delta^{r+1}\pi_n(t) = \frac{(-1)^r}{(n+r+1)!} \int_0^\infty e^{-\ell} \ell^{n+r+1} f_t^{(r+1)}(\ell)\, d\ell \tag{146.8}$$

For

$$u_a(x) = \frac{x}{R(x)} e^{-s(x)a} \qquad K_{n,r}(a) = G_{n,r}[-u_a](x_0)$$

local uniform derivative bounds justify every finite differentiation, difference, Gamma integral, and prime sum. Thus for each fixed finite (n,r),

$$\boxed{\begin{aligned} G_{n,r}[h](x_0) = &-a_\Gamma K_{n,r}(0) \\ &+ \int_0^\infty \frac{K_{n,r}(a) - e^{-a/2} K_{n,r}(0)}{1 - e^{-2a}}\, da \\ &+ \sum_{m \geq 2} \Lambda(m) K_{n,r}(\log m) \end{aligned}} \tag{146.9}$$

where $a_\Gamma = [\psi(1/4) - \log \pi]/2$ is the same scalar anchor as in §154. The local estimates depend on (n, r); (146.9) is not uniform in rank.

Finally, put

$$H_R(t) = [\beta_{i+j}(t)]_{i,j=0}^{R-1} \quad A = \frac{56}{15} \quad D_R(t) = \operatorname{diag}(1, At, \ldots, (At)^{R-1})$$

The exact leading coefficient gives

$$\boxed{\frac{15}{At} D_R(t)^{-1} H_R(t) D_R(t)^{-1} = M_R + O_R(t^{-1}) \qquad M_R = \left[\frac{1}{(i+j+1)!}\right]} \tag{146.10}$$

Since M_R is nonsingular with alternating $LDL^\intercal$ pivots,

$$\boxed{\operatorname{inertia} H_R(t) = \left(\left\lceil \frac{R}{2} \right\rceil, \left\lfloor \frac{R}{2} \right\rfloor, 0\right)} \tag{146.11}$$

for every fixed $R \geq 2$ and all sufficiently large t. Rank one is eventually positive. No effective or rank-uniform threshold is asserted.

147. Exact carrier weights and finite-anchor map

The raw Groskin jump readout is

$$\boxed{-\frac{u}{2d^2} \langle J_N, dM_N(u) \rangle_F = \sum_q \Lambda(q) q^{-1/2} \delta_{\log q}(du)} \tag{147.1}$$

Because $u_a = e^{-a/2} \kappa(\cdot, a)$, evaluation at $a = \log q$ absorbs the second square-root weight. At the one-point cell,

$$\boxed{\sum_q \Lambda(q) K_{n,r}(\log q) = \sum_q \frac{\Lambda(q)}{q} (-1)^r \Delta^{r+1} \pi_n(\log q)} \tag{147.2}$$

Equations (147.1)–(147.2) are exact arithmetic transport. The response matrix is already indefinite at $q = 2$ on the tested node pair; therefore the map is not a positive congruence and does not prove $L_\Gamma - L_P \succeq 0$.

The finite anchors now have the following exact grades:

anchor	certified statement	authority boundary
local rank 9, $x = 56$	$\mathfrak{B}_9^{\mathrm{conf}}[h; 56] \succ 0$; dyadic complement first becomes positive at depth $N = 79$ with final pivot $1.5436100114 \ldots \times 10^{-27}$	one basepoint; minimal only in that dyadic family
local rank 11, $x = 56$	directed confluent certificate	one basepoint
local rank 12, $x = 56$	controlling PP190-T certificate with (138.2)	one basepoint and one manifest-bound cutoff/tail proof
fifth rung, $x = 90$	$W_5(90) = 3.2334949506154321 \ldots \times 10^{-8} > 0$	this anchor is one point; global zero-assisted positivity is in Reading Volume §R13, while the independent source proof remains open
Connes–CvS $c = 100$ cell	current package rebuilds the 501×501 cell, selected positive value, ten recovery checks, and a directed normalized residual $\leq 9.1042746997704021 \ldots \times 10^{-501}$	exact supplied finite dyadic matrix only

The Connes–CvS bound is the normalized quantity

$$\boxed{\operatorname{dist}(\widehat{\lambda}, \sigma(A)) \leq \frac{\|Av - \widehat{\lambda}v\|_2}{\|v\|_2} \leq 9.1042746997704021 \ldots \times 10^{-501}} \tag{147.3}$$

The implementation encloses $\|v\|_2^2$ from below before division, so the certificate controls the normalized residual. The eleven preceding negative values are nondirected branch diagnostics; a directed inertia or branch-minimality certificate is not included.

Technical chapter XIII. Completion forms, reflection contours, and realization limits

Positive auxiliary forms are compared with the actual Gamma-minus-prime form. Reflection, conjugation and the topology of a proposed realization remain explicit.

103. Why the source problem becomes cancellation-first

The PP146–PP150 corridor closes a family of natural positive transports. It does not close all conceivable transports.

103.1 The Mills calibration and the Stieltjes-cone obstruction

The normalized Mills owner

$$G_M(x) = \frac{m(\sqrt{x})}{\sqrt{x}}$$

is the Stieltjes transform of the χ_1^2 probability measure

$$d\mu_M(t) = \frac{e^{-t/2}}{\sqrt{2\pi t}}\,dt \tag{103.1}$$

Its moments and Hankel determinants are

$$\mu_n = (2n-1)!!, \qquad \Delta_N = \prod_{j=0}^{N-1}(2j)! \qquad \Delta_N^{(1)} = \prod_{j=0}^{N-1}(2j+1)! \tag{103.2}$$

By contrast, one folded prime atom with log-frequency $a > 0$ is

$$p_a(x) = \frac{e^{-as(x)}}{R(x)} \qquad R(x) = \sqrt{1+4x} \qquad s(x) = \frac{1+R(x)}{2} \tag{103.3}$$

Its inverse Laplace density is

$$\kappa_a(u) = \frac{1}{2\sqrt{\pi u}} \exp\left[-\frac{(u+a)^2}{4u}\right] \tag{103.4}$$

This density is positive, so p_a is completely monotone. But

$$\frac{d}{du} \log \kappa_a(u) = -\frac{1}{2u} - \frac{1}{4} + \frac{a^2}{4u^2} \tag{103.5}$$

is positive near $u = 0$. Thus κ_a is not completely monotone and p_a is not Stieltjes. Positive mixtures or subordinations that remain inside the Stieltjes heat cone cannot map the Mills model to even one prime atom.

103.2 The triangular operator explains grading, not positivity

In Bargmann–Fock coordinates, with $N = zD_z$,

$$\mathcal{T} = \frac{1}{2}N(N+1) \qquad 2\mathcal{T} + \frac{1}{4}I = \left(N + \frac{1}{2}\right)^2 \tag{103.6}$$

The inverse on the zero-constant sector has the exact Beta representation

$$\mathcal{T}^{-1} f(z) = 2\int_0^1 \frac{1-t}{t} f(tz)\, dt \qquad \frac{1}{T_{k+1}} = \int_0^1 t^k\, 2(1-t)\, dt \tag{103.7}$$

This is a positive Hausdorff multiplier. The forward multiplier is not a moment or Löwner positivity preserver: applying T_{k+1} to the Hausdorff sequence $1, 1, 1, \ldots$ gives $1, 3, 6, \ldots$ and

$$\det \begin{pmatrix} 1 & 3 \\ 3 & 6 \end{pmatrix} = -3 \tag{103.8}$$

Because $\mathcal{T}$ and $\mathcal{T}^{-1}$ are functions of N, they commute with every mod-4 projector. They explain the residue grading but cannot supply the missing channel-changing positive operator.

103.3 One folded atom is not the matrix owner

For a prime log-atom $y > 0$, define

$$h_y(x) = \frac{x}{R} e^{-sy}$$

Exact differentiation gives

$$h_y'(x) = e^{-sy} \left[\frac{R^2+1}{2R^3} - \frac{xy}{R^2}\right] \tag{103.9}$$

Hence $h_y'(x) \geq 0$ precisely when

$$y \leq \eta(R) = \frac{2(R^2+1)}{R(R^2-1)} \tag{103.10}$$

At $R = 4$, $\eta(4) = 17/30 < \log 2$. Every prime atom is therefore decreasing for $x \geq 15/4$. Prime-atom PSD cannot be the full source mechanism.

Finally, the completed heat matrix has the cancellation-first identity

$$D_N H_N(x) D_N = \int_0^\infty e^{-xu}\Theta_\xi(u) E_N(u) K_N(xu) E_N(u)\, du \tag{103.11}$$

Here $H_N = [h^{(a+b+1)}/(a+b+1)!]_{a,b=0}^{N-1}$, $D_N = \operatorname{diag}((-1)^a)$, and $E_N(u) = \operatorname{diag}(u^a)_{a=0}^{N-1}$. The pencil is

$$K_N(t)_{ab} = \frac{1}{(a+b)!} - \frac{t}{(a+b+1)!} \qquad 0 \leq a, b < N \tag{103.12}$$

The constant heat mode cancels only after the completed integral is formed. The pencil itself is indefinite for every $N \geq 2$: for $N = 2m$ its inertia is $(m, m, 0)$ for $t \geq 0$; for $N = 2m+1$ there is one real crossing and otherwise both signs remain. Therefore the proof cannot be pointwise PSD. The owner is signed cancellation across the completed Gamma and prime components.

157. The endpoint-subtracted Beta–log Gram bridge

The Montgomery–Vaughan video factor is

$$J_y(\delta) = \int_0^y e^{2\pi i\delta x}\, dx = \frac{e^{2\pi i\delta y} - 1}{2\pi i\delta} \qquad J_y(0) = y \tag{157.1}$$

The terminal -1 is the lower-endpoint subtraction. It removes the apparent diagonal singularity and installs the derivative value y. Equivalently,

$$\boxed{J_y(\delta) = y\, e^{\pi i\delta y}\operatorname{sinc}(\delta y), \qquad \operatorname{sinc}(u) = \frac{\sin \pi u}{\pi u}} \tag{157.2}$$

For $L_n = \log n$ and $F(x) = \sum_n a_n e^{2\pi i L_n x}$,

$$0 \leq \int_0^1 \int_0^y |F(x)|^2\, dx\, dy = \int_0^1 (1-u)|F(u)|^2\, du \tag{157.3}$$

After normalization, the owner is the probability measure

$$\boxed{d\nu_\triangle(u) = 2(1-u)\, du, \qquad 0 \leq u \leq 1} \tag{157.4}$$

It simultaneously owns the reciprocal-triangular moments

$$\int_0^1 u^k \, d\nu_\triangle(u) = \frac{2}{(k+1)(k+2)} = \frac{1}{T_{k+1}} \tag{157.5}$$

and the log-character Gram kernel

$$\boxed{\begin{aligned}\mathcal{B}(\delta) &= \int_0^1 e^{2\pi i\delta u} \, d\nu_\triangle(u) \\ &= \frac{2(1+ic-e^{ic})}{c^2} \qquad c = 2\pi\delta, \qquad \mathcal{B}(0) = 1\end{aligned}} \tag{157.6}$$

Its real part is

$$\Re\mathcal{B}(\delta) = \left(\frac{\sin \pi\delta}{\pi\delta}\right)^2 = \operatorname{sinc}^2(\delta) \geq 0 \tag{157.7}$$

With the inner product conjugate-linear in its first slot, for any finite frequency set,

$$B_{mn} = \mathcal{B}(L_n - L_m) = \langle e^{2\pi i L_m u}, e^{2\pi i L_n u} \rangle_{L^2(\nu_\triangle)} \tag{157.8}$$

is Hermitian positive semidefinite. Monomials and log characters may be placed in the same Gram space, producing the positive block

$$\begin{bmatrix} [\langle u^i, u^j \rangle] & [\langle u^i, e^{2\pi i L_n u} \rangle] \\ [\langle e^{2\pi i L_m u}, u^j \rangle] & [\mathcal{B}(L_n - L_m)] \end{bmatrix} \succeq 0 \tag{157.9}$$

This is a genuine source-side sesquilinear form. It is not yet the missing completed source inequality. Its exact firewall is the accumulating gap

$$L_{n+1} - L_n = \log\left(1 + \frac{1}{n}\right) \sim \frac{1}{n} \tag{157.10}$$

No fixed compact positive window can orthogonalize infinitely many frequencies whose gaps approach zero. The PP204 replay shows that fixed-rank Jacobi projections resolve small frequencies but fail uniformly as the log frequency grows, and a window capable of separating adjacent labels near N must scale at least on the order of N in the nearest-neighbor model.

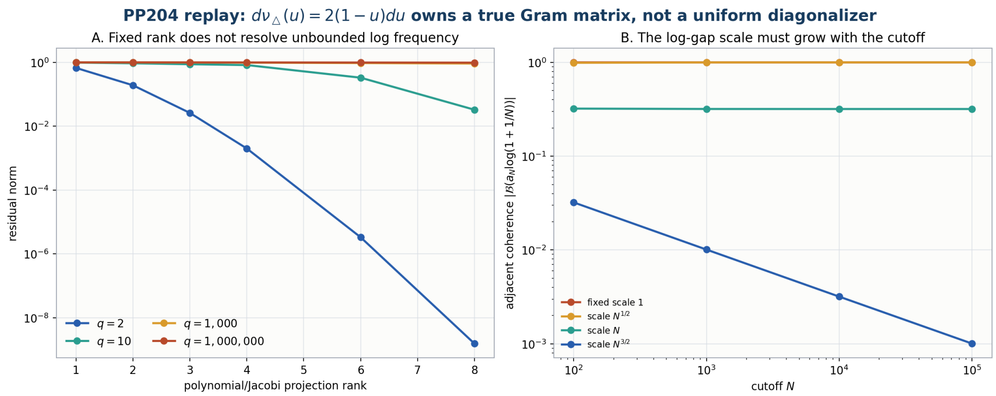

Figure 60: Projection and scale diagnostics for the Beta-logarithm model. Each curve is finite and replayed; the plotted trend is a firewall, not an asymptotic proof beyond the stated theorem.

The surviving target is not a larger scalar window. It is a source-defined, operator-weighted, nonstationary compression whose **final** form has the translation covariance required by the Weil functional while its internal lift still couples the two reflection sheets.

154. Completion-coupled translation defects and the PP97 carrier

Reserve $\Lambda_{\mathrm{vM}}(m)$ for the von Mangoldt function. For a real finite resolvent combination $F = \sum_i c_i f_{x_i}$ define

$$\begin{gathered} \widehat{F}(t) = \int_{\mathbb{R}} F(u)e^{-itu}\,du, \qquad g_F(v) = \langle F, \tau_v F\rangle \\ D_F(v) = g_F(0) - g_F(v) = \frac{1}{2}\|(I-\tau_v)F\|_2^2 \end{gathered} \tag{154.1}$$

Here $(\tau_v F)(u) = F(u+v)$ and

$$w_\infty(t) = \frac{1}{4\pi}\left[\Re\psi\left(\frac{1}{4}+\frac{it}{2}\right) - \log\pi\right] = \frac{1}{4\pi}\left[\Re\psi\left(\frac{s}{2}\right) - \log\pi\right]_{s=1/2+it} \tag{154.2}$$

The PP200/PP201 Gamma representation, independently rebuilt in PP205 and replayed in PP206, is

$$\boxed{\int_{\mathbb{R}} |\widehat{F}(t)|^2 w_\infty(t)\,dt = a_\Gamma \|F\|_2^2 + \int_0^\infty D_F(v)\,d\mu_\Gamma(v)} \tag{154.3}$$

where

$$\boxed{\begin{aligned} a_\Gamma &= \frac{1}{2}\left(\psi\left(\frac{1}{4}\right) - \log\pi\right) = -2.686091709612832791\ldots \\ d\mu_\Gamma(v) &= \frac{e^{v/2}}{2\sinh v}\,dv > 0 \end{aligned}} \tag{154.4}$$

The scalar anchor is negative; every translated defect is nonnegative. The formula is therefore a signed anchor plus a positive continuum, not a positive measure representation of the completed form by itself.

The density has the exact expansion

$$\frac{e^{v/2}}{2\sinh v} = \sum_{k\geq 0} e^{-(2k+1/2)v} \tag{154.5}$$

To read the poles in the expanded variable, analytically continue the Fourier height t. With $a_k = 2k + 1/2$,

continued height	$s = 1/2 + it$	folded point $q = s(1-s)$	behavior of e^{-itv}
$t = +ia_k$	$s = -2k$	$-2k(2k+1) = -2T_{2k}$	$e^{+a_k v}$ grows
$t = -ia_k$	$s = 2k+1$	$-2k(2k+1) = -2T_{2k}$	$e^{-a_k v}$ decays

These are the two sheets of the folded Gamma pole. The $k = 0$ point $s = 0$ is an endpoint of the completed factor, not a nontrivial zeta zero.

The functional equation at its own fixed point supplies the exact anchor:

$$\boxed{a_\Gamma = -\frac{\zeta'}{\zeta}\left(\frac{1}{2}\right)} \tag{154.6}$$

Indeed, $\xi'(1/2) = 0$, the terms $1/s$ and $1/(s-1)$ cancel at $s = 1/2 + i0$, and the completed logarithmic derivative leaves (154.6). This is analytic continuation. It is **not** permission to replace the divergent series $\sum_m \Lambda_{\mathrm{vM}}(m)/\sqrt{m}$ by a_Γ inside a positive sum.

The prime channel is nevertheless exactly computable on the resolvent span. Put

$$a_i = \sqrt{x_i + \frac{1}{4}}, \qquad s_i = \frac{1}{2} + a_i = \sigma_i + i0 > 1 \tag{154.7}$$

and

$$\begin{aligned} A_i &= \frac{x_i}{2a_i}\, 2\sum_{j\neq i} \frac{c_i c_j}{x_i - x_j} + c_i^2\,\frac{x_i + 1/2}{4a_i^3} \\ B_i &= c_i^2\,\frac{x_i}{4a_i^2} \end{aligned} \tag{154.8}$$

Then

$$g_F(v) = \sum_i (A_i - B_i v) e^{-a_i v} \tag{154.9}$$

and, because every $\sigma_i > 1$,

$$\boxed{\sum_{m\geq 2} \frac{\Lambda_{\mathrm{vM}}(m)}{\sqrt{m}} g_F(\log m) = \sum_i \left[A_i \left(-\frac{\zeta'}{\zeta} \right)(s_i) - B_i \left(\frac{\zeta'}{\zeta} \right)'(s_i) \right]} \tag{154.10}$$

No prime table, cutoff, zero table, or tail estimate is required in (154.10). This is the practical source-side closure of the carrier.

For one node, it agrees exactly with PP97:

quantity at $x = 0.05$	replayed source value	role
$(xG)'$	-1.205641588399722174914	archimedean channel
$(xP)'$	-1.228733588379453600229	prime channel
$W_1 = (xG)' - (xP)'$	$+0.023091999973142531$	completed difference

The completion is visible in the cancellation, not in separate positivity of the two channels.

For a cutoff M set

$$\theta^\sharp(M) = \sum_{2\leq m\leq M} \frac{\Lambda_{\mathrm{vM}}(m)}{\sqrt{m}} \tag{154.11}$$

Then

$$-\sum_{m\leq M} \frac{\Lambda_{\mathrm{vM}}(m)}{\sqrt{m}} g_F(\log m) = \sum_{m\leq M} \frac{\Lambda_{\mathrm{vM}}(m)}{\sqrt{m}} D_F(\log m) - \theta^\sharp(M)\|F\|_2^2 \tag{154.12}$$

Both terms on the right diverge. The tempting substitution $\theta^\sharp(M) \rightsquigarrow a_\Gamma$ is the named **regularization trap**: it keeps the divergent positive-defect sum and replaces only its compensator, manufacturing a false proof.

The geometric obstruction is sharper. The Gamma mass diverges at short shift,

$$d\mu_\Gamma(v) \sim \frac{dv}{2v} \quad (v \downarrow 0) \tag{154.13}$$

whereas the smooth prime mass grows at long shift like $e^{v/2}dv$. The densities differ by the factor e^v asymptotically. A positive scalar diagonal weight cannot move the required compensation from one end to the other; an operator-weighted, genuinely two-point mechanism remains the open class.

158. Two measures that must not be conflated

Two exact measures have different triangular roles:

measure	support and mass	exact moments	role
$d\nu_\triangle(u) = 2(1-u)du$	$[0,1]$, probability	$\int u^k d\nu_\triangle = 1/T_{k+1}$ for $k \geq 0$	Beta–Hankel and log-character Gram owner
$d\mu_\Gamma(v) = e^{v/2}(2\sinh v)^{-1}dv$	$(0,\infty)$, infinite total mass	finite moments only for $k \geq 1$	archimedean translation-defect owner

For $k \geq 1$, expand (154.5) and integrate termwise:

$$\boxed{\begin{aligned} \int_0^\infty v^k \, d\mu_\Gamma(v) &= \sum_{m\geq 0} \frac{k!}{(2m+1/2)^{k+1}} \\ &= \frac{k!}{2^{k+1}}\zeta\left(k+1, \frac{1}{4}\right) \\ &= \frac{(-1)^{k+1}}{2^{k+1}}\psi^{(k)}\left(\frac{1}{4}\right) \end{aligned}} \tag{158.1}$$

The first moment is

$$\int_0^\infty v \, d\mu_\Gamma(v) = \frac{1}{4}\psi^{(1)}\left(\frac{1}{4}\right) = \frac{\pi^2 + 8G}{4} \tag{158.2}$$

where G is Catalan's constant. At $k = 0$ the integral diverges; the finite quantity a_Γ in (154.4) is the renormalized scalar anchor and is not the zeroth moment of a finite measure.

The measure comparison figure in Reading Volume §R18 shows these distinct supports.

The phrase "triangular rail'' therefore names two different exact appearances: reciprocal-triangular **moments** on the compact side and doubled-even-triangular **pole locations** on the Gamma side. Their common arithmetic vocabulary is not a measure identity.

137. Exact completed Weil/resolvent identity

For positive nodes x_i, real coefficients c_i, and

$$q(s) = s(1-s), \qquad \Phi_c(s) = q(s)\left(\sum_i \frac{c_i}{x_i + q(s)}\right)^2$$

PP190-T identifies the completed Weil form exactly. Let $\mathcal{W}_{\text{pair}}$ denote the folded-orbit normalization used in this volume and let $\mathcal{W}_{GW}$ denote the classical convention that counts every zero. The compulsory fold factor is

$$\boxed{\mathcal{W}_{\text{pair}}(c) = c^\mathsf{T}(L_\Gamma - L_P)c = \frac{1}{2}\mathcal{W}_{GW}[H_c]} \tag{137.1}$$

On $s = \frac{1}{2} + it$, put

$$H_c(t) = \left(t^2 + \frac{1}{4}\right)\left(\sum_i \frac{c_i}{t^2 + x_i + \frac{1}{4}}\right)^2 \geq 0$$

and

$$g_c(u) = \frac{1}{2\pi}\int_{\mathbb{R}} H_c(t)e^{-itu}\,dt$$

Then

$$\boxed{\mathcal{W}_{\text{pair}}(c) = \frac{1}{4\pi}\int_{\mathbb{R}} H_c(t)\left[\Re\psi\left(\frac{1}{4} + \frac{it}{2}\right) - \log\pi\right]dt - \sum_{m\geq 2}\frac{\Lambda(m)}{\sqrt{m}}g_c(\log m)} \tag{137.2}$$

There is no endpoint remainder for this test family. If $a_x = \sqrt{x + \frac{1}{4}}$ and

$$f_x(u) = e^{-a_x|u|}\left(\frac{1}{4a_x} + \frac{1}{2}\operatorname{sgn} u\right)$$

then $H_c = |\widehat{f_c}|^2$ and $g_c(u) = \langle f_c, \tau_u f_c\rangle$. Thus (137.2) is a single completion-coupled nonlocal quadratic form. It is not yet a Hilbert norm square. Separating its two finite-cutoff norm channels produces divergent common backgrounds at infinite cutoff; only their coupled autocorrelation difference converges on the resolvent span.

At $x = 56$, $a_x = 15/2$, and the prime sampling factor is exactly

$$m^{-1/2}e^{-(15/2)\log m} = m^{-8} \tag{137.3}$$

This is the exact adapter between the PP189 common-tail arithmetic and the completed resolvent form.

148. Resolvent autocorrelation and the zero-margin firewall

For

$$a_x = \sqrt{x + \frac{1}{4}} \qquad f_x(u) = e^{-a_x|u|}\left(\frac{1}{4a_x} + \frac{1}{2}\operatorname{sgn} u\right)$$

put

$$\kappa(x,u) = \frac{x\,e^{-a_x|u|}}{2a_x}$$

Parseval and one partial-fraction identity give the exact translation divided difference

$$\boxed{\langle f_x, \tau_u f_y\rangle = \frac{\kappa(x,u)-\kappa(y,u)}{x-y}} \tag{148.1}$$

At $u=0$, $\kappa(x,0)=x/\sqrt{1+4x}$ is operator monotone and $\kappa(x,0)/x$ is Stieltjes. The prime channel is

$$\boxed{xP(x) = \sum_{m\geq 2} \Lambda(m) m^{-1/2}\kappa(x,\log m)} \tag{148.2}$$

and the archimedean channel is the signed spectral integral

$$\boxed{xG(x) = \int_{\mathbb{R}} \frac{x}{t^2+x+1/4}\, d\sigma_\infty(t)} \tag{148.3}$$

$$d\sigma_\infty(t) = \frac{1}{4\pi}\left[\Re\psi\left(\frac{1}{4}+\frac{it}{2}\right) - \log\pi\right] dt \tag{148.4}$$

Thus every prime power is a translate of one operator-monotone Gram anchor. The difficulty is exact: translation destroys positive definiteness, while completion restores only a coupled difference.

There is no pointwise symbol margin to exploit. Since $\Xi(t)=\xi(1/2+it)$ is real for real t,

$$\boxed{\Re\frac{\xi'}{\xi}\left(\frac{1}{2}+it\right) = 0} \tag{148.5}$$

away from its poles, unconditionally. The real parts of the analytically continued archimedean and prime symbols therefore agree on the critical line. Any proposed proof based on a strict Gamma-over-prime boundary margin is vacuous. The folded cut has no absolutely continuous jump from h; under RH the representing measure is purely atomic at the folded zero locations.

The PNT-mode endpoint also survives:

$$\int_0^\infty e^{u/2}\left(\frac{1}{4}K(u) - K''(u)\right) du = K'(0+) - \frac{1}{2}K(0) \tag{148.6}$$

For the $x=56$ resolvent, $K'(0+)=0$ and $K(0)=2/3375$, so

$$\boxed{K'(0+) - K(0)/2 = -1/3375 \neq 0} \tag{148.7}$$

A boundary counterterm or a test class with $K(0)=0$ is compulsory.

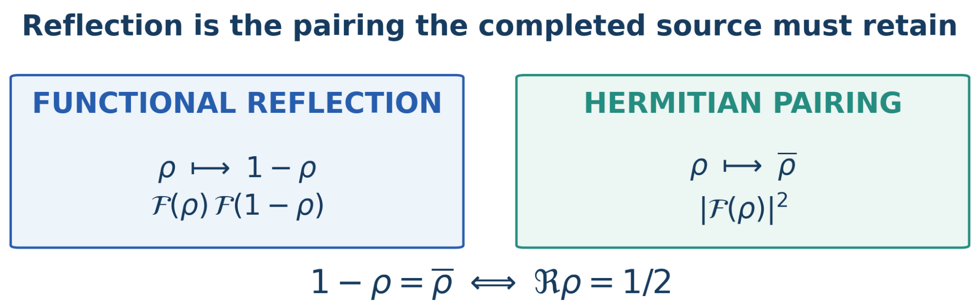

Figure 61: For a real-coefficient test, reflection and conjugation use different partners off the critical line. The full resolvent family separates the distinction; a single multinode test may annihilate an orbit. See §§159–160.

149. Cauchy–Löwner contour identities

The exploratory contour calculation is relevant because it identifies the precise complex-analytic owner of every finite Löwner and confluent entry. Let Γ be a positively oriented contour inside a domain of holomorphy of h, enclosing the positive nodes x_i and no singularities. Cauchy's formula gives

$$\boxed{L_h(x_i,x_j) = \frac{1}{2\pi i}\oint_\Gamma \frac{h(z)}{(z-x_i)(z-x_j)}\,dz} \tag{149.1}$$

Consequently, for real c_i,

$$\boxed{c^{\mathsf{T}} L_h c = \frac{1}{2\pi i}\oint_\Gamma h(z)\left(\sum_i \frac{c_i}{z-x_i}\right)^2 dz} \tag{149.2}$$

Coalescing all nodes at x yields

$$\boxed{\frac{h^{(i+j+1)}(x)}{(i+j+1)!} = \frac{1}{2\pi i}\oint_\Gamma \frac{h(z)}{(z-x)^{i+j+2}}\,dz} \tag{149.3}$$

For the signed Dobsch normalization, replace $z-x$ by $x-z$; this contributes $(-1)^{i+j}$. On the diagonal $i=j=n$, (149.3) reaches the native odd order

$$i+j+1 = 2n+1$$

which explains the repeated derivative order and factorial $(2n+1)!$ in the confluent/Hausdorff hierarchy.

Equations (149.1)–(149.3) are exact but do not prove positivity. The integrand contains a holomorphic square

$$\left(\sum_i \frac{c_i}{z - x_i}\right)^2$$

not an absolute square. A single contour therefore cannot create the conjugation demanded by the nonholomorphic folded moment. The sharpened next question is whether completion supplies a double-contour or sesquilinear kernel of the form

$$\iint \mathcal{K}_{\mathrm{comp}}(z,w)F(z)\overline{F(w)}\,dz\,d\bar{w} \tag{149.4}$$

whose compression is (149.2) and whose positivity is source-visible. No such kernel is constructed here.

159. Stationary-symbol blindness and the missing conjugation

Let

$$\Phi(s) := \frac{\xi'(s)}{\xi(s)}, \qquad s = \sigma + it \tag{159.1}$$

Away from zero ordinates, $\Xi(t) = \xi(1/2 + it)$ is real. Hence $i\Phi(1/2 + it) = d(\log \Xi(t))/dt$ is real and

$$\boxed{\Re\Phi(1/2 + it) = 0} \tag{159.2}$$

pointwise wherever the quotient is finite. There is no positive archimedean-over-prime margin on the critical boundary; their real parts cancel exactly after completion.

The distributional boundary value is also lossy. An off-line functional- equation pair at $\beta = 1/2 \pm \delta$ and height γ contributes, with $y = t - \gamma$,

$$-\frac{\delta}{\delta^2 + y^2} + \frac{\delta}{\delta^2 + y^2} = 0 \tag{159.3}$$

Thus the consistent distributional symbol is

$$\boxed{\Omega(t) = \pi \sum_{\rho:\,\beta_\rho = 1/2} m_\rho\,\delta_{\gamma_\rho}(t) \geq 0} \tag{159.4}$$

unconditionally, while the pointwise regularization is simply zero. Both versions erase the off-line content. A stationary difference kernel $K(u,v) = k(u - v)$ that compresses only to this scalar multiplier is therefore **blind**, not RH-equivalent.

For the meromorphic continuation

$$\mathcal{F}_-(s) = (1-s)\Psi_X(q(s)) \tag{159.5a}$$

the exact completed zero form uses reflection and one representative per functional-equation orbit:

$$Q_X(c) = \sum_{[\rho]} m_\rho \, \mathcal{F}_-(\rho)\mathcal{F}_-(1-\rho) \tag{159.5}$$

whereas the corresponding Hermitian comparison is normalized as

$$\frac{1}{2}\sum_{\rho \text{ all}} m_\rho \, |\mathcal{F}_-(\rho)|^2 \tag{159.6}$$

For one fixed real-coefficient test, pointwise equality of the reflection product with the Hermitian square holds exactly when

$$\boxed{\Re\rho = \frac{1}{2} \quad \text{or} \quad \Psi_X(q_\rho) = 0} \tag{159.7}$$

A multinode test can annihilate an off-line orbit, as the exact synthetic example in reader (20.6b) demonstrates. A separating family is needed for the RH equivalence. For the nonzero one-node carrier, no such annihilator exists, and equality is strict off the line. This names the missing operation precisely:

$$\boxed{\begin{array}{c}\text{Create the identification}\\ s \mapsto 1-s \quad \text{with} \quad s \mapsto \bar{s}\\ \text{without assuming RH}\end{array}} \tag{159.8}$$

The construction must retain reflection information lost by the scalar boundary compression (159.4). Internal nonstationarity is one design strategy, not a proved universal classification. Final translation covariance is compatible with the exact Weil form. Section 161 gives a separate precise obstruction for regular measurable multiplier norms; it leaves singular spectral measures and form limits open.

A finite conjugation-symmetric feature family can turn an aggregate holomorphic-square sum into a tensor norm; Lamzouri's Proposition 2.1 [66] provides a concrete example. This does not make individual off-line summands nonnegative, and it does not identify the resulting finite form with the completed source form. Its zeta application controls asymptotic proportions of zeros. The present fixed-scale criterion instead requires an independent bound through unbounded degree, with multiplicities and the complete source retained.

159.1 What the sesquilinear language contributes

Use the same convention as Reading Volume §R18A and technical §161: $\mathfrak{h}(u, v)$ is conjugate-linear in its first argument and linear in its second. It is Hermitian when

$$\mathfrak{h}(v,u)=\overline{\mathfrak{h}(u,v)} \tag{159.9}$$

and positive when $\mathfrak{h}(u,u)\geq 0$. In the complex setting the diagonal quadratic form determines a Hermitian form through polarization:

$$\boxed{\begin{aligned}4\mathfrak{h}(u,v)&=Q(u+v)-Q(u-v)\\&\quad -iQ(u+iv)+iQ(u-iv)\qquad Q(w)=\mathfrak{h}(w,w)\end{aligned}} \tag{159.10}$$

This elementary fact is useful because it makes the type mismatch visible. The reflected zero pairing

$$\mathfrak{b}_{\mathrm{ref}}(F,G)=\frac{1}{2}\sum_{\rho\ \mathrm{all}} m_\rho\,\mathcal{F}(\rho)\mathcal{G}(1-\rho) \tag{159.11}$$

is complex **bilinear** as printed; no conjugate appears. A Hermitian extension in the declared convention conjugates its first test factor and keeps its second factor linear. On RH, real-coefficient test functions obey

$$1-\rho=\bar{\rho},\qquad \mathcal{G}(\bar{\rho})=\overline{\mathcal{G}(\rho)} \tag{159.12}$$

so (159.11), restricted to real-coefficient tests, agrees with the Hermitian pairing. A complex Hermitian extension conjugates the coefficients in the first slot under our convention; a complex bilinear form does not become sesquilinear by a change of notation. Off RH the reflection/conjugation agreement is not available for a separating family. The lecture material on sesquilinear forms therefore helps by identifying the exact algebraic type a successful lift must have; it does not itself construct the missing lift. Any proposed polarization argument must first exhibit a genuinely positive diagonal Q on an enlarged two-sheet space. Applying (159.10) directly to (159.11) would merely conceal the unproved step.

160. The reflection-contour normal form

For a finite positive node set $X=(x_1,\ldots,x_N)$ and real coefficients c_i, define

$$\Psi_X(q)=\sum_{i=1}^{N}\frac{c_i}{x_i+q},\qquad q(s)=s(1-s) \tag{160.1}$$

and reserve

$$\boxed{\mathscr{L}_F(s):=q(s)\Psi_X(q(s))^2} \tag{160.2}$$

This is PP205's test symbol $\Lambda(s)$ under a collision-free name. With $s=\sigma+it$, its argument is explicitly

$$q(s) = \sigma(1-\sigma) + t^2 + i\,t(1-2\sigma) \tag{160.3}$$

Functional-equation symmetry gives

$$\mathscr{L}_F(1-s) = \mathscr{L}_F(s) \qquad \Phi(1-s) = -\Phi(s) \tag{160.4}$$

so $\mathscr{L}_F\Phi$ is antisymmetric under reflection. Put

$$\sigma_* = \min_i \frac{1+\sqrt{1+4x_i}}{2} > 1 \tag{160.5}$$

For every $1 < \sigma_0 < \sigma_*$, the exact single-contour formula is

$$\boxed{\begin{aligned} Q_X(c) &= \frac{1}{2\pi}\int_{\mathbb{R}} \mathscr{L}_F(\sigma_0+it)\Phi(\sigma_0+it)\,dt \\ &= \frac{1}{2\pi i}\int_{(\sigma_0)} \mathscr{L}_F(s)\Phi(s)\,ds \end{aligned}} \tag{160.6}$$

On this line $\sigma_0 > 1$, the source expansion of Φ is absolutely convergent. The poles of $\Psi_X(q(s))$ lie outside the contour window, the horizontal edges vanish like $O(\log|t|/|t|^2)$ or faster under moment cancellation, and the enclosed poles are the nontrivial zeros. Reflection turns the two vertical integrals into twice (160.6), while the residue sum is twice the folded form.

At the terminal line $s = 1/2 + it$,

$$\boxed{\mathscr{L}_F(1/2+it) = |\widehat{F}(t)|^2 \geq 0, \qquad \Phi(1/2+it) \in i\mathbb{R}} \tag{160.7}$$

The positive object and the pairing are exactly orthogonal there. With the poles of Φ treated by symmetric indentation and symmetric truncation, the critical-line statement is PV $I_F(1/2) = 0$; the integrand is not zero. The RH content lives in the contour shift and its residues, not in a pointwise boundary sign.

Define

$$I_F(\sigma) = \frac{1}{2\pi i}\int_{(\sigma)} \mathscr{L}_F(s)\Phi(s)\,ds \tag{160.8}$$

On any open interval containing no zero abscissae or test poles, I_F is constant. On its admissible contour lines it is odd about $1/2$. For endpoint lines avoiding poles and shifts crossing no test poles, the residue argument gives the exact jump law

$$\boxed{I_F(\sigma_2) - I_F(\sigma_1) = \sum_{\sigma_1 < \beta_\rho < \sigma_2} m_\rho \mathscr{L}_F(\rho)} \tag{160.9}$$

This is a classical contour/residue mechanism in project-native packaging. It is not yet a positivity theorem: $\mathscr{L}_F(\rho)$ is a holomorphic square at an off-line zero and has no manifest sign.

The contour figure in Reading Volume §R20 illustrates this jump law.

Three fast screening tests now govern every candidate:

1. **Reflection test.** If it produces $|\mathcal{F}_X(\rho)|^2$ in place of $\mathcal{F}_X(\rho)\mathcal{F}_X(1-\rho)$, it must prove the required equality for a separating family; a fixed test can have accidental zeros.
2. **Stationary-loss test.** If the internal construction reduces to the boundary multiplier (159.4), it has erased every off-line pair.
3. **Terminal test.** If it claims positivity from the integrand at $\sigma = 1/2$, it claims a sign for a contour integral forced to vanish.

The correct next object is a positive form before compression whose compression reproduces (160.6) on $\sigma_0 > 1$. Section 161 adds a regularity test to this completion-coupled, two-sheet target: an ordinary strong tensor-norm limit cannot supply the required spectral owner.

161. Regular translation energy: an obstruction

The varying-endpoint Gram in Reading Volume §R18B is a positive auxiliary object. Its natural tensor lift, however, has a further obstruction. The distinction is between an ordinary convergent vector series and a singular limit of forms.

Use the inner product conjugate-linear in the first slot. Put $L_n = \log n$, let ϕ_n be (EG.1), and take a finite index set $I \subset \{2, 3, \ldots\}$. Define

$$\mathcal{R}_{b,I}F = \sum_{n\in I} b_n\phi_n \otimes (I - \tau_{L_n})F \qquad g_F(v) = \langle F, \tau_v F\rangle \tag{161.1}$$

Translation unitarity gives the complete finite expansion

$$\begin{aligned}\|\mathcal{R}_{b,I}F\|^2 = \sum_{m,n\in I} \bar{b}_m b_n K_{mn}\big[&g_F(0) - g_F(L_n) - g_F(-L_m)\\ &+ g_F(L_n - L_m)\big]\end{aligned} \tag{161.2}$$

The final shifts are $\log(n/m)$. Pairs with the same reduced ratio must be grouped before a coefficient can be declared noncancellable. For a reduced ratio a/b, those pairs are $(m,n) = (\ell b, \ell a)$. In an infinite construction the four displayed channels must not be separated without an appropriate convergence argument.

Theorem 161.1 — regular translation-energy obstruction. Fix the coefficients and auxiliary vectors independently of the input test and its node. Suppose (161.1) is a finite sum, or its partial sums converge strongly in the fixed ordinary Hilbert space $\mathcal{H} \otimes L^2(\mathbb{R})$ on the resolvent tests. Here $\mathcal{H} = L^2(0,\infty)$ for (EG.1). Then its norm cannot satisfy

$\|\mathcal{R}_b f_x\|^2 = W_1(x)$ for every $x > 0$. In particular, it cannot reproduce the completed source form on every rational-resolvent test.

Proof. Under the forward transform e^{-itu}, translation by L_n acts as multiplication by e^{itL_n}. For finite I set

$$A_I(t) = \sum_{n\in I} b_n \phi_n (1 - e^{itL_n}) \qquad M_I(t) = \|A_I(t)\|^2_{\mathcal{H}} \geq 0$$

Plancherel gives

$$\|\mathcal{R}_{b,I} F\|^2 = \frac{1}{2\pi} \int_{\mathbb{R}} |\widehat{F}(t)|^2 M_I(t) dt \tag{161.3}$$

The same regular multiplier representation survives strong convergence. Fix $x_0 > 0$. The transform

$$\widehat{f}_{x_0}(t) = \frac{1/2 - it}{t^2 + x_0 + 1/4}$$

does not vanish on the real line. Strong convergence says that $A_I \widehat{f}_{x_0}$ converges in $L^2(\mathbb{R}; \mathcal{H})$. Divide its measurable limit by $\widehat{f}_{x_0}$ to define $A(t)$. For every other $x > 0$, the ratio $\widehat{f}_x / \widehat{f}_{x_0}$ is bounded, so the same multiplier works on all these tests. Thus (161.3) holds with $M(t) = \|A(t)\|^2 \geq 0$.

Push forward $M(t)dt/(2\pi)$ under $q = t^2 + 1/4$ and call the resulting positive measure ν. It is absolutely continuous on $(1/4, \infty)$ and has no atom at $1/4$. Equality of the one-node diagonal would give

$$W_1(x) = \int_{[1/4,\infty)} \frac{q}{(x+q)^2}\, d\nu(q) \tag{161.4}$$

Integrate from 0 to x. Tonelli applies to the nonnegative integrand; $W_1 = (xS_\xi)'$ and $xS_\xi(x) \to 0$ at the origin. Consequently

$$\boxed{S_\xi(x) = \int_{[1/4,\infty)} \frac{d\nu(q)}{x+q}} \tag{161.5}$$

This integral is finite: its kernel is comparable to the one in (161.4), since $q \geq 1/4$.

The completed fold has a different analytic requirement. Reflection removes the square-root branch in

$$\Phi_0(x) = \frac{\xi(s_x)}{\xi(1)} \qquad S_\xi(x) = \frac{\Phi_0'(x)}{\Phi_0(x)} \tag{161.6}$$

Thus Φ_0 is entire with real coefficients, and S_ξ is meromorphic in the full plane, with discrete poles and real values on real intervals away from them. A positive Stieltjes measure with this transform must be purely atomic. Indeed, on any compact interval whose reflected interval contains no pole, the two boundary values of S_ξ agree and are real. Stieltjes inversion gives zero measure there. Equivalently, integrate its Poisson-kernel form

$$-\frac{1}{\pi}\Im S_\xi(-y+i\varepsilon) = \int \frac{\varepsilon\, d\nu(q)}{\pi[(q-y)^2+\varepsilon^2]} \tag{161.7}$$

over such an interval and let $\varepsilon \downarrow 0$. Local finiteness and the weighted tail integrability supplied by (161.5) justify this inversion. Hence ν is supported on the discrete reflected pole set. Any off-cut pole would already contradict analytic continuation of (161.5).

The measure is thus both absolutely continuous and discretely supported, hence zero. That would imply $S_\xi = 0$, contradicting $S_\xi(0) = \lambda_1 > 0$. No RH assumption was used. ☐

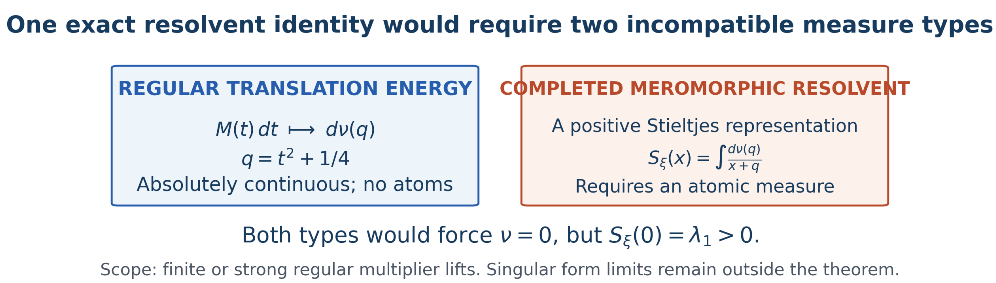

Figure 62: The regular-energy obstruction compares two measure types. An ordinary measurable multiplier produces an absolutely continuous measure; a positive Stieltjes representation of the completed meromorphic resolvent would require an atomic measure. Their only common measure is zero. Singular form limits lie outside the stated class.

Comparison with the completed source. Section 154's full Gamma-minus-prime form has exactly the one-node diagonal W_1 used above, so the candidate's regular Fourier density cannot reproduce it, even if mixed rational-log translations are reorganized. Its integer-label Gram may be nonstationary, yet its action on F reduces to a scalar Fourier density.

Scope and surviving route. This theorem excludes finite sums, strongly convergent series in the fixed ordinary tensor norm, and more generally regular measurable vector-multiplier realizations with finite test energies. It does not exclude singular spectral measures, a different source-defined norm, a discrete realization, or weak limits of quadratic forms that fail strong vector convergence. Absolutely continuous measures can converge weakly to atoms. Such a construction must specify its domain and topology, retain the Gamma/prime compensation, and prove exact equality on the full resolvent span. Sections 163–165 construct a source-defined discrete sequence and prove a sufficient variation criterion; that bound remains unproved.

The new requirement is therefore an atomic positive spectral owner, or a rigorously justified singular form limit, derived from the completed source. The trace target (23.3) and the all-node source sign remain open.

Technical chapter XIV. Completed Bernstein rows and the fixed-scale energy

Source derivatives determine the rows and their exact Pascal/Laguerre norm. The growth theorem leads to a fixed-scale prime estimate; the elementary/Gamma part is controlled.

163. Row mass, refinement, and the generating function

Fix $a > 0$ and abbreviate $S = S_\xi$. All zero sums below are folded sums, with multiplicities and conjugate folded values retained. Since $\Re q_\rho > 0$ and the zero count is $O(T \log T)$, $\sum_{[\rho]} m_\rho/|a + q_\rho| < \infty$. The existing Widder and shifted-zeta identities give

$$\begin{aligned} F_{n,k}(x) &= (-1)^n D^{n+k}[x^k S(x)] = (n+k)! \sum_{[\rho]} \frac{m_\rho q_\rho^k}{(x+q_\rho)^{n+k+1}} \\ Z_r(x) &= \frac{(-1)^{r-1}}{(r-1)!} S^{(r-1)}(x) \end{aligned} \tag{163.1}$$

Substitution into (BR.1) proves its Bernstein expansion. For each complex θ, the binomial theorem and degree-elevation identity imply

$$\begin{aligned} \sum_{j=0}^{N} B_{N,j} &= S(a) \\ B_{N,j} &= \frac{N+1-j}{N+1} B_{N+1,j} + \frac{j+1}{N+1} B_{N+1,j+1} \end{aligned} \tag{163.2}$$

Taking absolute values, then summing j, proves $S(a) \le \mathcal{V}_N(a) \le \mathcal{V}_{N+1}(a)$: each coefficient of the finer row is counted with total weight one. A negative entry at one degree forces a negative entry at every subsequent degree. This statement concerns a finite negative witness, not a method that guarantees one.

For the row polynomial $P_N(z) = \sum_j B_{N,j} z^j$, finite Leibniz expansion gives an independent formula entirely in source derivatives:

$$\begin{aligned} P_N(z) &= \frac{1}{N!} D_x^N \left[(x-az)^N S(x)\right]\Big|_{x=a} \\ &= \sum_{r=0}^{N} \binom{N}{r} \frac{S^{(r)}(a)}{r!} a^r (1-z)^r \end{aligned} \tag{163.3}$$

Summing for sufficiently small u, and then continuing meromorphically, produces

$$\begin{aligned} \sum_{N\geq 0} P_N(z) u^N &= \frac{1}{1-u} S\left(a \frac{1-uz}{1-u}\right) \\ &= \sum_{[\rho]} \frac{m_\rho}{a + q_\rho - u(q_\rho + az)} \end{aligned} \tag{163.4}$$

The first equality follows also from $\sum_{N\geq r} \binom{N}{r} u^N = u^r/(1-u)^{r+1}$. The completed source, including its prime-dependent part, occurs in (163.3)–(163.4). Its asymptotic coefficients alone do not determine these rows.

For later use, the falling moments satisfy

$$\sum_{j=0}^{N} (j)_r B_{N,j}(a) = (N)_r a^r Z_{r+1}(a) \quad (0 \leq r \leq N) \tag{163.5}$$

This is the binomial falling-moment identity, valid algebraically for complex θ. At $N \geq 1$, Stirling's finite change of basis between j^r and $(j)_\ell$ then shows

$$\sum_{j=0}^{N} (j/N)^r B_{N,j}(a) \longrightarrow a^r Z_{r+1}(a) \quad \text{for each fixed } r \geq 0 \tag{163.6}$$

This moment convergence is unconditional. Weak convergence of the signed measures requires a further bound on total variation.

163A. The exact Bernstein–Laguerre energy

The row coefficients admit a norm that keeps the completed source inside one polynomial. Let $L_j^{(0)}(t) = \sum_{r=0}^{j} \binom{j}{r} (-t)^r / r!$ be the ordinary Laguerre polynomials. Their coefficients are precisely the signed grid entries $c_{j,r}$ divided by $r!$, including $L_0 = 1$. Define

$$\mathcal{Q}_N(t;a) = \sum_{j=0}^{N} B_{N,j}(a) L_j^{(0)}(t) = \sum_{r=0}^{N} \binom{N}{r} \frac{a^r S^{(r)}(a)}{(r!)^2} t^r \tag{163A.1}$$

To prove the second equality, expand each L_j and use (163.5) in the form $\sum_j \binom{j}{r} B_{N,j} = \binom{N}{r} a^r Z_{r+1}$. The sign in $Z_{r+1} = (-1)^r S^{(r)}/r!$ cancels the Laguerre sign. Both factorials remain. Independently, finite coefficient comparison gives the classical polynomial identity

$$L_N^{(0)}(\theta t) = \sum_{j=0}^{N} \binom{N}{j} \theta^j (1-\theta)^{N-j} L_j^{(0)}(t) \tag{163A.2}$$

It holds for complex θ. Thus (163A.1) also equals $\sum_q m_q L_N^{(0)}(at/(a+q))/(a+q)$, with equal folded values combined into m_q. Every such sum is normally convergent for fixed degree, by the summable resolvent weights.

Rodrigues' formula $L_j = e^t D^j (e^{-t} t^j)/j!$ and integration by parts give $\int_0^\infty e^{-t} L_j L_k \, dt = \delta_{jk}$. The boundary terms vanish; when $j > k$, the j-th derivative of L_k vanishes, and when $j = k$, its leading coefficient gives norm one. Together with circle Parseval this proves

$$\boxed{\begin{aligned} \mathscr{E}_N(a) &:= \int_0^\infty e^{-t} |\mathcal{Q}_N(t;a)|^2 \, dt = \sum_{j=0}^{N} B_{N,j}(a)^2 \\ &= \frac{1}{2\pi} \int_{-\pi}^{\pi} |P_N(e^{i\vartheta};a)|^2 \, d\vartheta \end{aligned}} \tag{163A.3}$$

The finite linear map $z^j \mapsto L_j^{(0)}(t)$ is therefore an isometry between these two polynomial spaces. It sends $(1-z)^r$ to $t^r/r!$; this is the exact connection between the source polynomial in (163.3) and the second factorial in (163A.1). No equality with the earlier Laguerre flux hierarchy is asserted.

The elementary coefficient-norm inequalities give

$$\frac{S(a)^2}{N+1} \le \mathscr{E}_N(a), \qquad \sqrt{\mathscr{E}_N(a)} \le \mathcal{V}_N(a) \le \sqrt{N+1}\sqrt{\mathscr{E}_N(a)} \tag{163A.4}$$

Consequently (BR.4) is equivalent to the following estimate at the same fixed a: for every $\varepsilon > 0$ there is a finite $C_{a,\varepsilon}$ such that $\mathscr{E}_N(a) \le C_{a,\varepsilon}(1+\varepsilon)^{2N}$ for every N. The polynomial factor $N+1$ is absorbed by first using a smaller positive epsilon. Positivity of the norm is automatic; its upper growth bound is the missing assertion.

A finite algebraic form, useful for checking normalization, is

$$\mathscr{E}_N(a) = \sum_{r,s=0}^{N} \binom{N}{r}\binom{N}{s} \frac{(r+s)!}{(r!)^2(s!)^2} a^{r+s} S^{(r)}(a) S^{(s)}(a) \tag{163A.5}$$

The triangular row inside the energy matrix

The factorial coefficients in (163A.5) are the entries of a symmetric Pascal matrix. For a fixed $a > 0$, collect the real completed-source derivatives into a column $d^{(N)}$ and define

$$d_r^{(N)}(a) = \binom{N}{r}\frac{a^r S^{(r)}(a)}{r!} \qquad (0 \le r \le N)$$
$$(M_N^{\mathrm{Pas}})_{r,s} = \binom{r+s}{r}, \qquad (C_N)_{r,j} = \begin{cases}\binom{r}{j} & j \le r\\ 0 & j > r\end{cases} \tag{163A.6}$$

In the signed grid notation, $(C_N)_{r,j} = (-1)^j c_{r,j}$ and $(M_N^{\mathrm{Pas}})_{r,s} = (-1)^r c_{r+s,r}$. The figure shows cells with row index at most 17; these matrix identities use the same array for arbitrary finite indices.

The derivatives are real because the completed folded sum retains conjugate pairs. Direct regrouping of (163A.5), followed by Vandermonde's identity, gives

$$\boxed{\begin{aligned}&\mathscr{E}_N(a) = (d^{(N)})^{\mathsf T} M_N^{\mathrm{Pas}} d^{(N)}\\ &M_N^{\mathrm{Pas}} = C_N C_N^{\mathsf T}, \qquad \det M_N^{\mathrm{Pas}} = 1\end{aligned}} \tag{163A.7}$$

Indeed, $\sum_j \binom{r}{j}\binom{s}{j} = \binom{r+s}{r}$ and C_N is triangular with unit diagonal. This classical Pascal factorization is described in [65]. Its role here is to identify the exact matrix already present in the completed-source energy. The first four rows and columns make the earlier triangular numbers visible:

$$M_3^{\mathrm{Pas}} = \begin{pmatrix}1&1&1&1\\1&2&3&4\\1&3&6&10\\1&4&10&20\end{pmatrix}, \qquad \boxed{(M_N^{\mathrm{Pas}})_{2,s} = \binom{s+2}{2} = T_{s+1}} \tag{163A.8}$$

The last identity uses zero-based indices, $N \ge 2$, and $0 \le s \le N$. Thus the third row and column are triangular; the neighboring rows contain the constant, integer, and tetrahedral sequences. These are the Pascal coefficients of §171, now acting as a Gram matrix on source derivatives.

There is also an exact reflection of polynomial coefficients. Set $(U_N)_{j,r} = (-1)^j\binom{r}{j}$ for $j \le r$ and zero otherwise. The identity $P_N(z;a) = \sum_r d_r^{(N)}(a)(1-z)^r$ in (163.3) gives

$$\boxed{B_N = U_N d^{(N)}, \qquad U_N^2 = I, \qquad U_N^{\mathsf T} U_N = M_N^{\mathrm{Pas}}} \tag{163A.9}$$

Here $B_N = (B_{N,0},\dots,B_{N,N})^{\mathsf T}$ and $(U_N)_{j,r} = c_{r,j}$ is the transposed signed grid. The involution is the substitution $z \mapsto 1-z$ in the polynomial variable: applying it twice returns the original polynomial. This variable is independent of the source coordinate s and of the Cayley coordinate in Reading Volume §R7. For $N \ge 1$ the change of basis is involutive but not orthogonal in the ordinary coefficient norm; its Gram matrix is precisely M_N^{Pas}.

The smallest nontrivial case reconnects this matrix to the reciprocal sequence of §171:

$$M_1^{\mathrm{Pas}} = \begin{pmatrix} 1 & 1 \\ 1 & 2 \end{pmatrix}, \qquad \lambda_\pm = \frac{3 \pm \sqrt{5}}{2}, \qquad \mathrm{tr}((M_1^{\mathrm{Pas}})^m) = \mathcal{P}_m(3) \tag{163A.10}$$

Indeed $\lambda_+\lambda_- = 1$ and $\lambda_+ + \lambda_- = 3$. The trace sequence is $2, 3, 7, 18, 47, 123, \ldots$, with the same recurrence as (RP.2). The calligraphic $\mathcal{P}_m$ is the existing reciprocal polynomial; P_N continues to denote the source polynomial.

For general N, (163A.9) gives

$$(M_N^{\mathrm{Pas}})^{-1} = U_N M_N^{\mathrm{Pas}} U_N, \qquad \lambda_j \lambda_{N-j} = 1 \quad (0 \le j \le N), \tag{163A.11}$$

where $\lambda_0 \le \cdots \le \lambda_N$ are the positive eigenvalues. The first identity follows by multiplying $U_N^{\mathsf{T}} U_N$ and using $U_N^2 = I$; similarity then proves reciprocal pairing. The final diagonal entry and the Rayleigh bound imply

$$\mathrm{cond}_2(M_N^{\mathrm{Pas}}) = \lambda_N^2 \ge \binom{2N}{N}^2 \tag{163A.12}$$

Thus involution does not make this change of coefficients orthogonal or well-conditioned at large degree. This is the matrix counterpart of keeping the reflected coefficients and their attached basis functions distinct in (SW.4c).

The Pascal matrix is positive definite for every N, regardless of the zero locations. Its positivity explains the norm identity, while the degree-dependent vector $d^{(N)}$ carries the source information needed for an upper growth estimate. The diagonal entry $\binom{2N}{N}$ itself grows exponentially, so the factorization alone supplies no such bound.

In particular $\mathscr{E}_1 = S(a)^2 + 2aS(a)S'(a) + 2a^2 S'(a)^2$. The symbol $\mathscr{E}_N$ denotes a polynomial energy. The off-line heat defect $\mathcal{E}_H$ in (HG.2) is a different quantity.

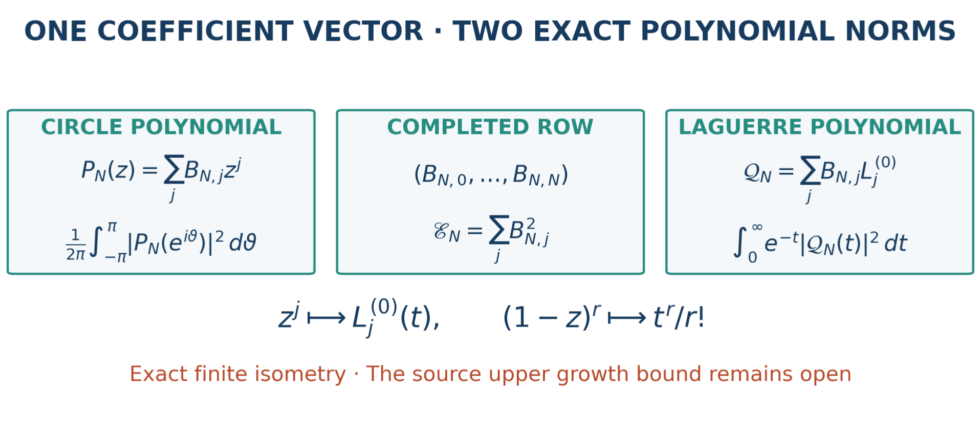

Figure 63: The completed row has two exact polynomial realizations with the same squared norm. The open assertion concerns the growth of that norm at one fixed source scale.

164. Exact growth and the heat comparison

Fix $a > 0$. For a folded point q put

$$R_q(a) = \frac{a + |q|}{|a + q|}, \qquad \mathcal{R}(a) = \sup_{[\rho]} R_{q_\rho}(a) \geq 1. \tag{164.1}$$

The completed Bernstein row of §163 has variation $\mathcal{V}_N(a)$ and Laguerre energy $\mathscr{E}_N(a)$. A verified zero height H gives the uniform finite-height estimate

$$\mathcal{V}_N(a) \leq S(a)\sqrt{1 + H^{-2}} \left(1 + \frac{a}{(a + H^2)^2}\right)^{N/2}. \tag{164.4b}$$

This is extremely sharp at fixed a but still has one fixed exponential factor greater than one, so it is not the arbitrary-ε source bound.

Theorem 164.2. Energy asymptotics and ordinary limits

There is $0 < \mathcal{K}(a) < \infty$ such that

$$\boxed{\mathscr{E}_N(a) \sim \mathcal{K}(a) \frac{\mathcal{R}(a)^{2N}}{\sqrt{N}}.} \tag{164.5}$$

Consequently

$$\boxed{\begin{gathered} \lim_{N \to \infty} \left(\frac{\mathcal{V}_N(a)}{S(a)}\right)^{1/N} = \lim_{N \to \infty} \left(\frac{\mathscr{E}_N(a)}{S(a)^2}\right)^{1/(2N)} = \mathcal{R}(a), \\ \lim_{N \to \infty} \frac{\mathscr{E}_{N+1}(a)}{\mathscr{E}_N(a)} = \mathcal{R}(a)^2. \end{gathered}} \tag{164.6}$$

The proof reduces to collisions of Bernstein rows. For $0 < p < 1$,

$$I_N(p) = \sum_j \binom{N}{j}^2 p^{2j}(1 - p)^{2N-2j} = \frac{1}{2\pi} \int_{-\pi}^{\pi} [1 - 4p(1 - p)\sin^2(\vartheta/2)]^N \, d\vartheta, \tag{164.7}$$

so Laplace scaling at $\vartheta = 0$ gives

$$I_N(p) \sim \frac{1}{2\sqrt{\pi N p(1 - p)}}, \qquad I_N(p) \leq \frac{C}{\sqrt{N p(1 - p)}}. \tag{164.8}$$

Distinct centers have a strictly smaller exponential collision rate. The finitely many maximizing folded orbits therefore determine the leading term (164.5), with equal folded values aggregated before squaring their weights.

Corollary 164.3. Bounded energy at one fixed scale

Since $\mathcal{R}(a) = 1$ exactly when every folded zero is positive real,

$$\boxed{\mathrm{RH} \iff \mathscr{E}_N[S_\xi](a) \to 0 \iff \sup_N \mathscr{E}_N[S_\xi](a) < \infty.} \tag{164.13}$$

A bounded subsequence at unbounded degrees also suffices because the ordinary root limit exists. Moving the basepoint with N is a different limit and can hide the obstruction. The longer collision-kernel and multiplicity proof is preserved in earlier editions.

165. Bounded variation and the atomic source representation

Theorem 165.1. If $\sup_N \mathcal{V}_N(a) < \infty$ at one prescribed $a > 0$, then the measures $\eta_N = \sum_j B_{N,j}(a)\delta_{j/N}$, $N \geq 1$, converge weakly on $[0,1]$ to the unique positive measure with moments $a^r Z_{r+1}(a)$. Its Stieltjes transform is the completed S_ξ. The hypothesis is unproved; the result is an implication from a source bound.

Proof. A uniform total-variation bound makes these signed measures weak-* relatively compact as functionals on $C[0,1]$. Any subsequential limit has the moments (163.6). Polynomial approximation implies uniqueness, so the whole sequence converges. Initially for $|x - a| < a$, the geometric series in the following integral is uniformly convergent:

$$S(x) = \int_{[0,1]} \frac{d\eta(t)}{1 + (x/a - 1)t} \tag{165.1}$$

Its Taylor coefficients at a are exactly those of S. The right side is analytic on $\mathbb{C} \setminus (-\infty, 0]$, even for signed finite η. Analytic continuation of (165.1) excludes every off-cut pole of S. Since its poles are $-q_\rho$, RH follows. Under RH the explicit positive measure

$$\eta = \sum_{[\rho]} \frac{m_\rho}{a + q_\rho} \delta_{a/(a+q_\rho)} \tag{165.2}$$

has precisely the same moments and therefore is that unique limit. No positivity of the original signed rows was assumed. ☐

The correct matrix normalization follows from $h = xS$. Put $A_x(t) = 1 + (x/a - 1)t$. Its divided differences, including the diagonal by continuity, are

$$L_h(x, y) = \int_{[0,1]} \frac{1 - t}{A_x(t)A_y(t)}\, d\eta(t) \tag{165.3}$$

For arbitrary complex coefficients this gives the Hermitian Gram norm $\int (1 - t)|\sum_i c_i/A_{x_i}(t)|^2 d\eta(t) \geq 0$. Thus the representation recovers all nodes at once. For the finite-vector normalization of §R10A, weight η by $1/(1 - t)$ and push forward under $d = t/[a(1 - t)]$. The resulting measure ν satisfies

$$S(x) = \int \frac{d\nu(d)}{1+xd}, \qquad \nu([0,\infty)) = S(0) = \lambda_1 \tag{165.4}$$

There is no extra numerator d in this finite-vector formula. The discrete measure (165.2) has no atom at $t = 1$; its weighted mass in (165.4) is finite by $S(0) < \infty$.

Completion before variation. The elementary source term $1/x$ alone produces $B_{N,j} = a^{-1}\delta_{j,N}$, a persistent endpoint atom at $t = 1$. The completed function removes the corresponding pole at $x = 0$. The exact row mass, endpoint cancellation, and limiting positive measure require the completed combination. Section 166A proves when separate channel bounds can nevertheless establish the qualitative subexponential energy criterion. The source basepoint $a = 2 = 2T_1$ gives $s_a = 2$, an available Euler-series location; it does not change this requirement or prove the variation bound.

166. What topology remains after the regular-energy obstruction

Section 161 excludes a regular measurable multiplier in the fixed ordinary L^2 norm. The discrete rows above are instead measures on a compact interval. A weak limit of measures is not a strong vector limit in that old norm. This difference is mathematical, not terminological.

For example, consider a sampling quadratic form $Q(f) = \sum_j c_j |f(t_j)|^2$ with $c_j > 0$, discrete support, and a domain containing compactly supported smooth functions. Choose an isolated atom t_0 and shrinking smooth bumps with $f_n(t_0) = 1$ and support avoiding the other atoms. Then

$$\|f_n\|_{L^2(dt)} \to 0, \qquad Q(f_n - f_m) = 0 \qquad Q(f_n) = c_0 > 0 \tag{166.1}$$

This violates closability in ordinary $L^2(dt)$. It does not exclude the same sampling form on a different domain with a norm controlling point values. A surviving source realization must state that domain and norm, and prove its source identity. Referring generally to a singular limit does not supply those data.

The existing dilation criterion and higher-moment support theorem give a second exact crosswalk. Write $\beta_* := \sup_\rho \Re\rho$ and $r_\xi := \sup_\rho |\Re\rho - 1/2|$. Functional-equation symmetry implies $2\beta_* = 1+2r_\xi$. The criterion of §143 and (GM.6) therefore give (HG.5). The normalized L^{2m} norms increase to this support radius, so finite moments supply lower bounds. A source proof reducing the dilation threshold to 1 remains missing.

The regular-energy obstruction, the discrete-measure proposal, and the dilation limit can therefore be read together: they specify which object must converge, in which topology, and which sign estimate has not yet been established. They do not turn the calibrated auxiliary model into the completed source.

166A. The remaining norm estimate and the fixed source scale

Extend (163A.1) linearly to $\mathcal{Q}_N[f]$, with S replaced by f, and let $\mathscr{E}_N[f] = \|\mathcal{Q}_N[f]\|^2_{L^2(e^{-t}dt)}$. Use the same replacement in (163.3) to define $P_N[f]$. The exact source in §54 gives

$$\mathcal{Q}_N[S] = a^{-1}L_N^{(0)} + \mathcal{Q}_N[G] - \mathcal{Q}_N[P] \tag{166A.1}$$

Indeed $\mathcal{Q}_N[1/x] = a^{-1}L_N^{(0)}$ by direct differentiation. The exact energy includes all cross terms. This identity concerns a degree-dependent source polynomial; it does not assert the existence of the fixed regular multiplier excluded in §161.

A cut-plane estimate closes the Gamma part

Lemma 166A.1. If f is holomorphic on $D = \mathbb{C} \setminus (-\infty, 0]$, then, at each fixed $a > 0$ and each $0 < r < 1$, a finite $C_{f,a,r}$ satisfies

$$\mathscr{E}_N[f](a) \le C^2_{f,a,r} r^{-2N} \quad (N \ge 0) \tag{166A.2}$$

Proof. The source-polynomial generating function is $(1-u)^{-1} f(a(1-uz)/(1-u))$. For $|u| < 1$, $|z| \le 1$, its argument lies in D. In fact, an argument $-v$ with $v \ge 0$ would require $u = (a+v)/(az+v)$, whose modulus is at least one; a zero denominator cannot give a finite solution. For $|u| = r$ the image is a compact subset of D. Its maximum, multiplied by $(1-r)^{-1}$, defines $C_{f,a,r}$. Uniform Cauchy coefficient estimates give $|P_N[f](z)| \le C_{f,a,r} r^{-N}$ on $|z| = 1$. Circle Parseval proves (166A.2). □

This lemma applies unconditionally to $A(x) = 1/x + G(x)$. On the principal branch $R(x) = \sqrt{1+4x}$ has positive real part in D, so $(1+R)/4$ has real part greater than $1/4$. The digamma function in $G = [\psi((1+R)/4) - \log \pi]/(2R)$ has no pole there. Taking $r = (1+\varepsilon)^{-1}$ proves the required subexponential estimate for the whole elementary/Gamma channel.

Consequently the triangle inequality, now using this proved channel bound, gives an exact qualitative reduction:

$$\boxed{\begin{aligned} &\forall \varepsilon > 0\ \exists C_{a,\varepsilon} < \infty: \quad \mathscr{E}_N[S](a) \le C_{a,\varepsilon}(1+\varepsilon)^{2N} \quad \forall N \\ &\qquad \iff \forall \varepsilon > 0\ \exists C'_{a,\varepsilon} < \infty: \quad \mathscr{E}_N[P](a) \le C'_{a,\varepsilon}(1+\varepsilon)^{2N} \quad \forall N \end{aligned}} \tag{166A.3}$$

Use $S = A - P$ in one direction and $P = A - S$ in the other; constants absorb the squared triangle bound. No positivity of A or P is required. Channel separation is therefore legitimate for this growth criterion after the Gamma estimate is proved. Exact row masses, endpoint cancellation, the limiting measure, and sharper numerical bounds still use the completed combination (166A.1).

The first unproved assertion is now the right-hand estimate in (166A.3) for the full prime term, at a fixed basepoint such as $a = 2$. The Dirichlet series for P and all its finite derivatives converge there. That local convergence gives no uniform estimate at arbitrary degree. For example, if $|u| < r < 1/3$, then $|x - a| \le 2ar/(1-r) < a$ and the transformed source remains in $\Re s > 1$, where the Euler series is available. Extending this argument to every $r < 1$ requires control outside that Euler-safe region. One cannot assume P holomorphic throughout D in order to apply the lemma: excluding its off-cut poles is the unresolved zero-location statement.

Each finite prime sum separately satisfies the lemma. Its constants need not be uniform in the prime cutoff, and the raw Euler partial sums do not converge throughout the larger domain. Thus neither finite prime truncation nor an exchange of the degree and cutoff limits proves (166A.3). This locates the remaining analytic task without replacing it by positivity of an auxiliary norm.

A moving basepoint erases the diagnostic

For every nontrivial zero, $q = A + ib$ satisfies $b^2 \leq A$. Writing $v = |q|$ gives $v - A = b^2/(v + A) \leq 1/2$; hence $R_q(a)^2 - 1 \leq a/(a + A)^2 \leq 1/a$. Also

$$\frac{|a+q|^{-1}}{\Re(a+q)^{-1}} = \sqrt{1 + \frac{b^2}{(a+A)^2}} \leq \sqrt{1 + \frac{1}{4a}} \tag{166A.4}$$

The last bound uses $A/(a + A)^2 \leq 1/(4a)$. Sum the positive real parts and apply (164.1) to obtain, without assuming RH,

$$\boxed{1 \leq \frac{\mathcal{V}_N(a)}{S(a)} \leq \sqrt{1 + \frac{1}{4a}}\left(1 + \frac{1}{a}\right)^{N/2}} \tag{166A.5}$$

Therefore every sequence $a_N \to \infty$ satisfies

$$\lim_{N\to\infty} \left(\frac{\mathcal{V}_N(a_N)}{S(a_N)}\right)^{1/N} = 1 \qquad \frac{\mathcal{V}_N(N)}{S(N)} \leq e^{1/2}\sqrt{1 + \frac{1}{4N}} \quad (N \geq 1) \tag{166A.6}$$

These conclusions are unconditional and cannot prove RH. As in the fixed-rung large-x theorem of §55, changing the source scale can hide the unbounded-order question. A sparse sequence of degrees at one fixed a is allowed by (164.6); sending a to infinity with degree is a different limit. The required fixed-scale source norm estimate remains open.

166B. Gamma Stieltjes repair and the bounded full-prime criterion

The Gamma-pole analysis gives a shorter derivation of the Gamma measure used in this criterion. Put $R_x = \sqrt{1 + 4x}$, $s_x = (1 + R_x)/2$, $b(x) = x/R_x$, and $a_\Gamma = [\psi(1/4) - \log \pi]/2 < 0$. The quarter-centered digamma split is

$$\boxed{h_\Gamma(x) = a_\Gamma b(x) + \sum_{m\geq 0} g_m(x), \qquad g_m(x) = \frac{2x}{(4m+1)(4m+1+R_x)}.} \tag{166B.1}$$

Each term has a positive Stieltjes representation. With $y = \sqrt{4u-1}$,

$$\frac{1}{R_x} = \int_{1/4}^{\infty} \frac{du}{\pi y(x+u)}, \qquad \frac{g_m(x)}{x} = \int_{1/4}^{\infty} \frac{2y\,du}{\pi(4m+1)((4m+1)^2+y^2)(x+u)}. \tag{166B.2}$$

Thus

$$\boxed{G(x) = \int_{1/4}^{\infty} \frac{d\sigma_\Gamma(u)}{x+u}} \tag{166B.3}$$

with signed density

$$\frac{d\sigma_\Gamma}{du} = \frac{a_\Gamma}{\pi y} + \frac{2}{\pi} \sum_{m\geq 0} \frac{y}{(4m+1)((4m+1)^2+y^2)}. \tag{166B.4}$$

The total baseline shift between the completion-centered pole terms and these positive quarter-centered terms is exact:

$$\sum_{m\geq 0} \frac{1}{(4m+1)(2m+1)} = \frac{\pi}{4} + \frac{\log 2}{2}. \tag{166B.4a}$$

The repaired positive part pushes forward exactly to the Catalan-resolvent reserve of (155C.5), plus the $m=0$ Catalan measure. This is a reconciliation, not a new reserve.

At fixed $a>0$, the weighted total variation is finite; its Bernstein endpoint is geometrically small and the Gamma collision energy tends to zero. In particular,

$$\mathcal{V}_N[G](a) \leq C_\Gamma(a), \qquad |B_{N,N}[G](a)| \leq C_\Gamma(a)\beta_a^N, \quad \beta_a = \frac{a}{a+1/4} < 1, \tag{166B.7}$$

and

$$\mathscr{E}_N[1/x+G](a) = a^{-2} + \mathscr{E}_N[G](a) + 2a^{-1}B_{N,N}[G](a) \longrightarrow a^{-2}. \tag{166B.8}$$

Theorem 166B.1. Bounded full-prime energy at one fixed scale

For $P(x) = -(\zeta'/\zeta)(s_x)/R_x$,

$$\boxed{\begin{aligned} \mathrm{RH} \iff & \sup_{N\geq 0} \mathscr{E}_N[P](a) < \infty \\ \iff & \mathscr{E}_N[P](a) \longrightarrow a^{-2} \\ \iff & \mathscr{E}_N[P-1/x](a) \longrightarrow 0. \end{aligned}} \tag{166B.9}$$

The proof is the identity $S_\xi = 1/x + G - P$ plus the decay above and Corollary 164.3. No separate sign is assigned to the Gamma and prime pieces.

At $a = 2$ this becomes the explicit all-degree criterion

$$\boxed{\mathrm{RH} \iff \forall N \geq 0 : \quad \mathscr{E}_N[P](2) \leq \left(1 + \log 2 + \frac{\pi}{6}\right)^2.} \tag{166B.11}$$

The constant has the triangular reading

$$1 + \log 2 + \frac{\pi}{6} = 2 - \sum_{n\geq 1} \frac{1}{2T_{2n}} + \frac{1}{2}\sqrt{1 + \frac{1}{12}\sum_{n\geq 1}\frac{1}{T_n^2}}, \tag{166B.12}$$

and the elementary bounds from §R4 imply the convenient rational equivalent

$$\boxed{\mathrm{RH} \iff \forall N : \ \mathscr{E}_N[P](2) < 5 \iff \forall N : \ \mathscr{E}_N[P](2) \leq 5.} \tag{166B.12a}$$

Theorem 166B.2. Prime plateau

With the same $\mathcal{K}(a), \mathcal{R}(a)$ as Theorem 164.2,

$$\boxed{\mathscr{E}_N[P](a) - a^{-2} \sim \mathscr{E}_N[P - 1/x](a) \sim \mathcal{K}(a)\frac{\mathcal{R}(a)^{2N}}{\sqrt{N}}.} \tag{166B.13}$$

The exact endpoint decomposition is

$$\mathscr{E}_N[P](a) = a^{-2} + \mathscr{E}_N[P - 1/x](a) + 2a^{-1}B_{N,N}[P - 1/x](a), \tag{166B.16}$$

and the completed resolvent endpoint satisfies

$$|B_{N,N}[S_\xi](a)| \leq \left(\sum_{[\rho]} \frac{m_\rho}{|a + q_\rho|}\right)\left(\frac{a}{d_a}\right)^N, \quad d_a = \min_{[\rho]} |a + q_\rho| > a. \tag{166B.17}$$

Hence the cross term is geometrically smaller than the leading spectral energy. The theorem describes the two alternatives; it does not select the bounded one.

The adversarial Gamma-pole analysis also closes a tempting shortcut: splitting the integer pole lattice into prime-power and complementary indices does not yield a positive Löwner reserve. The exact rank-two witness is recorded in §48C; adding the full repaired complement merely returns the RH-equivalent completed comparison above.

166C. Prime cutoffs, the persistent endpoint, and exponential cutoff depth

Fix $a > 0$ and truncate the actual von-Mangoldt source by integer value, including prime powers:

$$P_X(x) = \frac{1}{R_x} \sum_{2 \le n \le X} \Lambda(n) n^{-s_x}, \qquad R_x = \sqrt{1+4x}, \quad s_x = \frac{1+R_x}{2}. \tag{166C.1}$$

Every fixed cutoff converges at each fixed degree but loses the persistent endpoint at large degree. The recovery transition occurs only when the cutoff depth is exponential in N: the central-limit calculation retained in earlier editions gives the threshold $\log X_N \sim (N+1)/a$. Consequently no single cutoff-uniform subexponential cap can prove the full-prime criterion. The point is uniformity in degree, not failure of any fixed finite approximation.

The support-count shortcut fails even earlier. Only 40 prime powers lie at or below 113, while the true von-Mangoldt mass satisfies $\Psi(113) > 117.3867 > 114$. Sparse support is therefore not small weighted mass. The Gamma measure is continuous whereas $d\Psi(e^u)$ is atomic, so no finite constant gives literal measure domination of the prime source by the Gamma lattice.

A surviving cutoff argument must match the cutoff to the degree and control both pieces. One sufficient formulation is to construct X_N and nonnegative A_N, D_N with

$$\boxed{\|\mathcal{Q}_N[P_{X_N}]\|_2 \le A_N, \qquad \|\mathcal{Q}_N[P - P_{X_N}]\|_2 \le D_N, \qquad A_N + D_N \le \sqrt{5}.} \tag{166C.25}$$

Section 166D proves the remainder half for one explicit exponential schedule; the matched main-term bound remains open. The exact endpoint coefficient, central-limit window, and raw-cutoff negative control are archived in earlier editions (Zenodo version chain).

166D. An explicit full-row remainder for a growing prime cutoff

Section 166C proves that no bound is available uniformly over independent pairs (N, X), and (166C.25) names the two estimates a surviving cutoff argument needs. One of the two is now proved, unconditionally, for an explicit schedule. Throughout, $\alpha = (\sqrt{5}-1)/2$ and the norm is the weighted one of (163A.3), $\|\mathcal{Q}_N[f]\|_2^2 = \int_0^\infty e^{-t} |\mathcal{Q}_N[f](t;2)|^2 dt = \sum_{j=0}^N |B_{N,j}[f](2)|^2$ — not the unweighted $L^2(dt)$ norm and not the Euclidean norm of the monomial coefficients.

Theorem 166D.1. For every integer $N \ge 0$ and every integer $X \ge 2$, with no hypothesis,

$$\boxed{\big\|\mathcal{Q}_N[P - P_X](\cdot;2)\big\|_2 \le \frac{5^N}{\sqrt{5}} X^{-\alpha}\Big(\frac{\log X}{\alpha} + \frac{1}{\alpha^2}\Big)} \tag{166D.1}$$

In particular the schedule $X_N = 20^{N+1}$ gives

$$\big\|\mathcal{Q}_N[P - P_{X_N}]\big\|_2 \le D_N := \frac{20^{-\alpha}}{\sqrt{5}}\Big(\frac{(N+1)\log 20}{\alpha} + \frac{1}{\alpha^2}\Big)\kappa^N \longrightarrow 0,$$

$$\kappa = \frac{5}{20^\alpha} = 0.785035410093857\ldots < 1$$

Proof. On the closed complex disk $|x-2| \le 1$ put $\omega = 1+4x$. Since $\Re\omega \ge 5$, the principal root satisfies $\Re\sqrt{\omega} = \sqrt{(|\omega| + \Re\omega)/2} \ge \sqrt{5}$ and $|\sqrt{\omega}| \ge \sqrt{5}$, so $\Re s_x \ge 1 + \alpha > 1$ — and this is tight, the minimum $1+\alpha$ being attained on the boundary. The Euler tail is therefore absolutely and uniformly convergent on a neighbourhood of the disk. Since $0 \le \Lambda(n) \le \log n$ and prime powers enter by their integer value as in (166C.1),

$$M_X := \sup_{|x-2|\le 1} \left|P(x) - P_X(x)\right| \le \frac{1}{\sqrt{5}} \sum_{n>X} \frac{\log n}{n^{1+\alpha}} \le \frac{X^{-\alpha}}{\sqrt{5}} \Big(\frac{\log X}{\alpha} + \frac{1}{\alpha^2}\Big)$$

the comparison integrating $(\log t)t^{-1-\alpha}$, which decreases for $t \ge 2$ because $1-(1+\alpha)\log t < 0$ there. Cauchy's estimate gives $|(P-P_X)^{(r)}(2)|/r! \le M_X$. With the exact Pascal conversion (BE.1a), $d_r = \binom{N}{r} 2^r f^{(r)}(2)/r!$ and $B_{N,j} = \sum_{r\ge j}(-1)^j \binom{r}{j} d_r$, so

$$\|\mathcal{Q}_N[f]\|_2 \le \sum_{j=0}^{N} |B_{N,j}| \le \sum_{r=0}^{N} 2^r |d_r| \le M_X \sum_{r=0}^{N} \binom{N}{r} 4^r = 5^N M_X$$

which controls all $N+1$ coefficients simultaneously, both endpoints and degree zero included. For $\kappa < 1$ exactly: $\alpha > 3/5$ follows from $(11/5)^2 < 5$, and $20^3 = 8000 > 3125 = 5^5$ gives $20^\alpha > 5$. $\square$

The surviving obligation is now one prescribed diagonal sequence. Put $A_N = \|\mathcal{Q}_N[P_{20^{N+1}}](\cdot;2)\|_2$. The triangle and reverse triangle inequalities give $\big|A_N - \|\mathcal{Q}_N[P]\|_2\big| \le D_N$, so by Theorem 166B.1

$$\boxed{\mathrm{RH} \iff \sup_{N\ge 0} A_N < \infty} \tag{166D.2}$$

This does not contradict Theorem 166C.4, which rules out bounds uniform over *independent* cutoffs and degrees; here the cutoff is prescribed as a function of the degree. The exponentially small error also transfers the prime-energy asymptotics of Theorems 164.2 and 166B.2 to this schedule: under RH, $A_N^2 = \frac{1}{4} + \mathcal{K}(2)N^{-1/2} + o(N^{-1/2})$, using $|A_N^2 - e_N^2| \le D_N(2e_N + D_N) = o(N^{-1/2})$ with $e_N = \|\mathcal{Q}_N[P]\|_2$; and if RH fails, $A_N^2 \sim \mathcal{K}(2)\mathcal{R}(2)^{2N}N^{-1/2}$ with $\mathcal{R}(2) > 1$, since $D_N/e_N \to 0$. It is the **norm** error that is exponentially small; the energy statement needs that displayed extra factor. Neither alternative has been selected by any source estimate.

Precise advance and remaining gap. The remainder half of (166C.25) is now explicit for one generous exponential schedule; (166D.1) does **not** establish $A_N + D_N \le \sqrt{5}$, and no bound $\sup_N A_N < \infty$ is proved. A finite set of computed degrees, a positive endpoint, a bound depending uncontrollably on N, or one fixed exponential allowance above one does not discharge (166D.2). The schedule $X_N = 20^{N+1}$ is a mathematical construction and is **not** a proposal to enumerate 20^{N+1} integers.

Scope note on generalization. If the fixed basepoint $a = 2$ and radius one are replaced by a general Cauchy radius $h \in (0,a)$ with $\sigma_h = (1+\sqrt{1+4(a-h)})/2$ and matrix factor $(1+2a/h)^N$, the monotonicity step above needs $X \ge e^{1/\sigma_h}$; the uniform integer assumption $X \ge 3$ suffices. Near $\sigma_h = 1$ the integrand need not decrease from $X = 2$. This qualifies that generalization only, not the concrete $a = 2$ theorem.

A smaller sufficient whole-row cutoff

Theorem 166D.2 (radius four-fifths). Put $\alpha_4 = (\sqrt{29/5} - 1)/2$. For all integers $N \geq 0$, $X \geq 2$,

$$\boxed{\|\mathcal{Q}_N[P - P_X](\cdot; 2)\|_2 \leq \frac{6^N X^{-\alpha_4}}{\sqrt{29/5}} \left(\frac{\log X}{\alpha_4} + \frac{1}{\alpha_4^2} \right).} \tag{166D.3}$$

Proof. On $|x - 2| \leq 4/5$ the principal root $\sqrt{1 + 4x}$ has real part and modulus at least $\sqrt{29/5}$. The preceding tail argument gives that disk supremum with 6^N omitted. Cauchy's estimate for the r-th Taylor coefficient gains $(5/4)^r$, and the exact Pascal conversion now has sum $\sum_r \binom{N}{r} 5^r = 6^N$. The tail comparison is decreasing from $X = 2$. □

For the prescribed schedule $X_N = 13^{N+1}$, the error tends to zero with an explicit linear prefactor and exponential base

$$\kappa_{13} = \frac{6}{13^{\alpha_4}} = 0.985728931213\ldots < 1, \qquad \boxed{\mathrm{RH} \iff \sup_N \|\mathcal{Q}_N[P_{13^{N+1}}](\cdot; 2)\|_2 < \infty.} \tag{166D.4}$$

Exactly, $(12/5)^2 < 29/5$ implies $\alpha_4 > 7/10$, and $13^7 = 62{,}748{,}517 > 60{,}466{,}176 = 6^{10}$ implies $13^{\alpha_4} > 6$. The equivalence follows from the triangle and reverse triangle inequalities and Theorem 166B.1. No uniform norm bound is proved. The earlier base-twenty schedule remains valid and has faster decay in its displayed majorant. Neither base nor disk is asserted optimal. The base-five result below concerns recovered outputs and mixed derivative blocks, not the whole row.

166E. Common-source recovery and the positive-scale error transfer

Use $\mathcal{P}_m$ from Section 155A, $c_{m,j} = [y^j]\mathcal{P}_m(y)^2$, $J = 2m$, and the recovery weights of (104A.6) for rates $b_0, \ldots, b_J$. If all observations share one moment perturbation $\delta\mu$, finite summation proves

$$\delta\Lambda_m(k) = \sum_{j=0}^{J} c_{m,j} b_j^k \delta\mu_j \quad \Longrightarrow \quad \boxed{\sum_{k=1}^{J+1} w_k \delta\Lambda_m(k) = \sum_{j=0}^{J} c_{m,j} \delta\mu_j.} \tag{166E.1}$$

Indeed $\sum_k w_k b_j^k = 1$. A common error is combined before absolute bounds are taken. Independent rounding residuals e_k still contribute $\sum_k |w_k||e_k|$: if $|\delta\mu_j| \leq \epsilon_j$, the complete bound is $\sum_j |c_{m,j}|\epsilon_j + \sum_k |w_k||e_k|$. The correlation must be established and preserved, not assigned after rounding independent outputs.

Theorem 166E.1 (a row-norm transfer at one positive scale). Fix $a > 0$, $N \geq J$, and a real analytic source f near a. Define $\mu_j^{(a)}[f] = (-1)^j f^{(j)}(a)/j!$ and use exactly the row operator of (163.3), with coefficients $B_{N,r}[f](a)$. Then

$$\begin{aligned}
\mu_j^{(a)}[f] &= \frac{1}{\binom{N}{j}a^j}\sum_{r=j}^{N}\binom{r}{j}B_{N,r}[f](a),\\
t_{m,N,a,k}(r) &= \sum_{j=0}^{\min(r,J)} c_{m,j}b_j^k\frac{\binom{r}{j}}{\binom{N}{j}a^j},\\
\Lambda_{m,a}^{f}(k) &:= \sum_{j=0}^{J} c_{m,j}b_j^k\mu_j^{(a)}[f] = t_{m,N,a,k}^{\mathsf{T}}B_N[f],\\
\left|\sum_{k=1}^{J+1} w_k\Lambda_{m,a}^{f}(k)\right| &\le \|t_{m,N,a,0}\|_2\|\mathcal{Q}_N[f](\cdot;a)\|_{L^2(e^{-t}dt)}.
\end{aligned} \tag{166E.2}$$

Proof. Differentiate the polynomial in (163.3) at $z=1$; equivalently use its falling-moment identity (163.5). This gives the first line. Substitution gives the next two, and (166E.1) gives $\sum_k w_k t_{m,N,a,k} = t_{m,N,a,0}$. Cauchy–Schwarz with the actual isometry (163A.3) proves the last line. No sign assumption is used. □

For $a=2$, $f=P-P_X$, and $\alpha=(\sqrt{5}-1)/2$, Theorem 166D.1 gives

$$\left|\sum_{k=1}^{2m+1} w_k\Lambda_{m,2}^{P-P_X}(k)\right| \le \|t_{m,N,2,0}\|_2\frac{5^N}{\sqrt{5}}X^{-\alpha}\left(\frac{\log X}{\alpha}+\frac{1}{\alpha^2}\right). \tag{166E.3}$$

This keeps the integer-value prime-power cutoff, not a substituted Euler product. The completed positive-scale approximation $S_X = 1/x + G - P_X$ satisfies $S_\xi - S_X = -(P-P_X)$, so the same absolute bound applies. Furthermore

$$\|t_{m,N,a,0}\|_2 \le \sqrt{N+1}\,\mathcal{P}_m(-1/a)^2, \qquad \mathcal{P}_m(-1/2) = 2^{m+1}-2^{-m}. \tag{166E.4}$$

The binomial ratio is at most one and $c_{m,j}$ has sign $(-1)^j$; these give the first bound. The recurrence (155A.1) gives the second. Thus the prescribed schedule $X_N = 20^{N+1}$ makes the transferred error tend to zero for each fixed m as $N\to\infty$. Equations (166E.5)–(166E.9) below prove uniform growing-degree versions.

The shifted output at $a>0$ is not an actual Li coefficient. The full P has a pole $1/x$ at the origin, while finite P_X is regular there; S_X retains the uncancelled elementary pole. Setting $a=0$ in (166E.2) is invalid. Section 155B supplies the correctly regularized boundary functional, but no directed all-order boundary error bound or source sign is inferred from (166E.3). The uniform cutoff-row norm in (166D.2) remains unproved. The finite-polynomial reconstruction in Section 166G is a different operation, proved using a completed-source disk and the full mixed-block amplification. It is not inferred from (166E.3); independent rounding retains a separate budget.

Growing degree and direct recovery

Write $\mathcal{T}_{m,N}[f] = \sum_{j=0}^{2m} c_{m,j}(-1)^j f^{(j)}(2)/j!$, realized through row degree $N \geq 2m$. The earlier row-norm bound already gives a useful growing window. Put $C_\alpha = 20^{-\alpha}(\log 20/\alpha + \alpha^{-2})/\sqrt{5}$. For $0 \leq m \leq \lfloor N/8 \rfloor$, (166E.4) and (166D.1) imply

$$|\mathcal{T}_{m,N}[P - P_{20^{N+1}}]| \leq 4C_\alpha (N+1)^{3/2}(\kappa 4^{1/8})^N \longrightarrow 0. \tag{166E.5}$$

Here $\alpha > 3/5$ and $5^8 < 2^{19}$ prove $\kappa 4^{1/8} < 1$ exactly. More generally this row-norm argument works for a fixed $m \leq \theta N$ when $\kappa 4^\theta < 1$ and $2m \leq N$. It remains available for analytic errors known through their row norms. The prime-tail functional itself admits a sharper direct estimate.

Theorem 166E.2 (the full admissible recovery range). Put $\alpha_3 = (\sqrt{6}-1)/2$. On the disk $|x-2| \leq 3/4$,

$$M_X := \sup_{|x-2|\leq 3/4} |P(x) - P_X(x)| \leq \frac{X^{-\alpha_3}}{\sqrt{6}}\left(\frac{\log X}{\alpha_3} + \frac{1}{\alpha_3^2}\right). \tag{166E.6}$$

For all integers $N \geq 0$, $X \geq 2$,

$$\boxed{\max_{0\leq m\leq \lfloor N/2 \rfloor} |\mathcal{T}_{m,N}[P - P_X]| \leq \frac{9\,3^N X^{-\alpha_3}}{4\sqrt{6}}\left(\frac{\log X}{\alpha_3} + \frac{1}{\alpha_3^2}\right).} \tag{166E.7}$$

Proof. On this disk the principal root has real part and modulus at least $\sqrt{6}$, proving (166E.6) by the same decreasing tail comparison. Cauchy's bound is $|f^{(j)}(2)|/j! \leq M_X(4/3)^j$. The alternating coefficients of $\mathcal{P}_m^2$ give $|\mathcal{T}_{m,N}[f]| \leq M_X \mathcal{P}_m(-4/3)^2$. The polynomial recurrence has characteristic roots 3 and 1/3 at this argument; its initial values give

$$\mathcal{P}_m(-4/3) = \frac{3^{m+1} - 3^{-m}}{2}, \qquad \mathcal{P}_m(-4/3)^2 \leq \frac{9}{4}\,9^m \leq \frac{9}{4}\,3^N. \tag{166E.8}$$

This proves the theorem, including $m = N = 0$. There is no whole-row amplification because N enters the recovered functional only through its admissibility condition $2m \leq N$. $\square$

For any integer $b \geq 5$, define

$$\begin{gathered} q_b = \frac{3}{b^{\alpha_3}}, \qquad C_b = \frac{9b^{-\alpha_3}}{4\sqrt{6}}\left(\frac{\log b}{\alpha_3} + \frac{1}{\alpha_3^2}\right), \\ \max_{2m\leq N} |\mathcal{T}_{m,N}[P - P_{b^{N+1}}]| \leq C_b (N+1) q_b^N \longrightarrow 0. \end{gathered} \tag{166E.9}$$

Indeed $(12/5)^2 < 6$ and $5^7 > 3^{10}$ give $\alpha_3 > 7/10$ and $q_b < 1$. For orientation, $q_5 = 0.934429044142\ldots$ and $q_{20} = 0.342142037896\ldots$; the exact inequalities carry convergence. The result covers the full admissible range, not just the coarser window (166E.5). It controls one common analytic source error. Independent observation residuals still cost $\sum_k |w_k||e_k|$.

No actual Li coefficient at the boundary or sign of a recovered output is certified by this positive-scale estimate.

166F. Matched cutoff matrices at one fixed positive scale

The derivative cutoff can be attached to an equivalent target at its own basepoint. This defines a separate positive-scale moment form; it does not identify that form with the boundary Li matrix or take a limit $a \downarrow 0$.

For real analytic f near a and a polynomial $p(y) = \sum_j p_j y^j$, put

$$\mathcal{K}_a[f;p] = \sum_j [y^j]p(y)^2 \, \frac{(-1)^j f^{(j)}(a)}{j!}, \qquad (K_{a,d}[f])_{rs} = \mathcal{K}_a[f;\mathcal{P}_r,\mathcal{P}_s]. \tag{166F.1}$$

The bilinear notation in the matrix replaces p^2 by $\mathcal{P}_r\mathcal{P}_s$. The reserve R_d remains exactly (155C.8), in this same polynomial basis.

Theorem 166F.1 (exact common-error block constant). Let f be holomorphic on a neighborhood of $|x-2| \le 3/4$ and real on the real axis, with disk supremum at most M. For every $d \ge 1$,

$$\boxed{\left\|\mathsf{R}_d^{-1/2} K_{2,d}[f] \mathsf{R}_d^{-1/2}\right\|_{\mathrm{op}} \le 125\Sigma_d M, \qquad \Sigma_d = \frac{9}{128}(9^d - 9^{-d}) + \frac{3d}{8}.} \tag{166F.2}$$

Proof. The third-kind polynomials (155D.4) have alternating coefficients, since their j roots lie in $(0,4)$. At $-4/3$ their recurrence and initial values give $V_j(-4/3) = (3^{j+1} + 3^{-j})/4$. For $p = \sum_{j<d} a_j V_j$, the coefficient absolute sum evaluated at $4/3$ is at most $\sum_{j<d} |a_j| V_j(-4/3)$. Cauchy's derivative bound and multiplication of these coefficient majorants give

$$|\mathcal{K}_2[f;p]| \le M \left(\sum_{j<d} |a_j| V_j(-4/3)\right)^2 \le M\Sigma_d \|p\|^2_{L^2(\nu_C)} \le 125 M\Sigma_d \mathcal{R}[p].$$

Summing the geometric terms in $V_j(-4/3)^2$ gives the stated exact Σ_d. The supremum over all nonzero real polynomials of degree below d proves the normalized operator-norm bound. □

The coarser $(9^d - 1)/8$ also bounds Σ_d, but is unnecessary here. This is the full mixed block: its highest derivative order is $2d-2$. For $f = P - P_X$ use M_X in (166E.6). With

$$X_d = 5^{2d-1}, \qquad \varepsilon_d = 125\Sigma_d \frac{X_d^{-\alpha_3}}{\sqrt{6}} \left(\frac{\log X_d}{\alpha_3} + \frac{1}{\alpha_3^2}\right), \tag{166F.3}$$

one has $\varepsilon_d = O(dq_5^{2d-2}) \to 0$. The parameter match is $N = 2d-2$, so $X_d = 5^{N+1}$. This controls every admissible mixed entry together in reserve norm, not the entire Bernstein–Laguerre row at base five.

The equivalent target at scale two

Fix $a = 2$ once and for all, and write

$$\begin{aligned} y_{a,\rho} &= (a+q_\rho)^{-1}, \\ \mathcal{K}_a[p] &= \mathcal{K}_a[S_\xi;p] = \sum_{[\rho]} m_\rho y_{a,\rho} p(y_{a,\rho})^2, \\ \mathcal{D}_a[p] &= \mathcal{R}[p] - \mathcal{K}_a[p], \\ \beta^+_{a,d} &= \sup_{\substack{p\neq 0\\ \deg p<d}} \mathcal{D}_a[p]/\mathcal{R}[p]. \end{aligned} \tag{166F.4}$$

The actual shifted weights have finite absolute mass. Their bounded support accumulates only at zero, and

$$\Im y_{a,\rho} = -\frac{\Im q_\rho}{|a+q_\rho|^2}. \tag{166F.5}$$

Thus the shift preserves nonreality. Under RH the support is positive real and contained strictly inside $[0,4]$.

Theorem 166F.2 (positive-scale criterion). A finite uniform upper bound on $\beta^+_{2,d}$, a fixed polynomial upper bound, or an upper bound at every exponential rate in d is equivalent to RH.

Proof. Under RH $\mathcal{K}_2$ is positive and $\beta^+_{2,d} \le 1$. For the finite-bound converse repeat Theorem 155D.1 with shifted moments: their generating function is $S_\xi(a-z)$ and has genuine poles at $z = a + q_\rho$. Compact support of the hypothetical positive representing measure excludes a nonreal such pole. For the subexponential converse define the exterior root by $w+w^{-1} = 2-y_{2,\rho}$ and let $\mathfrak{L}_2 = \sup r(y_{2,\rho})$. If a nonreal point exists, $\mathfrak{L}_2 > 1$ is attained finitely often, with a strict gap to the remaining radii. The finite annihilator and real affine phase adjustment of Theorem 155D.3 apply to these shifted points and their summable weights. They yield $\beta^+_{2,d} \ge c\mathfrak{L}_2^{2d}$ at every sufficiently large rank. This contradicts any all-rate upper estimate. The universal polynomial upper estimate on test values proves the matching rate, exactly as in (155D.10). The rate is $\mathfrak{L}_2$, not an identification with the boundary Li modulus $\mathfrak{L}$. □

The cutoff approximates this very target

Retain the full completion and define

$$S_X(x) = \frac{1}{x} + G(x) - P_X(x), \qquad \widehat{\mathsf{D}}_{2,d} = \mathsf{R}_d - K_{2,d}[S_{X_d}], \qquad \widehat{\beta}^+_{2,d} = \lambda_{\max}(\mathsf{R}_d^{-1/2}\widehat{\mathsf{D}}_{2,d}\mathsf{R}_d^{-1/2}). \tag{166F.6}$$

The elementary and Gamma channels are present, not truncated out. Since $S_X - S_\xi = P - P_X$, the sign of the exact error is

$$\mathsf{D}_{2,d} - \widehat{\mathsf{D}}_{2,d} = K_{2,d}[P - P_{X_d}], \qquad |\widehat{\beta}^+_{2,d} - \beta^+_{2,d}| \le \varepsilon_d \longrightarrow 0. \tag{166F.7}$$

The second assertion is the variational eigenvalue bound applied to (166F.2). Hence

$$\boxed{\begin{aligned} \text{RH} &\iff \sup_d \widehat{\beta}^+_{2,d} < \infty \\ &\iff \exists C, A \geq 0\ \forall d : \widehat{\beta}^+_{2,d} \leq C(1+d)^A \\ &\iff \forall \epsilon > 0\ \exists C_\epsilon < \infty\ \forall d : \widehat{\beta}^+_{2,d} \leq C_\epsilon e^{\epsilon d}. \end{aligned}} \tag{166F.8}$$

The vanishing error cannot hide the eventual exponential escape. A fixed unbounded rank subsequence suffices for the all-rate condition by that same eventual escape, with rates measured in the actual rank. The varying-cutoff matrices need not be nested, so their extreme eigenvalues need not be monotone.

No upper bound in (166F.8) is proved from the prime source. This matched positive-scale approximation bypasses a boundary transfer for this route; it is not itself that transfer. Section 166G separately reconstructs the actual boundary matrix with Taylor degree $15d - 1$ and cutoff 8^{15d}. The raw cutoff retains its origin pole. Independent entry-rounding errors need their own matrix estimate in addition to the common analytic bound.

166G. Controlled reconstruction of the actual boundary matrix

The raw cutoff $S_X = 1/x + G - P_X$ has an uncancelled origin pole. The construction below instead evaluates a finite Taylor polynomial at zero. It uses the same boundary moments and compensated reserve as Section 155C, not the shifted target $K_{2,d}$ of Section 166F:

$$\mu_j = \frac{(-1)^j S_\xi^{(j)}(0)}{j!}, \qquad K_d = \mathsf{C}_d[\mu_{r+s}]\mathsf{C}_d^{\mathsf{T}}, \qquad \mathsf{D}_d = \mathsf{R}_d - K_d. \tag{166G.1}$$

Here C_d is the coefficient matrix of $\mathcal{P}_0, \ldots, \mathcal{P}_{d-1}$. The cutoff includes full elementary/Gamma completion and prime powers by their integer value; it is not a truncated Euler product. At the safe point two, $S_X - S_\xi = P - P_X$.

Lemma 166G.1 (completed disk). The carried low-height exclusion $|\Im\rho| > 1$ gives holomorphy on a neighborhood of $|z-2| \leq 23/8$ and

$$\sup_{|z-2|\leq 23/8} |S_\xi(z)| \leq 16\lambda_1 < 1. \tag{166G.2}$$

Proof. For $q = A + iB$ one has $A = \gamma^2 + \beta(1-\beta) > 1$ and $|B| < |\gamma| < A$. On this disk $\Re z \geq -7/8$, so $|z+q|^{-1} \leq (A-7/8)^{-1} \leq 8/A \leq 16\Re(1/q)$. The folded sum converges normally by this summable majorant, whose sum is $16\lambda_1$. Section 155C.1 gives $\lambda_1 < 1/16$. Every pole lies strictly outside a neighborhood of the disk. This uses the low-height exclusion, not RH or an unknown positive folded measure. □

For rank $d \geq 1$ set $L_d = 15d - 1$, $X_d = 8^{15d}$ and

$$\boxed{\widehat{S}_d(z) = \sum_{\ell=0}^{L_d} \frac{S_{X_d}^{(\ell)}(2)}{\ell!}(z-2)^{\ell}.} \tag{166G.3}$$

Write $\alpha = (\sqrt{6}-1)/2$, $r = 18/23$, $q_T = 3/8^{\alpha}$ and

$$\begin{aligned} E_d^{\partial} &= \frac{23}{5} r^{15d} + \frac{1}{2\sqrt{6}} \left(\frac{15d \log 8}{\alpha} + \frac{1}{\alpha^2} \right) q_T^{15d}, \\ \Theta &= 36(18/23)^{15} < 1. \end{aligned} \tag{166G.4}$$

Theorem 166G.2 (boundary disk and mixed block). Put $\widehat{\mu}_j^{(d)} = (-1)^j \widehat{S}_d^{(j)}(0)/j!$ and $\widehat{K}_d^{\partial} = \mathsf{C}_d[\widehat{\mu}_{r+s}^{(d)}]\mathsf{C}_d^{\mathsf{T}}$. Then

$$\begin{aligned} \sup_{|z|\le 1/4} |S_\xi(z) - \widehat{S}_d(z)| &\le E_d^{\partial}, \\ \|\mathsf{R}_d^{-1/2}(\widehat{K}_d^{\partial} - K_d)\mathsf{R}_d^{-1/2}\|_{\mathrm{op}} \le \varepsilon_d^{\partial} &:= 125\frac{36^d-1}{35} E_d^{\partial} = O(d\Theta^d) \longrightarrow 0. \end{aligned} \tag{166G.5}$$

Proof. Let T_L denote Taylor truncation at two. The completed remainder on $|z| \le 1/4$ is at most $r^{L+1}/(1-r) = (23/5)r^{L+1}$, since $|z-2| \le 9/4$. For $f_X = P - P_X$, the disk-3/4 estimate (166E.6) is $M_X = X^{-\alpha}(\log X/\alpha + \alpha^{-2})/\sqrt{6}$. Consequently $|T_L f_X(z)| \le M_X \sum_{\ell=0}^{L} 3^{\ell} \le M_X 3^{L+1}/2$. The exact polynomial identity

$$S_\xi - T_L S_X = (S_\xi - T_L S_\xi) - T_L(P - P_X) \tag{166G.6}$$

proves the first bound after $L+1 = 15d$ and $X = 8^{15d}$. Neither term continues the raw cutoff through its pole.

For a holomorphic boundary error f of supremum E, Cauchy bounds $|f^{(j)}(0)|/j!$ by $E4^j$. Write $p = \sum_{j<d} a_j V_j$ in the Catalan-orthonormal third-kind basis of Section 155D. Its alternating coefficients and the exact value at -4 give

$$V_j(-4) = \frac{\ell^{j+1} + \ell^{-j}}{\ell+1} \le 6^j, \quad \ell = 3 + 2\sqrt{2}, \qquad |\mathcal{K}_0[f;p]| \le E\frac{36^d-1}{35}\|p\|_{L^2(\nu_C)}^2, \tag{166G.7}$$

where $\mathcal{K}_0[f;p] = \sum_j [y^j]p^2(-1)^j f^{(j)}(0)/j!$. Cauchy–Schwarz proves the last inequality from $E(\sum |a_j| V_j(-4))^2$. Apply $\|p\|_{L^2(\nu_C)}^2 \le 125\mathcal{R}[p]$ and take the absolute Rayleigh supremum. This controls all mixed entries simultaneously. Finally $\alpha > 2/3$ gives $q_T < 3/4 < 18/23$, and the exact integer comparison $36\,18^{15} < 23^{15}$ proves the claimed decay. □

The required moment translation is finite:

$$c_\ell^X = \frac{(-1)^\ell S_X^{(\ell)}(2)}{\ell!}, \qquad \widehat{\mu}_j^{(d)} = \sum_{\ell=j}^{15d-1} \binom{\ell}{j} 2^{\ell-j} c_\ell^{X_d}. \tag{166G.8}$$

The highest boundary moment is μ_{2d-2}, while the source degree is $15d-1$. For $m<d$ the odd-Li diagonal error is at most $\varepsilon_d^{\partial}(\mathsf{R}_d)_{mm}$. This is a signed polynomial identity, not a replacement positive measure.

The matched boundary criterion and its error budget

Define $\widehat{\mathsf{D}}_d^{\partial} = \mathsf{R}_d - \widehat{K}_d^{\partial}$ and its largest normalized eigenvalue $\widehat{\beta}_d^{\partial,+}$. The error sign and variational estimate are

$$\mathsf{D}_d - \widehat{\mathsf{D}}_d^{\partial} = \widehat{K}_d^{\partial} - K_d, \qquad |\widehat{\beta}_d^{\partial,+} - \beta_d^{+}| \le \varepsilon_d^{\partial} \longrightarrow 0. \tag{166G.9}$$

Section 155D therefore gives

$$\boxed{\begin{aligned} \mathrm{RH} &\iff \sup_d \widehat{\beta}_d^{\partial,+} < \infty \\ &\iff \exists C, A \ge 0\ \forall d: \quad \widehat{\beta}_d^{\partial,+} \le C(1+d)^A \\ &\iff \forall \epsilon > 0\ \exists C_\epsilon < \infty\ \forall d: \quad \widehat{\beta}_d^{\partial,+} \le C_\epsilon e^{\epsilon d}. \end{aligned}} \tag{166G.10}$$

No bound in (166G.10) is proved from the arithmetic source. The order of operations is complete finite source at two, finite Taylor polynomial, boundary moments, then reflected mixed matrix. Holding X fixed while sending L to infinity would revive the original pole obstruction. Section 166F's smaller positive-scale cutoff is a separate result.

If the coefficients $S_X^{(\ell)}(2)/\ell!$ have independent errors e_ℓ, add $125(36^d-1)\sum_{\ell=0}^{15d-1}|e_\ell|(9/4)^\ell/35$ to the matrix error in (166G.5). The common analytic error is not a rounding budget. The bundled exact rational regression uses the retained synthetic model $q_0 = 17/4$ (multiplicity two), $q_\pm = 147/16 \pm 3i/2$. Its positive shifted moments through degree 284 reconstruct a negative $\lambda_{37}^{*} \in (-0.598, -0.597)$, with rational error below 10^{-30}. This tests the adapter, not the actual zeta source or an all-order upper bound.

Technical chapter XV. Remaining proof obligations and countermodels

The full criteria and proved finite results have been separated above. These final references identify the remaining source implication and its countermodels.

66. Finite results within the exact criteria

Reader §R12 gives the current scalar proof channels; §13 gives the zero-assisted finite rectangle. Technical §§92–93 and 138 distinguish global order eight from rank twelve at one node. These finite theorems are summarized once in Reading Volume §R22.

Their exact converse has no finite stopping rank: §49 gives an open interval with infinitely many negative rungs if RH fails, while §§51 and 145 give finite witnesses at every prescribed scale. A uniform source theorem is still needed to establish the positive side at every order.

67. The remaining source implication

The all-node inequality (54.8), restated at Reader (23.1), remains unproved. Sections 155D–155E reduce equivalent source tasks to the compensated form's one-sided growth or to ordinary-Laguerre curvature. A polynomial upper bound on either parity of I_n suffices under the explicit progression theorem; no such bound is proved. The compensation has a proved polynomial bound, but the signed prime integral has not.

At fixed positive scale two, Section 166F aligns a complete cutoff matrix with its own RH-equivalent target, with vanishing error at 5^{2d-1}. Section 166G separately reconstructs the actual boundary matrix by a controlled finite Taylor polynomial. Both one-sided source upper bounds remain open. Whole-row convergence at 13^{N+1} or 20^{N+1} does not supply them. Sections 155F–155G show why an envelope, positive prime-power weights and a long fixed exact prime prefix are insufficient. Sections 155H–155I restore the exact divisor law and identify its Mellin error with the denominator residual's Hardy norm. The remaining sufficient target is (155H.6), below every positive power of the actual prefix length; the two tested families do not meet it.

The independent seventh-rung source certificate is the next finite-order task. Global $W_7 > 0$ is not established by the independent source channel; $W_7 \rightsquigarrow F^{(14)}$ is the first open source rung. No historical certificate has been promoted by these all-order reformulations.

69. Smallest countermodels that remain decisive

- A coarse one-channel sample cannot distinguish a frequency from its Nyquist mirror.
- A nonnegative function can have a Fourier transform of changing sign.
- A fixed finite moment/Weil compression cannot determine a meromorphic target Cauchy functional.
- A finite set of Li/Hankel inequalities can be passed by an off-axis synthetic quartet.
- Any fixed positive Widder prefix can coexist with a later negative rung in a finite synthetic Stieltjes test model.
- The recurrence $W_{k+1} = -(2k + 1)W_k' - xW_k''$ does not preserve positivity without derivative control.
- Matching minimum eigenvalues does not determine ground-state parity.
- Exact roots-of-unity cancellation does not survive nonlinear logarithmic phase without curvature control.

The fixed counting and prime-supported countermodels in Sections 155F–155G additionally retain the specified positivity and PNT hypotheses without the actual arithmetic cancellation. The divergent balanced primitive product in Section 155H rejects that one construction, not all inverse-factor methods.

These countermodels should remain beside the positive theory. They prevent the next branch from silently rebuilding an already closed route.

Summary of the technical boundary

The Dossier starts with exact triangular arithmetic and reaches the completed source without identifying its comparison measures with the actual folded zero data. Its common index set is the reflection-pair set, with algebraic multiplicity retained. The canonical product and resolvent therefore count an off-line quartet as two conjugate folded nodes. This indexing is sufficient to recover the first-Li normalization and the Widder-zero-heat identities without an RH assumption.

The inherited finite source certificates and exact arithmetic identities remain the results recorded in the Reading Volume's status key. Their receipt provenance is v5.0, not a newly claimed replay. The independently unproved next source rung is W_7; the all-order, all-node and all-degree requirements in the corresponding criteria remain unproved. Countermodels exclude the listed shortcuts under their stated hypotheses, not every possible route to the required source inequalities.

Thus the proofs establish their own domains, the certificates establish their own finite ranges, and the empirical appendix establishes neither. Version 5.1 clarifies those interfaces but advances no RH status. No entropy construction or semantic interpretation is a premise of this Dossier.

Part E. Empirical context and historical transcriptions

EVIDENCE Under the single master status key in the Reading Volume, everything in this Part is numerical or transcribed evidence. It supports no theorem in Chapters I–XV, and no result anywhere in the program depends on it. It is retained so that the empirical claims that circulated alongside this work stay attached to the exact statements that replaced them.

Section 168 gives the exact counting and triangular-coordinate identities, including the transport rule (168.6): an unchanged event requires transporting the complete selection rule – windows, merging and support conditions – and applying T_x to the cumulative smooth zero count is a different operation. The historical comparisons below provide context and possible future tests; they are not an RH proof.

The broader report [62] scans 2.30–3.20 with lower controls and describes an enrichment shelf near 2.70–2.81. The rational marker $11/4 = 2.75$ is inside that reported interval. It is not established as an endpoint of that shelf, and it is not the mean normalized spacing. The statistic concerns random-surrogate preceding-marker hits near small-gap valleys. Different supported-block sets must not be treated as a common-support ranking. The five-marker figure retained below is a local comparison and cannot show the full shelf. The raw gap arrays and complete randomization replay are not included here, so no significance level and no shelf boundary is asserted.

The final three pages reproduce original report pages 11–13 as historical pages: not a fresh replay, and not a confirmation of every interpretation in that report. This Part uses its own `S` label namespace, and §168 retains tags (168.2)–(168.6).

Historical comparison, as transcribed

Historical section 168. What the reported spacing experiments contribute

The two historical reports [61–62] are retained as empirical instruments. They test different coordinates and have different controls. The present revision transcribes their reported counts and arithmetic comparisons; their raw gap arrays and full randomization replay are not included here. No fresh search-adjusted significance level is claimed.

Row-sector audit near the proposed modulus window

The orthogonal follow-up [61] scans 401 moduli from 800 to 1200 using six row sectors and 500 permutations. Its label "base-6" means six bins, not positional base-six notation. The windows give:

window	best reported modulus	rank of 1009	adjusted p at best modulus	adjusted p at 1009
900	1133	48	0.079840	1
1000	1087	151	0.235529	1
1100	1133	143	1	1
1300	1022	58	0.938124	1

This audit does not validate a special 990/1009 row-sector mechanism. It also does not test every possible gcd or TFG partition. A reduced-ray experiment should declare $q = n/\gcd(n,k)$ and its reciprocal weights in advance, then retain the scan correction. Arithmetic equality of totients or a useful decimal period remains true independently of this outcome.

A localized-enrichment comparison near 2.75

The second report [62] studies unfolded nearest-neighbor gaps $s_n = N_0(\gamma_{n+1}) - N_0(\gamma_n)$, with $N_0(T) = \frac{T}{2\pi}\log\frac{T}{2\pi} - \frac{T}{2\pi} + 7/8$. Its active marker is

$$a_+ = \frac{\pi}{2} + \frac{2}{\pi} + \cos 1 \approx 2.747718405031 \qquad a_- = \frac{\pi}{2} + \frac{2}{\pi} - \cos 1 \tag{S.1}$$

For $r = \pi - 3$, the identity $\cos 1 = \sin[(1+r)/2]$ is exact. The approximation $\cos 1 \approx 1/2 + 2r^2$ has error about 0.000205346767 at this fixed r; it is not the Taylor expansion of that sine function about $r = 0$. Both the exact marker and the useful approximation can be retained with this distinction stated.

The original reported 22-block comparison totals 736 observed preceding hits versus 218 random-surrogate hits, ratio 3.376146789; each of its printed block ratios exceeds one. The broader follow-up shows a band, with several neighboring markers:

marker	supported blocks	observed hits	surrogate hits	ratio
a_+	21	702	218	3.22018
11/4	22	743	224	3.31696
$7\pi/8$	21	692	190	3.64211
2.740	22	784	218	3.59633
2.780	21	570	158	3.60759

The primary summary reports 736 observed hits and 218 surrogate hits over 22 supported blocks. The follow-up row for the same active marker reports 702 and 218 over 21 supported blocks. These are different reported aggregates. The printed tables do not establish that the difference is exactly one removed block, or that the repeated surrogate count means the same random sample was reused. Those questions require the block ledger and the randomization record, neither of which is included here.

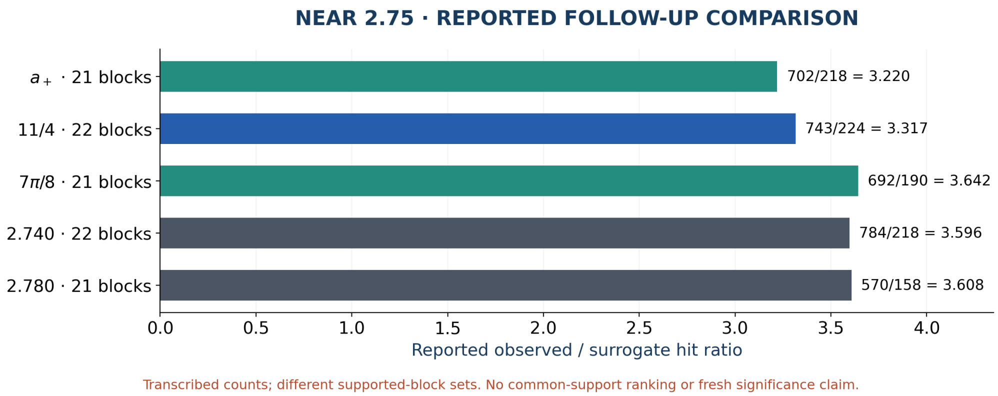

Figure 64: Reported follow-up counts near 2.75, transcribed from the empirical report [62]. Each label shows its own supported-block count. Observed/surrogate ratios use different block sets and cannot by themselves rank the markers on common support.

The denominator in this table counts random-surrogate hits, not hits at the sign-reversed marker a_-. The displayed support sets differ, so these ratios do not select a unique winner. The report's statistic searches a preceding window for a marker near a small-gap valley; it is a conditional gap-pattern statistic. An unconditional pair-correlation value at separation 2.75 does not test the same event. Its random-center controls likewise do not preserve all local gap correlations.

The useful next comparison is specific: use a common set of blocks for a_+, $7\pi/8$, $11/4$, and nearby prespecified controls; retain the same windows, merging rules, exclusions, and support thresholds; then run the complete statistic on held-out zeros and an appropriate correlated null, such as a matched sine-kernel/GUE simulation. Include the full selection procedure in any significance calculation. A decimal or triangular coordinate can organize this experiment without predetermining its result.

The exact arithmetic of §§98 and 167, the measured enrichment band, and the source positivity frontier therefore remain available side by side. Their proposed connection is a research question requiring a transport identity or a successful independent test. RH remains open.

Sources for this Part

[61] *A Search-Adjusted Audit of Row-Sector Modulus Signals in Terminal Zeta-Zero Data*, unpublished historical report. The table above preserves the transcribed audit; it has not been rerun.

[62] *A Finite-Count Search for Localized Enrichment Near 2.75 in Unfolded Zeta-Zero Gaps*, unpublished historical report, 24 pages. The final three pages of this Part reproduce pages 11–13 of that report; those pages match the original copy in both extracted text and rendered

pixels.

Original wider-scan pages follow

The next three pages reproduce pages 11, 12 and 13 of the original 24-page report, in order. They include the active-marker follow-up, alternative-marker support, and the broader threshold scan. Their original titles and page furniture are preserved so the historical source can be identified.

Their original page numbers, figure numbers, table numbers and internal references — including "Appendix D", the "R141H" and "R142A" ledgers and the named companion rails — belong to that report, not to this volume and not to this supplement. Consult the complete report for those references. The facsimiles preserve historical evidence; they are not a fresh replay and not a confirmation of every interpretation in that report.

References

1. E. Bombieri, *The Riemann Hypothesis - official problem description*, Clay Mathematics Institute, Millennium Prize Problems, Clay problem description.
2. NIST Digital Library of Mathematical Functions, Sections 5.5, 5.7–5.9, 5.11, 24.4, 25.4, 25.10, 25.11, and 25.16; in particular Hurwitz special values and derivatives, zero counting, and Gamma and digamma asymptotics.
3. E. C. Titchmarsh, revised by D. R. Heath-Brown, *The Theory of the Riemann Zeta-Function*, 2nd ed., Oxford University Press, 1986.
4. X.-J. Li, "The positivity of a sequence of numbers and the Riemann hypothesis," *Journal of Number Theory* 65 (1997), no. 2, 325–333, DOI 10.1006/jnth.1997.2137.
5. E. Bombieri and J. C. Lagarias, "Complements to Li's criterion for the Riemann hypothesis," *Journal of Number Theory* 77 (1999), no. 2, 274–287, DOI 10.1006/jnth.1999.2392.
6. L. de Branges, *Hilbert Spaces of Entire Functions*, Prentice-Hall, 1968.
7. G. Csordas, T. S. Norfolk, and R. S. Varga, "The Riemann hypothesis and the Turan inequalities," *Transactions of the American Mathematical Society* 296 (1986), 521-541.
8. J. Huckstead, *Divisor-Band Bijections and Totient Shells in the Triangular-Fractional Grid*, version 5, Zenodo (2026), DOI 10.5281/zenodo.21440877.
9. J. Huckstead, *Triangular Addressing, Null Coordinates, and Reciprocal-Metallic Locks in a Scale-Covariant Plane Geometry*, Working Draft III, Zenodo (2026), DOI 10.5281/zenodo.21444929.
10. J. Huckstead, *From Measure to Flux: Energy-Conjugate Bookkeeping and Exact Semidiscrete Scattering in Finite Radial Wave Models*, publication layer v0.6.13, Zenodo (2026), DOI 10.5281/zenodo.21444339.
11. J. Huckstead, *Two-Term Asymptotics for the Total Variation of Exponentially Weighted Laguerre Polynomials*, v0.1, Zenodo (2026), DOI 10.5281/zenodo.21861619.
12. J. Sondow and C. Dumitrescu, "A monotonicity property of Riemann's xi function and a reformulation of the Riemann hypothesis," *Periodica Mathematica Hungarica* 60 (2010), 37-40, DOI 10.1007/s10998-010-1037-3; arXiv:1005.1104.
13. Y. Matiyasevich, F. Saidak, and P. Zvengrowski, "Horizontal monotonicity of the modulus of the Riemann zeta function and related functions," arXiv:1205.2773 (2012).
14. J. C. Lagarias, "On a positivity property of the Riemann xi-function," *Acta Arithmetica* 89 (1999), 217-234.
15. A. D. Sokal, "Real-variables characterization of generalized Stieltjes functions," *Expositiones Mathematicae* 28 (2010), 179-185; arXiv:0902.0065.

16. D. V. Widder, "The Stieltjes transform," *Transactions of the American Mathematical Society* 43 (1938), 7-60.
17. F. Johansson, "Rigorous high-precision computation of the Hurwitz zeta function and its derivatives," arXiv:1309.2877 (2013).
18. GNU MPFR Project, *GNU MPFR 4.2.2 Manual*, https://www.mpfr.org/mpfr-current/mpfr.html.
19. F. Hausdorff, "Summationsmethoden und Momentfolgen. I," *Mathematische Zeitschrift* 9 (1921), 74-109, DOI 10.1007/BF01378337.
20. F. Hausdorff, "Summationsmethoden und Momentfolgen. II," *Mathematische Zeitschrift* 9 (1921), 280-299, DOI 10.1007/BF01279032.
21. A. Pringsheim, "Ueber Functionen, welche in gewissen Punkten endliche Differentialquotienten jeder endlichen Ordnung, aber keine Taylor'sche Reihenentwickelung besitzen," *Mathematische Annalen* 44 (1894), 41-56, EuDML 157700.
22. K. Löwner, "Über monotone Matrixfunktionen," *Mathematische Zeitschrift* 38 (1934), 177-216, DOI 10.1007/BF01170633.
23. R. L. Schilling, R. Song, and Z. Vondraček, *Bernstein Functions: Theory and Applications*, 2nd ed., De Gruyter, 2012, DOI 10.1515/9783110269338.
24. M. Riesz, "Sur l'hypothèse de Riemann," *Acta Mathematica* 40 (1916), 185-190, DOI 10.1007/BF02418544.
25. L. Báez-Duarte, "A sequential Riesz-like criterion for the Riemann hypothesis," *International Journal of Mathematics and Mathematical Sciences* 2005, 3527-3537, DOI 10.1155/IJMMS.2005.3527.
26. A. Agarwal, M. Garg, and B. Maji, "Riesz-type criteria for the Riemann hypothesis," *Proceedings of the American Mathematical Society* 150 (2022), DOI 10.1090/proc/16064.
27. H. L. Montgomery and R. C. Vaughan, "Hilbert's inequality," *Journal of the London Mathematical Society* (2) 8 (1974), 73–82.
28. H. L. Montgomery, *Ten Lectures on the Interface Between Analytic Number Theory and Harmonic Analysis*, CBMS Regional Conference Series in Mathematics 84, American Mathematical Society, 1994.
29. H. Iwaniec and E. Kowalski, *Analytic Number Theory*, American Mathematical Society Colloquium Publications 53, 2004.
30. J. B. Conrey and A. Gamburd, "Pseudomoments of the Riemann zeta-function and pseudomagic squares," arXiv:math/0307213v2; *Journal of Number Theory* 117 (2006).
31. M. Wahl, "On the mod-Gaussian convergence of a sum over primes," arXiv:1201.5295v3 (2013), especially equation (1.4).
32. M. Gerspach and Y. Lamzouri, "Low pseudomoments of Euler products," arXiv:2103.03870 (2021).
33. A. Connes, "The Riemann Hypothesis: Past, Present and a Letter Through Time," arXiv:2602.04022v1 (2026).
34. D. S. P. Salazar, "Order-Moment Transport and Hankel Determinants in Special-Function Inequalities," arXiv:2606.31647v2 (2026).
35. M. Bhowmik, A. Chatterjee, and M. Putinar, "Holomorphic Interpolation of Multivariate Completely Monotone Functions," arXiv:2606.12102 (2026).

36. L. Guth and J. Maynard, "New large value estimates for Dirichlet polynomials," *Annals of Mathematics* 203 (2026), no. 2, 623–675, DOI 10.4007/annals.2026.203.2.6; arXiv:2405.20552v2.

37. B. Chen, V. Gupta, and Y. C. Li, "Large Value Estimates for Dirichlet Polynomials with Characters and Zero Density of Dirichlet L-Functions," arXiv:2507.08296v2 (2026).

38. A. Bondarenko, O. F. Brevig, E. Saksman, K. Seip, and J. Zhao, "Pseudomoments of the Riemann zeta function," *Bulletin of the London Mathematical Society* 50 (2018), no. 4, 709–724, DOI 10.1112/blms.12183; arXiv:1701.06842v3.

39. E. Lill, "Résolution graphique des équations numériques de tous les degrés à une seule inconnue, et description d'un instrument inventé dans ce but," *Nouvelles Annales de Mathématiques*, 2e série, 6 (1867), 359–362.

40. E. Lill, "Résolution graphique des équations algébriques qui ont des racines imaginaires," *Nouvelles Annales de Mathématiques*, 2e série, 7 (1868), 363–367.

41. B. Bellotti and P.-J. Wong, "Improved estimates for the argument and zero-counting function of the Riemann zeta-function," arXiv:2412.15470v2 (2025), accepted by *Mathematics of Computation*.

42. D. J. Platt and T. S. Trudgian, "The Riemann hypothesis is true up to $3 \cdot 10^{12}$," *Bulletin of the London Mathematical Society* 53 (2021), 792–797; arXiv:2004.09765.

43. O. Dobsch, "Matrixfunktionen beschränkter Schwankung," *Mathematische Zeitschrift* 43 (1938), 353–388.

44. W. F. Donoghue, Jr., *Monotone Matrix Functions and Analytic Continuation*, Grundlehren der mathematischen Wissenschaften 207, Springer, 1974.

45. Euclid, *The Thirteen Books of The Elements*, translated with introduction and commentary by T. L. Heath, 2nd ed., Dover, 1956, Book VII, Definition 22, and Book IX, Proposition 36.

46. L. E. Dickson, *History of the Theory of Numbers*, Volume I: Divisibility and Primality, Carnegie Institution of Washington, 1919, Chapter I.

47. A. Groskin, "A finite Guinand–Weil dictionary and archimedean tail order for the truncated Weil quadratic form," arXiv:2607.02828v3 (2026), archival DOI 10.5281/zenodo.21124802.

48. A. Connes, C. Consani, and H. Moscovici, "Zeta Spectral Triples," arXiv:2511.22755v1 (2025), forthcoming in the EMS Lecture Notes in Mathematics volume *Applications of Noncommutative Geometry to Gauge Theories, Field Theories, and Quantum Space-Time*.

49. A. Connes and W. D. van Suijlekom, "Quadratic Forms, Real Zeros and Echoes of the Spectral Action," arXiv:2511.23257v1 (2025).

50. A. Connes, C. Consani, and H. Moscovici, "Zeta zeros and prolate wave operators," arXiv:2310.18423v2 (2024).

51. M. Suzuki, "Weil's quadratic form via the screw function," arXiv:2606.09096v2 (2026).

52. A. Groskin, "High-Precision Approximation of Riemann Zeros via the Truncated Weil Form," arXiv:2605.20224v4 (2026), archival DOI 10.5281/zenodo.19546514.

53. E. W. Weisstein, "Gamma Function," *MathWorld–A Wolfram Web Resource*, MathWorld entry, page captured 27 August 2026.

54. *Hermitian Spaces*, Chapter 12 lecture slides, CIS 5150, University of Pennsylvania, Sections 12.1–12.2, especially the definitions of sesquilinear/Hermitian forms and the complex polarization identities, https://www.cis.upenn.edu/~cis5150/cis515-20-sl9.pdf.

55. J. Huckstead, *The Polar Shell Renderer: A Lens, Not a Law*, revised 9 July 2026, Zenodo, DOI 10.5281/zenodo.21280464.

56. A. Voros, "Zeta functions for the Riemann zeros," *Annales de l'Institut Fourier* 53 (2003), no. 3, 665–699; first preprint 2001, arXiv:math/0104051v4. Equations (40)–(41), (59), (74), (81), and (91)–(95), and Table 1 supply the classical spectral-zeta formulas used here.

57. A. Voros, "Erratum - Zeta functions for the Riemann zeros," *Annales de l'Institut Fourier* 54 (2004), no. 4, 1139, DOI 10.5802/aif.2046.

58. J. B. Keiper, "Power series expansions of Riemann's ξ function," *Mathematics of Computation* 58 (1992), no. 198, 765–773, DOI 10.2307/2153215.

59. NIST, *Digital Library of Mathematical Functions*, §§5.4–5.5, Gamma special values, recurrence, reflection, and duplication. Official formulas.

60. S. M. Eisenberg, "Moment Sequences and the Bernstein Polynomials," *Canadian Mathematical Bulletin* 12 (1969), no. 4, 401–411. DOI 10.4153/CMB-1969-050-8. Classical background; the source-specific growth argument is printed independently in §164, without a claim of literature novelty.

61. *A Search-Adjusted Audit of Row-Sector Modulus Signals in Terminal Zeta-Zero Spacing Residuals*, unpublished historical report (2026), 10 pages. Only its reported tables are used; its raw arrays and permutation replay are not part of this work.

62. *A Finite-Count Search for Localized Enrichment Near 2.75 in Unfolded Riemann Zeta-Zero Gap Coordinates*, unpublished historical report, May 2026, 24 pages. Its reported counts and stated design are compared in §168.

63. NIST, *Digital Library of Mathematical Functions*, sine Maclaurin series and Euler infinite product, and the fourth-kind Chebyshev representation. The triangular factorization in (PR.6) is a direct regrouping of the factorial coefficients; Gamma reflection is covered by [59].

64. L. Euler, *De formulis exponentialibus replicatis*, E489 (1778), original paper in the Euler Archive. The fixed-point differentiation and stability calculation used here are displayed in §R5E.

65. A. Edelman and G. Strang, *Pascal Matrices*, MIT course essay. Classical symmetric Pascal matrix, Vandermonde factorization, and determinant one. Section 163A identifies this matrix inside the completed-source energy.

66. Y. Lamzouri, *A new proof that more than two thirds of the zeros of the Riemann zeta function are simple or on the critical line*, arXiv:2609.02882v2, 17 pages. Proposition 2.1, Lemma 3.1 and Theorem 1.1 are the statements compared in §159. Its notation is local to that paper; in particular its critical-line counting symbol is not the smooth approximation N_0 of §168.

Shared references [67]–[78] are listed in the Reading Volume; the numbering below retains that common bibliography.

79. H. L. Montgomery, "The pair correlation of zeros of the zeta function," in *Analytic Number Theory*, Proceedings of Symposia in Pure Mathematics 24, American Mathematical Society, 1973, 181–193. The historical theorem and conjectured density are distinguished in Section 61A; the comparison does not import the conjecture as an actual-source estimate.

80. L. Elaissaoui and Z. E.-A. Guennoun, "Fourier expansion of the Riemann zeta function and applications," *Journal of Number Theory* 211 (2020), 113–138, DOI 10.1016/j.jnt.2019.09.025; preprint arXiv:1809.02829. Theorem 1.1 and Corollary 2.4 of the preprint (v2): the zeta Fourier-coefficient and Parseval identities. Section 155G re-derives the Mellin normalization independently.

Entries 83–120 were added in the previous edition. They are the classical primary sources, and the modern accounts, for results that this volume uses or re-derives. Each is cited for the statement named where it is used.

83. Nicomachus of Gerasa, *Introduction to Arithmetic* (c. 100 CE), end of Chapter 20; used at (2.3).
84. J. Faulhaber, *Academia Algebrae*, Augsburg, 1631; used at (2.1).
85. C. G. J. Jacobi, "De usu legitimo formulae summatoriae Maclaurinianae," *Journal für die reine und angewandte Mathematik* 12 (1834), 263–272, DOI 10.1515/crll.1834.12.263. The first general proof of Faulhaber's assertion.
86. D. E. Knuth, "Johann Faulhaber and sums of powers," *Mathematics of Computation* 61 (1993), no. 203, 277–294, DOI 10.2307/2152953. The inverse form and derivative rule of §R2.
87. R. Wituła, K. Kaczmarek, P. Lorenc, E. Hetmaniok, and M. Pleszczyński, "Jordan numbers, Stirling numbers and sums of powers," *Discussiones Mathematicae – General Algebra and Applications* 34 (2014), 155–166, DOI 10.7151/dmgaa.1225. The case $r = 1$ of their product decomposition (13) is $3S_2 = j_n T_n$, the summed form of (2.2a).
88. N. Derby, "A search for sums of powers," *The Mathematical Gazette* 99 (2015), no. 546, 416–421, DOI 10.1017/mag.2015.77. Used in §§R2 and R5C; the printed quadratic should read $(p - T_{2n})(p + n) = 0$.
89. D. Singmaster, "How often does an integer occur as a binomial coefficient?" (Research Problems), *American Mathematical Monthly* 78 (1971), no. 4, 385–386, DOI 10.2307/2316907.
90. B. Pascal, *Traité du triangle arithmétique*, Paris, 1665 (written 1654).
91. P. Mengoli, *Novae quadraturae arithmeticae, seu de additione fractionum*, Bologna, 1650; the telescope (4.1).
92. L. Euler, "De summis serierum reciprocarum," *Commentarii academiae scientiarum Petropolitanae* 7 (1740), 123–134; Euler Archive E41, scholarlycommons.pacific.edu/euler-works/41.
93. L. Euler, "De progressionibus harmonicis observationes," *Commentarii academiae scientiarum Petropolitanae* 7 (1740), 150–161; Euler Archive E43, scholarlycommons.pacific.edu/euler-works/43. The paper that introduces Euler's constant.
94. J. Stirling, *Methodus Differentialis: sive Tractatus de Summatione et Interpolatione Serierum Infinitarum*, London, 1730.
95. J. L. Raabe, "Angenäherte Bestimmung der Factorenfolge $1{\cdot}2{\cdot}3{\cdot}4{\cdot}5 \cdots n = \Gamma(1{+}n) = \int x^n e^{-x}\,dx$, wenn n eine sehr grosse Zahl ist," *Journal für die reine und angewandte Mathematik* 25 (1843), 146–159, DOI 10.1515/crll.1843.25.146. The source of Raabe's integral $\int_0^1 \log\Gamma = \frac{1}{2}\log 2\pi$.
96. E. Cesàro, "Sur la série harmonique," *Nouvelles Annales de Mathématiques* (3) 4 (1885), 295–296.
97. M. B. Villarino, "Ramanujan's harmonic number expansion into negative powers of a triangular number," preprint (2007), arXiv:0707.3950; see also "Ramanujan's harmonic number expansion," preprint (2005), arXiv:math/0511335. Derives (GA.2), with an error estimate, from [120].
98. C. Mortici and M. B. Villarino, "On the Ramanujan–Lodge harmonic number expansion," *Applied Mathematics and Computation* 251 (2015), 423–430, DOI 10.1016/j.amc.2014.11.088.
99. C.-P. Chen, "On the coefficients of asymptotic expansion for the harmonic number by Ramanujan," *The Ramanujan Journal* 40 (2016), 279–290, DOI 10.1007/s11139-015-9670-3; and "Ramanujan's formula for the harmonic number," *Applied Mathematics and Computation* 317 (2018), 121–128, DOI 10.1016/j.amc.2017.08.053.
100. D. W. DeTemple, "A quicker convergence to Euler's constant," *American Mathematical Monthly* 100 (1993), no. 5, 468–470, DOI 10.2307/2324300.
101. L. J. Boya, "Another relation between π, e, γ and $\zeta(n)$," *RACSAM* 102 (2008), no. 2, 199–202, DOI 10.1007/BF03191819. The reciprocal-triangular series (GA.3), obtained from Stirling's formula.
102. E. T. Whittaker and G. N. Watson, *A Course of Modern Analysis*, 5th ed., Cambridge University

Press, 2021, Chapter 12 (the Gamma function), DOI 10.1017/9781009004091.
103. J. C. Lagarias, “Euler’s constant: Euler’s work and modern developments,” *Bulletin of the American Mathematical Society* 50 (2013), no. 4, 527–628, DOI 10.1090/S0273-0979-2013-01423-X.
104. O. Espinosa and V. H. Moll, “On some integrals involving the Hurwitz zeta function: Part 1,” *The Ramanujan Journal* 6 (2002), 159–188, DOI 10.1023/A:1015706300169.
105. H. Kinkelin, “Ueber eine mit der Gammafunction verwandte Transcendente und deren Anwendung auf die Integralrechnung,” *Journal für die reine und angewandte Mathematik* 57 (1860), 122–138, DOI 10.1515/crll.1860.57.122; J. W. L. Glaisher, “On the product $1^1 \cdot 2^2 \cdot 3^3 \cdots n^n$,” *Messenger of Mathematics* 7 (1878), 43–47.
106. B. Nyman, *On Some Groups and Semigroups of Translations*, thesis, Uppsala, 1950.
107. A. Beurling, “A closure problem related to the Riemann zeta-function,” *Proceedings of the National Academy of Sciences* 41 (1955), no. 5, 312–314, DOI 10.1073/pnas.41.5.312.
108. L. Báez-Duarte, M. Balazard, B. Landreau, and E. Saias, “Notes sur la fonction ζ de Riemann, 3,” *Advances in Mathematics* 149 (2000), 130–144, DOI 10.1006/aima.1999.1861.
109. L. Báez-Duarte, M. Balazard, B. Landreau, and E. Saias, “Étude de l’autocorrélation multiplicative de la fonction « partie fractionnaire »,” *The Ramanujan Journal* 9 (2005), 215–240, DOI 10.1007/s11139-005-0834-4.
110. J. Hadamard, “Étude sur les propriétés des fonctions entières et en particulier d’une fonction considérée par Riemann,” *Journal de Mathématiques Pures et Appliquées* (4) 9 (1893), 171–215, Numdam.
111. H. von Mangoldt, “Zur Verteilung der Nullstellen der Riemannschen Funktion $\xi(t)$,” *Mathematische Annalen* 60 (1905), 1–19, DOI 10.1007/BF01447494.
112. H. Davenport, *Multiplicative Number Theory*, 3rd ed., revised by H. L. Montgomery, Graduate Texts in Mathematics 74, Springer, 2000, Chapter 12, DOI 10.1007/978-1-4757-5927-3. The Hadamard constant $B = -\frac{1}{2}\gamma_{\mathrm{E}} - 1 + \frac{1}{2}\log 4\pi$ and $\sum_\rho \Re\rho^{-1} = -B$.
113. T.-J. Stieltjes, “Recherches sur les fractions continues,” *Annales de la Faculté des Sciences de Toulouse* (1) 8 (1894), no. 4, J1–J122, Numdam.
114. S. Bernstein, “Sur les fonctions absolument monotones,” *Acta Mathematica* 52 (1929), 1–66, DOI 10.1007/BF02592679.
115. D. V. Widder, *The Laplace Transform*, Princeton University Press, 1941.
116. A. Weil, “Sur les « formules explicites » de la théorie des nombres premiers,” *Communications du Séminaire Mathématique de l’Université de Lund*, tome supplémentaire (1952), 252–265.
117. E. C. Titchmarsh, *Introduction to the Theory of Fourier Integrals*, 2nd ed., Oxford University Press, 1948. Mellin inversion and the Mellin–Plancherel theorem used at (GA.6).
118. H. M. Edwards, *Riemann’s Zeta Function*, Academic Press, 1974.
119. B. C. Berndt, *Ramanujan’s Notebooks, Part V*, Springer-Verlag, New York, 1998, Chapter 38, Entry 9, p. 521; the expansion (GA.2).
120. D. W. DeTemple and S.-H. Wang, “Half-integer approximations for the partial sums of the harmonic series,” *Journal of Mathematical Analysis and Applications* 160 (1991), no. 1, 149–156, DOI 10.1016/0022-247X(91)90296-C.

Table 4: Support-filtered expected-affinity family near 2.75.

Rail	Active hits	Random hits	Enrichment
Primary valley crest near 2.7477	736	218	3.376×
Basin companion near 2.74475	721	251	2.873×
Tip companion near 2.7545	685	246	2.785×

The companion rails do not replace the primary sign-control result. They are retained as descriptive evidence that the enrichment appears in a small neighborhood of related marker values and morphology classes. A continuous coordinate scan is required before making a stronger claim about the width or peak location of this neighborhood.

4.4 Morphology rotation

The morphology-envelope diagnostic is descriptive. It shows that the active marker can rotate among morphology states. In the evaluated aggregate telemetry, the strongest morphologies were distributed among tip extreme, valley, and tight basin rows. This rotation explains altitude bands where the primary fixed-valley cross-section weakens while the broader active neighborhood remains enriched. Detailed rotation data is retained in Appendix D.

4.5 Coordinate-locality validation scan (R142A)

The primary R141H ledger establishes the frozen-design sign-control result. To test whether that result is tied to a single coordinate or to a broader neighborhood, we then performed a coordinate-locality validation scan, denoted R142A. This scan used the same frozen morphology grammar as the primary ledger:

$$\epsilon = 5 \times 10^{-4}, \qquad W = 4, \qquad R = 4, \qquad \tau = 0.10.$$

The scan evaluated a regular coordinate grid over $2.30 \leq x \leq 3.20$, the original active coordinate, sign-reversed controls, nearby perturbations, and named companion coordinates.

R142A changes the interpretation of the geometric prior in an important way. The original active marker remained enriched, but it did not emerge as a unique isolated maximum. Instead, it lies inside a broader enriched shelf spanning approximately

$$2.70 \leq x \leq 2.81.$$

The active coordinate

$$a_{\text{Euler+cos}} = \frac{\pi}{2} + \frac{2}{\pi} + \cos(1) \approx 2.747718$$

produced

$$702/218 = 3.220\times$$

over 21 support-qualified R142A blocks. Several nearby coordinates were comparable or stronger. In particular,

$$\frac{7\pi}{8} \approx 2.748894$$

produced $692/190 = 3.642\times$, while grid coordinates 2.740 and 2.780 produced $784/218 = 3.596\times$ and $570/158 = 3.608\times$, respectively.

Thus R142A supports a shelf interpretation: the original geometric marker successfully localized an enriched coordinate neighborhood, while the empirical crest rotates among nearby rails. This is stronger and more conservative than claiming that the prior identified a unique needle-point maximum.

Table 5: Representative R142A coordinate-locality results. Enrichment is computed as total pre-hits divided by total random-pre hits over support-qualified blocks. This table is not a top-rank table; it includes the sign-control floor, upper negative-control trend, frozen active coordinate, named companions, and representative shelf rails.

Coordinate	Value	Support blocks	Hits	Enrichment
Sign-control floor	1.667114	22	60332/40657	1.483927
Negative control upper trend	2.450000	22	3461/1382	2.504342
Active exact	2.747718	21	702/218	3.220183
Empirical basin companion	2.744750	22	707/226	3.128319
$7\pi/8$ companion	2.748894	21	692/190	3.642105
α_1 companion	2.749611	21	714/234	3.051282
2.750 grid / 22/8	2.750000	22	743/224	3.316964
R124 tip companion	2.754500	22	651/239	2.723849
Shelf rail	2.740000	22	784/218	3.596330
Shelf rail	2.780000	21	570/158	3.607595
Shelf rail	2.805000	19	487/137	3.554745

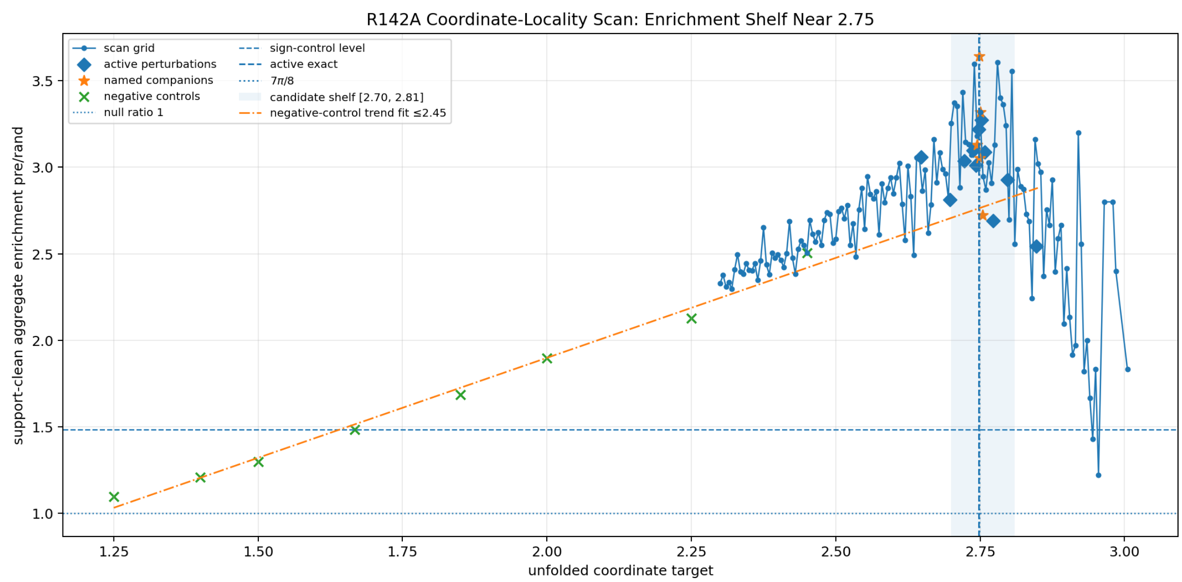

Figure 3: R142A coordinate-locality scan. The horizontal axis is the unfolded target coordinate and the vertical axis is support-clean aggregate enrichment, computed as total pre-hits divided by total random-pre hits. Negative controls below $x = 2.45$ follow a smooth rising background trend. The original active coordinate $a_{\mathrm{Euler+cos}} \approx 2.747718$ lies inside an elevated shelf spanning approximately 2.70–2.81. Nearby rails, including $7\pi/8$, 2.740, and 2.780, show comparable or stronger enrichment. The scan supports a shelf interpretation rather than a unique coordinate-local peak.

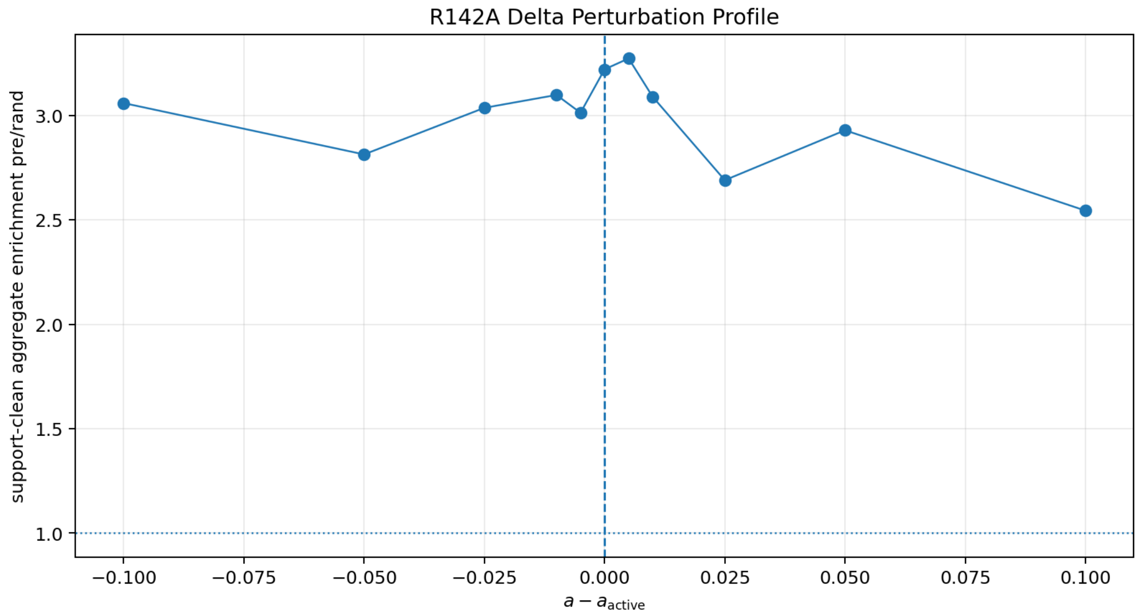

Figure 4: R142A perturbation profile around the active coordinate. The profile remains elevated across small perturbations of the active marker, with the local maximum occurring near $a_{\text{Euler+cos}} + 0.005$. This confirms that the active coordinate is embedded in a finite-width enrichment shelf rather than forming a sharp isolated spike.

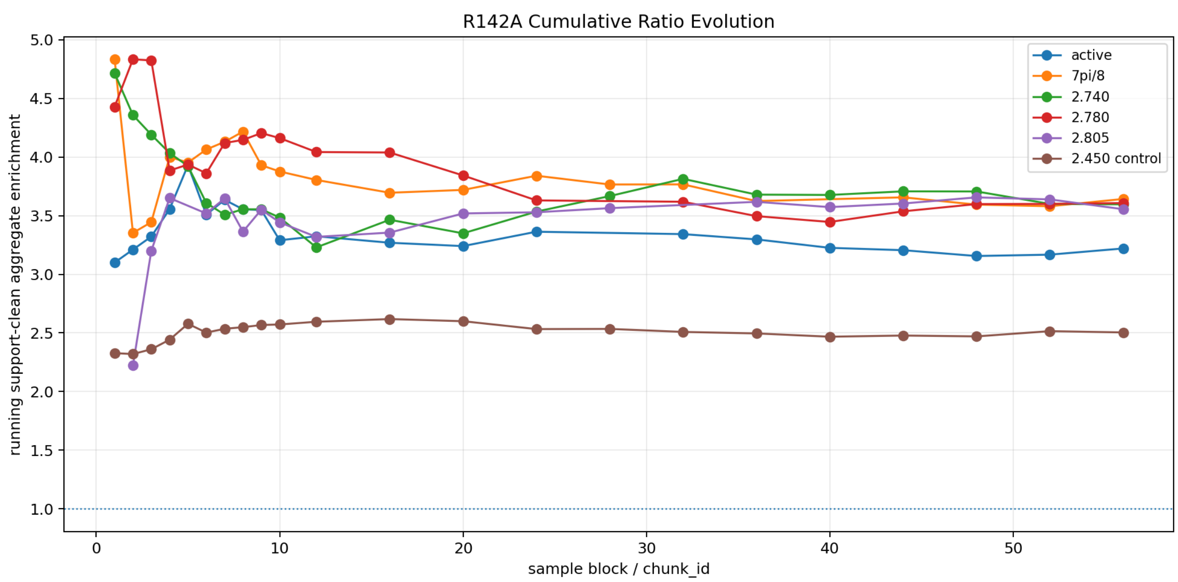

Figure 5: Cumulative aggregate enrichment for selected shelf coordinates and the 2.450 negative-control coordinate. The shelf coordinates stabilize above the negative-control trend as additional blocks are accumulated, while the 2.450 control remains distinctly lower. This supports the interpretation that the observed 2.75-neighborhood response is not driven solely by early-block transients.